

**GOLD AND BASE METAL MINERALIZATION IN  
THE NIPPERS HARBOUR OPHIOLITE,  
NEWFOUNDLAND**

**CENTRE FOR NEWFOUNDLAND STUDIES**

**TOTAL OF 10 PAGES ONLY  
MAY BE XEROXED**

**(Without Author's Permission)**

**KAREN A. HUDSON**



0004J

8



National Library  
of Canada

Bibliothèque nationale  
du Canada

Canadian Theses Service

Service des thèses canadiennes

Ottawa, Canada  
K1A 0N4

## NOTICE

The quality of this microform is heavily dependent upon the quality of the original thesis submitted for microfilming. Every effort has been made to ensure the highest quality of reproduction possible.

If pages are missing, contact the university which granted the degree.

Some pages may have indistinct print especially if the original pages were typed with a poor typewriter ribbon or if the university sent us an inferior photocopy.

Reproduction in full or in part of this microform is governed by the Canadian Copyright Act, R.S.C. 1970, c. C-30, and subsequent amendments.

## AVIS

La qualité de cette microforme dépend grandement de la qualité de la thèse soumise au microfilmage. Nous avons tout fait pour assurer une qualité supérieure de reproduction.

S'il manque des pages, veuillez communiquer avec l'université qui a conféré le grade.

La qualité d'impression de certaines pages peut laisser à désirer, surtout si les pages originales ont été dactylographiées à l'aide d'un ruban usé ou si l'université nous a fait parvenir une photocopie de qualité inférieure.

La reproduction, même partielle, de cette microforme est soumise à la Loi canadienne sur le droit d'auteur, SRC 1970, c. C-30, et ses amendements subséquents.

GOLD AND BASE METAL MINERALIZATION IN  
THE NIPPERS HARBOUR OPHIOLITE,  
NEWFOUNDLAND

BY

© Karen A. Hudson, B.Sc.(Honours)

A thesis submitted to the School of Graduate  
Studies in partial fulfillment of the  
requirements for the degree of  
Master of Science

Department of Earth Sciences  
Memorial University of Newfoundland

August, 1988

St. John's

Newfoundland

Permission has been granted to the National Library of Canada to microfilm this thesis and to lend or sell copies of the film.

The author (copyright owner) has reserved other publication rights, and neither the thesis nor extensive extracts from it may be printed or otherwise reproduced without his/her written permission.

L'autorisation a été accordée à la Bibliothèque nationale du Canada de microfilmer cette thèse et de prêter ou de vendre des exemplaires du film.

L'auteur (titulaire du droit d'auteur) se réserve les autres droits de publication; ni la thèse ni de longs extraits de celle-ci ne doivent être imprimés ou autrement reproduits sans son autorisation écrite.

ISBN 0-315-50466-8

Karen A. Hudson  
Department of Earth Sciences  
Memorial University of Nfld  
St. John's, Nfld.  
A1C 3E7

28 February, 1989

To Whom It May Concern:

Please note that the colour photographs on pages 34, 36, 44, 50, 58, 59, 61, 63, 75 and 76 of my Earth Sciences Master of Science thesis are necessary for the presentation of the field and petrographic observations. Many of the rocks and minerals described in the thesis have subtle colour variations which would not be readily apparent in black and white photographs.

Sincerely,

*Karen Hudson*  
Karen Hudson.

## Abstract

The Nippers Harbour Ophiolite is a southwesterly extension of the lower Ordovician Betts Cove Ophiolite. Extensive sheeted dyke and gabbro members, as well as minor ultramafic components, characterize the Nippers Harbour Ophiolite. The ophiolite is unconformably overlain by the Silurian Cape St. John Group, which consists of subaerial conglomerates, cross-bedded sandstones, basic pyroclastics and andesitic to rhyolitic ash-flow tuffs. The ophiolite also is intruded by the Late Silurian to Early Devonian Cape Brule quartz-feldspar Porphyry. The mafic members of the Nippers Harbour Ophiolite show similarities to Betts Cove boninite-type lavas in that they contain unusually low  $\text{TiO}_2$  and high  $\text{SiO}_2$ ,  $\text{MgO}$ ,  $\text{Cr}$  and  $\text{Ni}$  contents.

Mineralization is located commonly in shear or fault zones in mafic ophiolitic rocks. The Hill showing has characteristics resembling those of massive sulphide stockwork zones, with pyrite-chalcopyrite-quartz-chlorite breccia and sheared rock, surrounded by fragments of hydrothermally altered quartz-chlorite-albite rock. Relatively unaltered diabase dykes intrude these assemblages. The altered rocks have been enriched in  $\text{FeO}$ ,  $\text{Cu}$  and  $\text{Zn}$ , and depleted in  $\text{Na}_2\text{O}$ ,  $\text{CaO}$ ,  $\text{Sr}$  and LREE. Mineralization is believed to have been formed by the mixing of upwelling, hot, Fe-, Cu-, Zn-enriched seawater-derived hydrothermal fluids with cold seawater at the diabase-pillow basalt interface.

Anomalous gold contents have been documented at Burtons Pond, Gull Pond and Showing Number 2. The gold is spatially related to sulphides, mainly chalcopyrite and arsenopyrite, which have precipitated with quartz-calcite, quartz-albite and quartz in veins in altered host rocks. Three alteration assemblages are recognized: (1) quartz-chlorite+/-albite, (2) quartz-chlorite-sericite and (3) quartz-sericite-calcite. Only the Burtons Pond showing displays all three assemblages, whilst the others are associated with assemblage (2). The alteration is expressed chemically by the addition of  $\text{FeO}$ , S,  $\text{K}_2\text{O}$ ,  $\text{CO}_2$ , Au, Ag, As, Ba, Co, Cu, Se and Zn, and variable depletions of CaO, Sr and  $\text{Na}_2\text{O}$ . Fluid inclusion and sulphur isotope data (ranging from 4.5 to 6.7 per mil) suggest that the fluids were seawater-derived and had the following characteristics: temperature  $\sim 250^\circ\text{C}$ , pH 5, total reduced sulphur  $< 10^{-3}\text{M}$ ,  $a_{\text{O}_2} < 10^{-42}$  and  $a_{\text{S}_2} < 10^{-13.5}$ . Gold probably was carried predominantly as a thio-complex, but it also may have been a chloride- or thio-arsenide complex. Mineralization is believed to have formed by movement of seawater-derived fluids along shallow thrust planes, depositing sulphides and gold with associated chlorite and sericite, in splays.

Other sulphide showings include Pb-Zn and Cu-bearing quartz veins at Welshs Bight and Rogues Harbour respectively. Field evidence and sulphur and lead isotope data (-0.4 to 2.9 per mil, and  $^{206}\text{Pb}/^{204}\text{Pb} = 17.659$ ,  $^{207}\text{Pb}/^{204}\text{Pb} = 15.464$ ,  $^{208}\text{Pb}/^{204}\text{Pb} = 37.562$  respectively) suggest that these showings are related to the intrusion of the Cape Brule Porphyry.



## Acknowledgements

I would like to thank Dr. J.W. Lydon of the Geological Survey of Canada for suggesting this project and for his help and encouragement along the way. My supervisor, Dr. D.F. Strong provided constructive guidance and was very helpful with editing. Dr. D.H.C. Wilton acted as second supervisor and was a superb editor. Rio Algom Exploration Inc, Varna Resources and Pearce Bradley, Baie Verte Mines are to be thanked for their permission to examine and work on their properties. Rio Algom in particular provided drill logs and drill hole locations from their work on the Burtons Pond showing. Dr. R.I. Thorpe of the Geological Survey of Canada and Dr. H.S. Swinden of the Newfoundland Department of Mines assisted with lead isotope interpretations. Joan Dicks is thanked for her cheerful and competent field assistance. Peter Hudson also provided helpful field assistance. M. Prole and W. Starkes from Nippers Harbour provided boat transportation. I also would like to thank Gert Andrews, Jeff Veinott (MUN), Jamie Lavigne, Dan Richardson, and G. LeChance (GSC) for major and trace element analyses, Simon Jackson and Dave Healey for precious metal and REE analyses (MUN), Wilf Marsh for help with photography, Dr. H. Longerich and Jeff Veinott for help with the electron microprobe (MUN), Carolyn Emerson for assistance with the scanning electron microprobe (MUN), Cindy Saunders for help with fluid inclusion procedures, David Van Everdingen for help with computer

programs and Foster Thornhill and Rick Soper for making thin, polished and fluid inclusion sections (MUN). Finally, I would like to thank Steve Edwards for his unwavering moral support. Financial support was provided through a Memorial University fellowship and through NSERC Operating Grant No. A7975 to Dr. D.F. Strong. The Geological Survey of Canada provided field support and salaries for myself and J. Dicks during the summer of 1988, as well as funding for half of my analytical work.

## Table of Contents

<b>1. Introduction</b>	<b>1</b>
1.1. Objective	1
1.2. Location and Access	1
1.3. Regional Geology	4
1.4. Local Geology	9
1.4.1. Nippers Harbour Ophiolite	10
1.4.2. Ultramafic Member	10
1.4.3. Gabbro Member	11
1.4.4. Sheeted Dyke Member	11
1.4.5. Cape St. John Group	12
1.5. Mineral Occurrences	13
1.5.1. Major Deposits	13
1.5.2. Other Metallic Mineral Occurrences	16
1.6. Ophiolitic Stockwork-type and Gold Deposition	16
1.6.1. Sulphide Deposits in Subsurface Ophiolitic Units	20
1.7. Summary	21
<b>2. General Geology</b>	<b>24</b>
2.1. Introduction	24
2.2. Ultramafic Unit	24
2.3. Gabbro Unit	28
2.4. Diabase Dyke Unit	30
2.5. Cape St. John Group	37
2.6. Cape Brule Porphyry	38
2.7. Structure	41
2.8. Summary	45
<b>3. Mineralization Features</b>	<b>46</b>
3.1. Introduction	46
3.2. History of Exploration	47
3.3. Geology and Mineralogy of Mineralized Showings	47
3.3.1. Showing No. 1 - Hill	48
3.3.2. Burtons Pond	53
3.3.2.1. Host Rock Alteration	54
3.3.2.2. Vein Mineralogy	62
3.3.3. Gull Pond	67
3.3.4. Showing No. 2	71

3.3.5, Rogues Harbour	72
3.3.6, Welshs Bight	74
3.4. Metal Contents of Sulphide Samples	77
3.5. Summary	82
<b>4. Geochemistry</b>	<b>84</b>
4.1. Introduction	84
4.2. Geochemical Characteristics and Tectonic Environment	85
4.2.1. Previous Work on Betts Cove / Tilt Cove lavas	85
4.2.2. Nippers Harbour Results	88
4.3. Chemical Gains and Losses	100
4.4. Hill Showing	109
4.5. Gold-Bearing Showings: Burtons Pond, Gull Pond, Showing No. 2	113
4.5.1. Burtons Pond	114
4.5.1.1. Relationship of Metasomatism to Gold Content	116
4.6. Rogues Harbour, Welshs Bight	124
4.7. Rare Earth Elements	125
4.8. Sulphur Isotopes	131
4.8.1. Introduction	131
4.8.2. Background	132
4.8.3. Nippers Harbour Results	134
4.9. Lead Isotope, Welshs Bight Showing	140
4.9.1. Summary	146
<b>5. Fluid Inclusions</b>	<b>149</b>
5.1. Introduction	149
5.2. Description of Inclusions	150
5.3. Freezing Results	156
5.3.1. Eutectic Temperature	156
5.3.2. Salinity	158
5.4. Heating Results	161
5.4.1. Homogenization Temperature	161
5.5. Discussion	163
5.6. Summary	167
<b>6. Characteristics of Ore-Bearing Hydrothermal Fluids and Genetic Models</b>	<b>169</b>
6.1. Hill Showing	169
6.1.1. Introduction	169
6.1.2. Application to the Hill Showing	170
6.2. Gold-Rich Showings - Burtons Pond, Gull Pond, Showing No. 2	172
6.2.1. Source of Gold	174
6.2.2. Modes of Gold Transport	175
6.2.3. Genetic Models	182
6.3. Rogues Harbour, Welshs Bight	185

<b>7. Summary and Recommendations</b>	<b>188</b>
Summary	188
7.2. Recommendations for Future Work	192
<b>References</b>	<b>193</b>
<b>Appendix A. Mineralogy of Samples</b>	<b>212</b>
<b>Appendix B. Analytical Methods</b>	<b>218</b>
B.1. Major Elements	218
B.1.1. Memorial Samples	218
B.1.2. GSC Samples	219
B.2. Trace Elements	220
B.2.1. Memorial Samples	220
B.2.2. GSC Samples	220
B.3. Precious Metals	223
B.3.1. Memorial Samples	223
B.3.2. GSC Samples	226
B.4. Rare Earth Elements and Traces - MUN	226
B.5. Sulphur Isotopes	227
B.6. Lead Isotopes	228
B.7. Sample Calculation - Mass Balancing	229
B.7.1. Part A' - Determination of Ratio of Oxide to Immobile Element Zr	229
B.7.2. Part B - Determination of Gain/Loss of Component , as g/kg of original rock	230
B.7.3. Atomic Weight used in Calculations	231
B.7.4. Graphs Used to Estimate Metasomatic Enrichments and Depletions	231
<b>Appendix C. Major and Trace Element Analyses</b>	<b>235</b>
<b>Appendix D. REE Analyses, Chondrite Normalizing Values, and Sulphur Isotopes</b>	<b>261</b>
D.1. REE analyses	261
D.2. Chondrite Values	269
D.3. Sulphur Isotopes	270
<b>Appendix E.</b>	<b>272</b>
<b>Precious and Base Metal Analyses</b>	
E.1. Precious and Base Metal Analyses	272
E.2. Sample Descriptions and Locations	280
E.2.1. Sample Descriptions	280
E.2.2. Sample Locations	283
<b>Appendix F. Electron Microprobe Data</b>	<b>290</b>
<b>Appendix G. Fluid Inclusion Methodology</b>	<b>301</b>

## List of Figures

<b>Figure 1-1:</b>	General Geology of the Baie Verte Peninsula	2
<b>Figure 1-2:</b>	Gold Occurrences in Ophiolitic Rocks on the Baie Verte Peninsula	3
<b>Figure 1-3:</b>	Essential characteristics of an idealized massive sulphide deposit	18
<b>Figure 1-4:</b>	The listwaenite model of gold mineralization	22
<b>Figure 2-1:</b>	Geology and mineral occurrences in the Nippers Harbour Ophiolite	25
<b>Figure 2-2:</b>	Photographs of ultramafic rocks	27
<b>Figure 2-3:</b>	Photographs of gabbro and pegmatitic gabbro	29
<b>Figure 2-4:</b>	Photographs of sheeted dyke outcrops, Northwest Arm	31
<b>Figure 2-5:</b>	Photographs of dyke contacts in outcrop	32
<b>Figure 2-6:</b>	Photomicrograph of diabase texture	34
<b>Figure 2-7:</b>	Photographs of dyke breccia and epidotized dyke outcrops	38
<b>Figure 2-8:</b>	Photographs of rhyolite and intrusive breccia outcrops, Cape St. John Group	39
<b>Figure 2-9:</b>	Photomicrographs of quartz-feldspar porphyry	40
<b>Figure 2-10:</b>	Structural features of the Nippers Harbour Ophiolite	42
<b>Figure 2-11:</b>	Photograph of chloritic shear zone in diabase outcrop, Northwest Arm	44
<b>Figure 3-1:</b>	Geology of the Hill Showing	49
<b>Figure 3-2:</b>	Photographs of mineralized units one and two, Hill Showing	50
<b>Figure 3-3:</b>	Photographs of unit three rocks, Hill Showing	51
<b>Figure 3-4:</b>	Photomicrograph of quartz-chlorite alteration, Hill showing	52
<b>Figure 3-5:</b>	Geology of the Burtons Pond showing	55
<b>Figure 3-6:</b>	Subsurface geology of the Burtons Pond showing	58
<b>Figure 3-7:</b>	SEM photomicrograph of sulphide replacement texture, Burtons Pond	57
<b>Figure 3-8:</b>	Photomicrographs of Burtons Pond unaltered and altered samples	58
<b>Figure 3-9:</b>	Photomicrographs of altered Burtons Pond samples	59
<b>Figure 3-10:</b>	Photomicrographs of altered Burtons Pond samples	61

<b>Figure 3-11:</b>	Photomicrographs of Burtons Pond sulphide veins	63
<b>Figure 3-12:</b>	Photomicrographs of sulphide textures	65
<b>Figure 3-13:</b>	SEM photomicrographs of electrum grains, Burtons Pond	66
<b>Figure 3-14:</b>	Paragenetic sequence of hydrothermal events, Burtons Pond	67
<b>Figure 3-15:</b>	Geology of the Gull Pond showing	68
<b>Figure 3-16:</b>	Paragenetic sequence of hydrothermal events, Gull Pond	69
<b>Figure 3-17:</b>	SEM photomicrograph of electrum grain in arsenopyrite, Gull Pond	70
<b>Figure 3-18:</b>	Photomicrograph of chlorite-sericite alteration, Gull Pond	71
<b>Figure 3-19:</b>	Paragenetic sequence of hydrothermal events, Showing No. 2	72
<b>Figure 3-20:</b>	Sulphide textures, Showing No. 2	73
<b>Figure 3-21:</b>	Photograph and photomicrograph of Rogues Harbour sulphides and quartz vein	75
<b>Figure 3-22:</b>	Photomicrograph of Welshs Bight sulphides	76
<b>Figure 3-23:</b>	Paragenetic sequence for hydrothermal minerals, Welshs Bight showing	77
<b>Figure 3-24:</b>	Au enrichment vs. Cu+Zn enrichment diagram for the Nippers Harbour showings	81
<b>Figure 4-1:</b>	Variation diagrams for altered and unaltered Nippers Harbour diabases	90
<b>Figure 4-2:</b>	Variation diagrams for altered and unaltered Nippers Harbour diabases	91
<b>Figure 4-3:</b>	Variation diagrams	93
<b>Figure 4-4:</b>	Rare-earth element diagrams	95
<b>Figure 4-5:</b>	Variation diagrams	96
<b>Figure 4-6:</b>	Variation diagrams	97
<b>Figure 4-7:</b>	Variation diagrams	99
<b>Figure 4-8:</b>	Variation diagrams	103
<b>Figure 4-9:</b>	Variation diagrams	104
<b>Figure 4-10:</b>	Variation diagrams	105
<b>Figure 4-11:</b>	Triangular diagrams of 'immobile' elements for unaltered and altered samples	107
<b>Figure 4-12:</b>	Alteration assemblages produced by varying seawater/rock ratios	110
<b>Figure 4-13:</b>	Triangular diagrams	115
<b>Figure 4-14:</b>	Relationship of gold content to metasomatism Burtons Pond Section A	117
<b>Figure 4-15:</b>	Relationship of gold content to metasomatism Burtons Pond drill hole No. 2	118
<b>Figure 4-16:</b>	Relationship of gold content to metasomatism Burtons Pond drill hole No. 4	119

<b>Figure 4-17:</b>	Chemical reactions affecting Burtons Pond rocks	121
<b>Figure 4-18:</b>	Rare-earth element diagrams	127
<b>Figure 4-19:</b>	Rare earth element diagram	128
<b>Figure 4-20:</b>	Rare earth element diagrams	129
<b>Figure 4-21:</b>	Rare earth element diagrams	130
<b>Figure 4-22:</b>	Sulphur isotopic variation in nature	133
<b>Figure 4-23:</b>	Sulphur isotope histograms, Nippers Harbour showings	135
<b>Figure 4-24:</b>	Temperature vs $\delta^{34}\text{S}$ , Burtons Pond samples	140
<b>Figure 4-25:</b>	$^{206}\text{Pb}/^{204}\text{Pb}$ vs $^{207}\text{Pb}/^{204}\text{Pb}$ diagram for Welshs Bight and other Newfoundland samples	142
<b>Figure 4-26:</b>	$^{206}\text{Pb}/^{204}\text{Pb}$ vs $^{208}\text{Pb}/^{204}\text{Pb}$ for Welshs Bight sample	145
<b>Figure 5-1:</b>	Photomicrographs of fluid inclusions	153
<b>Figure 5-2:</b>	Nippers Harbour eutectic temperatures	157
<b>Figure 5-3:</b>	NaCl-H <sub>2</sub> O system, temperature-composition diagram at 1 atm	159
<b>Figure 5-4:</b>	Nippers Harbour fluid inclusion salinities	160
<b>Figure 5-5:</b>	Nippers Harbour fluid inclusion homogenization temperatures	162
<b>Figure 6-1:</b>	Schematic model for mineralization at the Hill showing	173
<b>Figure 6-2:</b>	Calculated oxygen activity diagram for the system Au-NaCl-S-H <sub>2</sub> O at 250°C	177
<b>Figure 6-3:</b>	Calculated oxygen activity-sulphur activity diagram for the system Au-NaCl-S-H <sub>2</sub> O at 250°C and pH 5	178
<b>Figure 6-4:</b>	Calculated oxygen activity-sulphur activity diagram for the system Au-Fe-As-NaCl-S-H <sub>2</sub> O at 250°C and pH 5	180
<b>Figure 6-5:</b>	Calculated oxygen activity-sulphur activity diagram for the system Au-Fe-As-NaCl-S-H <sub>2</sub> O at 250°C and pH 5	181
<b>Figure 6-6:</b>	Model for gold mineralization at Burtons Pond	186
<b>Figure B-1:</b>	Variation diagrams	232
<b>Figure B-2:</b>	Variation diagrams	233
<b>Figure B-3:</b>	Variation diagrams	234
<b>Figure E-1:</b>	Locations for regional diabase/gabbro, pyroxenite/dunite, Cape St. John Group and QFP samples	284
<b>Figure E-2:</b>	Locations for Hill Showing samples	285
<b>Figure E-3:</b>	Locations for Burtons Pond samples	286
<b>Figure E-4:</b>	Locations for Gull Pond samples	287
<b>Figure E-5:</b>	Locations for Rogues Harbour samples	288
<b>Figure E-6:</b>	Locations for Showing No.2, Welshs Bight, and Regional Quartz Vein samples	289
<b>Figure G-1:</b>	Calibration curve for fluid inclusion runs	302
<b>Figure G-2:</b>	Freezing points of pure NaCl solutions	303



## List of Tables

<b>Table 1-1:</b>	Published and unpublished works on the Betts Cove Complex, particularly Nippers Harbour Ophiolite	5
<b>Table 3-1:</b>	Metal and Other Characteristics of Nippers Harbour mineralized samples	78
<b>Table 4-1:</b>	Analyses of 'typical' basalts, Betts Cove and Nippers Harbour diabases	89
<b>Table 4-2:</b>	Partial list of major and trace element data, Hill showing	101
<b>Table 4-3:</b>	Metasomatic changes affecting hydrothermally altered rocks, Nippers Harbour showings	108
<b>Table 4-4:</b>	Chemical changes of Gull Pond and Showing No.2 altered samples	123
<b>Table 4-5:</b>	Chemical changes of Rogues Harbour altered samples	124
<b>Table 4-6:</b>	Sulphur Isotope Thermometers After Kajiwara and Krouse, 1971	138
<b>Table 4-7:</b>	Nippers Harbour geological temperatures calculated from sulphur isotope pairs	139
<b>Table 4-8:</b>	Lead isotope results, Welshs Bight	141
<b>Table 4-9:</b>	Lead isotope analyses from the Silverdale deposit, Lushs Bight Group	145
<b>Table 5-1:</b>	Characteristics of fluid inclusion solids	152
<b>Table 5-2:</b>	Characteristics of Nippers Harbour Fluid Inclusions	155
<b>Table 5-3:</b>	Fluid Inclusion and Other Characteristics of Selected Hydrothermal Deposits, and of Nippers Harbour Inclusions	164
<b>Table B-1:</b>	Precision and accuracy estimate for MUN trace element analyses	221
<b>Table B-2:</b>	Detection limits, precision and accuracy estimates for MUN precious metal analyses	225
<b>Table B-3:</b>	Precision and accuracy estimates for MUN REE analyses	228
<b>Table G-1:</b>	Salinities obtained from freezing point measurements	304
<b>Table G-2:</b>	Eutectic temperatures corresponding to common salts	305

# Chapter 1

## Introduction

### 1.1. Objective

The aim of this thesis is to describe the chemical and mineralogical characteristics of several gold and sulphide showings in the Nippers Harbour Ophiolite, in order to provide some understanding of their origins. The showings within the ophiolite exhibit characteristics of stockwork-type sub-seafloor deposition, but they also may have been influenced by a large quartz-feldspar porphyry which intrudes the ophiolite. Consequently, a discussion of the features of this type of mineralization also is given. In light of the gold-bearing nature of some of the showings, reference is made to both modern and ancient gold deposits in this summary.

### 1.2. Location and Access

The Nippers Harbour Ophiolite is located on the south-east side of the Baie Verte Peninsula, at latitude  $49^{\circ}49'18''$  to  $49^{\circ}45'0''$  and longitude  $55^{\circ}49'35''$  to  $55^{\circ}55'25''$  (Fig. 1-1). It is accessible by Highway 415 to the community of Nippers Harbour. The outer extremities of the ophiolite are accessible by foot and boat.

Saunders (1985) has eloquently summarized the published work on the Baie

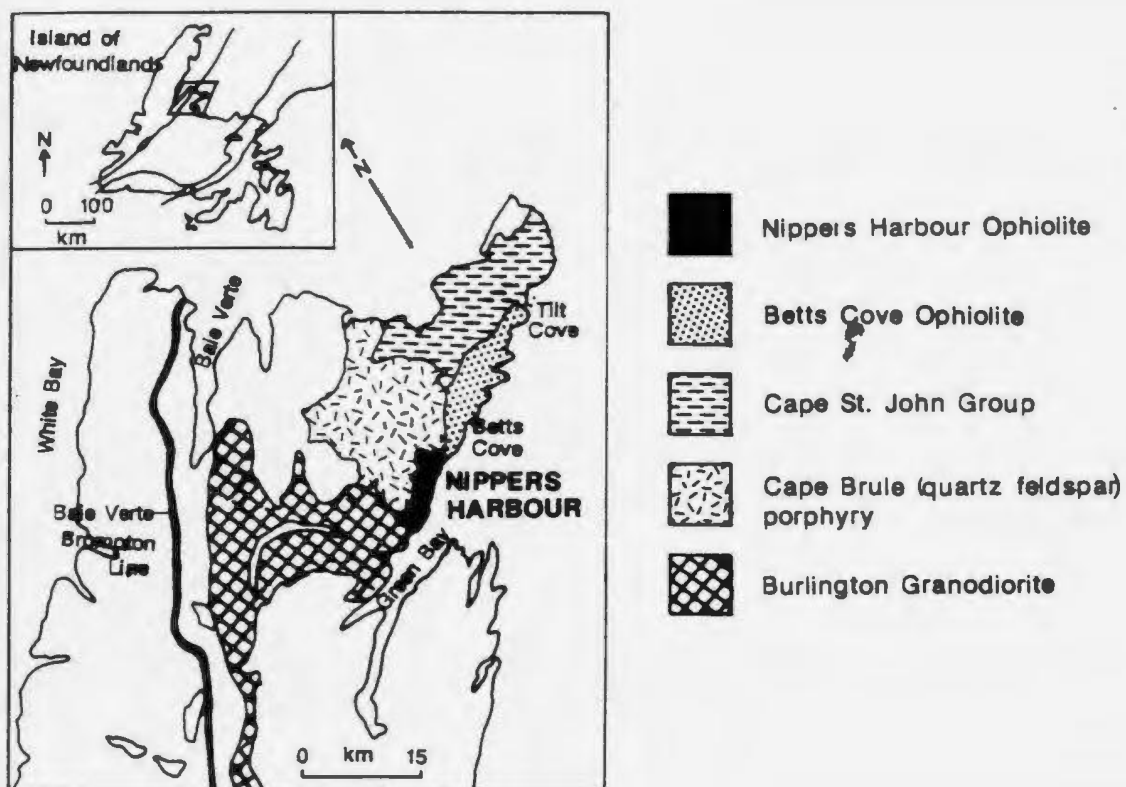


**Figure 1-1:** General Geology of the Baie Verte Peninsula

(From Strong (1984) - simplified from DeGrace et al. (1976)

and Hibbard (1983)).

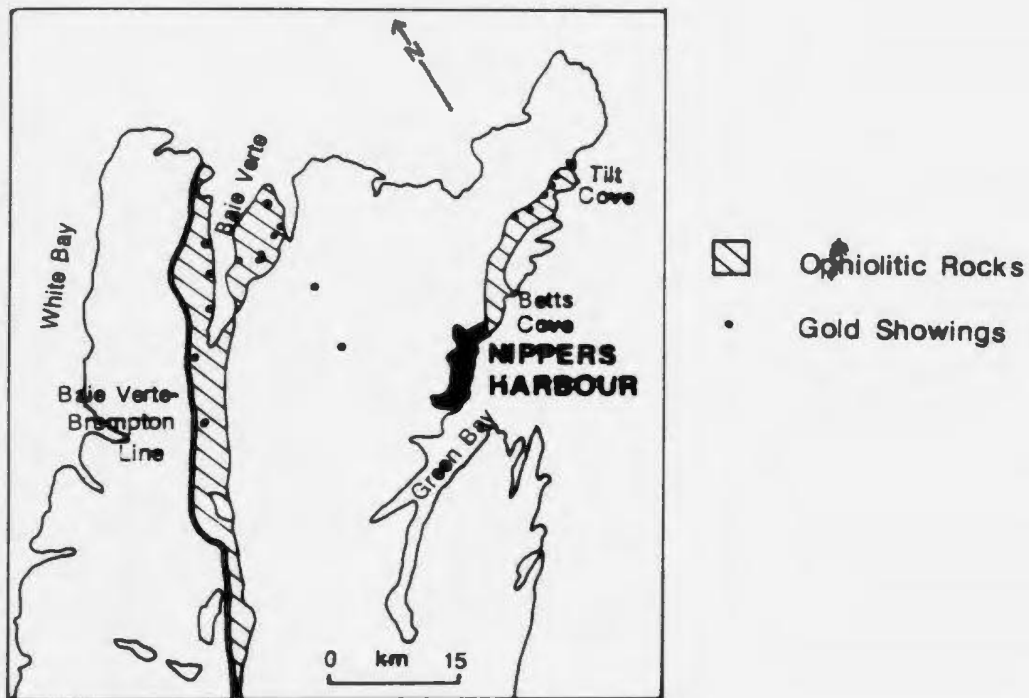


**Figure 1-2:** Gold Occurrences in Ophiolitic Rocks on the Baie Verte Peninsula

(After Tuach *et al.* (1988)).

Verte Peninsula. Table 1-1 is a subset of her comprehensive summary of contributions, with additional specific references to Nippers Harbour work. Recently, the peninsula has experienced an explosion of exploration activity with several important gold discoveries in correlative ophiolites 30 km to the west (Fig 1-2).

### 1.3. Regional Geology

Williams (1976) divided the island of Newfoundland into four tectonostratigraphic zones. These zones, from west to east, are known as the Humber, Dunnage, Gander and Avalon zones, and extend throughout most of the Appalachian Orogen (Williams, 1978). The rocks of the westernmost Humber zone record the formation and destruction of the ancient continental margin of eastern North America. The Dunnage zone, which contains the Nippers Harbour Ophiolite, represents the remains of an Early Paleozoic Iapetus ocean, and contains ophiolite suites and volcanic complexes. The easterly Gander and Avalon zones represent the eastern margin of Iapetus and an easternmost possible continent-based terrane, respectively.

Hibbard (1983) has informally named that part of the Baie Verte Peninsula to the east of the Baie Verte-Brompton Line as the Baie Verte Belt. It contains three ophiolitic units, the Advocate, Point Rousse and Betts Cove (which includes both the Betts Cove and Nippers Harbour Ophiolites) Complexes, which can be distinguished on the basis of geographical distribution and structural history. The Pacquet Harbour Group, characterized by both ophiolitic and island arc volcanics, defines a fourth ophiolitic-type unit. The ophiolites are overlain conformably and unconformably by later volcanic cover sequences and are cut by later intrusions.

**Table 1-1: Published and unpublished works on the Betts Cove Complex, particularly Nippers Harbour Ophiolite**

Year	Author(s)	Subject
1929	Snelgrove	Unpublished report on Betts Cove Copper Mine
1931	Snelgrove	Ph.D. thesis on Betts Cove and Tilt Cove ore deposits
1947	Baird	Ph.D. thesis on Betts Cove and Tilt Cove ore deposits
1948	Baird	Paper on copper deposits in the Betts Cove-Stocking Harbour district
1951	Baird	Report on Burlington Peninsula, including mineralized prospects
1964	Papezik	Paper describing nature and origin of nickel minerals at Tilt Cove
1967	Advocate Mines Ltd.	Report on diamond drilling data in Nippers Harbour area
1971	Upadhyay <u>et al.</u>	Description and interpretation of mode of formation of the ophiolite.

Year	Author(s)	Subject
1971	Schroeter	M.Sc. thesis on Nippers Harbour ophiolite.
1972	Riccio	M.Sc. thesis on ophiolite in Betts Cove area.
1973	Upadhyay	Ph.D. thesis on the entire Betts Cove ophiolite.
1973	Upadhyay & Strong	Outlined a genetic model for Betts Cove massive sulphide deposit
1974	Upadhyay	Unpublished report on mineral potential of Betts Cove/Tilt Cove area
1975	Neale <u>et al.</u>	Describe unconformity between the Betts Cove ophiolite and the overlying Cape St. John Group.
1975	Riccio	Unpublished report of mineral exploration on the Burlington Peninsula for 1975
1976	DeGrace <u>et al.</u>	Report on mapping of Nippers Harbour area and eastern Baie Verte Peninsula
1977b	Coish	Ph.D. thesis on geochemistry of the mafic units of the ophiolite near Betts Cove
1977a	Coish	Paper on subaqueous metamorphism in the Betts Cove Ophiolite
1978	Upadhyay	Proposed that some lavas within the ophiolite are komatiitic
1979	Coish and Church	Paper on geochemistry of mafic units of the ophiolite near Betts Cove

Year	Author(s)	Subject
1981	Squires	B. Sc. thesis on Tilt Cove deposit
1982	Upadhyay	Described komatiitic lavas from the Betts Cove ophiolite
1982	Coish <u>et al.</u>	Discussed REE geochemistry of mafic ophiolitic rocks
1982	Hurley	B.Sc. thesis on gold mineralization in Cape St. John Group volcanics at Tilt Cove
1985	Hurley and Crocket	Paper on gold-sphalerite association mineralization at Tilt Cove
1985	Saunders	M.Sc. thesis on mineralization in the Betts Cove Ophiolite
1988	Strong and Saunders	Paper on origin of lavas and sulphide mineralization at Tilt Cove

There are also confidential drill logs on file at the Newfoundland Department of Mines and Energy for the Burtons Pond area drilled by Rio Algom Exploration in 1984 and 1985.

The Nippers Harbour Ophiolite is considered to be a southward extension of the Betts Cove Ophiolite in the Betts Cove Complex, one of the four ophiolites in the Baie Verte Belt (DeGrace et al., 1976; Hibbard, 1983; Saunders, 1985). The Betts Cove Ophiolite occupies an arcuate belt stretching from Tilt Cove in the north to Betts Cove in the south (Figs 1-1 and 1-2). It has been dated isotopically as Early Ordovician (488.6±3.1/-1.8 Ma for the gabbro member of the ophiolite in the Tilt Cove area; Dunning (1984)), and is overlain conformably by the fossiliferous Arenigian Snooks Arm Group, a cover sequence of mafic volcanic, volcanoclastic and epiclastic rocks.



The Nippers Harbour Ophiolite is overlain unconformably by the Cape St. John Group, consisting of subaerial conglomerates, cross-bedded sandstones, mafic pyroclastics and andesitic to rhyolitic tuffs and ignimbrites. The main outcrop area occupies the Cape St. John Peninsula north of Tilt Cove (Fig. 1-1). In the immediate Nippers Harbour area, small outliers lie immediately north of Rogues Harbour. These rocks were assigned previously to the informal Rogues Harbour Group by Schroeter (1971), but later were included in the Cape St. John Group by DeGrace *et al.* (1976).

The Cape St. John Group is correlative with other Silurian volcanic sequences on the Baie Verte peninsula, such as the Springdale Group. The Group is considered to be Silurian in age based on a Rb/Sr whole rock isochron (353+/-15 Ma and 441+/-50 Ma (Pringle, 1978) and 385+/-15 Ma and 520+/-40Ma (Bell and Blenkinsop, 1978)) and indirect stratigraphic evidence.

Several major intrusions cut the rocks of the Baie Verte Belt (Fig. 1-1). Of these, the Cape Brule porphyry intrudes the Nippers Harbour Ophiolite. DeGrace *et al.* (1976) subdivided the porphyry into two field units, one fine-grained porphyry with a felsic matrix and one coarse-grained with a matrix rich in mafic minerals. The porphyry contains many fragments of both ophiolitic and Cape St. John rocks, which range in size from about 1 cm to hundreds of metres across. Hibbard (1983) noted that portions of the porphyries appear to be extrusive, possibly massive welded ash-flow tuff, and suggested that the porphyries may comprise composite bodies with both intrusive and extrusive portions.

Three isotopic dates have been obtained from the Cape Brule porphyry. The oldest date (475 $\pm$ 10 Ma, a U/Pb zircon age) has been interpreted as the original age of the pluton (Mattinson, 1975) while the other two Rb/Sr whole rock ages of 404 $\pm$ 25 Ma and 334 $\pm$ 14 Ma have been interpreted as disturbed ages (Bell and Blenkinsop, 1978; Pringle, 1978). Since the Cape Brule Porphyry shares a gradational contact and similar age with the volcanic rocks of the Cape St. John Group, they appear to be lithologically and geochemically correlative.

The Burlington Granodiorite also cuts the Nippers Harbour Ophiolite (Fig. 1-1). It is medium- to coarse-grained and heterogeneous, consisting mainly of massive hornblende and biotite granite, granodiorite and quartz diorite (DeGrace *et al.*, 1976). Various dating techniques yielded ages which cluster around the dates 460 Ma, 410 Ma and 345 Ma (Hibbard, 1983). The dates are interpreted, from oldest to youngest, as the emplacement age of the pluton, the results of slow cooling of the granodiorite, and an Acadian thermal event respectively. A dyke which is believed to be related to the Burlington Granodiorite, and which cuts the Nippers Harbour Ophiolite, has been dated by U/Pb-zircon methods at 463 $\pm$ 6 Ma (Mattinson, 1975; D.F. Strong pers. comm. to G. Dunning, 1980; Epstein, 1983).

#### 1.4. Local Geology

#### 1.4.1. Nippers Harbour Ophiolite

The Nippers Harbour Ophiolite consists of a crudely layered ultramafic unit and extensive gabbroic and sheeted dyke units. Contacts between the ultramafic and other units are generally fault-bounded while contacts between the latter units tend to be gradational. The following brief descriptions of these lithologies are taken from the work of Baird (1951), Neale (1957), Schroeter (1971), Riccio (1972), Upadhyay (1973), DeGrace et al. (1976), Coish (1977b) and Saunders (1985).

#### 1.4.2. Ultramafic Member

All of the well-preserved ultramafic rocks of the Betts Cove Complex appear to be cumulates, and include dunite, pyroxenite and wehrlite, with subordinate harzburgite and minor lherzolite (Upadhyay, 1973). Rhythmic layering has been noted by Riccio (1972), who described repeated cycles of layered dunite-harzburgite +/- orthopyroxenite, cycles of dunite-orthopyroxenite-websterite +/- harzburgite and an upper portion of sequences of dunite-wehrlite-olivine clinopyroxenite. Upadhyay (1973) noted size-graded layers, reverse gradations, cross laminations, slump, primary pinch and swell structures in the layered ultramafic sequences south of Kitty Pond in the Betts Cove area. In the Nippers Harbour area, layering is developed best in the ultramafics north of Burtons Pond and in the Rogues Harbour area to the southwest (DeGrace et al., 1976).

Ultramafic rocks in the Betts Cove Complex are extensively serpentinized. Talc schists and talc-carbonate are developed at Tilt Cove. Neale (1957), Schroeter (1971), Riccio (1972) and Upadhyay (1973) described steatitization and

carbonatization in the ultramafic rocks, especially those northeast of Betts Big Pond and at Green Head. Schroeter (1971) noted quartz-fuchsite-carbonate alteration of the ultramafic rocks in Northwest Arm.

#### 1.4.3. Gabbro Member

Upadhyay (1973) divided the gabbro member into two zones with a gradational contact. The lower zone comprises pyroxenite and gabbro which grade vertically into an upper zone of leucogabbro and diorite. In the basal zone, Upadhyay (1973) described the pyroxenite and gabbro as being either interlayered, or, as diffuse pods of one into the other. Lens-shaped ultramafic pods ranging from less than a meter to tens of metres are common in the transitional zone between the upper and lower zones, and share a sharp contact with their hosts.

The upper leucogabbro zone consists of quartz gabbro, urilitized gabbro and minor diorite. Schroeter (1971) noted a pegmatitic phase of the gabbro, on the northwest shoreline of the Rogues Harbour peninsula where it occurs as an irregular pod within metagabbro.

#### 1.4.4. Sheeted Dyke Member

The gabbro and ultramafic members are cut by diabase dykes and pass vertically upward into the sheeted dyke unit (DeGrace *et al.*, 1976). The latter unit consists of mainly diabase dykes, but also contains picritic, perknitic and silicic dykes, dyke breccia and screens of granodiorite, gabbro and ultramafics. The dykes dip steeply (vertically or subvertically), and sharp changes in orientation have been noted (Upadhyay, 1973; DeGrace *et al.*, 1976).

Coish (1977b) described the diabasic rocks as follows:

"Diabase dykes are the most common and the latest set of intrusions in the sheeted dyke member. They cut all other types of dykes and often branch and vein older dykes and gabbro in random directions... They range from 15 cm to 0.5 m in width... The diabase dykes comprise nearly equal proportions of cpx/actinolite and albite"

Most diabase dykes show chilled margins, although the contacts locally are obscured by fracturing and shearing (Saunders, 1985). Dyke breccias are developed along and across dyke margins as both veins and irregular patches (Upadhyay, 1973).

In the Betts Cove area, the dykes average 20 to 30 cm in width and weather red, red-brown, grey and green. Actinolite is the major fresh mafic mineral of the green-weathering dykes, while augite predominates in the red-weathering dykes (Saunders, 1985).

#### **1.4.5. Cape St. John Group**

The Cape St. John Group was originally named by Baird (1951), who defined it as "...that sequence of lava flows, with interbedded sedimentary and pyroclastic rocks, that overlies the Spooks Arm Group". DeGrace *et al.* (1976) concluded that the Cape St. John Group comprises a subvertical calc-alkaline volcanic pile about 3500 m thick (based on the interpretation that the Group is deformed into a syncline). The Group overlies the Nippers Harbour Ophiolite unconformably at Rogues Harbour, and in the area north of Northwest Arm.

At Rogues Harbour, gabbro is overlain unconformably in ascending order by red and green coarse-grained sandstone with interbedded siltstone and mudstone, and conglomerate (interpreted as subaerial fluvial deposits). They are overlain by rhyolite flows, ignimbrites, and vesicular to amygdaloidal basaltic flows. Schroeter (1971) assigned the name 'Rogues Harbour Group' to this package of rocks but on the basis of lithological and petrochemical similarity, DeGrace *et al.* (1976) correlated and included these rocks with the Cape St. John Group.

An intrusive breccia unit north of Nippers Harbour, described by DeGrace *et al.* (1976), contains subangular to rounded fragments of ophiolitic mafic rocks and acid volcanic rocks of the Cape St. John group, set in a fine-grained matrix of rock fragments and crystals of quartz and feldspar. The basal conglomerates appear to be the reworked equivalent of this breccia.

## 1.5. Mineral Occurrences

### 1.5.1. Major Deposits

The Betts Cove Complex hosts major sulphide deposits at both Betts Cove and Tilt Cove, as well as a number of other smaller occurrences. The Betts Cove deposit was mined from 1875 to 1883. 130,682 tons of copper ore were produced during this period, as well as 2,450 tons of iron pyrite (Martin, 1983).

Upadhyay and Strong (1973) and Saunders (1985) concluded that the Betts Cove deposit is similar to other modern and ancient ophiolite-type massive sulphide deposits (e.g. Cyprus, East Pacific Rise and Galapagos Ridge deposits). The Betts Cove deposit consists of a massive pyrite-chalcopyrite-sphalerite body

underlain by a stockwork of pyrite-chalcopyrite, and is located at the sheeted dyke-pillow lava interface. A distinctive footwall alteration with a core of quartz-chlorite and a halo of chlorite-albite-quartz has been superimposed on the background greenschist assemblage of actinolite-epidote-chlorite-albite-quartz (Saunders, 1985). Later faulting and shearing resulted in modification of the deposit by the remobilization of the sulphides and their redeposition in chloritic fault zones (Upadhyay and Strong, 1973).

The Tilt Cove mine originally opened in 1864 and operated until 1917, during which time 1,491,136 tons of copper ore, 78,015 tons of regulus (matte) and 5,416 tons of copper ingots were produced. The mine was re-opened in 1954 by First Maritime Mining Corporation Ltd. Production was carried out from 1957 to 1967, over which time 183,597,125 pounds of copper and 42,425 ounces of gold were extracted from approximately 7,400,000 tons of ore (DeGrace et al., 1976).

The deposits at Tilt Cove comprise massive and stockwork sulphide bodies. The main constituents of the ores are pyrite, chalcopyrite and magnetite with minor sphalerite, pyrrhotite and local concentrations of silver and gold (Donaghue et al., 1959). Pyrite is the major sulphide, and is found in massive, stockwork, and disseminated form. It is associated with chalcopyrite, which itself is locally altered to covellite. Magnetite forms patchy masses throughout the ore. Minor nickel mineralization (niccolite, maucherite, chloanthite, gersdorffite, arsenopyrite, millerite and violarite) occurs mainly near the contact of the pillow lava and a subsurface fault sliver of talc-carbonate rock (Snelgrove, 1931; Papezik, 1964).

Both Upadhyay and Strong (1973) and Strong (1980) suggested that the Tilt Cove orebodies are stratigraphically controlled and formed at an oceanic spreading center. Strong (1980) showed that the sulphide deposits are confined to the base of the pillow lava member, and that the massive ore overlies the stockwork ore. The nickel deposits may have originated from the ultramafic member, and been deposited through remobilization along faults and shears (Papezik, 1964; Squires, 1981). All of the orebodies have undergone some degree of tectonism and local remobilization (Squires, 1981).

Hurley (1982), and Hurley and Crocket (1985) have documented an occurrence of pyrite-sphalerite-chalcopyrite-native gold near the base of the Cape St. John Group near Tilt Cove. Gold contents range from 569 ppb to 28,820 ppb, with an anomalous value of 143,430 ppb, and grains are associated spatially with sphalerite and chalcopyrite that occur in spilitized magnesian tholeiites. Hurley and Crocket (1985) considered these tholeiites to be Cape St. John basalts but Strong and Saunders (1988) confirmed chemically that the basalts are actually ophiolitic. Hurley and Crocket (1985) suggested that the sulphides are remobilized sea-floor hydrothermal exhalations deposited originally at a spreading center.



### 1.5.2. Other Metallic Mineral Occurrences

The Betts Cove Complex hosts a multitude of smaller metallic mineral occurrences. Many of these have characteristics that are similar to the Betts Cove deposits, that is, they lie within the sheeted dyke units and have simple sulphide mineralogies (pyrite-chalcopyrite-pyrrhotite). Other types of showings include veins of chalcopyrite-pyrite +/- galena and pyrite-chalcopyrite. The showings in the Nippers Harbour area form the basis of this thesis and are discussed in more detail in later chapters.

Baird (1948) noted that many of the prospects in the Nippers Harbour/Betts Cove area occur along a major fault, designated the Stocking Harbour fault, or along shear zones which are offshoots of it (Fig. 2-1, 2-10). He also found that the Betts Cove deposit occurs at the intersection of two sets of shear zones, one which trends parallel to the main Stocking Harbour fault and another which trends east-west. The implications of faulting on sulphide deposition will be discussed in Chapters two and three.

### 1.6. Ophiolitic Stockwork-type and Gold Deposition

Massive sulphide deposits in ophiolites generally are thought to be formed at ocean-floor spreading centers, which may represent mid-ocean ridges, island arcs, or spreading back-arc basins (Miyashiro, 1973; Lydon, 1984). The deposits typically consist of a massive sulphide lens underlain by a stockwork or stringer zone (Fig. 1.3) (Hutchison and Searle, 1971; Lydon, 1984). This zone is interpreted as the near-surface conduit for the metal-bearing hydrothermal solutions which discharge at varying rates and precipitate sulphides above and

around the discharge vent (Solomon and Walshe, 1979; Constantinou, 1980; Lydon, 1984). The stockwork zone comprises a network of fractures and veinlets, in basalt and possibly extending into sheeted dykes, filled with sulphides (chalcopyrite, pyrite, pyrrhotite +/- sphalerite +/- galena) and silica (quartz or chalcidony) (Constantinou, 1980). Altered peripheral host rocks are impregnated frequently with disseminated pyrite.

Stockworks typically are zoned, reflecting the intensity and type of metamorphism. In certain Abitibi Belt deposits (Millenbach and Corbet), an inner core, characterized by chloritic hydrothermal alteration, results from additions of  $\text{FeO}_t$  and  $\text{MgO}$ , and depletion of  $\text{CaO}$ ,  $\text{Na}_2\text{O}$ ,  $\text{K}_2\text{O}$  and  $\text{SiO}_2$  (Riverin and Hodgson, 1980; Knuckey *et al.*, 1982; Knuckey and Watkins, 1982). The core is surrounded by a sericite-chlorite zone, where the  $\text{K}_2\text{O}$  removed in the chloritic core is enriched. Contacts between the zones are gradational, possibly reflecting a single metasomatic gradient (Lydon, 1984).

At the Mafhiathi deposit in Cyprus, Lydon and Galley (1986) described a similarly zoned subvertical alteration pipe which consists of an inner silicified, chloritized and pyritized zone, representing depletions in  $\text{CaO}$ ,  $\text{Na}_2\text{O}$ ,  $\text{K}_2\text{O}$  and enrichments in  $\text{SiO}_2$ ,  $\text{FeO}_t$  and S. Surrounding it is an intermediate zone which is more enriched in  $\text{MgO}$ , and a peripheral zone characterized by  $\text{K}_2\text{O}$  enrichment in the form of K-spar and illite.

Studies of the alteration zone beneath the present-day Galapagos Ridge sulphide mounds by Jonasson and Franklin (1987) have demonstrated similarities

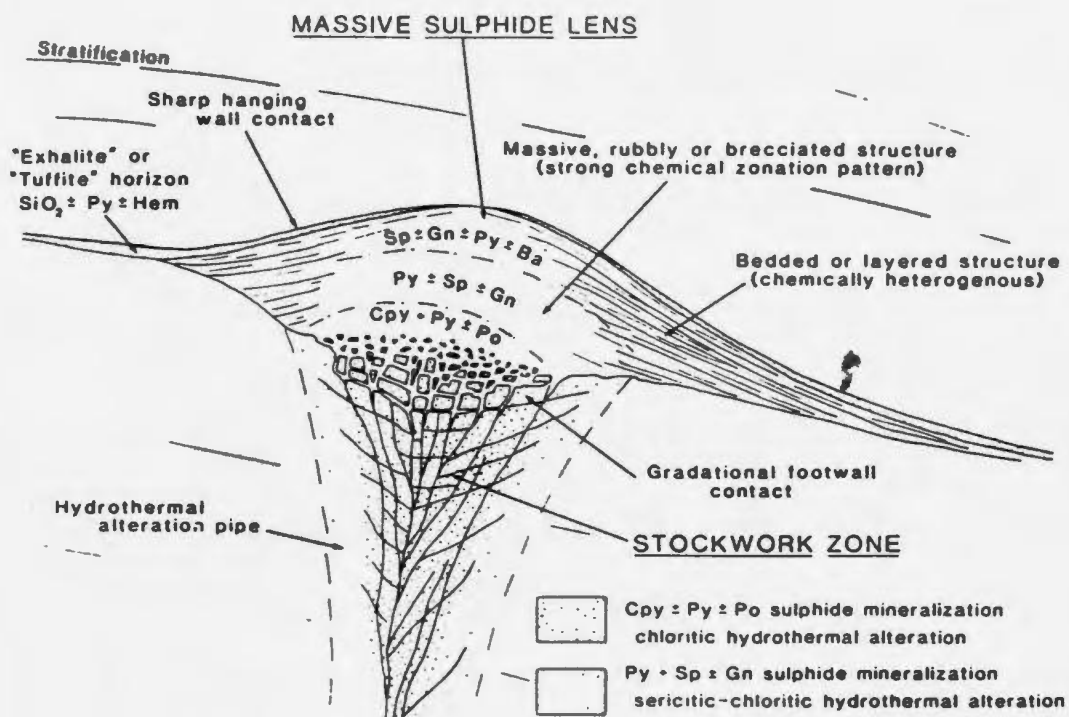


**Figure 1-3:** Essential characteristics of an idealized massive sulphide deposit

(From Lydon (1984))

to ancient stockwork deposits. The upflow zone encloses a stockwork of veinlets filled by silica, clays (Mg-chlorite) and sulphides (chalcopyrite and pyrite). Analyses of altered rocks show them to be strongly depleted in CaO, Na<sub>2</sub>O, K<sub>2</sub>O, MnO and SiO<sub>2</sub> and enriched in S, FeO, Cu and Zn.

Stockwork zones and massive sulphide deposits are believed to be generated by the passage of hot hydrothermal fluids through the ocean crust to the seafloor (Sillitoe, 1972; Spooner and Fyfe, 1973; Upadhyay and Strong, 1973; Andrews and Fyfe, 1976; Fryer and Hutchinson, 1976; Spooner, 1977; Parmentier and Spooner, 1978; Solomon and Walshe, 1979 and Lydon, 1984). The hydrothermal solutions are formed by initially cold, oxygenated, alkaline, Na-Mg-SO<sub>4</sub>-Cl seawater which is drawn down into the crust and heated, possibly by sub-surface magma chambers. The fluids evolve into a reduced, slightly acid, dominantly Na-Ca-Cl brine which is capable of leaching and transporting metals as chloride complexes (Andrews and Fyfe, 1976). A convection cell is set up, through which circulating fluids scavenge metals from the rock. Both the hydrothermal fluid and host rock are altered chemically. The hot solutions rise through fractures to exhale on the sea floor, producing the massive sulphide lens and underlying stockwork zone.

Gold is an important constituent of some Archaean and Paleozoic volcanogenic massive sulphide deposits. High gold concentrations are correlated with zinc-rich horizons at the Corbet mine (Knuckey and Watkins, 1982), and with the copper-rich core at the Millenbach mine (Riverin and Hodgson, 1980). The Ordovician Tilt Cove mine yielded 42,000 ounces of gold during its second phase of mining in the 1960's (DeGrace *et al.*, 1976).

Gold contents of modern massive sulphide deposits are highly variable, but generally low (Scott, 1987). Recently, however, elevated gold values have been found in sulphide samples from the Axial Seamount (45°57'N, 130°02'W) and southern Explorer Ridge (49°45.6'N, 130°16.2'W) by Hannington *et al.* (1986). The former yields gold contents up to 6700 ppb, averaging 4900 ppb, while the latter site gives slightly lower values up to 1500 ppb Au, averaging 660 ppb Au. The authors suggested that gold, preconcentrated in high-temperature (>300°C), Cu-Fe-rich sulphides, is remobilized by late, low-temperature (<250°C) fluids and precipitated in SiO<sub>2</sub>-Ba-Zn-rich sulphosalts near the surface.

#### 1.6.1. Sulphide Deposits in Subsurface Ophiolitic Units

Sulphide deposits have been observed in sheeted dyke, gabbroic and ultramafic units of ophiolites. Isotopic evidence has shown that hydrothermal circulation can extend to the gabbro level, several kilometres below the sea floor (Spooner *et al.*, 1977). A slight change in a physico-chemical parameter of metal-bearing hydrothermal fluids (pH, pressure, etc.) may cause sulphide deposition (Bonatti, 1975).

In the Agrokippia "B" deposit and Drill Hole 504B from Cyprus, zones of metal enrichment have been observed at the dyke-basalt transition zone. Gillis (1987) suggested that these isolated bodies are related to mixing of hot, rising, metal-enriched fluids with cold, circulating seawater. Such sulphide zones have also been documented in many ophiolites (Hutchinson and Searle, 1971; Upadhyay and Strong, 1973).

Panayiotou (1986) has documented sulphide and sulphide-arsenide mineralization in ultrabasic and gabbroic rocks in areas of the Troodos ophiolite, Cyprus. Fe-Cu-Ni-Co sulphide and arsenide lenses, veins and disseminations occur in highly sheared and serpentized ultrabasic rocks in the Limassol Forest and Mount Olympus, and in highly sheared and chloritized gabbros. This mineralization is believed to be related to the serpentization of the ultramafic host rocks by seawater-derived hydrothermal solutions.

Gold values of 1 to 10 ppm have been reported from carbonatized ultramafic rocks (listwaenites) from ophiolite complexes. Buisson and LeBlanc (1985, 1986) and LeBlanc (1986) have related these gold values to pyrite-rich Co-As mineralization, and late quartz veins with pyrite-arsenopyrite in these rocks. Acid gold-bearing solutions, derived from hydrothermal circulation through ultramafic rocks during serpentization, are assumed to precipitate sulphides and gold when they react with carbonatized listwaenites (Fig. 1-4).

### 1.7. Summary

The Ordovician Nippers Harbour Ophiolite hosts many sulphide-gold showings. It is located on the east side of the Baie Verte Peninsula, and is considered to be an extension of the neighbouring Betts Cove Ophiolite. The Nippers Harbour Ophiolite is overlain unconformably by the Silurian Cape St. John Group, a sequence of subaerial conglomerates, sandstones, basic pyroclastics and andesitic to rhyolitic welded tuffs. The Nippers Harbour Ophiolite also is intruded by the Silurian Cape Brule Porphyry, a medium to coarse grained quartz-feldspar pluton.

## Listwaenite Model of Gold Mineralization

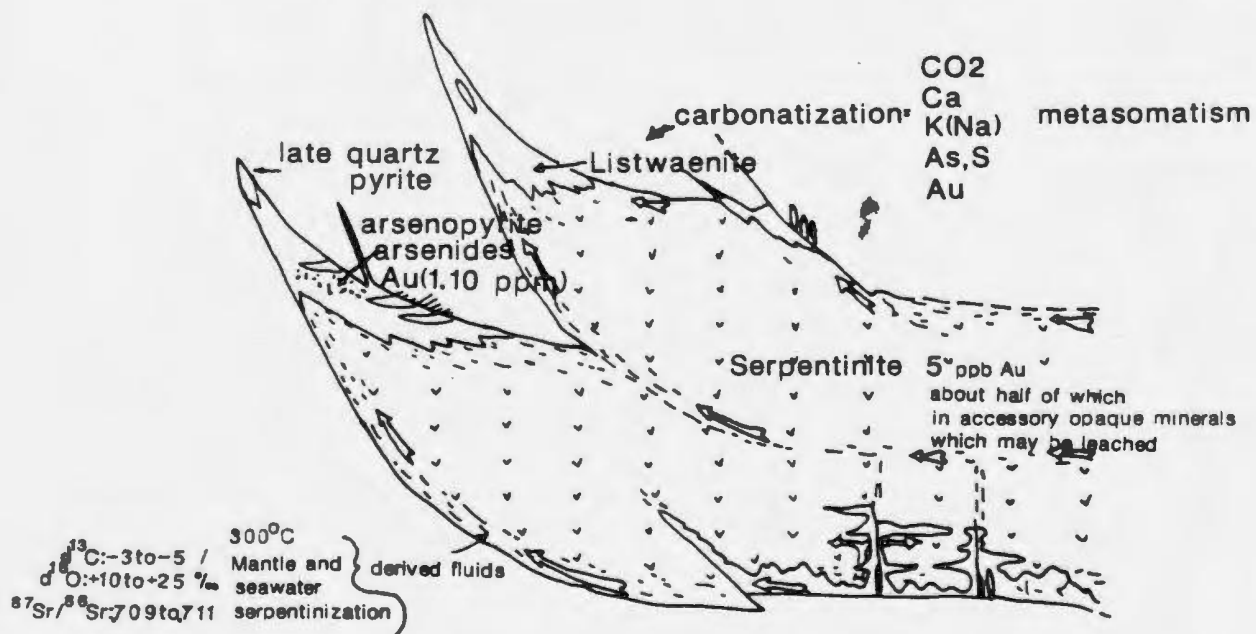


**Figure 1-4:** The listwaenite model of gold mineralization

(From Buisson and LeBlanc (1986))

Mineralized showings in the Nippers Harbour area have characteristics typical of other ophiolite-hosted mineralization. Examples of the latter are: basalt-hosted massive sulphide lenses and their associated underlying stockwork zones (often with significant gold concentrations), fault zones in diabase and gabbro hosting less significant concentrations of sulphide, and gold-sulphide bodies in carbonatized ultramafic rocks (listwaenites). In the Nippers Harbour area, the Silurian Cape Brule Porphyry, which cuts the ophiolite, also may have had an influence on mineralization. This thesis attempts to classify the Nippers Harbour showings genetically according to the above and possibly other geological settings, by discussing and evaluating field, petrographic and geochemical evidence.



## Chapter 2

# General Geology

### 2.1. Introduction

This chapter contains the field and petrographic observations completed for this study, supplemented by descriptions from Schroeter (1971) and DeGrace *et al.* (1976). Ultramafic, gabbro and sheeted dyke units are represented in the field area, as well as the Cape Brule porphyry and volcanic and volcanoclastic rocks of the Cape St. John Group. Mineralization and related alteration are detailed in chapter three.

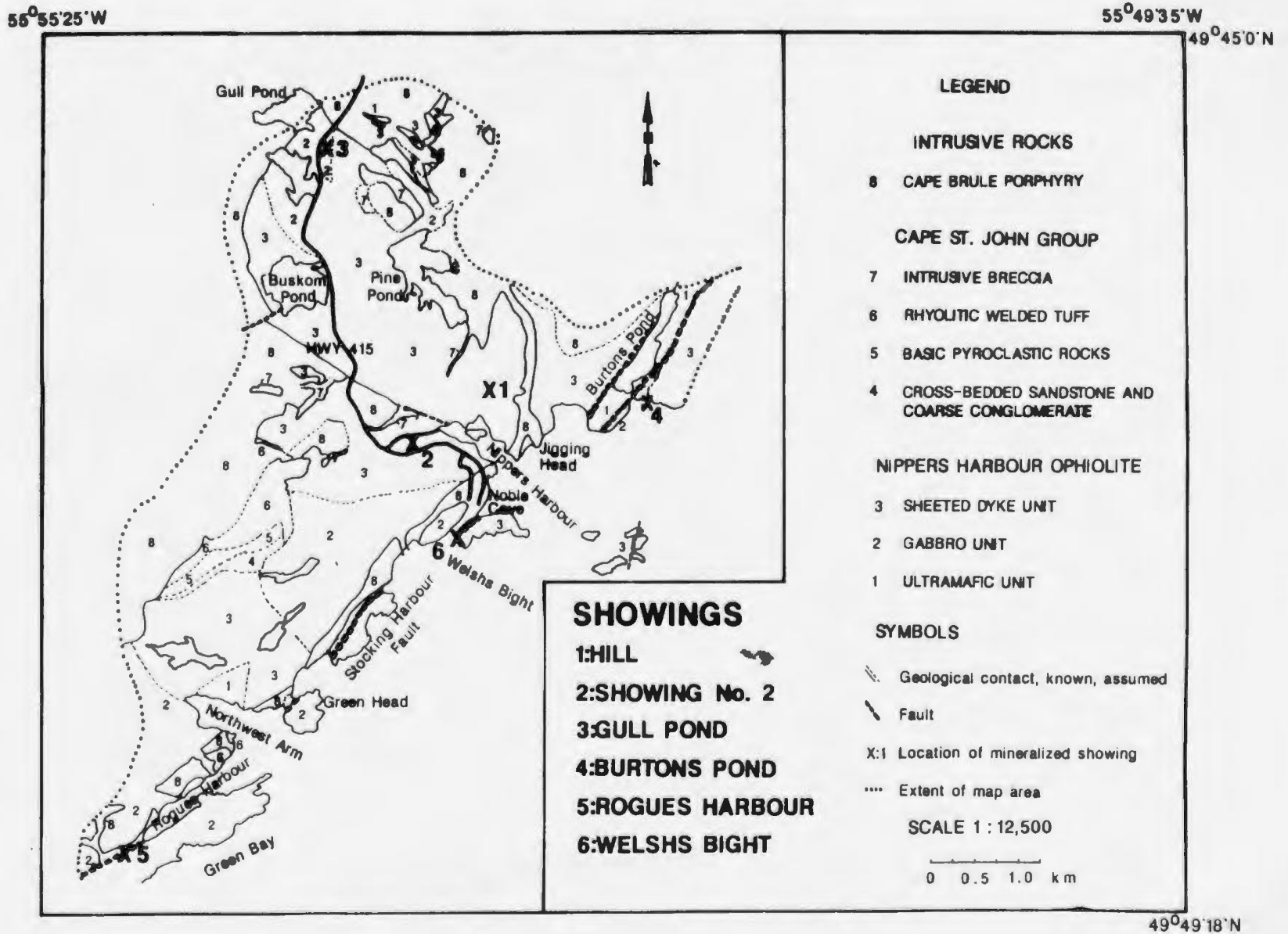
### 2.2. Ultramafic Unit

Ultramafic rocks crop out in belts east of Burtons Pond and north of Northwest Arm (Fig 2-1). In the Burtons Pond area, ultramafic rocks weather rusty brown or dark green on unweathered serpentized surfaces and are mainly altered dunites, consisting of more than 80 percent serpentine with clusters of large, 2 to 3 cm clinopyroxene crystals. These rocks contain no more than 1 percent chromite and often have a streaky, mottled appearance due to alignment of serpentine fibres.

Pyroxenite dykes and bands ranging in width from 1 to 10's of cm cut the

(After DeGrace et al. (1976))

**Figure 2-1:** Geology and mineral occurrences in the Nippers Harbour Ophiolite



Dunites and are discontinuous along their length (Fig. 2-2a). In thin section they contain greater than 90 percent clinopyroxene which has been altered to coarse and fibrous actinolite. A few plagioclase grains were noted in some samples.

A fairly extensive section of layered ultramafic rocks is exposed in a cliff just north of Burtons Pond (Fig. 2-2b). These layers are variable in thickness, ranging from 8 cm up to 1 m, strike roughly north-south and have moderate dips. They consist of alternating layers of pyroxenite and dunite with both sharp and gradational contacts. One contact displays pyroxene crystals oriented perpendicular to the contact. The layers may be an original magmatic feature as no structural elements such as foliations or lineations were noted, or they may represent dunitic bodies intruded by pyroxenite dykes as noted above.

East of Gull Pond, large xenoliths of ultramafic material are found in Cape Brule quartz-feldspar porphyry, and are aligned in a southeast-northwest direction, parallel to many other shears and faults in the ophiolite (Fig. 2-1). A strong lineation, defined in the ultramafics by alignment of magnetite crystals and rodding of pyroxenes, trends parallel to the trend of the xenoliths.

Ultramafic rocks north of Northwest Arm are similar to those at Burtons Pond although there is a higher percentage of pyroxenite present at the former. Locally along the coastline and at Green Head, talc-carbonate-filled shears are developed in ultramafic rocks and gabbros.

A



B



**Figure 2-2:** Photographs of ultramafic rocks

(a) Pyroxenite bands in dunite, Burtons Pond;

(b) Layered ultramafic rocks north of Burtons Pond.

### 2.3. Gabbro Unit

Gabbros crop out throughout the map area, and are found in abundance at Burtons Pond and in the area south of the Nippers Harbour highway. The gabbros generally are medium-grained, consisting of approximately equal parts of 1 mm plagioclase and mafic mineral with minor quartz. Laths of yellowish plagioclase, generally 0.5 to 1 mm long, comprise 40 to 60 percent of the rock, and in thin section, are altered partially to completely to a fine grained mass of sericite, epidote, albite and calcite. These crystals subophitically enclose actinolite, which is largely an alteration product of clinopyroxene. Very few relict grains of pyroxene remain, and where they do, they constitute no more than 5 percent of the rock. Actinolite grains carry accessory sphene and are altered in patches to a fibrous amphibole (uralite).

Variable-textured gabbros are present, particularly at Burtons Pond and Green Head. Here, pegmatitic bands and patches with crystals of sizes up to 1 cm, but generally 4 to 6 mm, stream through homogeneous gabbro (Fig 2-3a,b). At Green Head, homogeneous, fine-grained gabbro blocks floating in a granodioritic matrix themselves contain xenoliths of pegmatitic gabbro. A crude banding has been observed in the area south of Rogues Harbour in which layering is defined by fluctuations in the amount of amphibole and plagioclase.

Ultramafic xenoliths are common in gabbro from the Rogues Harbour area. Their edges are frayed and enhanced by fine chlorite rims, indicating reaction between the xenoliths and gabbro melt.

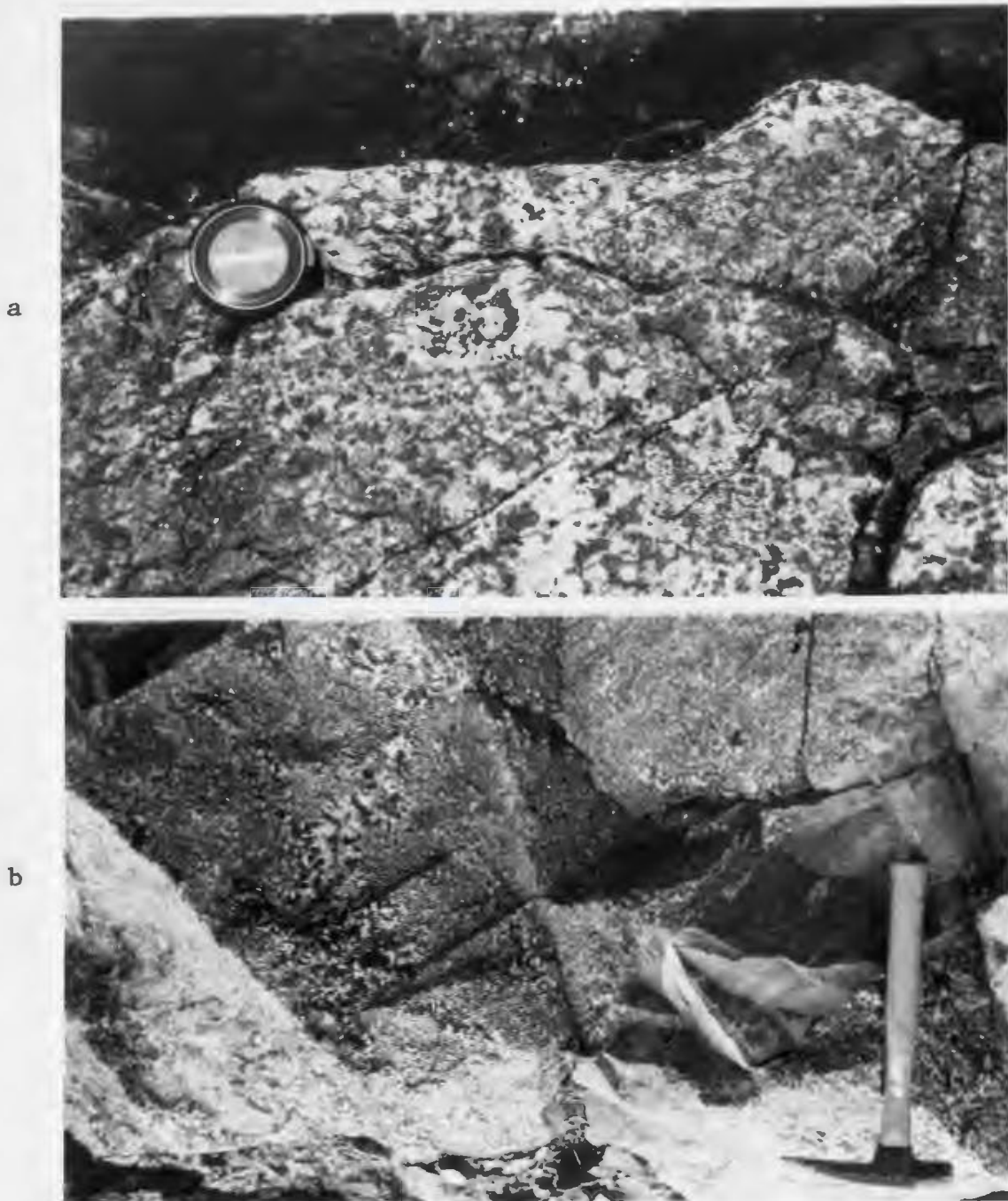


**Figure 2-3:** Photographs of gabbro and pegmatitic gabbro  
(a) Pegmatitic gabbro, Green Head; (b) Pegmatitic gabbroic  
patches in medium-grained gabbro, Burtons Pond. Width of Minolta  
lens cap in these and following photos: 5 cm.

The dyke-gabbro contact is gradational. Massive gabbro bodies commonly are intruded by aphyric, siliceous 5 to 25 cm wide dykes which display narrow chilled margins. The dykes become more numerous towards the margins of gabbro pods until they become sheeted. Although there is abundant evidence of dykes intruding gabbros, the reverse relationship was not observed except at one locality where rounded diabase xenoliths in gabbro display plagioclase rims. Riccio (1975), and Saunders (1985) also cited evidence that the gabbro pods intruded the sheeted dyke and pillow lava units and were subsequently cut by dykes.

#### 2.4. Diabase Dyke Unit

Diabase dykes constitute the major part of the Nippers Harbour ophiolite. They generally dip steeply but have variable strikes, which are discussed in Section 2.7. They are sheeted in most areas (Fig. 2-4a,b), forming swarms of multiple and composite dykes, except where they grade into massive gabbro. In the latter case, they contain many screens and pods of gabbro, especially at Burtons Pond and south of Nippers Harbour.

The sheeted dykes vary in width from a few centimetres up to 1 to 2 metres. They are chilled normally on one side with 1 to 5 cm margins (Fig. 2-5a), although dyke contacts often are obscured by shearing and related brecciation. 1 mm bands of quartz frequently are developed near and parallel to dyke edges and may be related to cooling (Fig. 2-5b). Late joints commonly cause minor offset of dykes.

The dykes are altered wholly or partly to a greenschist facies assemblage



a



b

**Figure 2-4:** Photographs of sheeted dyke outcrops,  
Northwest Arm

(a) North of Northwest Arm- hammer points upwards.

(b) Northwest Arm - same orientation as (a).



a



b



**Figure 2-5:** Photographs of dyke contacts in outcrop

(a) Diabase/pyroxenite chilled dyke contact, Northwest Arm;

(b) Diabase cooling-related quartz veins, Hill Showing.

(albite + chlorite + quartz + actinolite + epidote + magnetite + sphene) and are termed 'diabase' in the Betts Cove Complex (Coish, 1977b). Several types of dyke which tend to intrude each other so that no genetic sequence could be identified, are present. The first type of dyke is an aphyric to very finely crystalline, pale green weathering siliceous diabase with microlites of plagioclase on fresh surfaces. These commonly intrude massive gabbros, and may be the earliest dykes.

The most common dykes are the red and grey-green weathering types. As suggested by Saunders (1985) for dykes at Betts Cove, the red colour is due to the weathering of augite while the green colour can be ascribed to actinolite. In thin section, these diabases are holocrystalline and medium- to fine-grained except where they are highly propylitized. Three textures are dominant and can be gradational even on the scale of a thin section:

(a) An intergranular/subophitic texture in which blocky pyroxene crystals, often altered partially to totally to uralitic actinolite, are located interstitial to, and are enclosed by plagioclase laths (Fig. 2-6). The latter normally are altered to fine grained sericite, calcite and epidote.

(b) Euhedral, 0.3 to 0.5 mm laths of pyroxene set in a matrix of quartz, albite and penninitic chlorite. Pyroxene crystals are clouded by a reddish brown alteration product with a felted appearance and also are more rarely altered to calcite. Quartz is anhedral, forming a drusy mosaic of sutured crystals. It constitutes normally about 5 percent of the diabase, but can reach up to 15 percent, when a knobby weathering texture is developed.

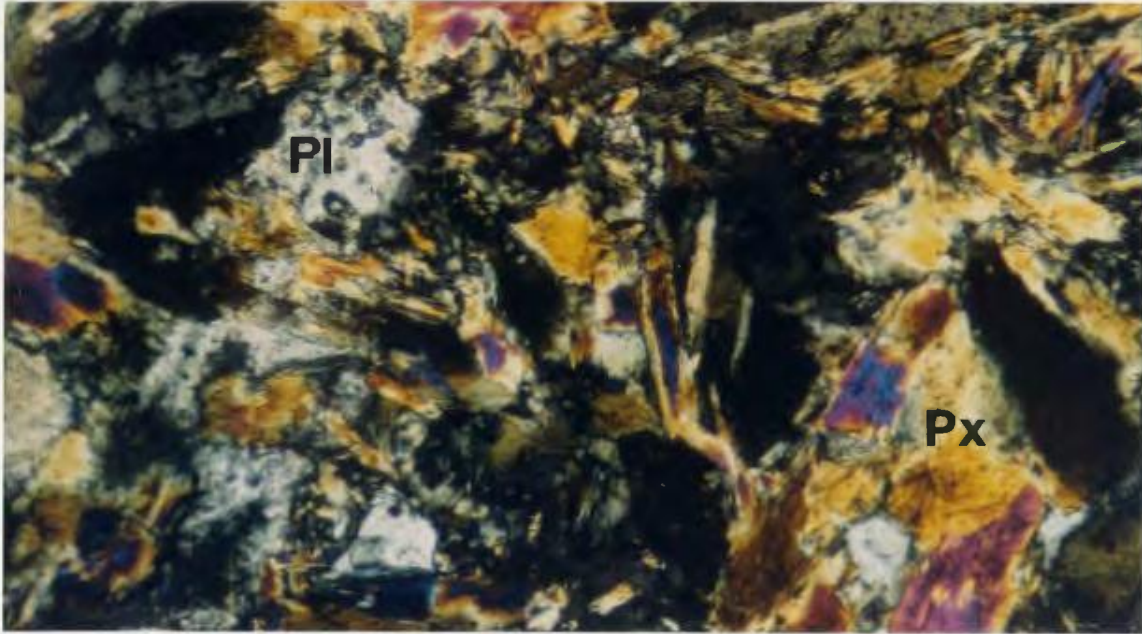


**Figure 2-6:** Photomicrograph of diabase texture Sample 21, XP, Subophitic diabase, note uralitized pyroxene laths (Px) enclosed by plagioclase (Pl). Photo width 3.3 mm.

Abbreviations for this and following figures: PL-plane light, XP-cross polars, RL-reflected light.

(c) A rare ophitic texture in which fine ( $<0.4$  mm) plagioclase laths are enclosed by chloritized and uralitized pyroxene.

Areas of brecciation are common, especially near Buskom Pond (Fig. 2-1). Anastamosing networks of quartz and quartz-carbonate veinlets characterize these breccias whose fractures also contain minor epidote, pyrite and chalcopyrite. Bleached diabase breccia is developed, especially along dyke contacts locally at Nippers Harbour. Fragments ranging in size from 1 mm to several cm commonly are cemented by yellow-green epidote (Fig. 2-7a).

Within the diabase are zones in which the dykes are wholly or partly replaced by epidote, quartz and sphene bands. The banding is subparallel to the dyke margins, and may break up into pods or cylindrical pipes. When well developed, as at Burtons Pond (Fig. 2-7b) and near the Hill showing, the rocks acquire a striped appearance. Several authors have described such zones in the Troodos ophiolite, Cyprus. Smewing (1975) suggested that epidiosites represent the residues after leaching of metals from the dykes, while Varga and Moores (1985) described epidiosites associated with major faults in the sheeted dyke complex which they believed were hydrothermal feeders to the massive sulphide deposits in Cyprus. Richardson *et al.* (1987) noted that the epidiosite zones are located at the base of the sheeted dyke unit. Based on this and other observations, they suggested that major epidiosite zones were areas of intensive, high temperature water-rock interaction resulting in the hydrothermal fluids that ultimately formed massive sulphides.

Diabase dykes have been noted to intrude pyroxenites, particularly on the east side of Burtons Pond. The contacts again normally are sheared and occasionally have pyroxene crystals growing across the interface, possibly representing a zone of minor melting and recrystallization. The pyroxenites therefore may represent high level, 'diapiric' ultramafic bodies, fault blocks, or other tectonically or magmatically emplaced bodies.

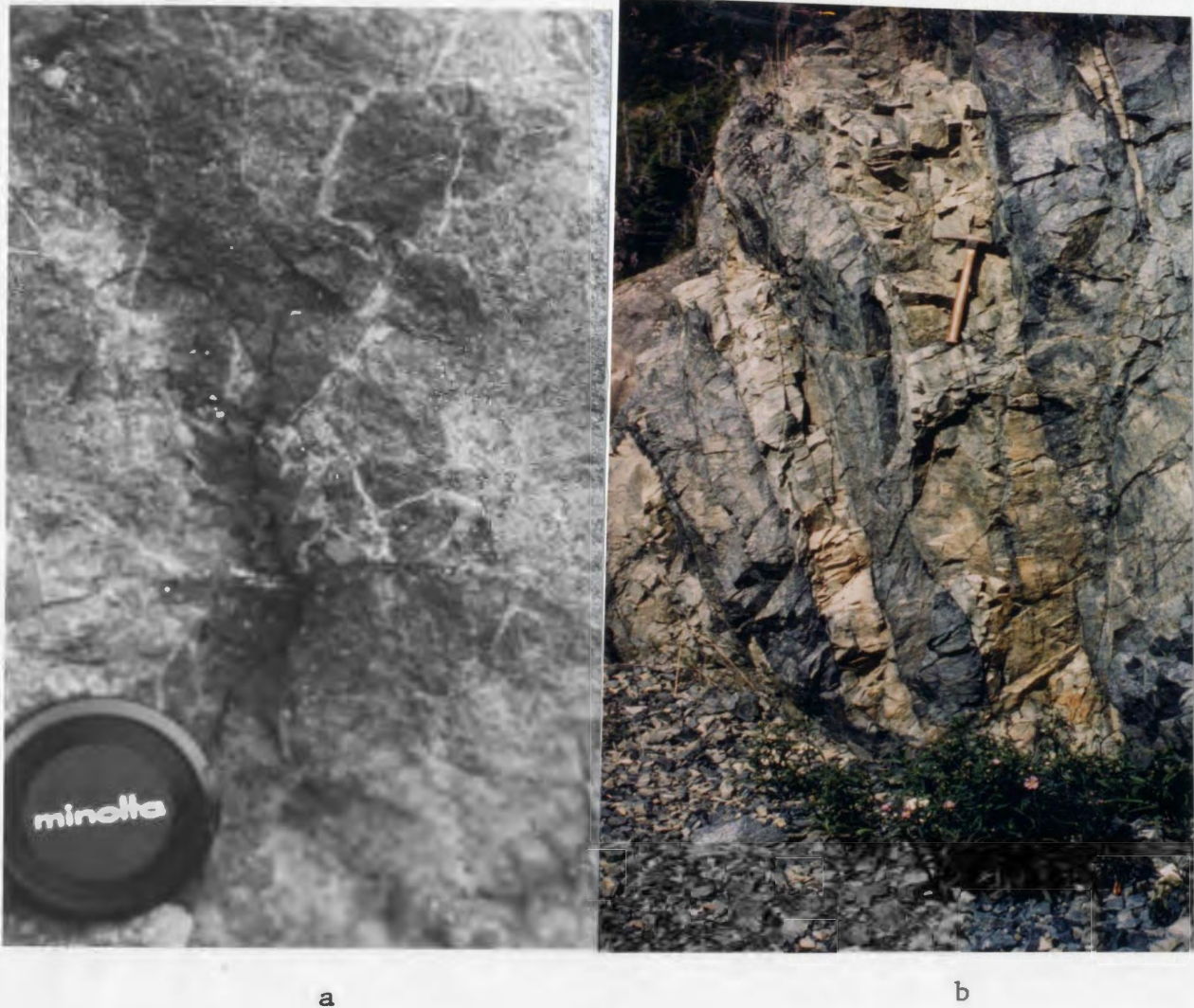


**Figure 2-7:** Photographs of dyke breccia and epidotized dyke outcrops

(a) Dyke breccia, Nippers Harbour

(b) Striped epidote-quartz zones in diabase, Burtons Pond;

## 2.5. Cape St. John Group

The general geology of the Cape St. John Group is described in Section 1.4.5. This unit was not mapped in detail for this study but a few noteworthy observations are made below.

Rhyolite and rhyolitic tuff (unit 6, Fig. 2-1) crop out sporadically throughout the map area, especially east of Gull Pond, north of Northwest Arm, and at Rogues Harbour. In the first area, rhyolite pods are aligned in roughly the same orientation as diabase and ultramafic xenoliths in a large shear zone in Cape Brule Porphyry.

The rhyolite weathers purple and crops out in spectacular purple hills which are easily identifiable. It consists of phenocrysts of plagioclase, quartz and rare K-feldspar in a matrix of plagioclase microlites, opaque minerals and alteration products of glass (chlorite, epidote and calcite). Plagioclase phenocrysts often are squarish, 2 to 3 mm in diameter, and are altered to epidote, sericite and calcite. Phenocrysts of quartz are smaller (1 mm) and rounded, while pink K-feldspar crystals attain dimensions of up to 4 to 5 mm.

Rhyolitic tuff crops out north of Northwest Arm. Flow-banding here is defined by pink, recessive-weathering bands (Fig. 2-8a) and alignment of plagioclase laths. The banding dips moderately to the northwest.

Basic flows and pyroclastics (unit 5) crop out north of, and sporadically in, Northwest Arm. Outcrop in the former area is poor but the rocks seem to be

mainly basic flows. These weather maroon to purple and have dark green, fine grained and equigranular fresh surfaces.

Conglomerates and crossbedded sandstones (unit 4) occur just south of the basic flows. The conglomerates contain boulders up to a metre wide with pebbles and cobbles whose long axes lie in the bedding plane. The framework consists of rhyolite, quartz-feldspar porphyry and tuff, and brown ultramafic fragments.

Intrusive breccia (unit 7) described by DeGrace *et al.* (1976) crops out irregularly throughout the map area. It consists of blocks of rhyolite, quartz-feldspar porphyry, and chloritized diabase and gabbro, up to several metres in dimension, set in a matrix of crystals of quartz and feldspar (Fig. 2-8b). A spectacular breccia is developed at Green Head, where blocks of pegmatitic gabbro are cemented by a granodioritic matrix. This host rock may be a phase related to the Burlington Granodiorite rather than the Cape Brule Porphyry.

## **2.6. Cape Brule Porphyry**

The Cape Brule quartz-feldspar porphyry (QFP) crops out throughout the entire map area. It clearly intrudes the Nippers Harbour ophiolite and commonly contains xenoliths of ophiolitic material. In some areas, especially on the highway near Gull Pond (Fig. 2-1), fragments of chloritized mafic material are roughly bedded, suggesting that they may be extrusive, tuffaceous features first suggested by Hibbard (1983).

The QFP is largely homogeneous over the entire area. It weathers a buff white to pink colour and crops out resistantly as hills and mounds. It consists of



**Figure 2-8:** Photographs of rhyolite and intrusive breccia outcrops, Cape St. John Group

(a) Flow banded rhyolite, north of Northwest Arm;

(b) Intrusive breccia, south of Pine Pond, note large rhyolite and smaller diabase fragments, as shown by J. Dicks.



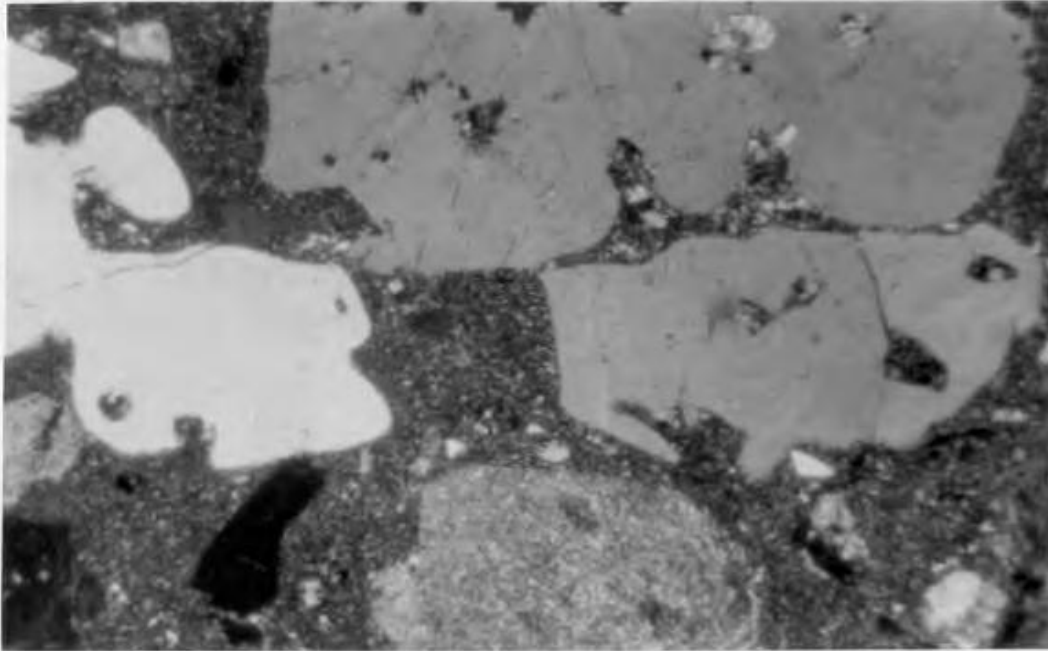


**Figure 2-9:** Photomicrographs of quartz-feldspar porphyry

Sample 227, XP, Fine-grained porphyry, note embayed quartz phenocrysts in fine-grained quartz-feldspar groundmass. Photo width 3.3 mm.

15 to 30 percent quartz, plagioclase and orthoclase phenocrysts in a fine-grained groundmass (Fig. 2-9). Quartz is the most abundant phenocryst, constituting about 20 percent of the rock volume, and generally is 1.5 to 1.75 mm in diameter. Most quartz crystals are wholly to partly embayed and broken. Very fine grained, radiating fibres of sericite were observed around the edges of some embayed crystals. These embayments sometimes contain inclusions of highly altered mafic material.

Feldspar phenocrysts range in size from 2 to 3 mm in maximum dimension. They comprise 10 to 15 percent of the rock volume and are represented by both orthoclase and lesser plagioclase. Orthoclase is altered variably to a rusty brown

product, and displays occasional perthitic texture and intergrowths with plagioclase. Plagioclase crystals have variable compositions. They also are altered, but to a mixture of sericite and epidote, and have generally subhedral to euhedral outlines.

A coarser phase of the porphyry crops out along the coast parallel to the Stocking Harbour Fault (Fig. 2-1). It weathers a deep salmon pink colour and contains a greater percentage of orthoclase phenocrysts. The groundmass is defined by finely intergrown, <1 mm, orthoclase and altered plagioclase crystals as well as comminuted chloritized mafic pieces. This may be a separate phase of the intrusion related to the Stocking Harbour Fault, but contacts with the fine-grained porphyry were not observed.

## 2.7. Structure

Structurally the Nippers Harbour area is dominated by faults and shear zones. Attitudes of diabase dykes define three structural blocks within the ophiolite, which are illustrated in Fig 2-10. The smallest block (A) lies to the east of Burtons Pond and is actually the southernmost extension of the Betts Cove ophiolite. Block (B), containing the Gull Pond showing, hosts dykes which form a northeast-facing arc, while dykes of the southern block (C) define a broad southeasterly-facing box fold. These latter two structural units are separated by a fault which originates in Nippers Harbour. Schroeter (1971) suggested that the rocks north of Nippers Harbour (Block B, Fig 2-10) have been rotated and/or tilted as a result of faulting and/or the intrusion of the Cape Brule porphyry.

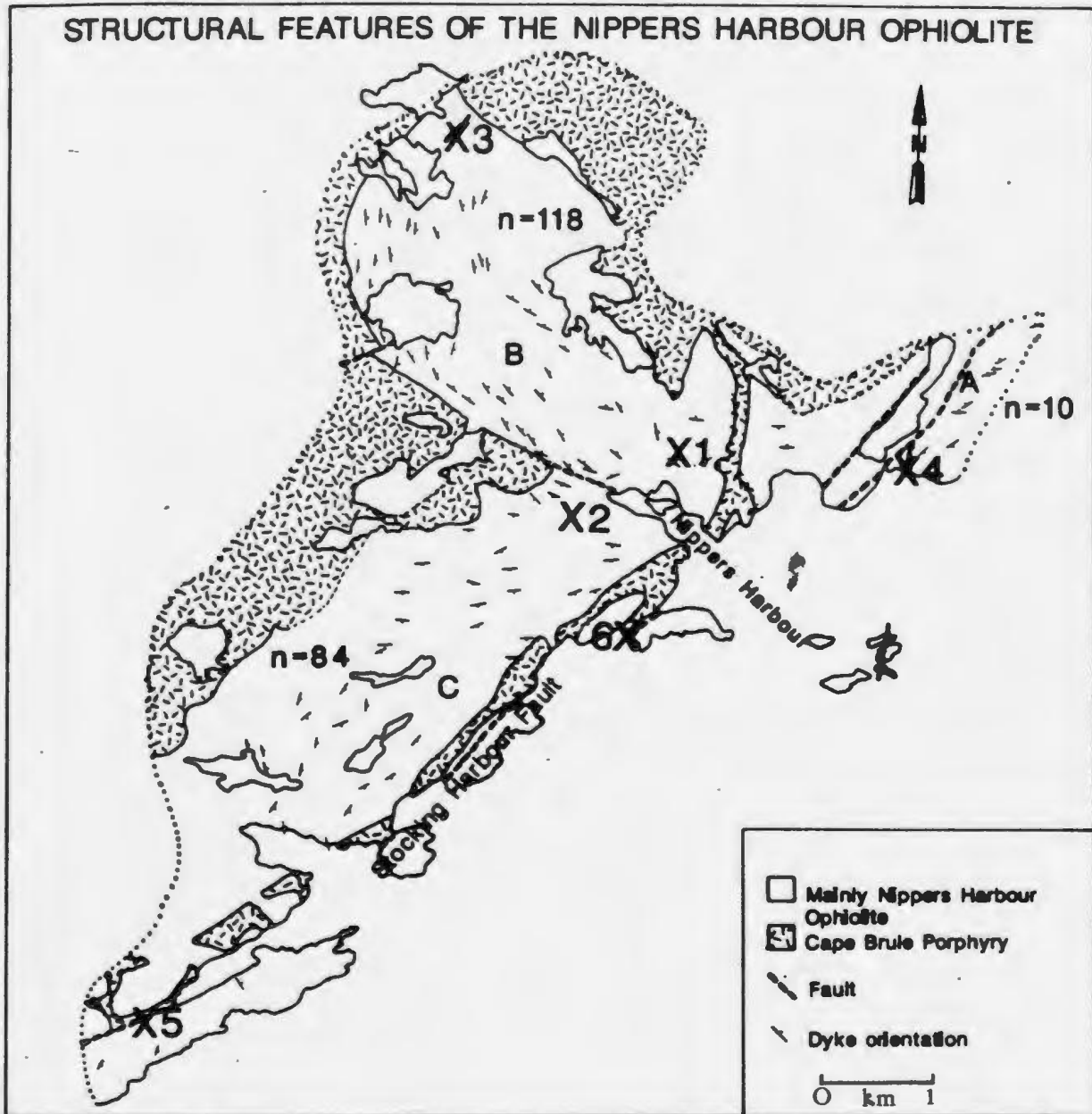


**Figure 2-10: Structural features of the Nippers Harbour Ophiolite**

Mineralized showings are numbered as in Figure 2-1.

'n' refers to the number of observations of dyke orientations for each structural block (A, B, and C).

The most prominent fault in the area is the Stocking Harbour Fault (Fig 2-10). It was traced by Baird (1951) over a total length of over 32 km, as far north as Betts Cove. Neale (1957) disagreed with Baird and demonstrated that the fault intersects and coincides with faults bounding the Betts Cove ophiolite at Jigging Head. Nevertheless, the Stocking Harbour Fault is marked by a prominent topographic depression and at Welshs Bight, is exposed as a 10 m wide vertical shear zone. Two of the main mineralized showings, the Rogues Harbour and the Welshs Bight, occur directly on the fault. The Burtons Pond showing occurs in a fault zone which is an offset of the Stocking Harbour fault. The significance of this is discussed in chapters three and six.

The sense of displacement and timing of movement on the fault are not discernable directly. However, a right-lateral displacement of over 30 m, first noted by Schroeter (1971), is recorded on a fault west of Buskom Pond (Fig. 2-1 and 2-10). Displacement appears to have involved uplift to the south with respect to rocks of the north, as the older Burlington Granodiorite is juxtaposed against younger Cape St. John Group rocks just to the north of Middle Arm in Green Bay.

On the Baie Verte Peninsula, all pre-Carboniferous strata and structures, including the Baie Verte Line, wrap around a major structure named the Baie Verte Flexure (Hibbard, 1982). This is expressed as a change in structural trends from a north-northeasterly to an easterly orientation. Hibbard (1982) suggested that the flexure was an early feature that pre-dated deformation of the Baie Verte rocks, and that younger structures followed its form. The Stocking Harbour and

other north-northeasterly trending faults in the Nippers Harbour area may be related to this primordial feature, and may even have been re-activated since their formation. The close association of the Cape Brule Porphyry and the faults in the ophiolite suggest that the faults acted as magma conduits or that they formed coevally with the Late Silurian to Early Devonian porphyry.



**Figure 2-11:** Photograph of chloritic shear zone in diabase outcrop, Northwest Arm

Other faults and shear zones are delineated by narrow valleys or topographic depressions. Their dips are not always easy to measure, but where present, are generally steep ( $80^{\circ}$  to  $90^{\circ}$ ). Most are marked by chloritic shear zones (Fig. 2-11) which often carry milky quartz veins containing less than 1 percent sulphide (pyrite or chalcopyrite).

## 2.8. Summary

Ultramafic, gabbro and sheeted diabase dyke units of the Nippers Harbour ophiolite are represented in the map area. Ultramafic rocks mainly are serpentized dunites with veins of pyroxenite. Gabbros generally are medium-grained to pegmatitic, and are unlayered. Dykes form the largest part of the ophiolite and for the most part, are sheeted, displaying narrow chilled and sometimes brecciated margins. Contacts between these ophiolitic units are both gradational and faulted.

The Cape Brule quartz-feldspar porphyry forms a substantial portion of the map area. For the most part, it contains quartz and feldspar phenocrysts in a fine-grained, quartz-plagioclase dominant matrix. A distinct phase whose matrix is dominated by K-feldspar crops out along the Stocking Harbour fault along the coast. Scattered outcrops of Cape St. John Group conglomerate, basaltic dyke, rhyolite and intrusive breccia occur throughout the area.

Structurally the map area is dominated by shear zones and faults; in particular, the Stocking Harbour Fault. Much of the mineralization occurs along, and may be controlled by this fault. The major faults in the area may be early pre-obduction features which have been re-activated upon intrusion of the Cape Brule Porphyry.

## Chapter 3

# Mineralization Features

### 3.1. Introduction

The six sulphide showings mapped and sampled for this study are located in Figure 2-1. The Burtons Pond showing (No. 4) is the most extensive of the six, and consequently the most detailed sampling was concentrated there. Showing No. 1 has been named the 'Hill' showing due to its location on a prominent hill overlooking Nippers Harbour. Mineralization at Showing No. 2, Gull Pond (No. 3) and Rogués Harbour (No. 5) is less extensive but the degree of exposure permitted comprehensive examination and sampling. The shaft at Welshs Bight (No. 6) was surrounded by a few scattered sulphidic samples, but as it was several metres away from any related outcrop, no samples of country rock were taken.

Regional mapping of the ophiolite was carried out in order to detect any new areas of mineralization. Although no new major showings were discovered, a great many chloritic shear zones hosting sulphide- (mainly chalcopyrite and pyrite) bearing milky quartz veins were documented. Several of these veins were sampled and are discussed in this chapter. In addition, sheared mafic rocks in places contain significant disseminated pyrite.

Sulphide mineralization occurs ubiquitously in faults, fault zones, or smaller shear zones. It is hosted by altered diabase or gabbros.

### 3.2. History of Exploration

The Nippers Harbour area has been actively explored at various times since the late nineteenth century. The Burtons Pond showing was discovered in the 1860's and mined from 1876 to 1892, during which 1500 tons' of copper ore were extracted (Martin, 1983). An inclined shaft and surface workings are present at the showing. The Gull Pond (originally called Muirs Pond) prospect also was actively explored at this time. Later, Advocate Mines (1967) reported grades of 0.90% Cu, 0.28 oz/ton Au and 1.26 oz/ton Ag on a 2-foot channel sample here.

At Rogues Harbour (No. 5), two shafts and two adits are present, with grades of up to 2.64% Cu (Douglas *et al.*, 1940; Baird, 1951). Shafts also are present at Showing No. 1 ('Hill') and at Welshs Bight (No. 6) (Baird, 1951). An assay of 2.75% Cu, 1.05 oz/ton Au and 1.30 oz/ton Ag was reported by Riccio (1975) for ore from Showing No. 2. Advocate Mines (1967) explored other showings near Jigging Head and Noble Cove (Fig. 2-1), but no remaining trace of mineralization was found during the present study. At this time, the entire area is under investigation for gold.

### 3.3. Geology and Mineralogy of Mineralized Showings



### 3.3.1. Showing No. 1 - Hill

Mineralization at the Hill showing consists of two major concentrations of sulphide in parallel, northwest-striking shear zones (Fig. 3-1). Unit one crops out along the southernmost major shear, but much of the surface outcrop has been removed by previous excavation. The unit consists of a chloritic breccia, cemented by quartz, pyrite, chalcopyrite and minor calcite (Fig. 3-2a). Breccia fragments generally are small (<5 cm diameter) and very angular, and are comprised of rounded quartz spherules in a matrix of dark green chlorite. They display a dominant fabric which is likely related to shearing. Sulphides (mainly pyrite) are concentrated around fragment edges, and are associated with and rimmed by minor epidote.

Unit two is composed of intensely sheared and chloritized rock with disseminated pyrite and chalcopyrite. (Fig. 3-2b). It crops out mainly along the more northern major shear, but smaller plugs occur sporadically throughout the area. Pyrite in units one and two occurs as idiomorphic cubes which are often embayed and corroded, and contain inclusions as well as overgrowths of chalcopyrite. Rare inclusions of arsenopyrite have been observed using a scanning electron microprobe (SEM).

Unit three comprises a dark green weathering, chloritized rock which often contains abundant quartz spherules and stockwork-like patches of quartz (Fig 3-3). These quartz veinlets frequently are epidote-lined and host minor disseminated pyrite. Dyke contacts are preserved, and are enhanced by shearing, producing chloritic and pyritic shear zones.

Figure 3-1: Geology of the Hill Showing

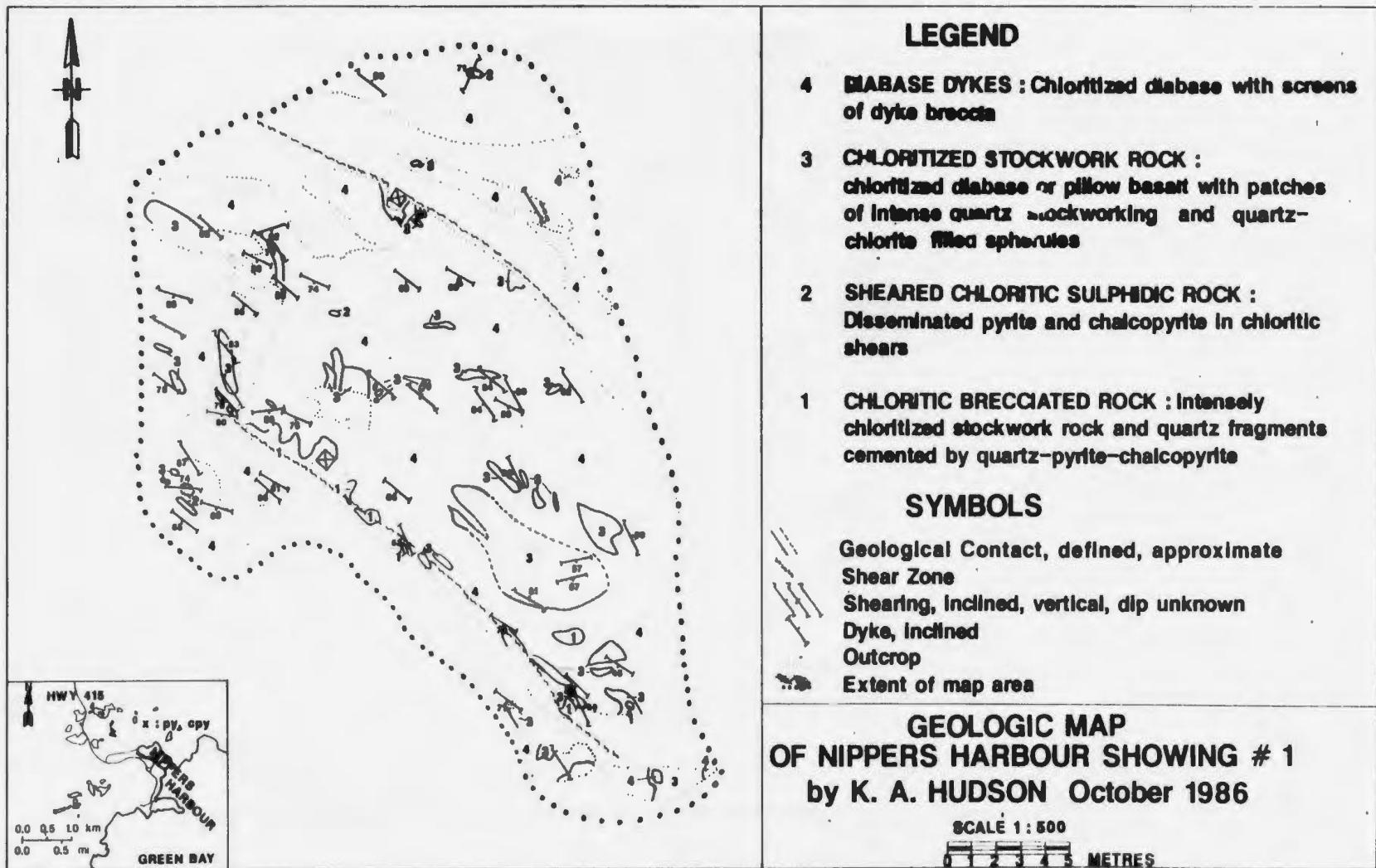




**Figure 3-2:** Photographs of mineralized units one and two, Hill Showing

(a) Unit one green chloritic breccia, cemented by quartz, pyrite, and chalcopyrite; (b) Unit two sheared chlorite-quartz-sulphide rock.



**Figure 3-3:** Photographs of unit three rocks,  
Hill Showing

(a) Quartz spherules in chlorite+/-albite rock (b) Stockwork  
quartz in unit three rock, intruded by fresh unit four diabase.

Quartz spherules are very common throughout map units one to three, giving the rocks a spotty, mottled appearance. In thin section, the quartz grains are equant and rounded (Fig. 3-4). Saunders (1985) has documented a similar texture for quartz-chlorite rocks in the altered core zone to the Betts Cove massive sulphide lens. The Hill spherules originally were thought to be vesicles, but their distribution is too homogeneous and their shapes are too angular to be identified as such with any confidence. Vesicles should be concentrated in areas such as pillow rims or dyke contacts; no such features were noted here. It appears that, in fact, the quartz spherules are alteration features (Fig. 3-4).

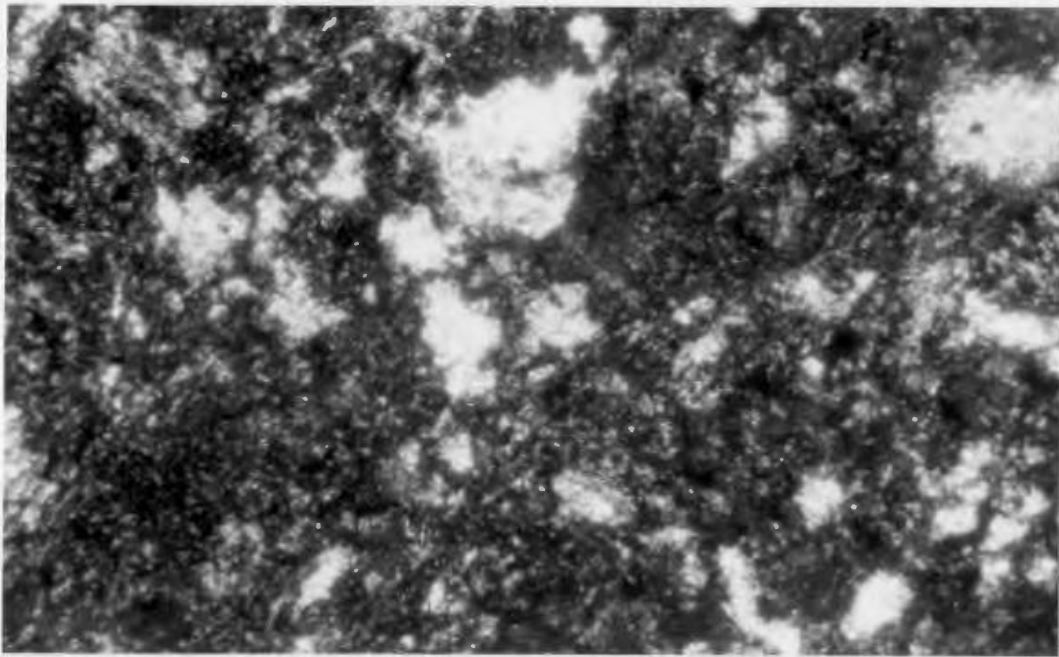


**Figure 3-4:** Photomicrograph of quartz-chlorite alteration, Hill showing

Sample 198, XP, note rounded quartz grains (spherules) (white) in chlorite+/-albite (dark) matrix. Photo width 3.3 mm.

Units one to three are intruded by a fine-grained, relatively unaltered, light

green weathering diabase dykes (unit four), which strike parallel to both major and minor shears of the area, implying that their distribution is controlled by these structures (Fig. 3-1). Furthermore, unit three xenoliths are aligned parallel to shearing and probably are controlled by it. Where unit four dykes have intruded unit two material, shearing in the latter has been folded (Fig. 3-2b). Thin quartz veinlets are developed in a circular manner in unit four rocks around xenoliths of altered rock.

The mineralogy of each unit is distinct. Units one and two have simple mineralogies, consisting only of sulphides, quartz and chlorite with minor epidote and calcite. Less altered unit three lithologies contain the above assemblages as well as albite, while unit four rocks are characterized by actinolite and feldspar, with minor chlorite and epidote. The implications of these assemblages are discussed in the forthcoming geochemistry chapter (number four).

### **3.3.2. Burtons Pond**

The Burtons Pond showing (No. 4) is located in the most eastern part of the map area (Fig 2-1). It is situated in fact in the western edge of the Betts Cove rather than the Nippers Harbour ophiolite.

The geology of the Burtons Pond showing is presented in Figure 3-5. Mineralization occurs in altered diabases and coarse-grained gabbros which are faulted to the north against serpentized dunites. Chalcopyrite, pyrrhotite and pyrite were focussed along a fault zone which has a surface width of up to 5 m, extends for at least 100 m in a northerly direction, and is terminated to the south

by the ocean. Sulphides occur as (1) sulphide-only veinlets filling shearing-related fractures in altered host rock, (2) patchy intergrowths with quartz, calcite and minor albite, in secondary but also shear-related veins, and (3) Disseminated grains in intensely silicified and chloritized areas.

Rio Algom Inc. drilled six holes on the Burtons Pond property in 1984. Their drill locations are depicted in Fig. 3-5 and in Fig. 3-6. The core was examined in detail, focussing attention on holes two and four which intersected representative Burtons Pond sulphide zones. These drill holes were sampled at regular intervals for petrographic, geochemical and precious metal work.

A schematic illustration of the main sulphidized and altered zones, as outlined by drilling, is portrayed in Fig. 3-6. The zone appears to wane at depths of 70 m, although hole five terminated in a fairly intensely altered and sulphidized zone.

#### **3.3.2.1. Host Rock Alteration**

Host rock alteration is not completely pervasive, but is concentrated in areas of intense shearing and faulting. Elsewhere alteration is confined to areas around veins associated with shearing. Three types of mineral associations can be recognized in the alteration of the host diabases and gabbros: (A) chlorite-quartz+/-albite alteration, (B) chlorite-sericite alteration and (C) carbonate (calcite)-sericite alteration.

The chlorite-quartz+/-albite alteration (A) is characterized by the diagnostic minerals chlorite and quartz and in most cases, albite, as well as minor

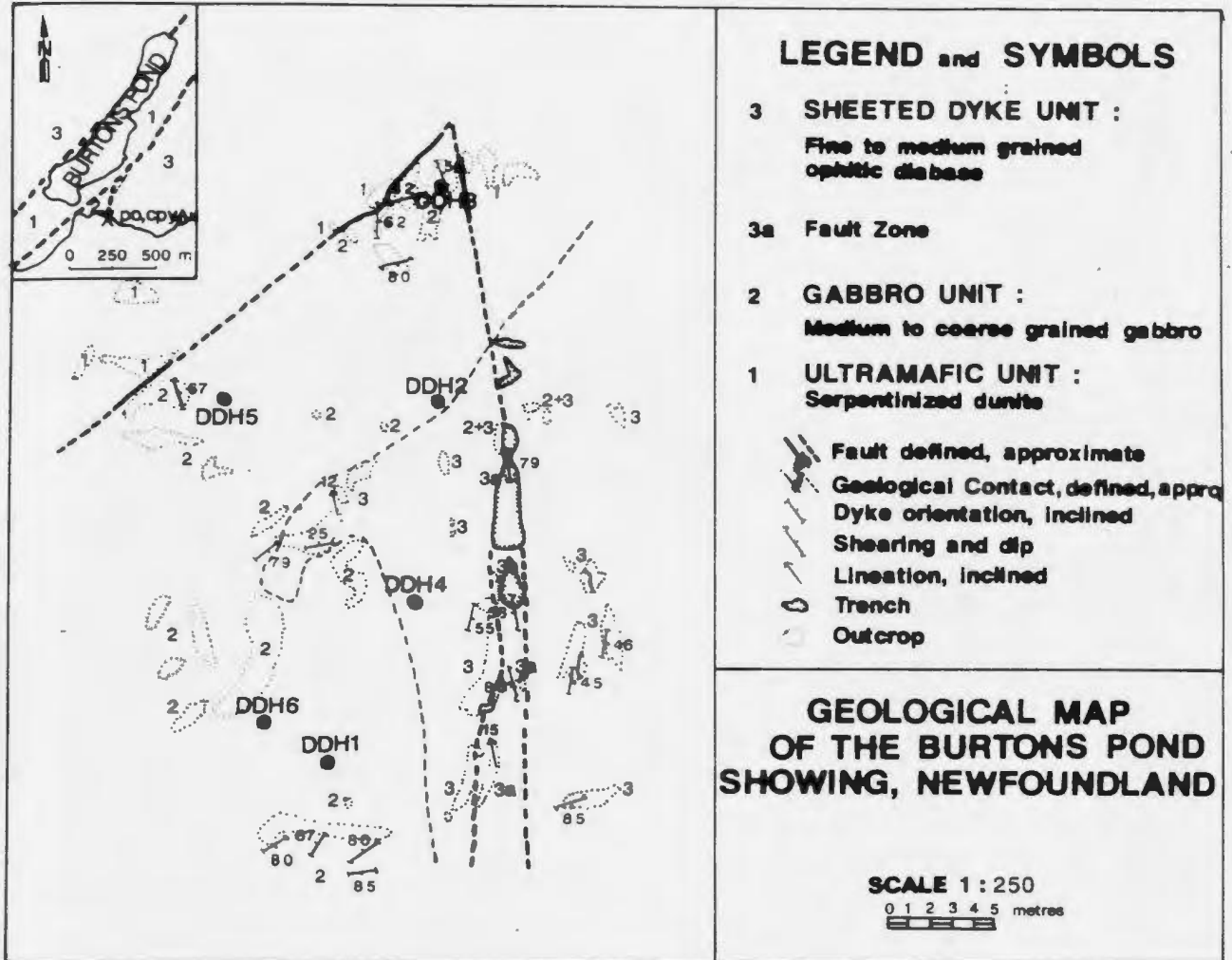
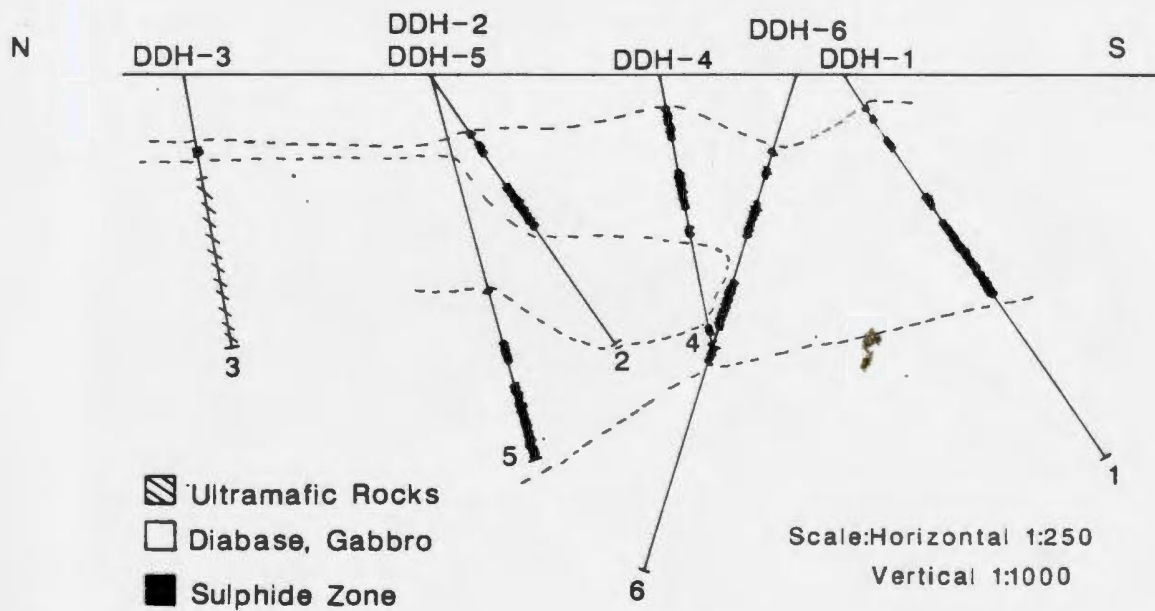


Figure 3-5: Geology of the Burtons Pond showing





**Figure 3-6:** Subsurface geology of the Burtons Pond showing

Section is oriented from north (N) to south (S), striking  $000^{\circ}$ . It runs through the fault zone (unit 3a) outlined in Fig. 3-5.

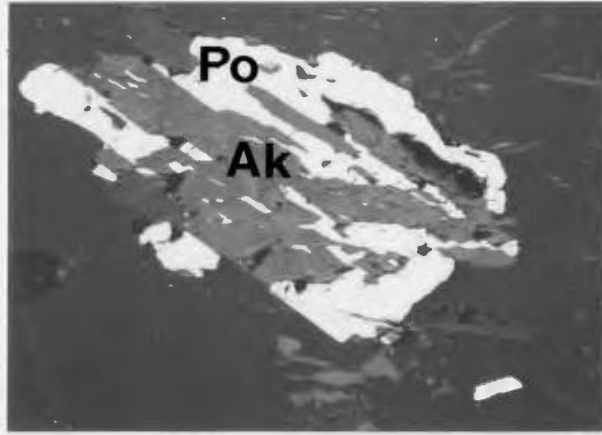


**Figure 3-7:** SEM photomicrograph of sulphide replacement texture, Burtons Pond

Sample K1275, 350X, note pyrrhotite (Po) replacing actinolite (Ak) grain.

Photo width 190  $\mu\text{m}$ .

epidote and sphene. Chlorite and quartz commonly are intergrown, and range in grain size from  $<0.5$  mm up to 0.5 mm depending on the original grain size of the rock, and on the amount of shearing that has taken place. Massive veins and minor disseminations of sulphide are dispersed throughout areas of intense silicification and chloritization. These sulphides fill fractures and replace amphibole (Fig. 3-7). Alteration tends to be patchy (Fig. 3-8) but in some samples is pervasive (Fig. 3-9a) and banded, consisting of alternating bands of chlorite, calcite and quartz-sulphide intergrowths (Fig. 3-9b). This banding is aligned parallel to shearing and thus likely is controlled by it.

Chlorite-sericite alteration (B) is distinguished by the presence of chlorite and sericite, with minor quartz, calcite, and relict amphibole and plagioclase (large original oligoclase grains). Chlorite partially to totally replaces amphibole

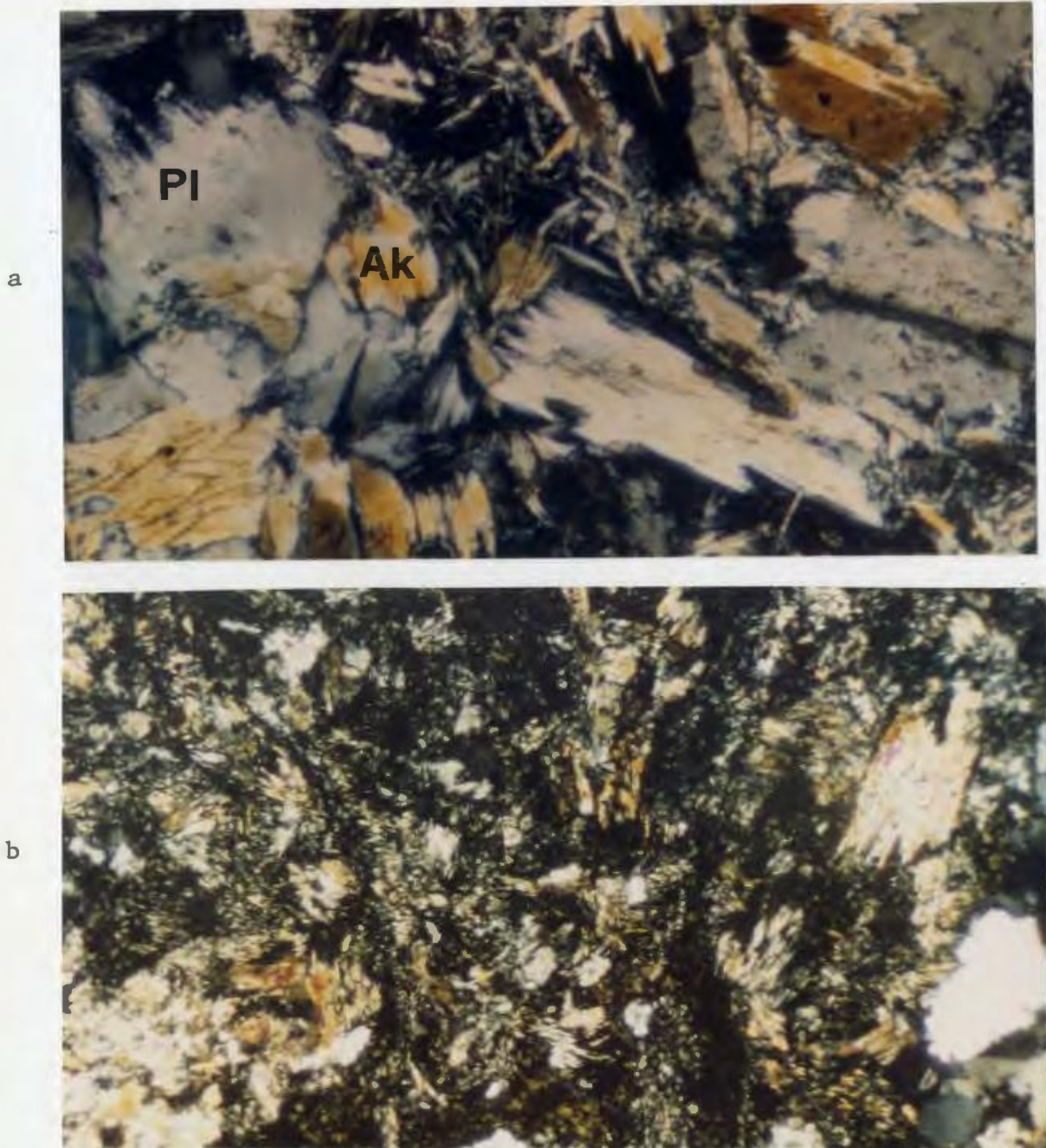


**Figure 3-8:** Photomicrographs of Burtons Pond unaltered and altered samples

(a) Sample 2, XP, uralitized gabbro, note large plagioclase (Pl) grains, intergrown with small to large actinolite (Ak) crystals; (b) Sample 298, XP, patchy quartz-chlorite +/- albite alteration assemblage (A), note fresh actinolite (white) crystals. Photo widths a,b 3.3 mm.

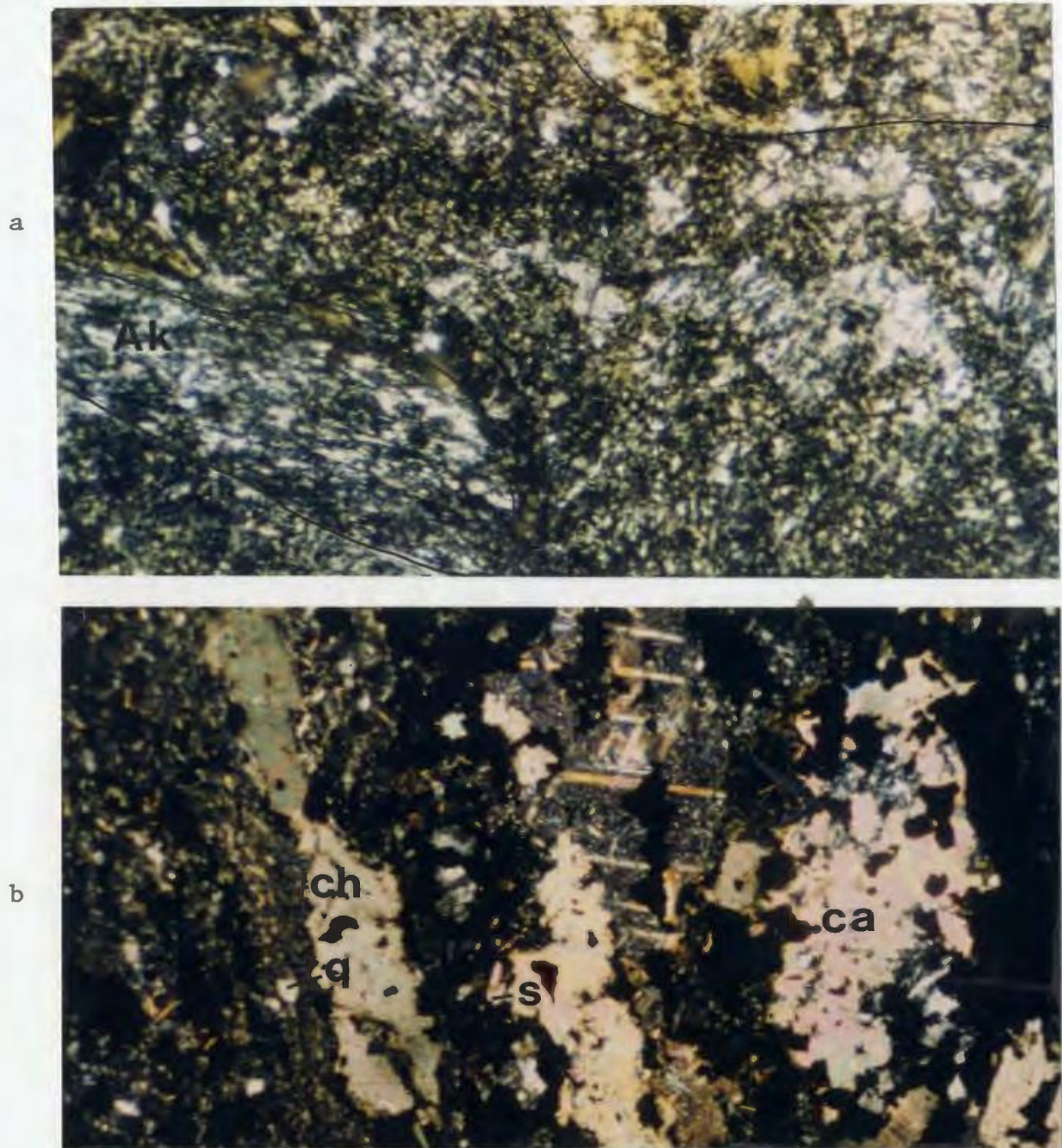


**Figure 3-9:** Photomicrographs of altered  
Burton's Pond samples

(a) Sample K1375, XP, pervasive quartz-chlorite alteration, note relict actinolite (Ak) outlines; (b) Sample K3075, XP, banded quartz(q)-chlorite(ch)+calcite(ca)+sulphide(s) alteration. Photo widths a, 2.4 mm, b, 3.3 mm.

grains, and minor sphene is located in the cores of these relict grains. Extensive sericitization of primary oligoclase and albite grains and laths has obliterated internal features such as twinning, but has preserved crystal outlines. Some chloritization of plagioclase also has occurred, resulting in minor replacement of sericite, as well as oligoclase.

The third alteration assemblage (C) is recognized by the diagnostic minerals calcite and sericite, and is formed in two ways. The first results from the replacement of chlorite in the chlorite-sericite assemblage by calcite, leaving the sericitic alteration of feldspar intact. The second mode of formation occurs by the partial to complete replacement of primary amphibole (actinolite) by calcite along edges and cleavage planes (Fig. 3-10a,b), and of feldspars by sericite (Fig. 3-10a). Sphene, quartz, epidote and fibrous amphibole (uralite) are minor phases.

The alteration types appear to be distinct, except where the chlorite-sericite (B) assemblage gives way to the calcite-sericite (C) assemblage by means of replacement of chlorite by carbonate, suggesting that the calcite alteration is a late phenomena. Of the three types, the chlorite-quartz+/-albite (A) assemblage is the most common and the most intense, as it leaves few traces of original minerals. Carbonate distribution is random, and appears to be controlled by the presence of ferromagnesian minerals, except where it is found in veins.

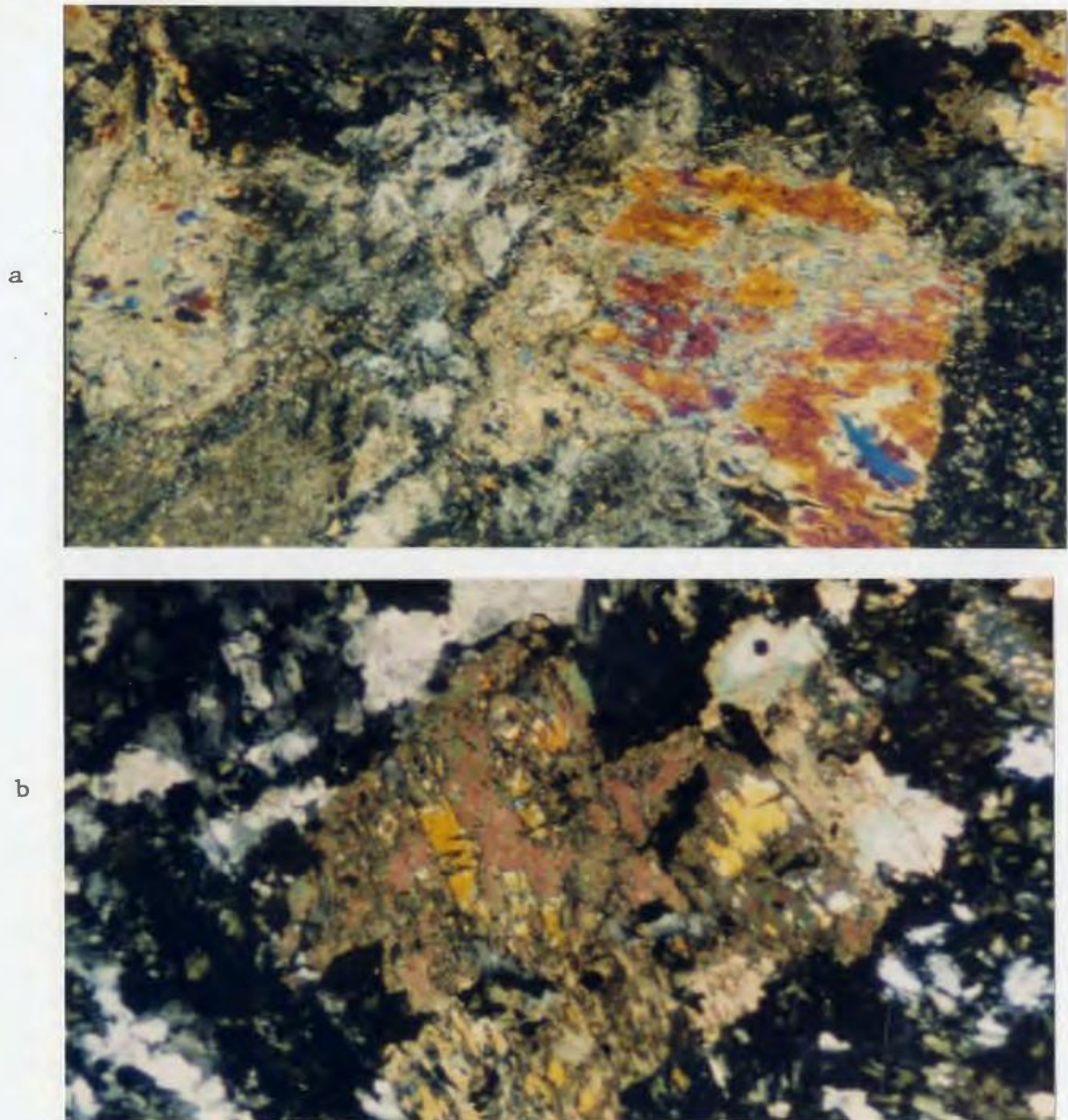


**Figure 3-10:** Photomicrographs of altered  
Burtons Pond samples

(a) Sample K4293, XP, calcite-sericite alteration, note calcite replacement of actinolite and sericitic replacement of plagioclase; (b) Sample K3728, XP, isolated calcite replacement of actinolite in quartz-chlorite-albite rock.

Photo widths, a, 3.3 mm, b, 1.8 mm

### 3.3.2.2. Vein Mineralogy

Stockworks are extremely common in altered Burtons Pond rocks, and consist of veins, normally only a few millimetres or less wide, but up to 0.5 m. Many vein types, most of which contain sulphides, were distinguished. Veining generally is intimately associated with shearing although barren milky quartz veins, commonly displaced by shearing-related fractures, probably are early features.

Sulphide-albite veins are common (Fig. 3-11a), and generally are enveloped by fine-grained sericite and epidote. The albite appears to be confined to the outer walls of the fractures.

Quartz-calcite-sulphide veins are the most typical. These have no marked alteration rims, and sulphides generally are intergrown with blocky quartz and calcite (Fig. 3-11b). Quartz-sulphide assemblages also were observed; in one section early formed fracture-wall lining sulphides are cemented by quartz. Feathery chlorite envelopes some of the quartz sulphide veins, while rare chlorite rosettes rim isolated sulphide microveinlets.

The major sulphides are non-magnetic, pure  $\text{FeS}$  pyrrhotite and chalcopyrite. The former is altered to marcasite along cracks and fractures, resulting in a 'bird's eye' texture (Fig. 3-12a), while the latter contains sphalerite inclusions. Arsenopyrite probably represents a later sulphide phase, as it heals fractures and overgrows pyrrhotite and chalcopyrite (Fig. 3-12a), and also is found as isolated, idiomorphic crystals. Euhedral cubes of cobaltite  $((\text{Co,Fe})\text{AsS})$ ,

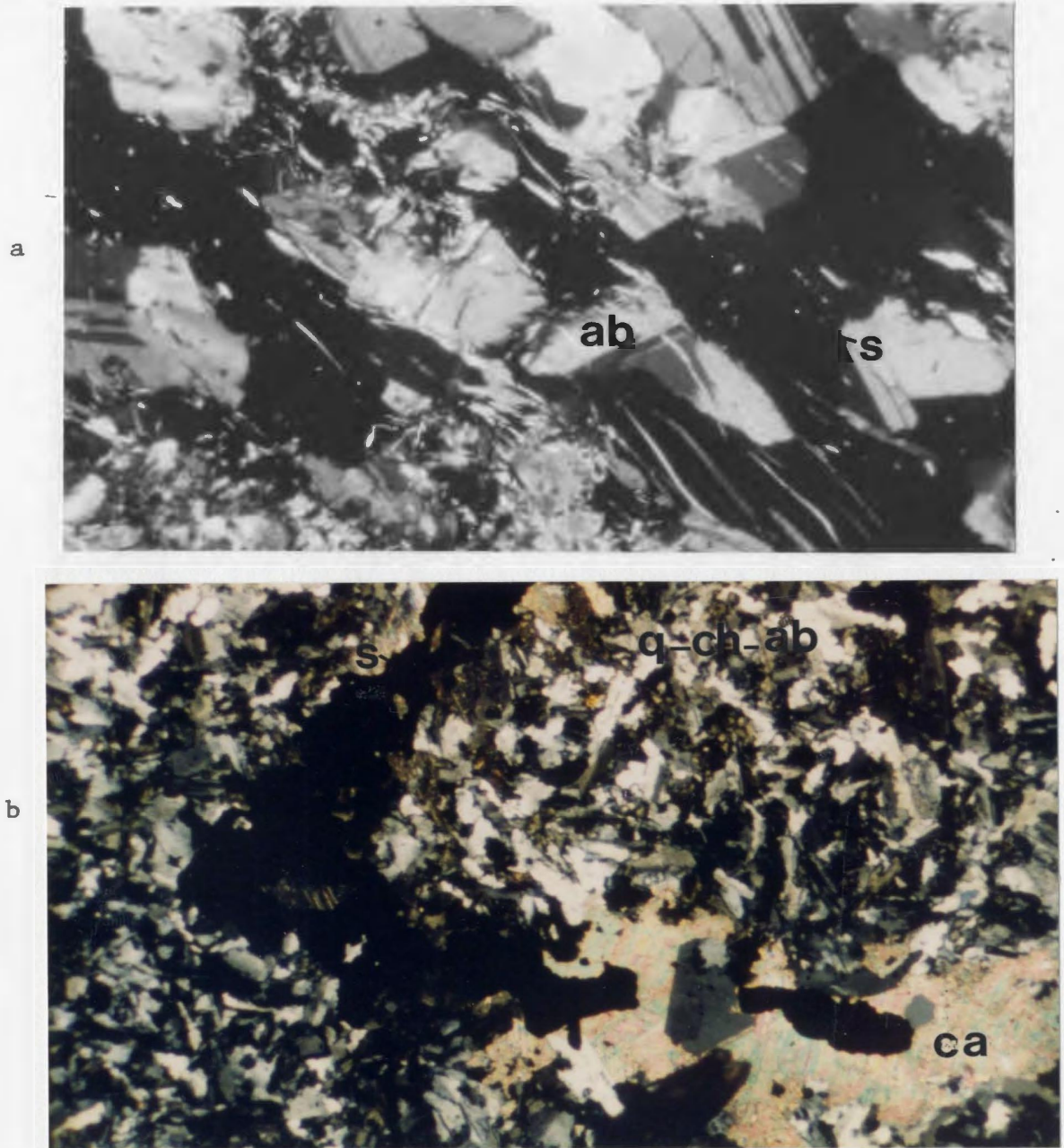


**Figure 3-11:** Photomicrographs of Burtons Pond sulphide veins

(a) Sample KA3175, XP, sulphide(s)-albite(ab) vein (b) Sample K3728, XP, calcite(ca)-sulphide(s) vein in quartz-chlorite-albite(q-ch-ab) rock.

Photo widths a,b 3.3 mm.



coatings of gersdorffite ((Ni,Co,Fe)AsS) (Fig. 3-12b), as well as segregated grains of native Bi are present in quartz gangue in veins.

Burtens Pond samples contain microscopically visible electrum (Au-Ag) as grains ranging from 1 to 3.5  $\mu\text{m}$ . These were found most commonly in and on the edges of chalcopyrite grains (Fig. 3-13a), while other flecks were located in quartz and calcite, near pyrrhotite or chalcopyrite (Fig. 3-13b).

Fig. 3-14 defines a paragenetic sequence of hydrothermal events at Burtens Pond. Early, barren quartz veins are cut by fractures containing pyrrhotite and chalcopyrite. Host-rock alteration to chlorite-quartz-albite, chlorite-sericite and calcite-sericite assemblages may have begun during the pyrrhotite and chalcopyrite precipitation. Sphalerite exsolved from or replaced chalcopyrite. Arsenopyrite, cobaltite and gersdorffite are placed in later positions in the sequence, as they overgrow and heal fractures in pyrrhotite and chalcopyrite, and are euhedral. Quartz and calcite appear to be the last hydrothermal precipitates, because they overgrow all of the other sulphides and seal the veins. The position of gold, though based on limited observations, is considered to be mid- to late in the sequence. It probably precipitated at least in part coevally with chalcopyrite, as it is found on chalcopyrite grain edges, or it even may have exsolved from the chalcopyrite. Gold grains also were located in quartz and calcite gangue, suggesting they may have formed with these minerals, late in the sequence. The paragenetic position of gold thus appears to coincide with that of the arsenic minerals, although no Burtens Pond gold grains actually were enclosed in them. The formation of marcasite by replacement of pyrrhotite is considered to be a very late, post-vein formation, event.

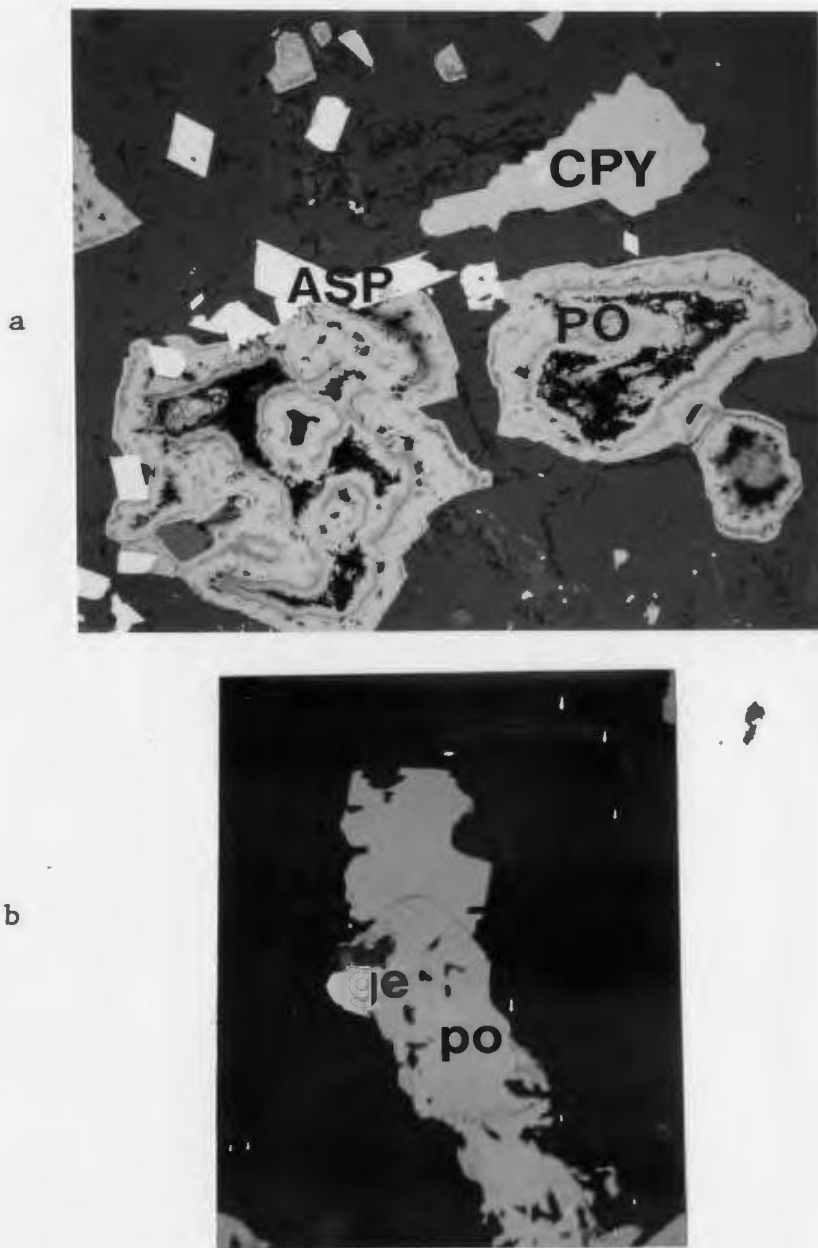


**Figure 3-12:** Photomicrographs of sulphide textures

(a) Sample K2825, 192X, note altered pyrrhotite (Po), now bird's eye marcasite, chalcopyrite (Cpy) and idiomorphic arsenopyrite (Asp). Photo width 363  $\mu\text{m}$ .

(b) Sample K875, 600X, gersdorffite (ge) coating on pyrrhotite (Po). Photo width 40  $\mu\text{m}$ .

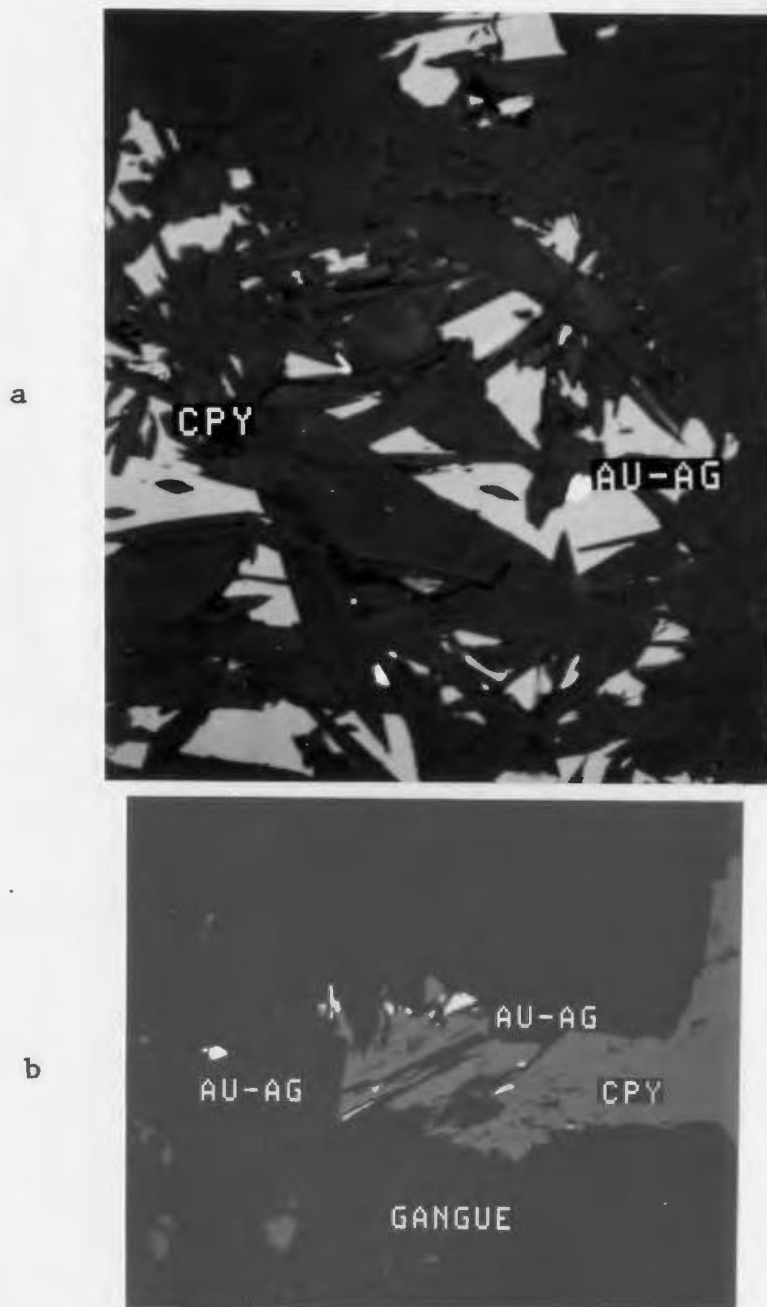


**Figure 3-13:** SEM photomicrographs of electrum grains, Burtons Pond

(a) Sample K3075, RL,690X, electrum in chalcopyrite, intergrown with actinolite (b) Sample KA3350, RL,790X, electrum in chalcopyrite and in quartz-calcite gangue. Photo widths, a, 102  $\mu\text{m}$ , b, 90  $\mu\text{m}$ .

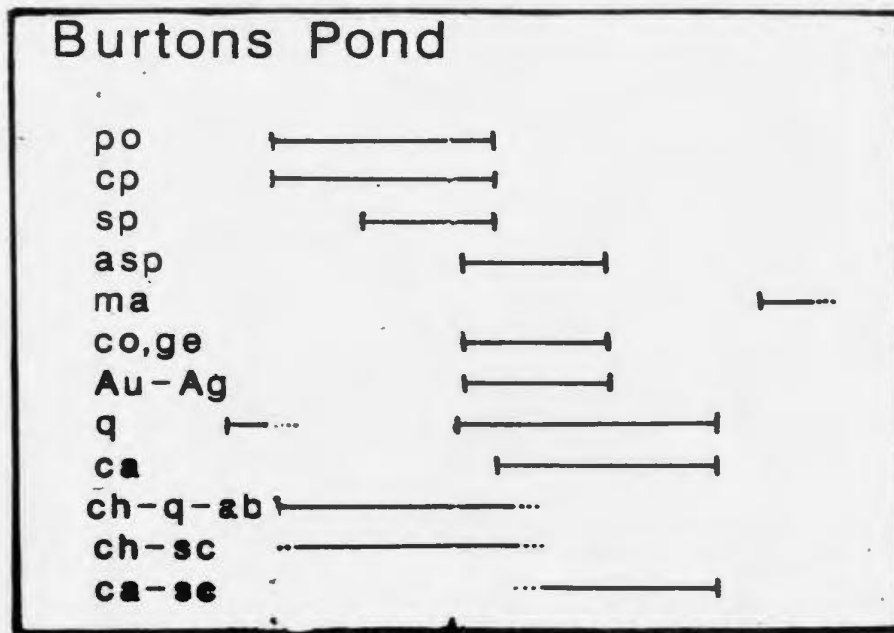


**Figure 3-14:** Paragenetic sequence of hydrothermal events, Burton's Pond

Abbreviations are as follows: po-pyrrhotite, cp-chalcopyrite, sp-sphalerite, asp-arsenopyrite, ma-marcasite, co-cobaltite, ge-gersdorffite, Au-Ag-electrum, q-quartz, ca-calcite, ch-q-ab-chlorite-quartz-albite, ch-sc-chlorite-sericite, ca-sc-calcite-sericite. See text for discussion.

### 3.3.3. Gull Pond

The Gull Pond showing (No. 3) crops out on Highway 415 in the northern part of the map area (Fig. 2-1). In outcrop, the mineralization consists of a 6 to 20 cm wide band of sulphide occurring along a fault in silicified, carbonatized and chloritized diabase (Fig. 3-15), whose core is composed of pyrrhotite and chalcopyrite in a gangue of calcite, quartz and minor epidote. This core is rimmed by chalcopyrite, arsenopyrite, pyrrhotite, calcite and quartz, which passes into pyrite, calcite and quartz.

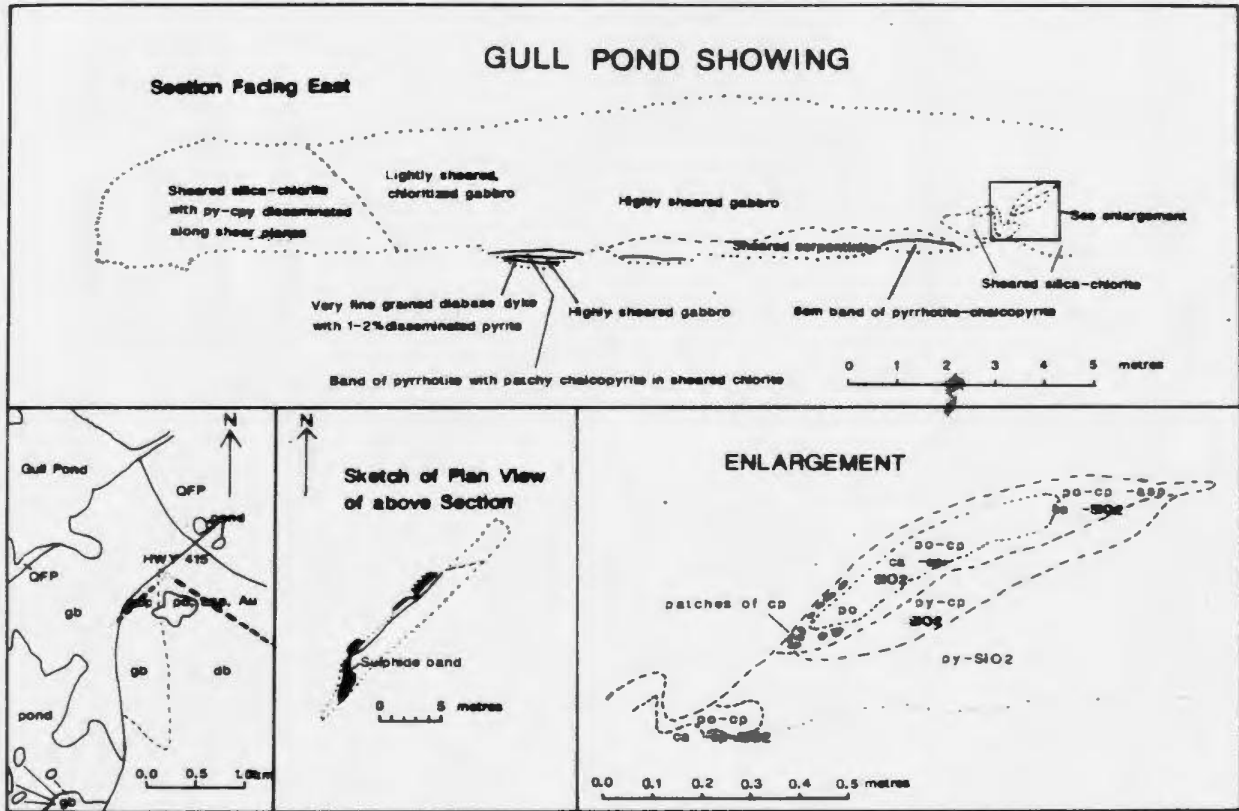


**Figure 3-15:** Geology of the Gull Pond showing  
 Symbols: gb-gabbro, db-diabase, QFP-quartz-feldspar porphyry,  
 ep-epidote; all others as in Fig. 3-14.

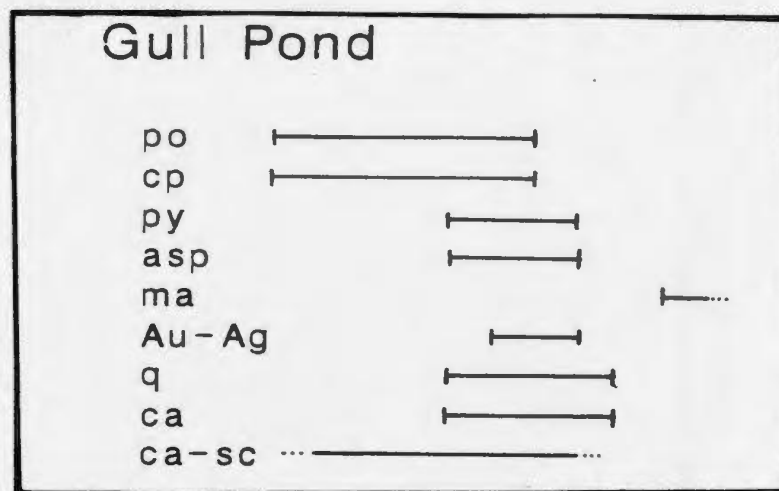


**Figure 3-16:** Paragenetic sequence of hydrothermal events, Gull Pond

Abbreviations are as in Fig. 3-14.

The sulphides and their paragenesis are identical to those at Burtons Pond with two exceptions (Fig. 3-16). Idiomorphic pyrite is found in the outer zone of the sulphide band at Gull Pond, while it is absent at Burtons Pond. Cobaltite and gersdorffite were not found in the Gull Pond sulphides; their presence at Burtons Pond may reflect the close proximity of ultramafic rocks to the host diabase there (Fig. 3-5). Nickel may have been remobilized from the dunites and been re-deposited in the main fault zone, along with Co, Fe, As and S. Ultramafic rocks are absent in the Gull Pond area. 1 to 18 $\mu$ m grains of electrum are found in arsenopyrite, quartz and pyrrhotite in three samples (53, 205, 262) (Fig. 3-17). Gold thus again is placed in a late position in the paragenetic sequence (Fig 3-16), due to its association with late, euhedral arsenopyrite and vein-cementing quartz.

The alteration halo extends only up to 4 metres away from the sulphide



**Figure 3-17:** SEM photomicrograph of electrum grain in arsenopyrite, Gull Pond

Sample 205, RL, 600X. Photo width 116  $\mu\text{m}$ .

band. Outcrop is restricted to the west by the highway, but even so, gabbros on the opposite road cut are unaltered. The host gabbros have been altered to a fine-grained, banded assemblage of chlorite-sericite-quartz (Fig. 3-18), reminiscent of alteration assemblage (B) at Burtons Pond. Away from the main sulphide band, quartz-calcite-sulphide+/-epidote offshoots pervade the altered rock. The rocks are sheared extensively along the faulted roadcut; this shearing event probably produced the host-rock foliation and may have localized the sulphides into their present band-like morphology.

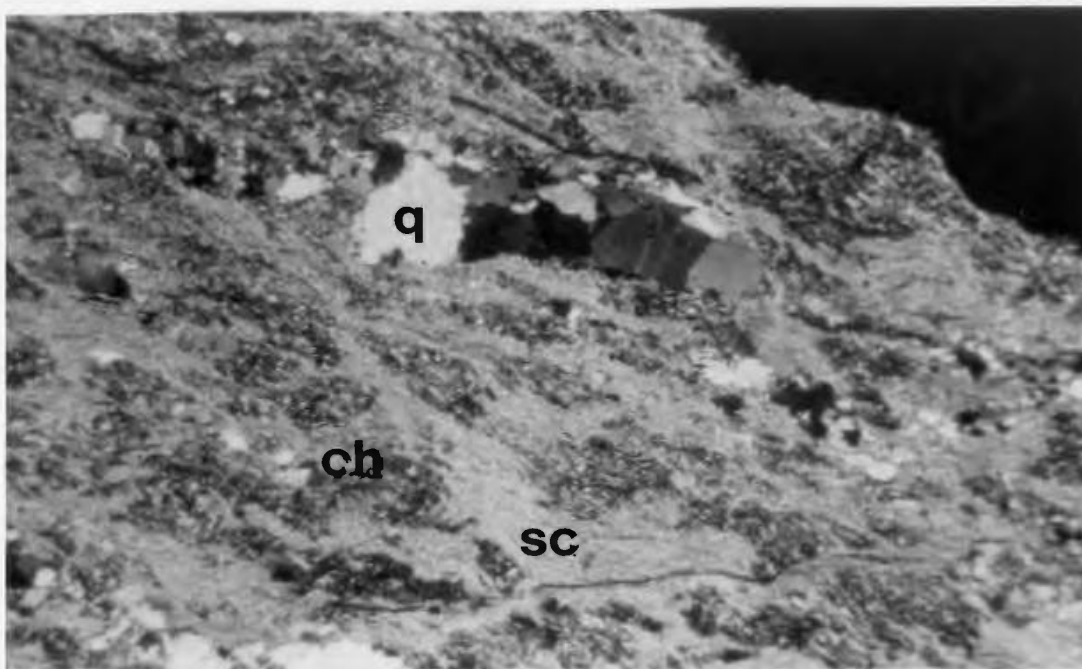


**Figure 3-18:** Photomicrograph of chlorite-sericite alteration, Gull Pond

Sample 262, XP, sc-sericite, q-quartz, ch-chlorite. Photo width 3.3 mm.

#### **3.3.4. Showing No. 2**

Showing No. 2 in the Nippers Harbour community consists of a 16 to 35 cm wide, sulphide-bearing quartz vein in diabase. Contacts with diabase are sharp and the host diabase is unaltered (except for the background spilitic assemblage common to much of the diabase in the area). The sulphides in the vein are roughly banded parallel to the vein walls. A paragenetic sequence, as determined by slab, polished and thin section study, is outlined in Fig. 3-19.

Pyrite is an early phase, forming colloform growths nucleated on quartz fragments and enclosing rare globules of chalcopyrite. It also is present as idiomorphic cubes floating in quartz, as well as irregular-shaped patches intergrown with arsenopyrite. These sulphides were subjected to a period of



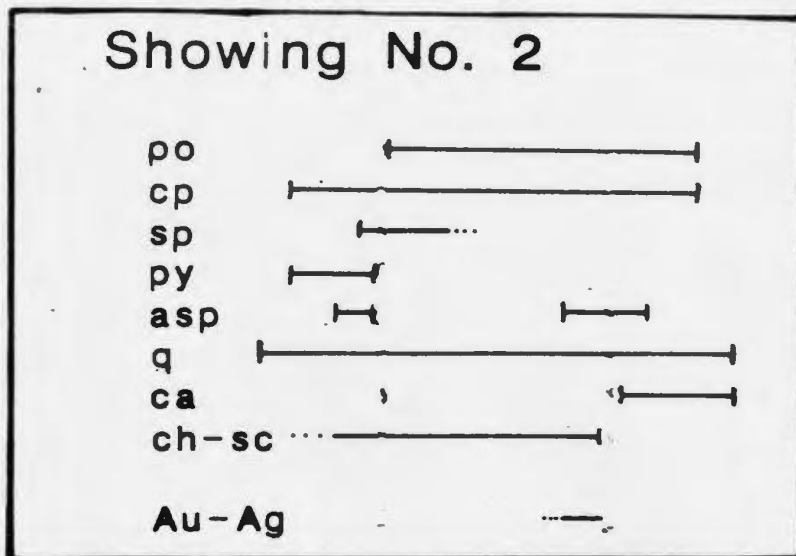


**Figure 3-19:** Paragenetic sequence of hydrothermal events, Showing No. 2

Abbreviations are as in Fig. 3-14.

brecciation, followed by precipitation of pyrrhotite, and further chalcopyrite and arsenopyrite. Quartz and calcite were the last phases to precipitate, filling microfractures and voids in sulphides (Fig. 3-20).  $1\mu\text{m}$  flecks of electrum (Au-Ag) were detected in one Showing No. 2 sample (292), where they were associated with and enclosed in arsenopyrite, similar to electrum at Gull Pond (Fig. 3-17).

Angular, elongate chlorite-sericite-quartz fragments are aligned parallel to the vein selvages, and may represent modified diabase.

### 3.3.5. Rogues Harbour

The quartz vein at Rogues Harbour (showing No. 5) hosts chalcopyrite and pyrite. The vein averages 1 m wide and extends for 825 m across the Rogues Harbour peninsula, but is most extensively mineralized where it is in contact with the Stocking Harbour Fault. Here, pyrite, chalcopyrite and chlorite fill

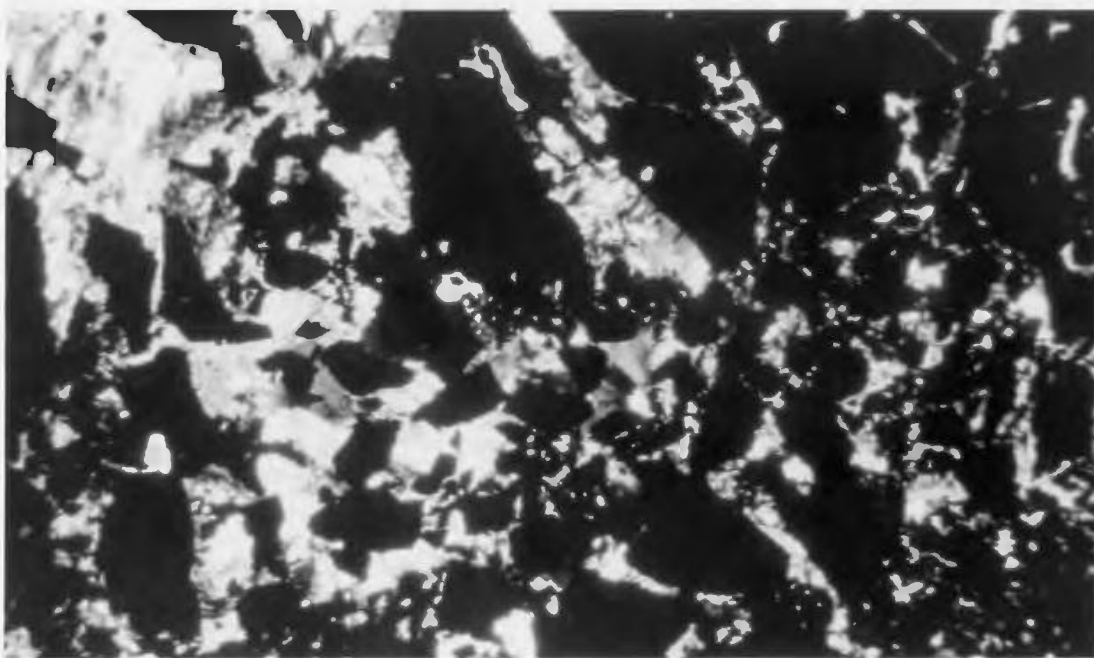


**Figure 3-20:** Sulphide textures,  
Showing No. 2

Sample 296, XP, hydrothermal sulphide breccia, healed by quartz and calcite. Photo width 3.3 mm.

honeycomb-like networks in milky white quartz. Sulphides generally comprise 10 percent of hand samples but reach quantities of up to 40 to 50 percent, where pyrrhotite becomes a common constituent. In thin section, sulphides found along the Stocking Harbour Fault are brecciated, with cracks in pyrite healed by chalcopyrite and sphalerite (Fig. 3-21a). These sulphides host a variety of accessory phases, including arsenopyrite, Bi-telluride, bravoite (Fe, Ni, Co) $S_2$  and Ni-telluride.

There is at least one other generation of quartz in this area which cements the sulphide-rich quartz and contains only minor sulphide-filled fractures. Vuggy quartz crystals were observed in open cracks.

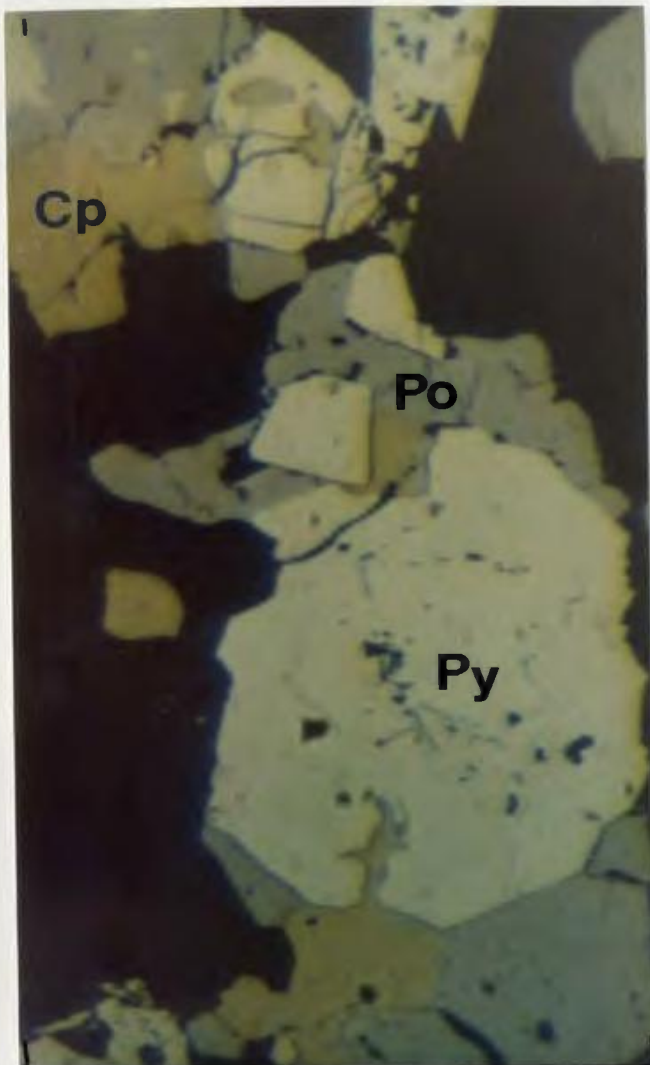
Patches of chlorite schist are common in the quartz vein along the Stocking Harbour Fault, and carry idiomorphic pyrite cubes with microscopic blebs of sheared and streaky chalcopyrite dispersed along shear planes. In most cases, the boundaries of these chloritic patches are very diffuse, although a few pods with sharp edges are visible. These may represent pods of altered gabbro, as fragments of unaltered gabbro were mapped in the quartz vein on the Rogues Harbour peninsula and on the margins of the quartz vein along the Stocking Harbour Fault. The degree of shearing probably was more intense along the fault and produced schists.

On the Rogues Harbour peninsula, minor pyrite is focussed at the margins of the quartz vein and in surrounding gabbro (Fig. 3-21b). The quartz vein here is fairly competent and is hematite-stained.

### **3.3.6. Welshs Bight**

The Welshs Bight showing (No. 6) occurs on a fault between Cape Brule quartz-feldspar porphyry and ophiolitic diabase (Fig. 2-1). Samples collected near the adit at the site contain sphalerite and galena. The nature of the host rock and its alteration were not directly discernable, as only dump samples were available. The porphyry near the adit is pyritized and sericitized, especially near contacts with diabase, and a spectacular stockwork of quartz veinlets is developed within 10 m of the major porphyry/diabase interface.

The Welshs Bight vein comprises strained and undulose quartz fragments, up to several mm in diameter, cemented in a groundmass of calcite, finely



a



b

**Figure 3-21:** Photograph and photomicrograph of Rogues Harbour sulphides and quartz vein

(a) Sample 245, RL, pyrrhotite (Po) overgrowing pyrite (Py) and chalcopyrite (Cp). (b) Rogues Harbour quartz vein, note sheared gabbro at margins containing minor pyrite mineralization. Photo width, a, 0.55 mm.

granulated quartz and sulphide. Intra-granular fractures are healed mainly by calcite and more rarely, by sulphides.

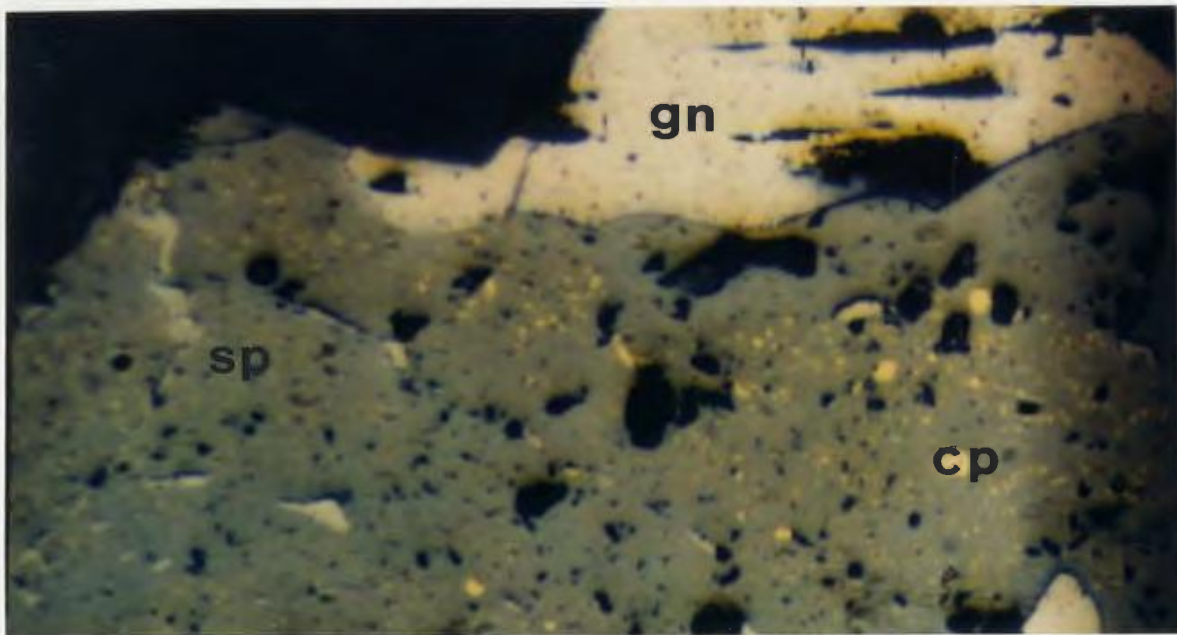


**Figure 3-22:** Photomicrograph of Welsh Bight sulphides

Sample 191, RL, note chalcopyrite disease (Cp) in sphalerite (Sp), which replaces galena (Gn). Photo width 3.3 mm.

The main sulphide is sphalerite, which replaces chalcopyrite and galena (Fig. 3-22). Remnant chalcopyrite and galena inclusions are angular and intergrown, and have an average diameter of 0.05 mm. Microscopic fragments of galena and sphalerite with 'chalcopyrite disease' (Fig. 3-22) are dispersed throughout the silicate matrix. A second generation of galena expresses itself as fracture healings in cracks in sphalerite. Isolated grains of pyrite and idiomorphic arsenopyrite form a minor component of the vein. The arsenopyrite appears to be a very late phase, as it overgrows sphalerite (Fig. 3-23).

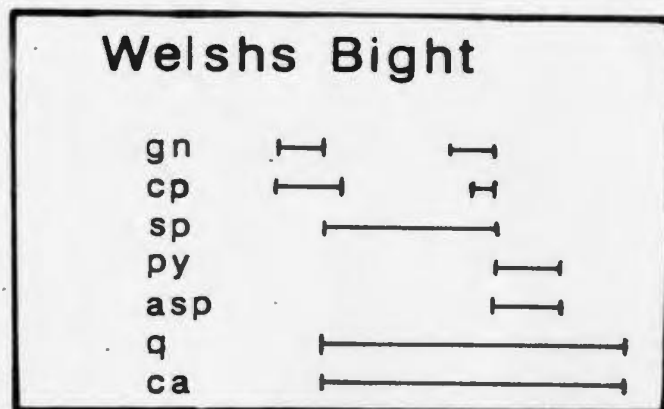


**Figure 3-23:** Paragenetic sequence for hydrothermal minerals, Welshs Bight showing

Abbreviations are as in Fig. 3-14, and gn-galena, py-pyrite.

### 3.4. Metal Contents of Sulphide Samples

Sulphide-rich samples from each showing were analysed at Memorial University for Cu, Zn, Pb, Au, Pt, Pd, and the remaining Platinum-group elements (PGE). Samples from the Burtons Pond showing were analysed at the GSC for the above elements, as well as Co and Ag. Analyses of several unaltered and non-sulphidized samples also were provided to establish background metal levels. The results, sample locations and sample descriptions are presented in Appendix E, and the metal characteristics of sulphide samples from each showing are summarized in Table 3-1.

Copper values for sulphidic samples range from 25 to 52627 ppm (0.0025% to 5.26%) (mean 8470 ppm), Zn values from 0 to 840 ppm (0% to 0.084%) (mean 149 ppm, and one from Welshs Bight at 16118 ppm), and Pb from 0 to 275 ppm (0% to 0.025%) (mean 28 ppm, and two from Welshs Bight at 4930 and 12353 ppm). The Rogues Harbour chalcopyrite-pyrite-bearing quartz vein contains the

	Hill	Burtons Pond	Gull Pond	Showing No. 2	Rogues Harbour	Welshs Bight
Major Sulphide Minerals	py cp	po, cp sp	po, cp asp	py, cp asp	py, cp sp, po	sp, gn cp, asp
Form of Sulph	Bx shear ore	Stkwk ore	Lens and stkwk	Qtz sulph vein	Stkwk in qtz vein	Qtz sulph vein
Alteration Assemblages	q-ch, q-ch- ab	q-ch-ab, ch-sc, ca-sc	q-ch- sc	q-ch- sc	ch-sc	
Au ppb	M-L 21.8- 191.2 (80)	H 310- 19970 (3965)	H 9831- 24713 (15438)	H 329.8- 14033 (4946)	M 80.2- 535.4 (227)	L 41.2
Cu ppm	M-H 463- 20460 (4406)	M-H 930- 46000 (7987)	M-H 2785- 30482 (15462)	M 220- 12604 (2955)	H 6534- 52627 (17659)	L 0- 473
Zn ppm	M 34- 290 (101)	M-H 49- 840 (225)	M 2- 296 (124)	L 10- 107 (36)	L-M 0- 269 (100)	H 16118
Pb ppm	L 0- 14 (1.5)	L 2- 68 (7)	M 0- 410 (222)	L 0- 97 (23)	L 0- 13 (4)	H 4930- 12353 (8642)

**Table 3-1: Metal and Other Characteristics of Nippers Harbour mineralized samples**

Symbols are as follows: Py: pyrite; Cp: chalcopyrite; Po: pyrrhotite; Sp: sphalerite; Asp: arsenopyrite; Gn: galena; q: quartz; ch: chlorite, sc: sericite; ab: albite; ca: calcite; L: low, M: medium; H: high; sulph: sulphide; stkwk: stockwork; bx: breccia. Range of values for each element are given, as well as mean values (in brackets) where applicable.

most Cu, followed closely by the Gull Pond, Burtons Pond and Hill samples, which also contain chalcopyrite. High Zn contents are recorded at Welshs Bight and Burtons Pond, with lesser values found at Gull Pond, Rogues Harbour and the Hill. Sphalerite inclusions are common in other sulphides (pyrrhotite and chalcopyrite) at these showings.

The Welshs Bight galena-bearing quartz vein is the only one to yield very high Pb values, although massive sulphide samples at Gull Pond contain up to 275 ppm Pb. Petrographic and SEM examination did not confirm the presence of galena in these samples; it may be extremely finely dispersed, or the Pb may have been taken up by another sulphide mineral such as chalcopyrite (Deer *et al.*, 1966).

Gold values range from 2.1 to 24713 ppb (mean 3807 ppb) in sulphide samples. The 'regional' quartz veins have the lowest values (2.1, 2.4, 3.4, 19.4 ppb), except for a pyritic quartz vein outcropping near Pine Pond, which yielded a value of 271.6 ppb Au. Background values in relatively unaltered diabase samples ranged from 1.9 to 10.7 ppb, while an ultramafic and quartz-feldspar porphyry sample gave contents of 2.5 and 1.3 ppb, respectively. These values are compatible with abundances of gold in other primary igneous rocks (Tilling *et al.*, 1973).

The Gull Pond, Burtons Pond and Showing No. 2 samples display the highest gold values in the Nippers Harbour area. SEM analysis of approximately 32 gold grains reveals a variety of associations. More specifically, the grains are



situated on the chalcopyrite grain edges, in cracks in chalcopyrite, in vein quartz, on pyrrhotite edges, and enclosed in arsenopyrite. Semi-quantitative analysis has revealed that the gold is fixed in electrum (Au-Ag metal) which contains up to 50 percent Ag.

Most Archaean lode gold deposits are essentially gold-only deposits, as they possess lower-than-background levels of transition metals (Co, Ni, Cu, Zn, Pb). They are, however, characterized by extreme concentrations of certain rare elements including Ag, As, Sb and W (Kerrich, 1979; Kerrich and Fryer, 1981; Kerrich, 1983). Archaean base metal deposits, on the other hand, contain anomalous amounts of both base metals and gold (Kerrich and Hodder, 1982; Kerrich, 1983) (Fig. 3-24). The diagram shown in Fig. 3-24 indicates that the Nippers Harbour showings have characteristics closer to base metal deposits than to lode gold deposits.

LeBlanc (1986) and Buisson and LeBlanc (1986) have described and modelled gold-bearing arsenide mineralization in ultramafic ophiolitic rocks from Morocco (Fig. 1-4). This Moroccan mineralization consists of quartz-carbonate lenses with Co-Ni-Fe arsenides, and gold associated with skutterudite, as well as small chromite Ni-arsenide veins with accessory gold. Arsenide occurrences have been described in serpentinized ultramafic ophiolitic massifs elsewhere. Carbonate-quartz veins with Co-Ni-Fe arsenides and accessory sulphoarsenides and sulphides are found in serpentinite lenses in Turkey (Legros). The Caucasus ophiolite hosts the Zod deposit, comprised of gold-sulphide-arsenide lenses in quartz-carbonate-talc assemblages (Smirnov, 1977). Sulphide-arsenide

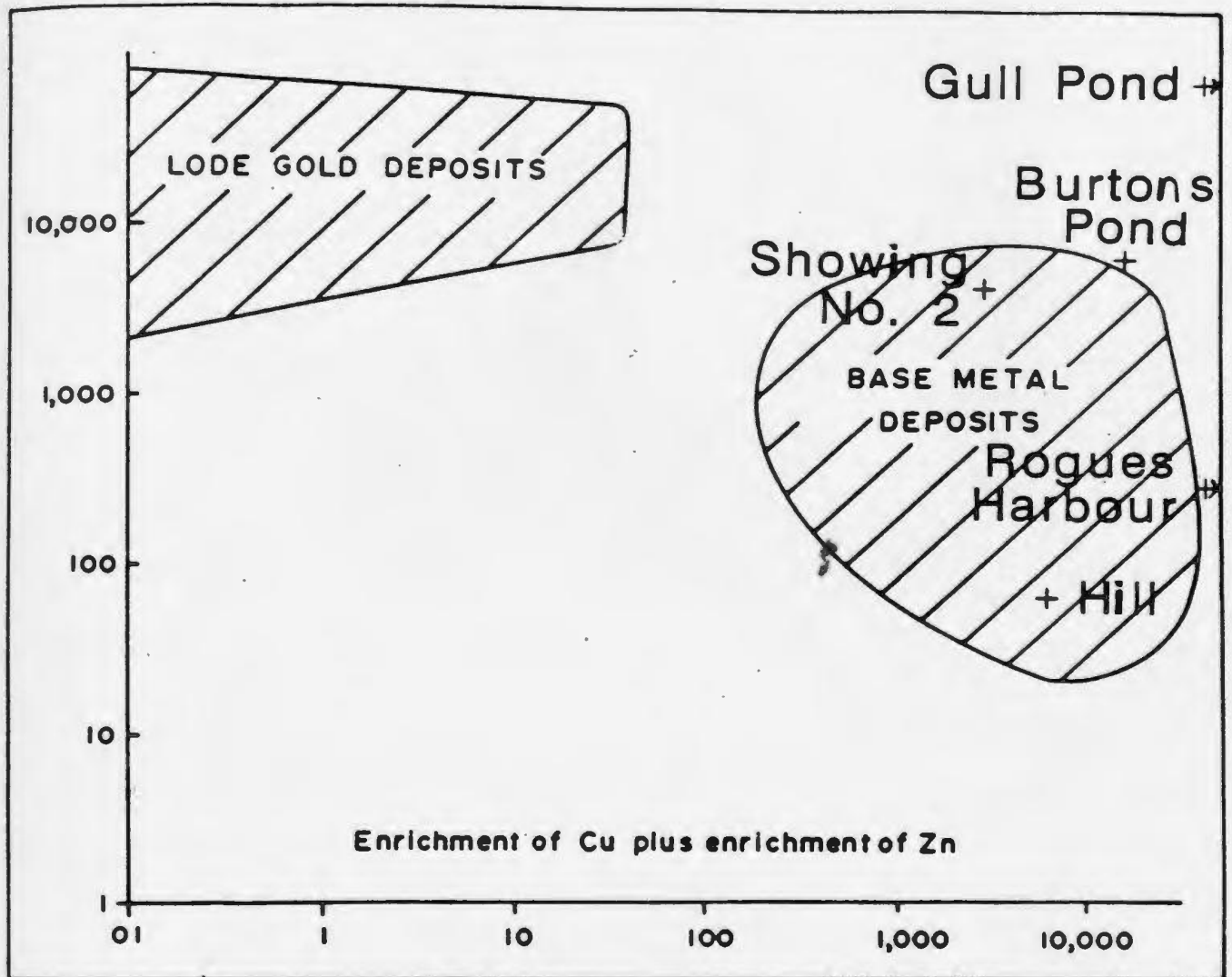


**Figure 3-27:** Au enrichment vs. Cu+Zn enrichment diagram for the Nippers Harbour showings

From Kerrich (1983). See text for discussion.

mineralization has been documented in serpentinites of the Limassol forest in the Troodos ophiolite, Cyprus (Panayiotou, 1980), where gold grains are found in loellingite ( $\text{FeAs}_2$ ) and pyrrhotite.

Arsenides are a common though not extremely abundant phase in ore samples at the gold-rich showings (Burtons Pond, Gull Pond, Showing No. 2). At Burton's Pond in particular, sulphide samples contain minor cobaltite ( $(\text{Co,Fe})\text{AsS}$ ) and gersdorffite ( $(\text{Ni,Co,Fe})\text{AsS}$ ) as well as arsenopyrite. At each of these showings, arsenopyrite is generally a later phase than early-forming pyrrhotite and chalcopyrite. The gold also appears to precipitate during the waning stages of pyrrhotite and chalcopyrite formation, as it is generally located on grain edges of these sulphides, in quartz-carbonate gangue and even in arsenopyrite. This suggests that there is probably a genetic link between gold and sulphide, and perhaps even gold and arsenide, formation at these showings, which is discussed at greater length in chapter six.

Platinum-group element (PGE) abundances are low in the Nippers Harbour sulphides (7.4 to 23.78 ppb total PGE from ICP analyses). These do not differ significantly from background levels in relatively unaltered diabases (Appendix E) and thus do not constitute economically interesting mineralization.

### 3.5. Summary

Six major showings were examined in detail for this study. They all are found in fault zones in altered diabase and gabbro. Sulphide mineralogy is fairly simple, comprising pyrrhotite or pyrite, and chalcopyrite in abundance, with

lesser and varying amounts of sphalerite, arsenopyrite, and electrum (Au-Ag). Galena is found only at the Welshs Bight showing.

The Hill showing is believed to have been formed below the seafloor prior to obduction of the ophiolite. Mineralization there consists of pyrite and chalcopyrite in shear zones in quartz-chlorite rocks, as well as minor pyrite in quartz-chlorite-albite rocks. These hydrothermally altered rocks have been intruded by relatively fresh diabase dykes.

The Burtons Pond, Gull Pond and Showing No. 2 areas are characterized by high base metal (Cu, Zn) and gold contents. Host rocks are altered to assemblages of chlorite-sericite-quartz (at all three showings) and chlorite-quartz+/-albite and calcite-sericite (Burtons Pond only). Gold is found on the edges of chalcopyrite grains, enclosed in pyrrhotite, quartz-calcite gangue and arsenopyrite, all of which are found in veins cutting altered host rocks.

Anomalous values of Cu, Zn, Pb, Ag and Au are recorded at the various showings. The showings have metal characteristics more typical of base metal rather than lode gold Archaean deposits. PGE contents of samples from all of the showings are low, near background levels.

## Chapter 4

# Geochemistry

### 4.1. Introduction

Almost all of the rocks in the vicinity of sulphide mineralization in the Nippers Harbour Ophiolite have been affected by metasomatism at least to some degree. In order to assess these chemical changes, it is necessary first to define the primary geochemical nature of unaltered rocks. The mafic and ultramafic ophiolitic rocks have been subjected to widespread sub-seafloor metamorphism of varying degrees of intensity. Their primary geochemistry also may have been inhomogeneous.

This chapter examines the primary chemistry of the Nippers Harbour ophiolitic rocks and uses the information obtained to deduce the metasomatic changes of hydrothermally affected rocks. Sulphur and lead isotope, as well as rare earth element (REE) data, also are presented and discussed.

Major and trace element analyses of 161 ophiolitic rock samples were provided for this study and are tabulated in Appendix C. Thirty of these were selected to represent 'background', non-hydrothermally altered samples on the basis of their greenschist mineralogy deduced from petrographic observation. A

number of samples were chosen from each showing and from samples collected during regional examination of the ophiolite. Twenty-five whole-rock samples were analysed for rare earth elements by ICP-MS at Memorial University. Seven analyses of Cape St. John Group volcanics and 8 analyses of Cape Brule quartz-feldspar porphyry also were provided. These are not discussed in detail for this study, but are tabulated in Appendix C. Sample descriptions and locations are presented in Appendix E.

## **4.2. Geochemical Characteristics and Tectonic Environment**

### **4.2.1. Previous Work on Betts Cove / Tilt Cove lavas**

Previous geochemical analyses of sheeted dyke and pillow basalt members of the Betts Cove Ophiolitic Complex have been published by Upadhyay (1973, 1978, 1982), Upadhyay and Neale (1979), Coish (1977a, b), Coish and Church (1979), Riccio (1972), Saunders (1985) and Strong and Saunders (1988). The geochemical characteristics interpreted to date are summarized as follows:

(1) The pillow lava member consists of three geochemically distinct sequences: the lower, intermediate and upper pillow lavas (Coish, 1977a; Coish and Church, 1979), with  $\text{TiO}_2$  contents of  $\text{TiO}_2 < 0.25\%$ ,  $0.25 < \text{TiO}_2 < 0.50\%$  and  $\text{TiO}_2 > 0.70\%$ , respectively. Upadhyay (1978, 1982) recognized only the upper and lower lava units.

(2) The Betts Cove basalts display 'boninitic' affinities (Sun and Nesbitt, 1978; Upadhyay and Neale, 1979; Cameron *et al.*, 1979, 1980; Cameron and Nisbet, 1982; Upadhyay, 1982). Boninites have been described at Papua, the

Bonin islands and the Mariana Trench by Hickey and Frey (1982) and Cameron *et al.* (1979). They are rich in  $\text{SiO}_2$  and  $\text{MgO}$  (> 55% and 9% respectively) and poor in  $\text{Al}_2\text{O}_3$ ,  $\text{CaO}$ , Ti, P, Zr, Y and REE. The presence of abundant low-Ca pyroxene (high Mg-orthopyroxene and clinoenstatite) is characteristic of boninites, although Cameron *et al.* (1979) require only one or more varieties of pyroxene in their boninites. Boninitic lavas from the Mariana Trench and the Bonin Islands typically display convex upwards REE patterns (Hickey and Frey, 1982).

(3) Some of the Betts Cove rocks are classified as komatiites and basaltic komatiites by Upadhyay (1982), based on quench textures, high  $\text{MgO}$ , Ni and Cr, and low  $\text{TiO}_2$  and  $\text{K}_2\text{O}$  contents. He expanded his findings by suggesting the basalts formed a continuum from komatiite through boninite to magnesian andesite. The Till Cove lavas are basaltic, not boninitic (Strong and Saunders, 1988).

(4) A crystallization order of (olivine + chromite)  $\rightarrow$  orthopyroxene  $\rightarrow$  clinopyroxene  $\rightarrow$  plagioclase was proposed by Church and Riccio (1977) for the Betts Cove lavas.

(5) REE concentrations in Betts Cove lavas have been shown to be low, generally less than 10 times chondrite (Coish, 1977a,b; Coish *et al.*, 1982). The lower Ti-lavas of Coish *et al.* (1982) display concave-upward chondrite-normalized patterns and lower REE concentrations than higher-Ti lavas and some intermediate Ti-lavas, which have convex-upward patterns.

(6) The Betts Cove Ophiolite is believed to have been formed in a supra-subduction zone environment. At this setting, an assortment of mantle types may have been partially melted to form the parental oceanic magmas. (Upadhyay, 1973; Sun and Nesbitt, 1978; Upadhyay and Neale, 1979; Coish *et al.*, 1982; Hickey and Frey, 1982). Sun and Nesbitt (1978), Coish and Church (1978) and Hickey and Frey (1982) suggested that the low-Ti, boninitic-like depleted Betts Cove lavas were derived from refractory upper mantle which had been previously partially melted and depleted. Secondary melting would be caused by fluids exhaled from newly subducted ocean crust, under hydrous, but not necessarily H<sub>2</sub>O-saturated, low pressure conditions.

Various tectonic settings have been proposed for the Betts Cove Ophiolite (e.g. Upadhyay, 1973: marginal ocean basin; Coish, 1977a,b: mid-ocean ridge; Sun and Nesbitt, 1978: incipient island arc or interarc basin; Coish *et al.*, 1982: interarc basin or back-arc basin). Saunders (1985), and Strong and Saunders (1988) most recently have suggested that the ophiolite formed in a fore-arc setting. Boninites occur most frequently in fore-arc regions (Cameron *et al.*, 1980; Hickey and Frey, 1982). Strong and Saunders (1988) furthermore have proposed that the Betts Cove lavas formed at the front of the advancing arc, and uphold the idea that melting was due to dehydration of previously altered oceanic crust (cf. Coish *et al.*, 1982). They suggested that subduction of metalliferous sediments or massive sulphides may have occurred to produce the abnormally large massive sulphide bodies at Tilt Cove.



#### 4.2.2. Nippers Harbour Results

Table 4-1 presents a partial list of some common basalt types, and average compositions of diabases from Betts Cove diabases and from 30 unaltered diabases in the Nippers Harbour area. The Nippers Harbour diabases have remarkably similar chemistry to those at Betts Cove in that they have anomalously low  $\text{TiO}_2$  contents, and high  $\text{SiO}_2$ ,  $\text{MgO}$ ,  $\text{Cr}$  and  $\text{Ni}$  relative to the other basalts. The  $\text{Cr}$  values in particular are high, probably reflecting the presence of chromite in many of the Nippers Harbour diabases (especially at Burton's Pond).

The total range of  $\text{TiO}_2$  contents for unaltered and altered ophiolitic rocks (including gabbros and ultramafics) is  $0.00 < \text{TiO}_2 < 0.37$  wt%, with two higher values at 0.41 wt% and 0.57 wt%. These contents, as well as  $\text{Zr}$  contents, are very low compared with MORB analyses and with those from the Marianas boninitic-type lavas.  $\text{Ti}$ ,  $\text{Y}$ ,  $\text{V}$ ,  $\text{Zr}$ ,  $\text{Cr}$ ,  $\text{Ni}$  and  $\text{FeO}_4/\text{MgO}$  probably are immobile, as partially shown in Figs. 4-1 and 4-2. These plots suggest that the Nippers Harbour ophiolitic rocks (particularly diabases) are more depleted than other oceanic basalts.

Strong and Saunders (1988) delineated two groups of low-Ti lavas at Tilt Cove: a "high-Zr" group which overlaps the low-Ti samples at Betts Cove, and a "low-Zr" group which is intimately associated with massive sulphide mineralization, and is more depleted than any lavas at Betts Cove. The authors regarded the two lava types to be formed by different degrees of partial melting of different upper mantle sources. Fig. 4-3 depicts the Nippers Harbour samples plotted with fields for these low- and high-Zr groups at Tilt Cove, as well as fields

Wt%	MORB	MTB	MAT	NIPPERS HARBOUR	BETTS GOVE
SiO <sub>2</sub>	49.61	50.2	53.0	54.7	56.2
TiO <sub>2</sub>	1.43	1.00	0.85	0.13	0.19
Al <sub>2</sub> O <sub>3</sub>	16.01	16.8	15.9	13.5	12.6
Fe <sub>2</sub> O <sub>3</sub>	11.49	8.7	10.6	9.52	10.4
MnO	0.18	0.1	0.2	0.17	0.16
MgO	7.84	8.4	5.9	11.1	11.0
CaO	11.23	11.7	10.5	7.09	7.32
Na <sub>2</sub> O	2.76	2.5	2.5	3.4	1.72
K <sub>2</sub> O	0.22	0.49	0.56	0.25	0.38
P <sub>2</sub> O <sub>5</sub>	0.14	0.10	0.11	0.03	0.03
TOTAL	100.91	99.99	100.12	99.89	100.00
Ba	14	43	50	57	54
Rb	1.2	3-10	2-10	11	4
Sr	130	190	145	67	93
Cr	297	260	20	789*	408
Ni	97	120	25	239*	140
V	292	225	330	260*	292
Zr	95	100	55	17.5*	16
Zn	-	50	70	76	57
Cu	77	-	-	131	81
Y	-	-	-	6.3	7

**Table 4-1:** Analyses of 'typical' basalts,  
Betts Cove and Nippers Harbour diabases

MORB = Mid-ocean ridge basalt; MTB = Mariana Trough basalt; MAT = Mariana Arc tholeiite. Rock analyses for MORB, MTB, MAT are average analyses taken from Hawkins (1980); Betts Cove (BC) values are based on an average of 21 diabase dyke analyses taken from Saunders (1985); Nippers Harbour (NH) values are based on averages of analyses of 30 unaltered diabase dykes. Starred values are based on averages of 91 analyses (Cr, Ni, V) and 68 analyses (Zr and Y). Major elements are quoted in Wt. % oxide; minor elements in ppm.

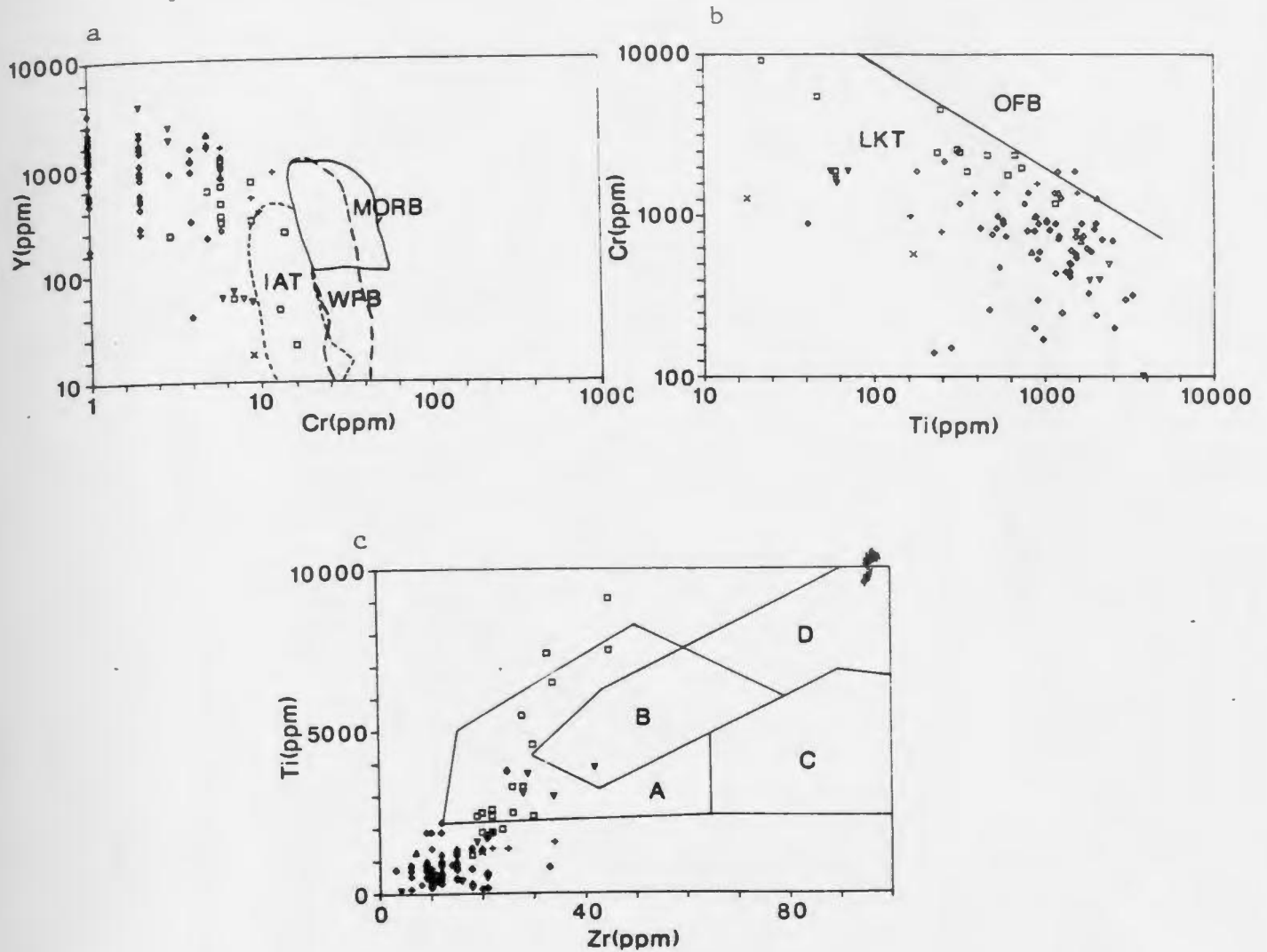


**Figure 4-1:** Variation diagrams for altered and unaltered Nippers Harbour diabbases

(a) Log Y vs Log Cr. Fields from Pearce (1980). IAT-island arc tholeiite, WPB-within plate basalt, MORB-mid-ocean ridge basalt. (b) Log Cr vs log Ti. Fields from Pearce (1975). LKT-low-K tholeiite, OFB-ocean floor basalt. (c) Zr vs Ti. Fields from Pearce and Cann (1973): low K tholeiites plot in fields A and B; ocean floor basalts in fields D and B; calc-alkaline basalts plot in fields C and B. Symbols are: Hill Showing ( $\square$ ); Burtons Pond ( $\diamond$ ); Gull Pond (+); Showing No. 2 ( $\times$ ); Rogues Harbour ( $\triangle$ ); Regional diabase samples ( $\nabla$ ).

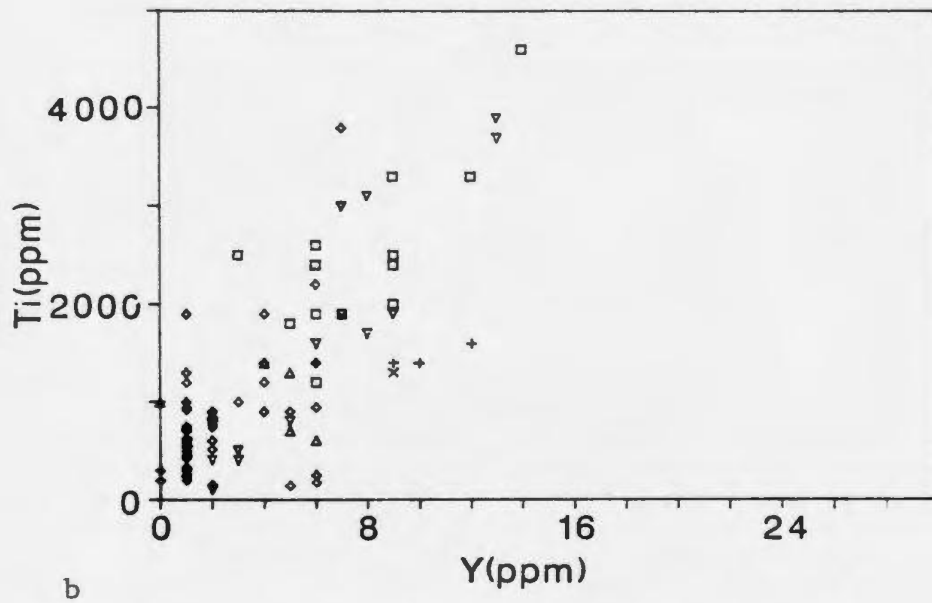
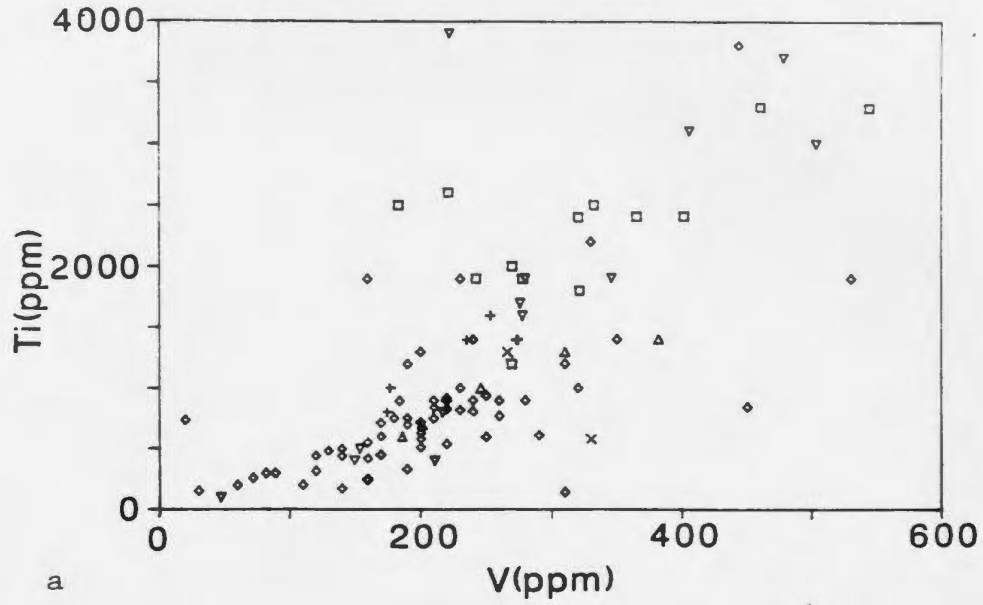


**Figure 4-2:** Variation diagrams for altered and unaltered Nippers Harbour diabbases

(a) V vs Ti; (b) Y vs Ti; Symbols as in Fig. 4-1.

for Betts Cove basalts from Coish *et al.* (1982) and Saunders (1985). Clearly, there are no extremely low-Zr diabases in the depicted Nippers Harbour samples, except for a few Burtons Pond samples.

The Nippers Harbour samples most closely resemble the Betts Cove and Tilt Cove low-Ti, (relatively) high-Zr lavas, although many samples have elevated Zr/Y ratios. The Zr contents are slightly higher than Betts Cove (Table 4-1), while Y values are comparable.  $\text{TiO}_2$  contents of Nippers Harbour diabases are also higher on average than Betts Cove diabases (Table 4-1). As pointed out above, Cr and Ni contents are very much higher than those at Betts Cove. As these elements (Ti, Zr, Y, Cr, Ni) have been shown to be immobile (Figs. 4-1 and 4-2), these differences are probably not due to secondary metasomatic processes. Regional diabase samples are remarkably enriched in normally low abundance elements such as Au (average  $\sim 7$  ppb for 7 samples) and Pd (average 16.5 ppb for 7 samples). In an analogous but opposite situation to the low-Zr Tilt Cove lavas, the Nippers Harbour diabases and microgabbros may have been derived from a different, but slightly more incompatible element-enriched source than that of Tilt Cove or Betts Cove.

REE abundances of unaltered Nippers Harbour rocks generally concur with these suggestions. The abundances are very low, ranging from  $\sim 0.1$  to  $\sim 2$  times chondrite in ultramafic rocks, 1 to  $\sim 5$  times chondrite in gabbros, and 6 to 8 times chondrite in diabases (Fig. 4-4). Gabbro and ultramafic samples display concave-upwards patterns typical of the lower-Ti lavas of Coish *et al.* (1982). Altered diabases and gabbros from the Hill, Burtons Pond, Gull Pond and Rogues

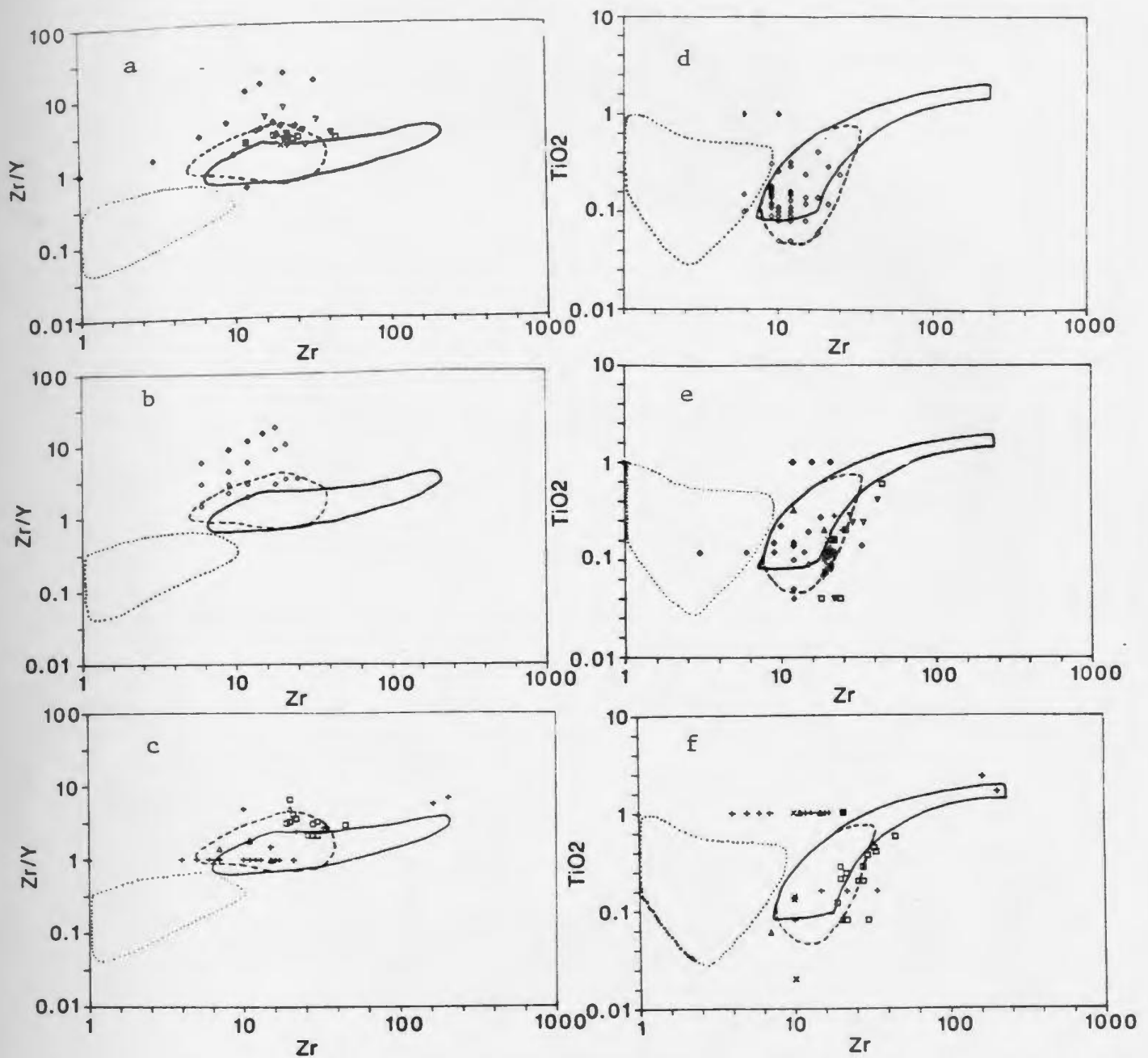


**Figure 4-3:** Variation diagrams

(a),(b),(c) Log Zr vs log Zr/Y, (a) unaltered samples, (b) Burton's Pond, (c) other altered samples; (d),(e),(f) Log Zr vs log  $TiO_2$ , (d) unaltered samples, (e) Burton's Pond, (f) other altered samples. Fields for Betts Cove pillow lavas shown are from Coish *et al.* (1982) (dashes), Saunders (1985) (solid lines) and Strong and Saunders (1988) (dots).

Harbour (see Section 4.7) also display similar patterns. The unaltered diabase sample (250) from unit 4 of the Hill showing, however, displays a convex-upwards pattern typical of the intermediate and upper higher-Ti lavas and of boninites (Fig. 4-4). This particular sample has a Ti content of 0.60 wt%  $\text{TiO}_2$ , which is higher than the majority of Nippers Harbour diabbases (0 to  $\sim 0.37$  wt%  $\text{TiO}_2$ ).

The Nippers Harbour relatively unaltered diabbases show similar trends but higher MgO contents than komatiites from the Munro Township (Fig. 4-5). These higher contents probably are due to MgO addition during sub-seafloor alteration or to greater fractionation of Cr-spinel and olivine, or both. The  $\text{TiO}_2$  vs  $\text{Al}_2\text{O}_3/\text{TiO}_2$  and  $\text{CaO}/\text{TiO}_2$  plots (Sun and Nesbitt, 1978) shown in Figure 4-6, however, indicate that the rocks are closer to boninites.  $\text{Al}_2\text{O}_3/\text{TiO}_2$  and  $\text{CaO}/\text{TiO}_2$  ratios of Archaean komatiites are low ( $<20$  and  $<17$ ) and are close to chondrite, suggesting that their source is undepleted. Nippers Harbour ratios are of the order of  $<368$  and  $<93$ , which correspond to values from Betts Cove basalts (up to 492, Saunders, 1985;  $\sim 60$ , Sun and Nesbitt, 1978). The scatter of  $\text{CaO}/\text{TiO}_2$  seen in Figure 4-6 may be attributed to the mobility of CaO during sub-seafloor alteration. The high MgO and  $\text{SiO}_2$ , low  $\text{TiO}_2$ , Zr, Y and REE contents of Nippers Harbour diabbases are also reminiscent of boninites.

Several plots using relatively unaltered diabase samples were made to attempt to deduce the fractionation history of the Nippers Harbour ophiolitic rocks. The  $\text{FeO}_t/\text{MgO}$  vs Ni plot shown in Fig. 4-7a reflects the fractionation and accumulation of Ni-bearing olivine and possibly clinopyroxene. The flatter slope at higher  $\text{FeO}_t/\text{MgO}$  values indicates the cessation of such precipitation.

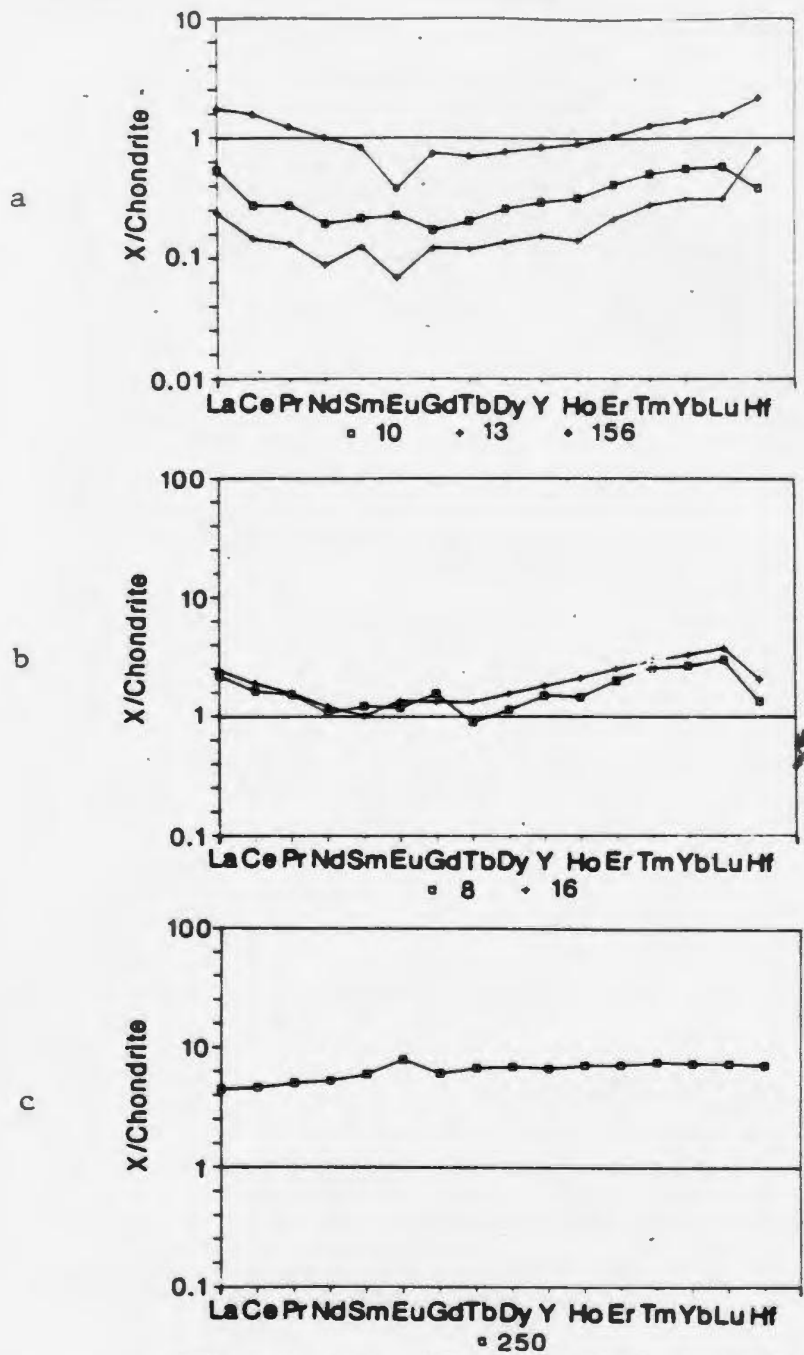
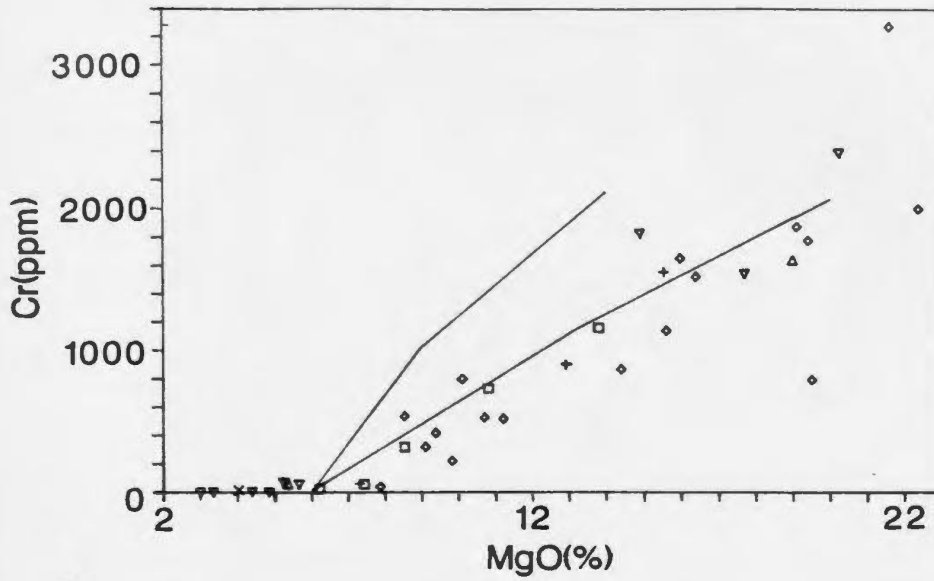


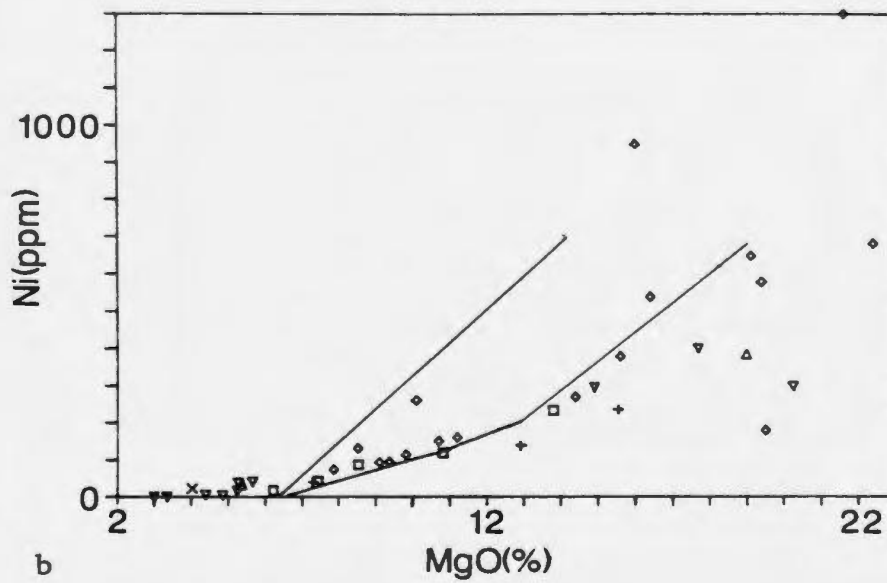
**Figure 4-4:** Rare-earth element diagrams

(a) Ultramafic samples, (b) gabbro samples, (c) unaltered diabase sample from unit 4, Hill showing. Sample numbers are depicted below plots. (Normalized according to Taylor and McLennan (1985))





a

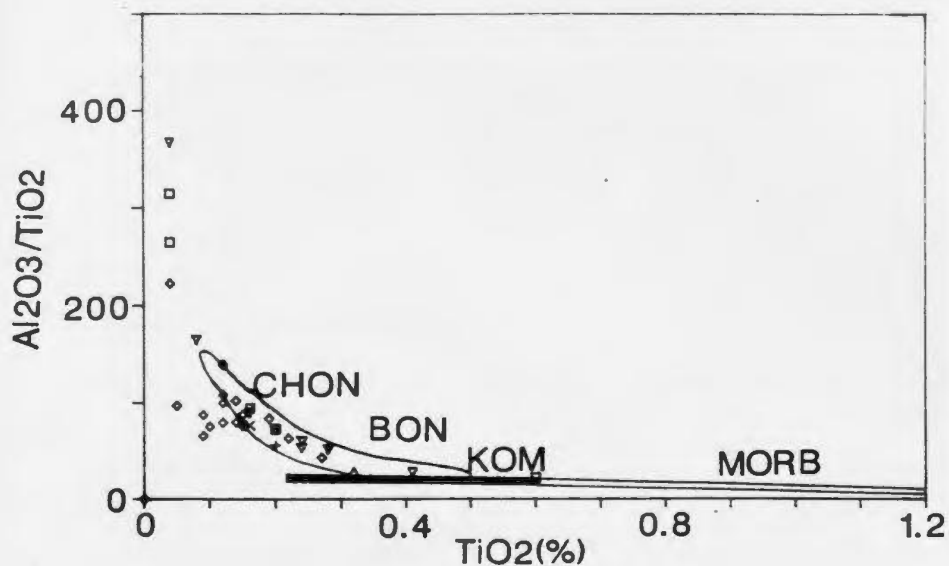


b

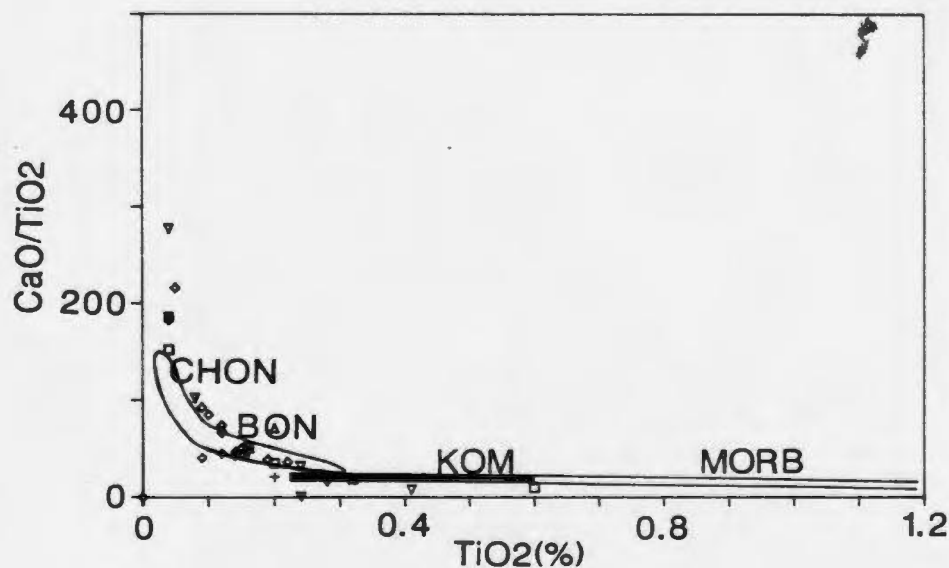
**Figure 4-5:** Variation diagrams

(a) MgO vs Ni, (b) MgO vs Cr. Areas between solid lines represent fields of komatiitic basalts from Munro townships (Arndt and Nesbitt (1982)).

Symbols as in Fig. 4-1.



a



b

**Figure 4-6:** Variation diagrams

(a)  $\text{Al}_2\text{O}_3/\text{TiO}_2$  vs  $\text{TiO}_2$ , (b)  $\text{CaO}/\text{TiO}_2$  vs  $\text{TiO}_2$ . Fields from Sun and Nesbitt (1978): KOM-komatiites and MORB-Mid-ocean ridge basalt, CHON-chondrite values; and from Hickey and Frey (1982): BON-boninites. Symbols as in Fig. 4-1.

Chromite is also an abundant minor phase in many diabase dykes. The Cr vs  $\text{FeO}_4/\text{MgO}$  (Fig. 4-7b) trend parallels the Ni vs  $\text{FeO}_4/\text{MgO}$  trend, reflecting the presence of chromite and suggesting that this mineral precipitated coevally with the Ni-olivine. The high Ni and Cr, and low  $\text{FeO}_4/\text{MgO}$  contents of many of the Betts Cove dykes led Coish and Church (1979) to suggest that the dykes were in part accumulative, the high values resulting from postcumulus growths on clinopyroxene and chromite. The similar contents of these elements in Nippers Harbour dykes also may result from such a process. Here, however, no postcumulus growth was observed due to the extensive uralitization of clinopyroxene.

Other plots of elements versus the mafic index Cr (not shown) show some curvilinear, but mainly poorly-defined trends, suggesting that their abundances may be controlled by factors other than crystal-liquid fractionation. MgO and Ni versus Cr trends support the argument for olivine and orthopyroxene precipitation. Negative Eu anomalies noted in some gabbro samples (Fig. 4-4b) suggest that low-pressure plagioclase fractionation may have occurred, as this tends to produce noticeable negative Eu anomalies in the melts which produce these rocks (Hanson, 1980). Some of the unaltered Nippers Harbour samples show positive Eu anomalies. This may be due to clinopyroxene fractionation, as clinopyroxene is an important phase in terms of removing REE from melts and in selectively enriching REE.

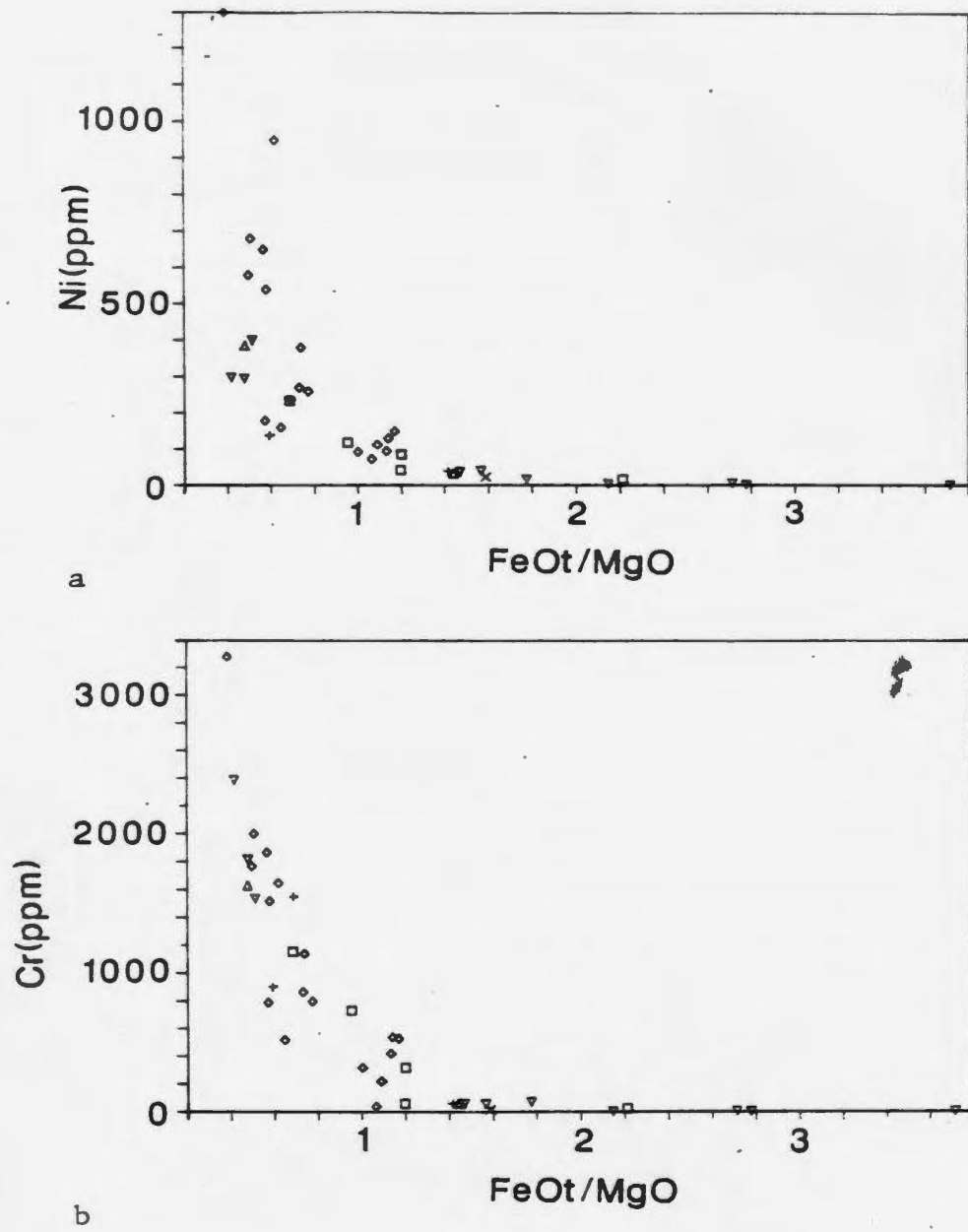


**Figure 4-7:** Variation diagrams

(a)  $\text{FeO}_t$  vs Ni (b)  $\text{FeO}_t$  vs Cr for unaltered samples. Symbols as in Fig. 4-1.

### 4.3. Chemical Gains and Losses

There are several methods that can be utilized to determine metasomatism with respect to major oxides and trace elements for hydrothermally altered rocks. Three techniques were used interactively for the study of chemical changes in Nippers Harbour rocks.

The first method is the simplest, and involves the comparison of normalized major and trace element data for rocks believed to be unaltered and altered. Table 4-2 displays a partial list of chemical data from the Hill showing. It is obvious that unit one, two and three rocks are enriched in  $\text{FeO}_t$ , Cu and Zn relative to unaltered unit four samples. It is somewhat surprising that unit four rocks are enriched in Zn relative to the other units, especially unit three. This may reflect the fact that unit four dykes are relatively fresh, and have not been subjected to metal leaching by hydrothermal fluids. The first three units also are depleted in CaO and  $\text{Na}_2\text{O}$  at varying degrees.

The second method involves the comparison of unaltered to altered samples by means of variation diagrams. Figure 4-8a and b depict trends for unaltered rocks showing MgO and Cr increase and little  $\text{SiO}_2$  variation, and can be related to olivine fractionation, as discussed above in Section 4.2.2. Minor deviations may be related to seafloor greenschist alteration or analytical error. When plots of Hill samples (Fig. 4-8c,d) are compared to these trends, it becomes obvious that there are deviations which relate to minor silica gain or loss, especially in unit one and two samples which contain the alteration assemblage chlorite-quartz-sulphide. Some chlorite compositions of altered rocks are plotted on Fig. 4-8. The loss of

UNIT	Fe <sub>2</sub> O <sub>3</sub> (%)	CaO (%)	Na <sub>2</sub> O (%)	Cu (ppm)	Zn (ppm)
UNIT 1					
159	19.63	0.78	0.01	5849	98
170	27.12	0.78	0.01	2468	43
199	15.99	2.40	0.05	20460	290
235	20.91	1.60	1.59	463	34
UNIT 2					
260	23.48	1.98	2.12	4164	57
175	17.52	1.32	0.03	479	217
195	27.62	1.46	1.29	748	42
261	14.88	1.36	1.57	2546	54
UNIT 3					
231	18.77	3.02	0.14	63	55
248	12.55	5.88	3.14	91	63
253	16.85	2.60	0.38	150	97
232	16.99	2.90	0.84	241	60
258	18.32	8.22	3.18	113	62
174	17.24	1.32	0.03	2478	78
UNIT 4					
256	8.75	8.22	3.18	106	148
250	13.66	5.66	2.28	248	127
251	10.18	6.98	3.04	156	327
252	9.33	7.36	1.65	48	436
254	10.18	6.00	3.04	54	145

**Table 4-2:** Partial list of major and trace element data, Hill showing

silica noted may reflect the inverse process of chloritization, as discussed by Strong and Saunders (1988) for the Tilt Cove lavas.

The Hill plots shown in Fig. 4-9c,d (compared to the fields for unaltered samples (Fig. 4-9a,b)) also show enrichments in  $\text{FeO}_t$ , as discussed above. Unit one and two rocks (squares, Fig. 4-9c,d) show greater enrichments in  $\text{FeO}_t$  than do unit three rocks (triangles). The Hill chlorites plotted are iron-rich, suggesting that they, pyrite and chalcopyrite may have accommodated some of the iron.

Plots of  $\text{Na}_2\text{O}$  vs  $\text{SiO}_2$  for unaltered samples (Fig. 4-10a) show several samples with relatively high  $\text{Na}_2\text{O}$  contents, possibly reflecting albitization, as noted in thin section. In comparison, Hill samples, especially units one and two, are more depleted in  $\text{Na}_2\text{O}$  (Fig. 4-10b). The plot of  $\text{CaO}$  vs  $\text{SiO}_2$  for unaltered samples showed considerable scatter, which may also be attributable to primary albitization, and was not used in these arguments.

Plots such as those in Figs. 4-8, -9 and -10 were made for each showing. They are compiled in Appendix B and are used in later discussions.

The above two methods of determining metasomatism are qualitative. The third method is more quantitative, facilitating comparison between the showings. It involves calculations of element and element oxide change with respect to an immobile element.

Studies of hydrothermal alteration in oceanic basalts have revealed that  $\text{Al}_2\text{O}_3$ ,  $\text{TiO}_2$ ,  $\text{P}_2\text{O}_5$ , Zr, Nb, V and Cr are generally immobile (Cann, 1970; Pearce

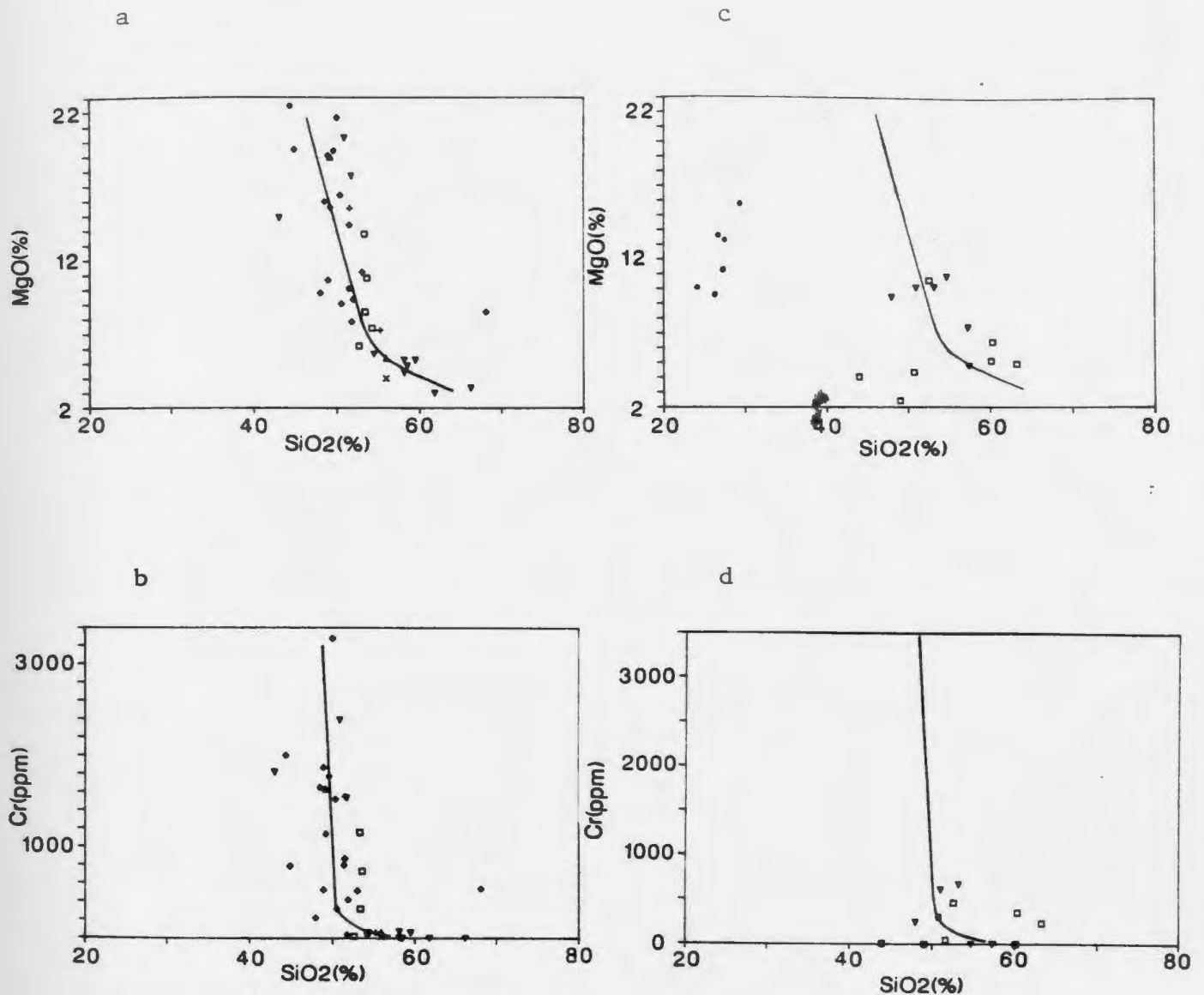


**Figure 4-8:** Variation diagrams

(a) SiO<sub>2</sub> vs MgO (b) SiO<sub>2</sub> vs Cr for unaltered samples. (c), (d) Similar plots for Hill samples. Symbols (a,b) as in Fig. 4-1; (c,d): Hill Units 1&2 (□), Hill Unit 3 (▽); chlorites (c,d): (•). Lines represent trends for unaltered samples shown in (a) and (b). See text for discussion.



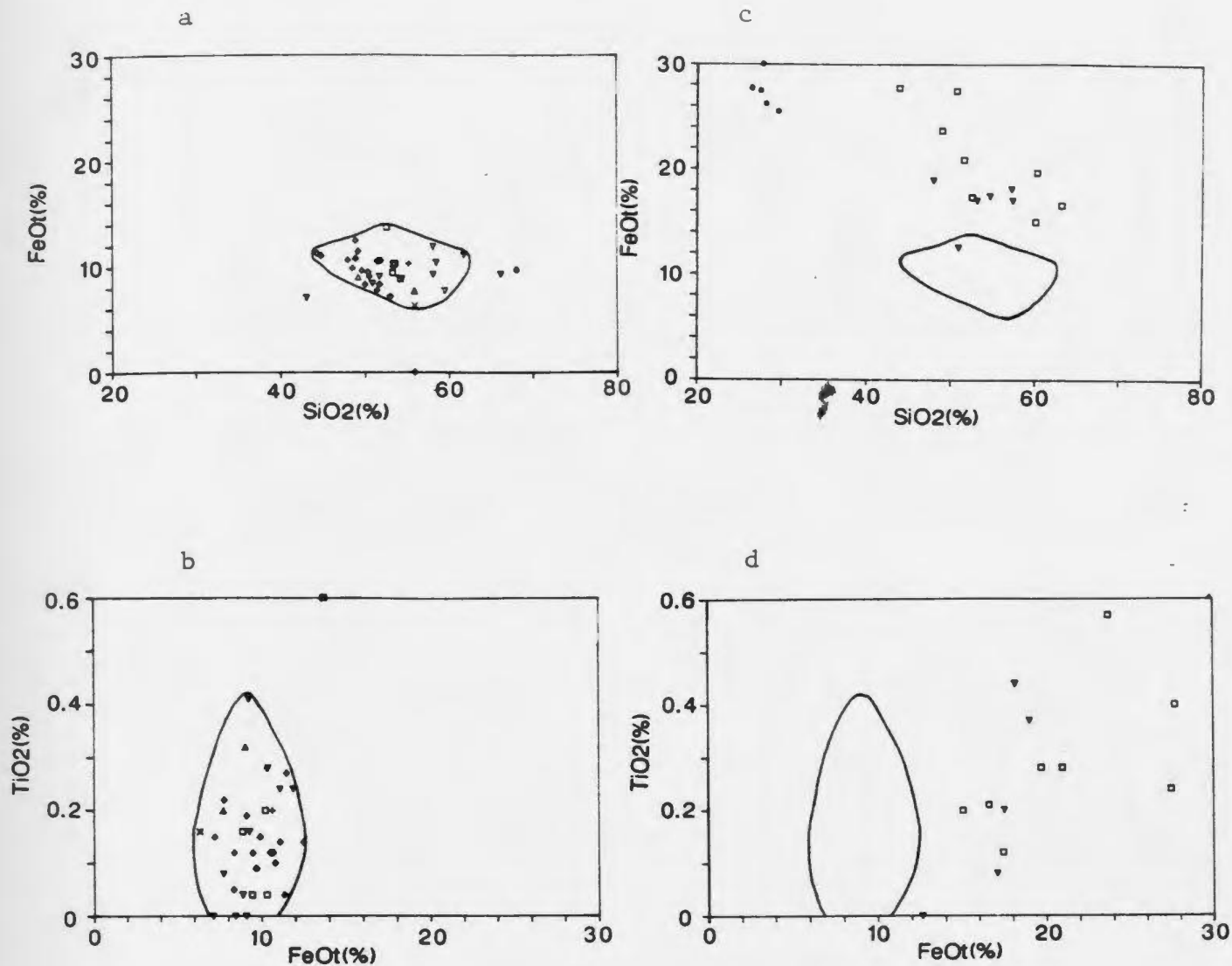
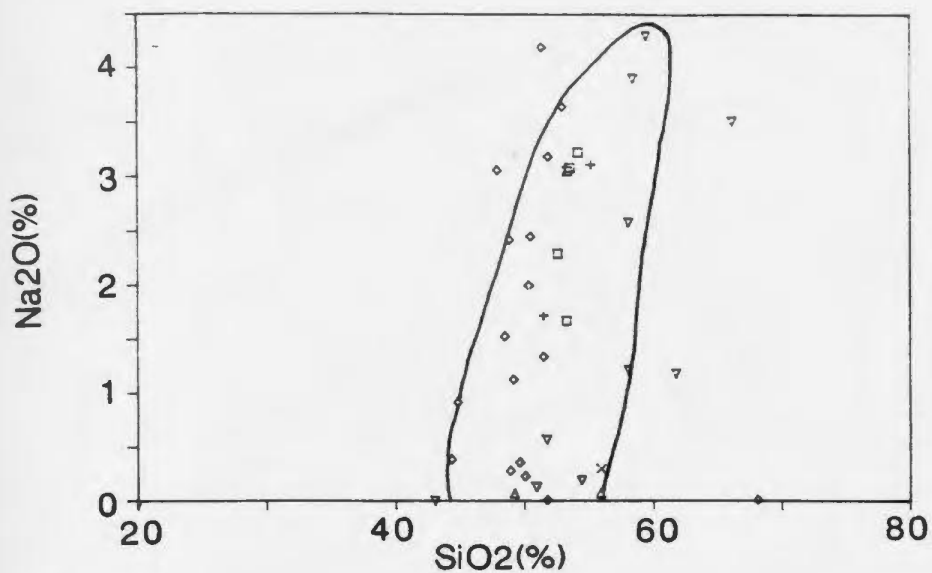


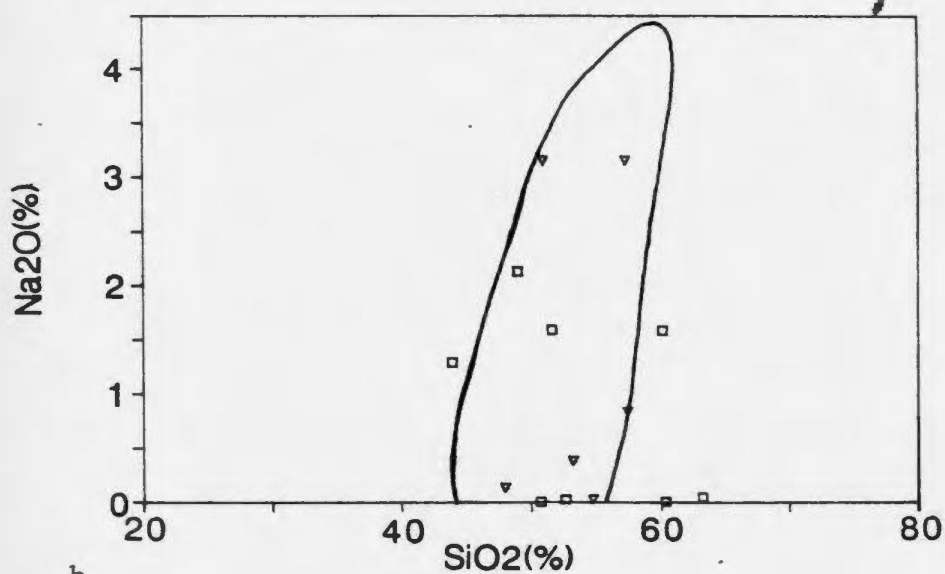
**Figure 4-9:** Variation diagrams

(a)  $\text{SiO}_2$  vs  $\text{FeO}_t$  (b)  $\text{FeO}_t$  vs  $\text{TiO}_2$  for unaltered samples. (c),(d)-Similar plots for Hill samples. Symbols as in Fig. 4-1 (a,b), and as in Fig 4-8 (c,d).

Envelopes represent fields for unaltered samples shown in (a) and (b).



a



b

**Figure 4-10:** Variation diagrams

(a)  $\text{SiO}_2$  vs  $\text{Na}_2\text{O}$ , unaltered samples; symbols as in Fig. 4-1. (b)  $\text{SiO}_2$  vs  $\text{Na}_2\text{O}$ , Hill samples; symbols as in Fig. 4-8 (c,d). Envelopes represent fields for unaltered samples shown in (a).

and Cann, 1973; Winchester and Floyd, 1976; Pearce, 1980). Concentrations of these elements in the Nippers Harbour mafic ophiolitic rocks were used as a basis for comparison to see which were the most immobile. Fig. 4-11 illustrates that relative proportions of  $\text{TiO}_2$ ,  $\text{Al}_2\text{O}_3$  and Zr for altered rocks from each showing are essentially identical to those from related unaltered rocks.

Zr was chosen as the reference immobile component in preference to the other two, because of the scatter of  $\text{TiO}_2$  and  $\text{Al}_2\text{O}_3$  shown in Fig. 4-11 and because  $\text{Al}_2\text{O}_3$  may have been mobile in some of the Gull Pond altered host rocks.

Calculations of enrichments and depletions of components were carried out by comparing the ratio of a major element to Zr in hydrothermally altered rocks to the range of this ratio in unaltered rocks. This method is outlined in Lydon and Galley (1986) and was used in preference to other mass-balancing methods (Gresens, 1967; Grant, 1986) because of the relative ease of the method and because it can be used even if density data are unavailable.

Diabases displaying greenschist (spilitic) assemblages were chosen as the unaltered rocks for this study. A sample calculation is documented in Appendix B, along with the atomic weights of elements for which chemical changes were calculated. Qualitative calculations showing the actual amounts of constituents that have been enriched or depleted per unit weight of original rock were carried out, assuming original Zr contents of 15 ppm for the Burton's Pond samples and 21 ppm for the remaining samples (see Section B.7). Volume changes could not be calculated due to the absence of specific gravity data.

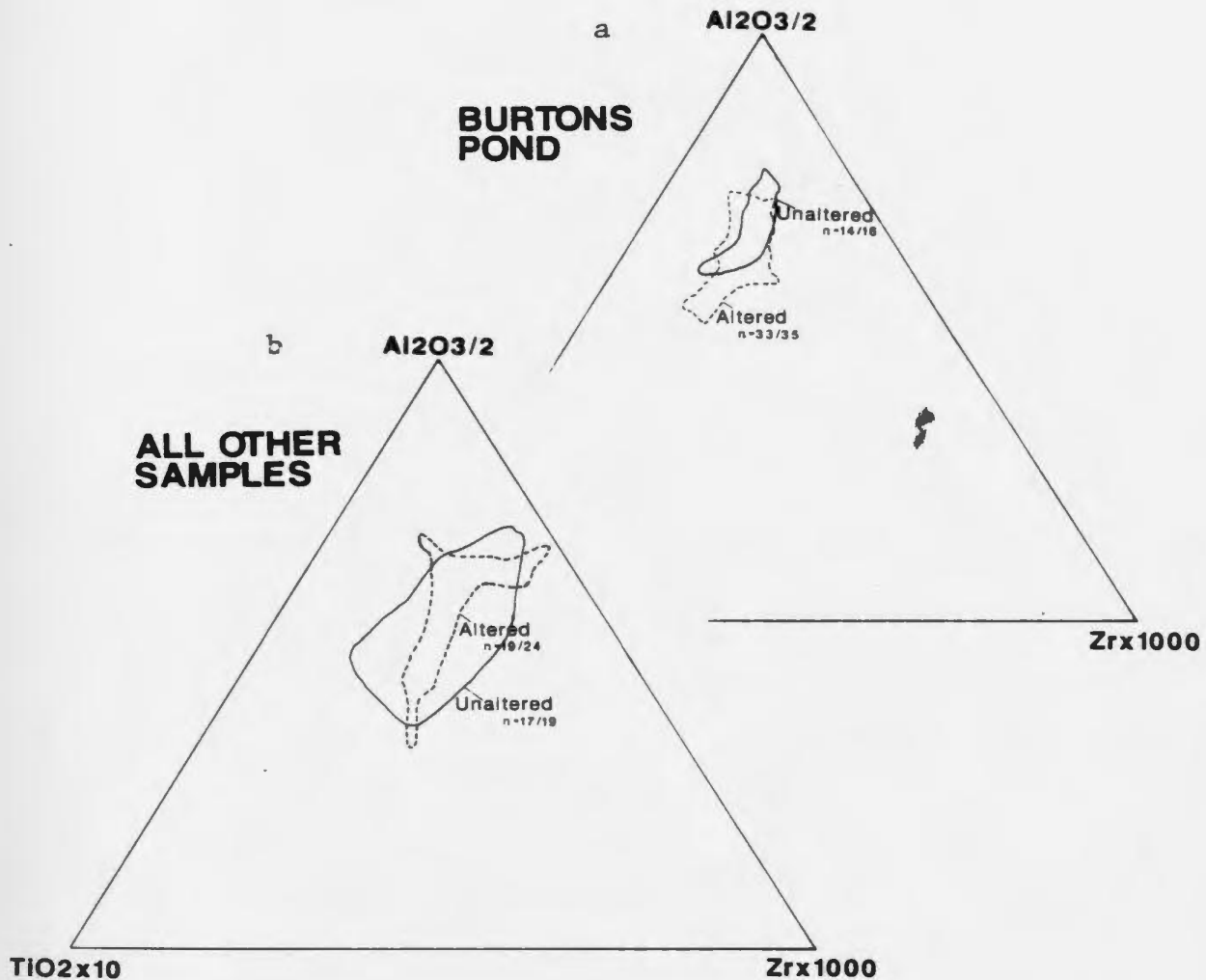


**Figure 4-11:** Triangular diagrams of 'immobile' elements for unaltered and altered samples

$n=(x/y)$  refers to the total number of samples included in the outlined field (x) compared with the total number of samples plotted of that type (y). (a) Burton's Pond samples, (b) All other samples.

The general results are recorded in Table 4-3. It should be noted that the changes recorded are the sums of all metasomatic changes which have affected the samples, and may not specifically relate to the hydrothermal events in question. More detailed discussions for each showing are given in following sections.

	Hill	Burtens Pond	Gull Pond	Showing No.2	Rogues Harbour
SiO <sub>2</sub>	-	-,+	-	nc	nc
FeO <sub>t</sub>	++	+	-,+	+	+
FeO <sub>t</sub> *		+			
CaO	--	+,-	-	--	--
MgO	nc	-	-	--	+
K <sub>2</sub> O	nc	+	++	++	++
Na <sub>2</sub> O	--	-,+	-	--	--
CO <sub>2</sub>		+			
H <sub>2</sub> O		+,-			
S		+			
Ba	nc	++	+	+	+
Sr	-	-,+	--	--	--

**Table 4-3:** Metasomatic changes affecting hydrothermally altered rocks, Nippers Harbour showings

Symbols are as follows: +:enrichment, ++:large enrichment, -:depletion, --:large depletion, nc: no change, FeO<sub>t</sub>\*:non-sulphide iron.

The showings, with the exception of Gull Pond, all show enrichments in  $\text{FeO}_4$  and no changes in  $\text{SiO}_2$ . Strong to weak depletions in  $\text{CaO}$  and  $\text{Na}_2\text{O}$  are noted for each showing. The Burtons Pond, Gull Pond, Showing No. 2 and Rogues Harbour showings display enrichments in  $\text{K}_2\text{O}$  and Ba, and depletions in Sr. Altered Hill rocks show no change in these components, or in  $\text{MgO}$ . All showings except the Rogues Harbour show depletions in  $\text{MgO}$ . Gains of  $\text{CO}_2$ ,  $\text{H}_2\text{O}$  and S were calculated for the Burtons Pond showing. Data for these three components were not available for the other showings.

The calculations indicated that  $\text{TiO}_2$ ,  $\text{P}_2\text{O}_5$ , Zr, Y, Cr, Ni, Sc, Nd, and to a great extent,  $\text{Al}_2\text{O}_3$ , are relatively immobile in even the most altered rocks.

#### 4.4. Hill Showing

The mineralogical characteristics of each of the four lithological units of the Hill showing are summarized in Appendix A. Units one and two comprise rocks composed solely of sulphides, quartz and chlorite with minor epidote and calcite. Rocks of unit three host these minerals as well as albite and unit four diabases which intrude the other units contain actinolite and feldspar, with minor chlorite and epidote.

Mottl (1983) composed an alteration assemblage diagram (Fig. 4-13) based on water-basalt reaction experiments at  $300^\circ\text{C}$ , 500 to 600 bars and seawater to rock ratios (w/r ratios) of 1, 3, 10, 50, 62 and 125 (Mottl and Holland, 1978; Mottl *et al.*, 1979; Seyfried and Bischoff, 1981; Seyfried and Mottl, 1982) and on mineral assemblage and composition data from Mid-Atlantic Ridge basalts (Humphris and Thompson, 1978).

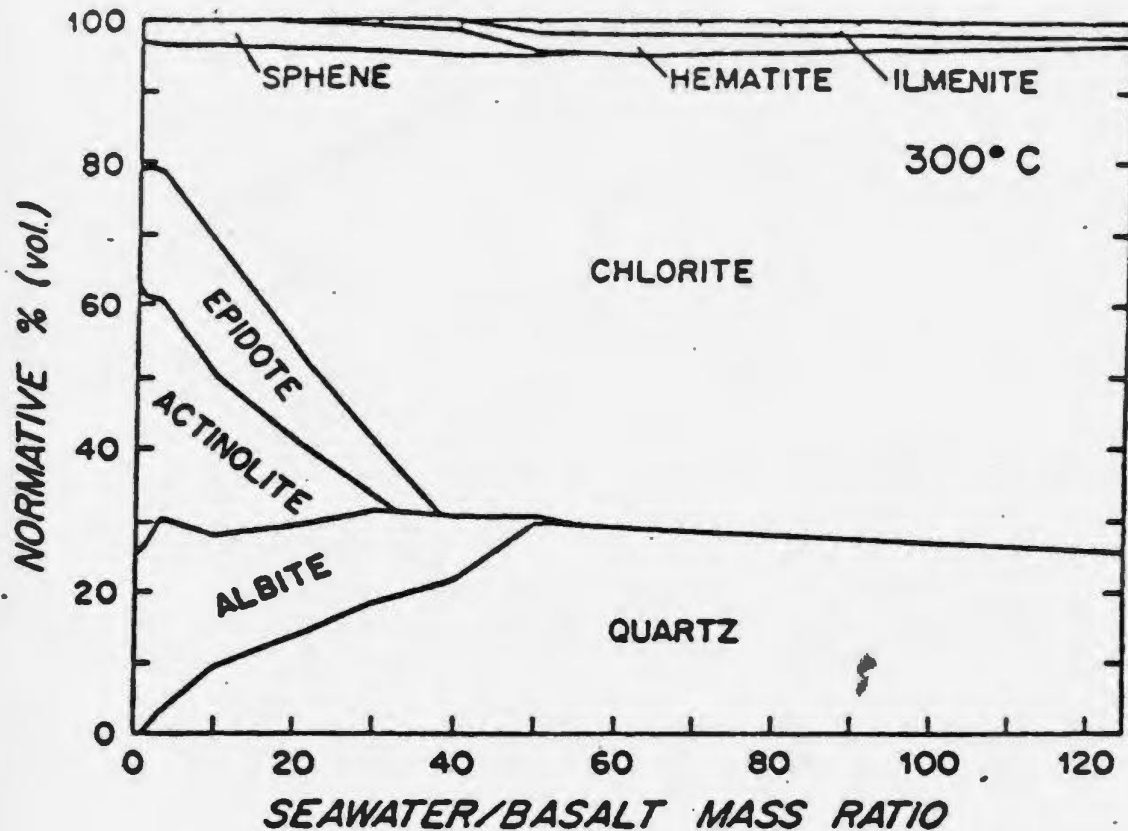


**Figure 4-12:** Alteration assemblages produced by varying seawater/rock ratios

From Mottl (1983). See text for details.

Mineral assemblages for the Hill lithologies correspond well to those depicted in Fig. 4-12. At 300°C and high w/r ratios (>50) a chlorite-quartz assemblage, as is present in units one and two, is stable. The chlorite-quartz-albite plus minor epidote assemblage of unit three is illustrated on Mottl's diagram for w/r ratios from 35 to 50. At w/r ratios of 2 to 35 the assemblage chlorite-albite-epidote-actinolite-quartz is stable and corresponds well to the unit four spilitic assemblages.

The metasomatic changes in Hill samples as calculated given the guidelines in section 4.3 are partially summarized in Table 4-3.  $\text{FeO}_1$ , Cu, and Zn have been added to the rocks, while CaO and  $\text{Na}_2\text{O}$  have been substantially removed. Unit one and two rocks show the most dramatic changes, while unit three rocks show the same changes to a lesser degree.

Much of the iron is fixed in the iron sulphides pyrite and chalcopyrite but some is fixed in iron-rich chlorite (Appendix F). Little change in  $\text{SiO}_2$  or MgO was noted. The presence of quartz in the alteration assemblage, therefore, probably is due to the release of free silica during a chemical reaction, possibly chloritization. The obvious explanation for the loss of CaO and  $\text{Na}_2\text{O}$  from the rocks is the destruction of feldspar by the hydrothermal fluid.

The three mineralogical assemblages and their associated chemical changes bear strong resemblance to alteration zones beneath massive sulphide deposits. At Betts Cove, the stockwork zone beneath the sulphide lens consists of a chlorite-quartz inner core enveloped by a chlorite-quartz-albite outer zone. This has been shown to be directly related to sulphide deposition by Saunders (1985). Almost all of the  $\text{Na}_2\text{O}$ , CaO and Sr has been removed from the core zone rocks, while  $\text{FeO}_1$ , Cu and Zn have been added to these rocks in significant quantities. Saunders (1985) explained the Fe enrichment by the addition of iron sulphides and iron-rich chlorites (with iron contents up to 27 percent). She suggested that Cu was leached from pyroxene and basalt glass and Zn from feldspar by acidic, convecting hydrothermal seawater fluids and subsequently redeposited in altered rocks. The depletion of  $\text{Na}_2\text{O}$ , CaO and Sr probably resulted from the destruction of feldspar in the fluid conduit.



At Tilt Cove, mineralization-related alteration is characterized by stockwork chlorite-quartz-pyrite, but is distributed non-uniformly over a larger area than the pipe described for Betts Cove (Strong and Saunders, 1988).

In general, the cores of stockwork zones beneath massive sulphides from the Canadian Archaean, Newfoundland, Cyprus, and modern-day settings are characterized by the formation of chlorite and quartz, generally accompanied by sulphide (pyrite). Fe-rich chlorites have been documented in alteration assemblages for Newfoundland massive sulphide stockwork zones (Lushes Bight Group, Lady Pond, Little Deer, Little Bay, (Gale 1969; Papezik and Fleming 1967); Whalesback (Bachinski, 1977); Betts Cove (Saunders, 1985); Tilt Cove (Strong and Saunders, 1988)). They result from the addition or non-removal of  $\text{FeO}_t$  to the original rock during alteration of pyroxenes, amphiboles or plagioclase. Chlorites in Archaean and recent deposits are Mg-rich (Millenbach (Riverin and Hodgson, 1980); Corbet (Knuckey *et al.*, 1982; Knuckey and Watkins, 1982); Galapagos sulphide mounds (Jonasson and Franklin, 1987).

Extreme metasomatic changes resulting from additions of  $\text{FeO}_t$  and  $\text{MgO}$  are reflected by the talc-actinolite assemblages reported at Mattagami Lake. Metamorphism in the Flin-Flon-Snow Lake and Manitouwadge area has resulted in the formation of cordierite-anthophyllite rather than chlorite (Pye, 1960; Froese, 1969; Whitmore, 1969; James *et al.*, 1978; Walford and Franklin, 1982).

In many cases (Mattiathi, Cyprus, Millenbach, Corbet, Kuroko) the inner zones are surrounded by outer sericite/illite or kaolinite zones. These reflect

addition of  $K_2O$  to the rocks;  $K_2O$  which may have been removed from the core zone and re-deposited in this zone. Such  $K_2O$ -rich zones are absent in Newfoundland deposits.

The presence of free quartz in the alteration zones is not necessarily a result of the addition of  $SiO_2$ . Only at Cyprus is a hydrothermal addition of  $SiO_2$  recorded. In most cases, the formation of quartz is due to the redistribution of other elements during alteration. An example is the chloritization of amphiboles or feldspars, releasing free silica, as suggested above for altered Nippers Harbour rocks.

In most documentations of alteration zones,  $CaO$ ,  $Na_2O$ , and to a lesser extent,  $K_2O$  are depleted in the alteration zones. This reflects the destruction of feldspar by hydrothermal fluids.  $Al_2O_3$  is removed only under extreme conditions.

A discussion of the genesis of the Hill showing is given in Chapter six.

#### **4.5. Gold-Bearing Showings: Burtons Pond, Gull Pond, Showing No. 2**

The Burtons Pond, Gull Pond and Showing No. 2 sulphide-bearing samples carry significant gold and are characterized by similar alteration, thus their geochemistries are discussed collectively. Because the Burtons Pond showing is the largest and displays the most intricate alteration, it will be used as the basis for description of the alteration at the other two localities.

#### 4.5.1. Burtons Pond

Metasomatic calculations carried out for Burtons Pond in Section 4.3 showed additions of  $\text{FeO}_t$ , Ba, K,  $\text{H}_2\text{O}$ ,  $\text{CO}_2$ , S, depletions of  $\text{MgO}$ ,  $\text{Na}_2\text{O}$ , Sr and variable to minor enrichments and depletions of  $\text{CaO}$  and  $\text{SiO}_2$ . The most abundant alteration minerals are sulphides, chlorite, quartz, albite, calcite and minor sericite. Burtons Pond chlorites are iron-rich (Appendix F). Clearly enrichments in  $\text{FeO}_t$  can be attributed, as they were at the Hill showing, to formation of this mineral and of iron-bearing sulphides (pyrrhotite, chalcopyrite, arsenopyrite).

The  $\text{SiO}_2$  vs  $\text{CaO}$  plot of unaltered samples (not shown) displayed no definitive magmatic trend. This may be due to spilitization of diabases, removing  $\text{CaO}$  from plagioclase, replacing it with  $\text{Na}_2\text{O}$  from seawater, and forming albite. The scatter of data seen in the Burtons Pond data, therefore, may also reflect this process. However, the triangular plots shown in Fig. 4-13 may confirm the enrichments and depletions of  $\text{CaO}$  as calculated in Section 4.3. Both of these plots depict additions and depletions of  $\text{CaO}$  above and below the trends shown by unaltered rocks. Samples rich in Au (above 500 ppb, shown as open circles) are particularly affected.

Burtons Pond samples show mainly depletions in  $\text{Na}_2\text{O}$ , although some samples are enriched in this compound. Several Burtons Pond sulphide-bearing veinlets carry fresh albite, suggesting that the sodium depleted in host rocks may have been re-deposited in part in veins.

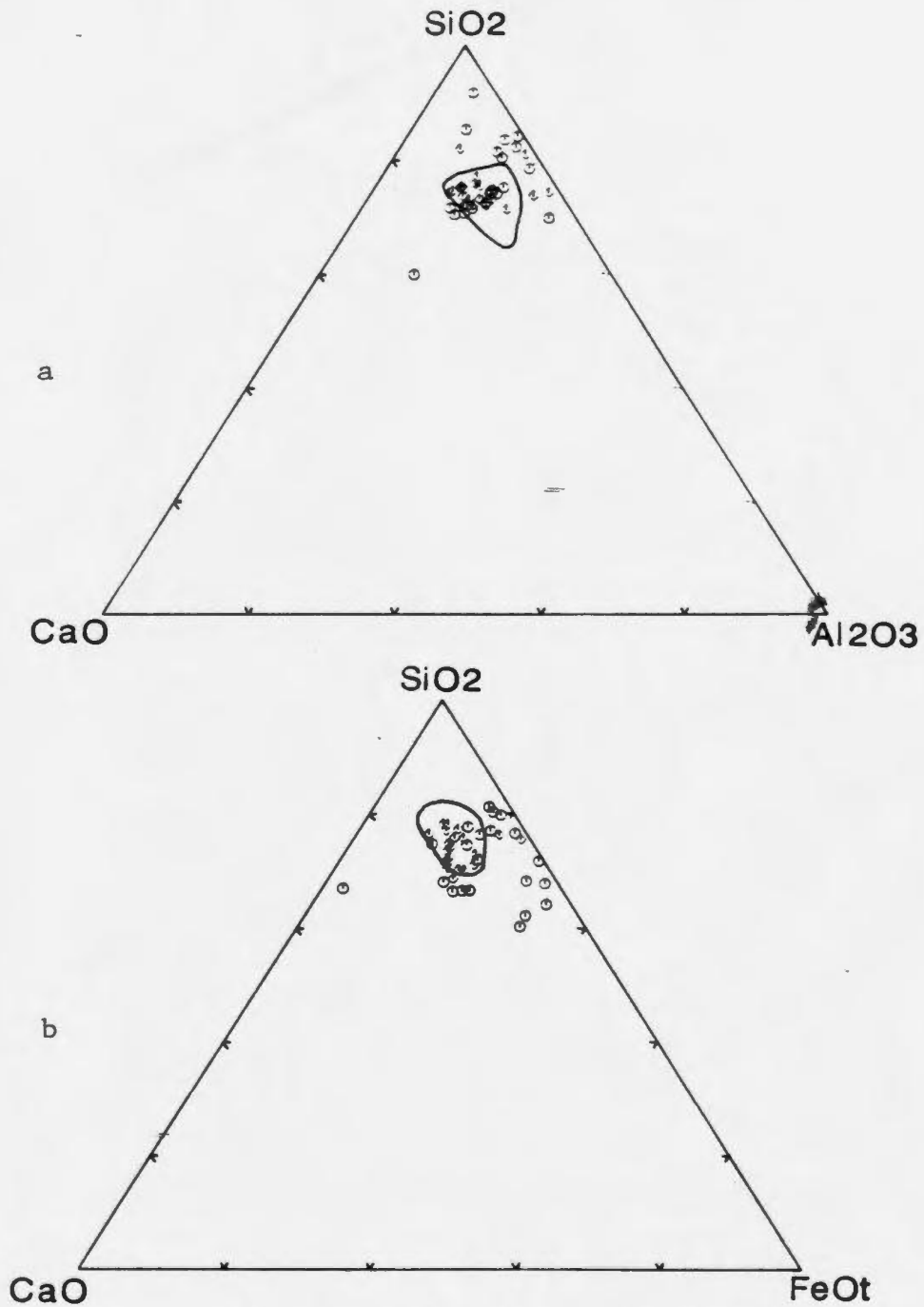


**Figure 4-13:** Triangular diagrams

(a)CaO-SiO<sub>2</sub>-Al<sub>2</sub>O<sub>3</sub> (b)CaO-SiO<sub>2</sub>-FeO<sub>t</sub> for Burton's Pond samples. Circled fields represent unaltered samples.

Enrichments in  $K_2O$  are minor, and generally correspond to samples of alteration type B, where albitized plagioclase is altered to sericite. Likewise, samples carrying calcite generally show the most distinctive  $CO_2$  enrichments.

#### 4.5.1.1. Relationship of Metasomatism to Gold Content

Gains or losses of components (as g/kg per original rock) were plotted against distance (Figs. 4-14, -15, -16) for the two Burtons Pond drill holes studied in detail, and against sample number for a series of samples (Section A-see Appendix E for sample locations) taken across the main fault zone. These plots were compared with plots of gold content, in order to evaluate the relationship between gold deposition and metasomatism. The method for the calculation of g/kg values is outlined in Appendix B.7. Briefly, it involves the comparison of an oxide/Zr molar ratio of a hydrothermally altered rock to that of a range of unaltered rocks, for a 100 g sample. The absolute value of the difference between the altered and unaltered molar ratio per 100 g is then converted to g/kg, using the atomic weight of the oxide or element in question.

In each of the three sets of plots, high gold contents correspond best (but not ubiquitously) with enrichments in total iron, non-sulphide total iron, and sulphur. This suggests that some gold deposition may be related to sulphides and iron-chlorite formation. Gold grains have been detected on chalcopyrite and pyrrhotite edges, and enclosed in pyrrhotite and arsenopyrite, supporting the above correlation between sulphur enrichment and gold content. It is possible that, even if the gold did not form coevally with sulphides, the latter may have acted as a nucleus for gold precipitation. Samples altered to chlorite-quartz and chlorite-quartz-albite display the most anomalous gold contents.

## SECTION A

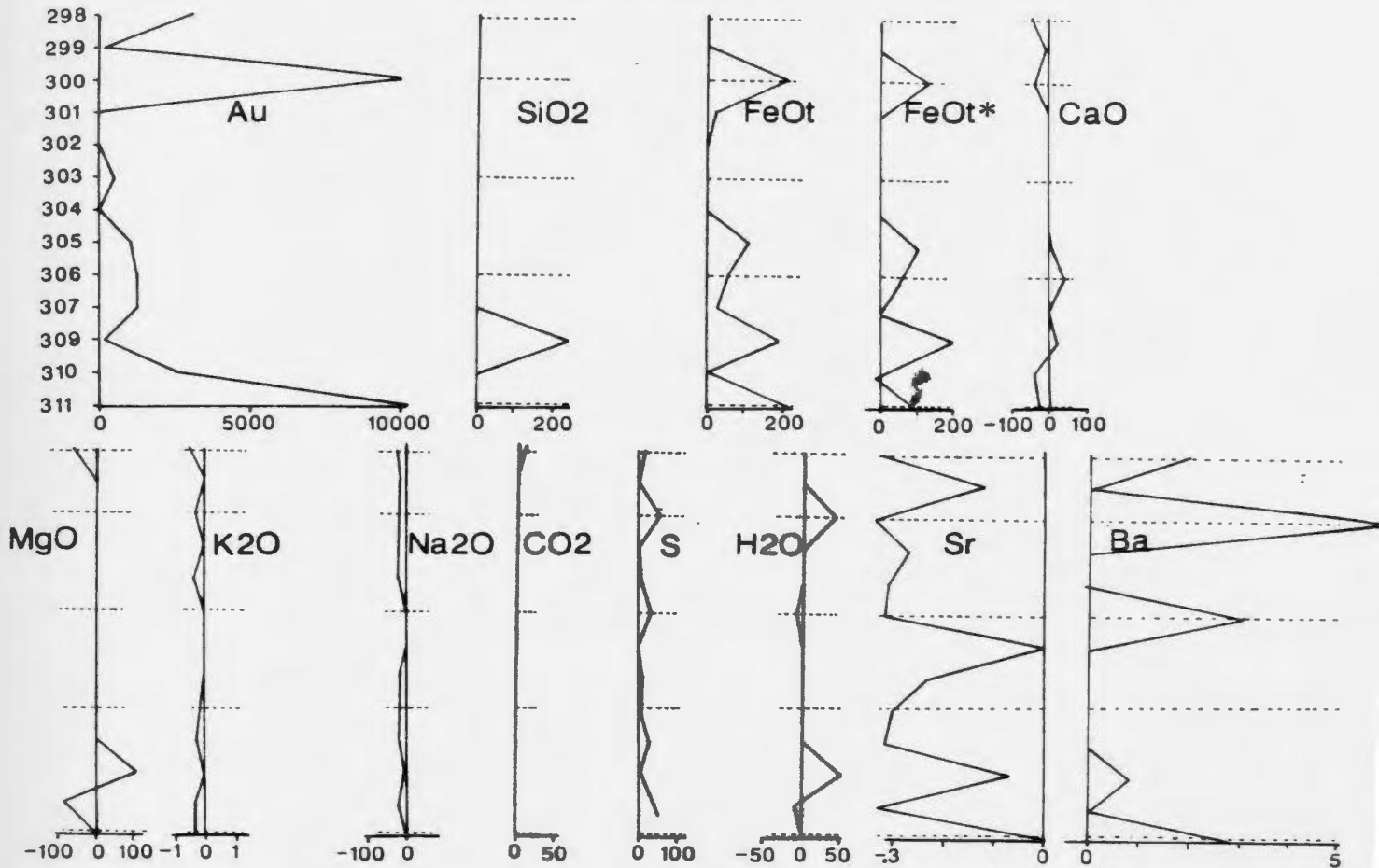


**Figure 4-14:** Relationship of gold content to metasomatism  
Burtons Pond Section A

Au is expressed in ppb; all other oxides and elements in g/kg; positive number indicates enrichment, negative number indicates depletion. FeOt\* represents non-sulphide iron.

## HOLE 2

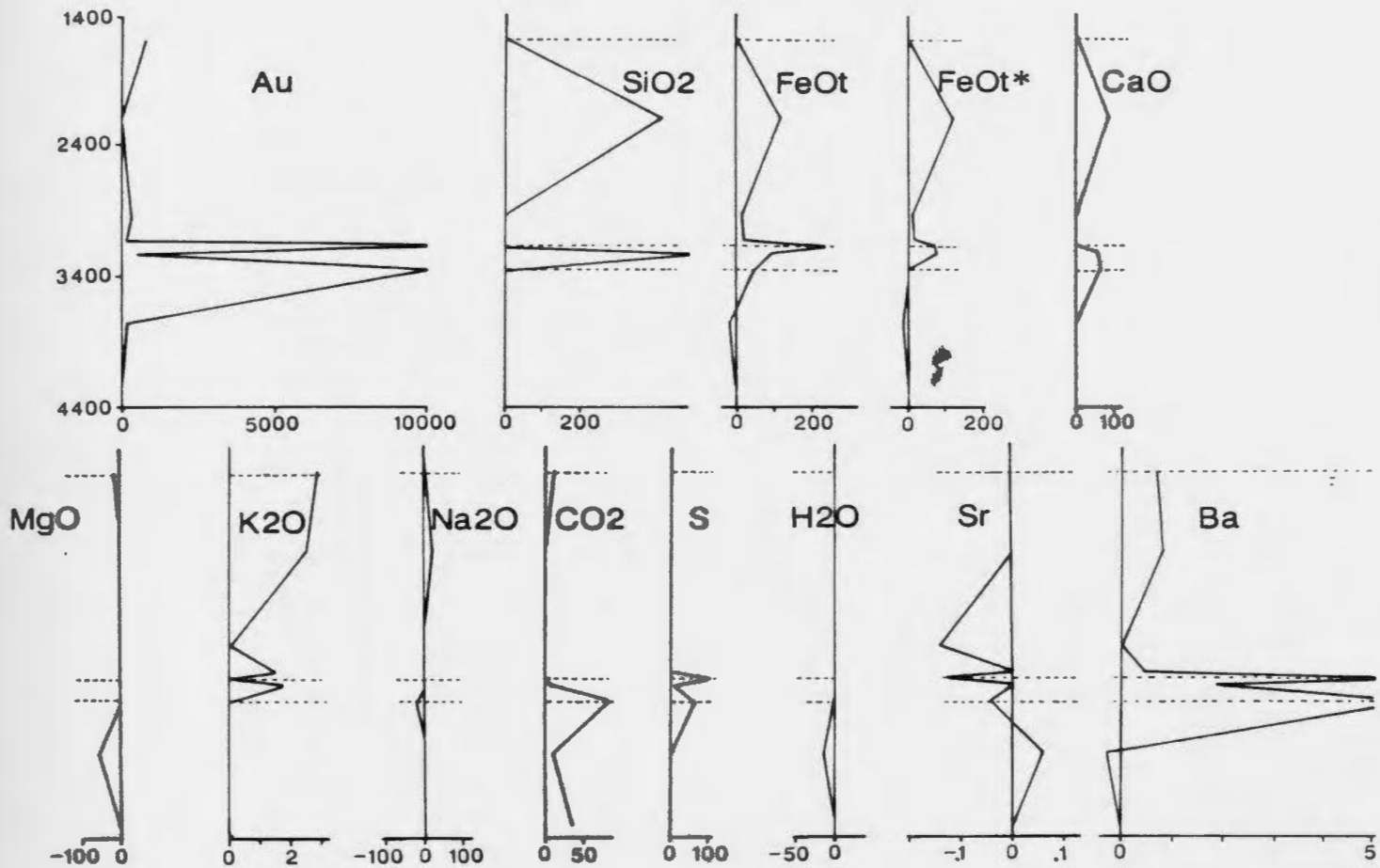


**Figure 4-15:** Relationship of gold content to metasomatism  
Burtons Pond drill hole No. 2

See Fig. 4-14 for explanation.

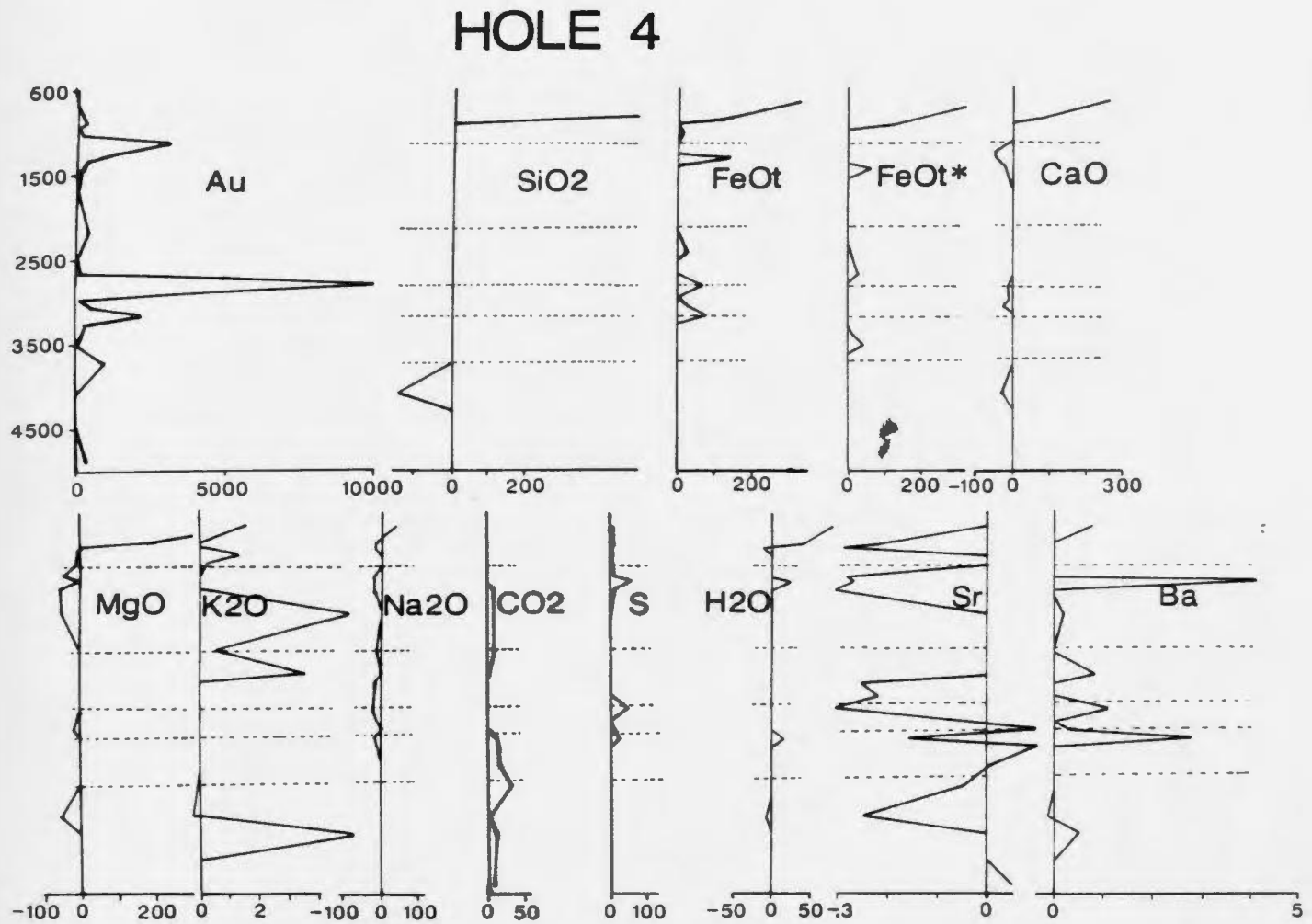


**Figure 4-16:** Relationship of gold content to metasomatism  
Burton's Pond drill hole No. 4

See Fig. 4-14 for explanation.



Enrichments of  $\text{CO}_2$ , though not large in magnitude (generally  $< 35 \text{ g/kg}$  original rock) correlate well with gold. Gold grains have been detected in quartz-calcite veins. This suggests that the fluids which carried gold also carried minor quantities of  $\text{CO}_2$ , and furthermore, that they precipitated at similar sites, under similar conditions.

There is a good correlation between gold enrichment and Sr depletion which may reflect the partial destruction of feldspar by the hydrothermal fluids. CaO and  $\text{Na}_2\text{O}$  depletions also correlate reasonably well with high Au content, confirming this hypothesis. Albite forms a significant component of the quartz-chlorite alteration assemblage in some samples; this may explain the relatively small and sometimes insignificant depletions of  $\text{Na}_2\text{O}$  noted. Scattered enrichments of CaO are recorded in Hole 2 and Section A, these correlate with  $\text{CO}_2$  enrichments in samples containing calcite, implying that some of the CaO mobilized from any remaining feldspar or from actinolite was fixed as calcium carbonate (calcite).

$\text{K}_2\text{O}$  and especially Ba also may be a minor component of the gold-bearing fluid, as some of their enrichments also correspond to high gold contents. These elements are both components of sericite, which is a member of alteration assemblage B (chlorite-sericite) and C (calcite-sericite). These assemblages therefore may have been produced by the same fluids which deposited gold.

$\text{MgO}$ ,  $\text{SiO}_2$  and  $\text{H}_2\text{O}$  enrichments and depletions do not correlate well with gold enrichment.

The alteration assemblages and their parageneses, as well as these metasomatic changes can be used to write unbalanced chemical reactions for the processes involved (Fig. 4-17). Mineral formula were calculated from averages of electron microprobe analyses for Burtons Pond amphiboles (average of 11), epidotes (2) and chlorites (2) (Appendix F). Reaction I is suggested to form the predominant chlorite-quartz+/-albite assemblage, A. Reactions II and III probably resulted in alteration assemblage (B), sericite-chlorite and (C), sericite-calcite. These reactions suggest that the  $X_{CO_2}$  of the fluids is very low,  $<0.01$  for temperatures below  $350^{\circ}C$  (Carmichael, 1984; Clarke *et al.*, 1986).

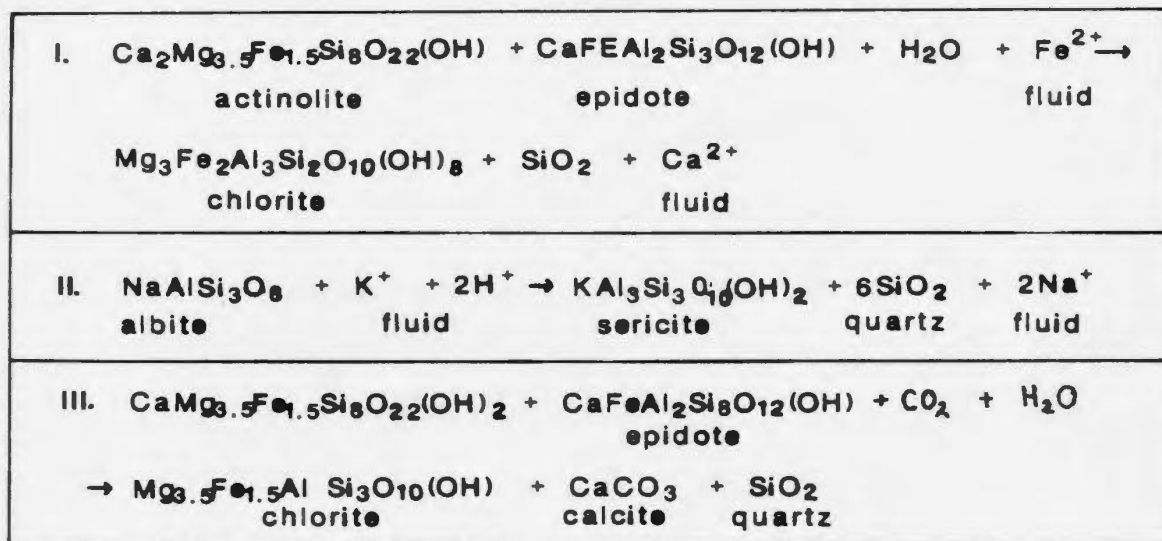


**Figure 4-17:** Chemical reactions affecting Burtons Pond rocks

Altered host rocks carrying sulphides at Gull Pond and Showing No. 2 are composed of sericite, chlorite and quartz. The Gull Pond rocks also contain minor calcite, and are cut by quartz-calcite veinlets. Brecciated Showing No. 2 sulphides are cemented by quartz and calcite.

Table 4-4 documents the chemical changes which have modified the Gull Pond rocks and two samples from Showing No. 2. As most of the diabase alteration at the latter is now represented by small (1 cm to 5 cm) chlorite-sericite-quartz fragments in the quartz vein, attempts to quantify their alteration were not definitive. The two representative samples were taken from a large diabase fragment in the quartz vein and from diabase in immediate contact with the vein.

Essentially all of the samples have gained  $K_2O$  and Ba, which are accommodated in sericite. They likewise have lost CaO,  $Na_2O$  and Sr, reflecting the consumption of feldspar to produce sericite and possibly chlorite.

It is interesting to note that there are no anomalous changes in total iron at Gull Pond. It is true that there are iron sulphides there (pyrrhotite altering to pyrite, and pyrite), but the chlorites are Mg-rich rather than Fe-rich (Appendix F). Chlorites of Showing No. 2 altered rocks are Fe-rich. The silica losses may be attributable to chloritization which releases free silica as outlined in reactions I and II. (Fig. 4-17).

Anomalous gold values show no exclusive correlations, but in general seem

Gull Pond

Sample	Au	FeOt	SiO <sub>2</sub>	CaO	MgO	Na <sub>2</sub> O	K <sub>2</sub> O	Ba	Sr
206	9832	-	-	-67	-56	-23	+27	+1.2	-
269	-	-	-	-	-	-5	+38	-	-.4
262	-	+177	+315	-48	-10	-22	+42	-	-.5
209	74.2	-	-281	-	-	-3	+19	+2.1	-.7
207	48.4	-	-365	-7	-	-8	+15	+1.7	-.7
54	-	-	-925	-69	-	-	-	-.45	-.9

Showing No. 2

11002	>10000	+199	-307	-69	-80	-23	+36	+2.6	-.8
11009	7	+99	-	+154	-	-20	-	+5.0	+5

**Table 4-4:** Chemical changes of Gull Pond and Showing No.2 altered samples

Gains and losses calculated as g per kg oxide of original rock. -:loss, +:gain.

See Appendix B, Section B.7 for calculation method.

to be related to gains of K<sub>2</sub>O and Ba, found in sericite and losses of CaO, MgO and Na<sub>2</sub>O. The association of gold mineralization with sericite is a feature common to many Archaean gold deposits (Bain, 1933; Kerrich and Fryer, 1979; Whitehead et al., 1980; Kerrich and Fyfe, 1981; Colvine et al., 1984).

#### 4.6. Rogues Harbour, Welshs Bight

Altered gabbro samples were selected from the quartz vein along the Stocking Harbour Fault (Fig 2-1) for alteration studies. Regretably, no immediate host rock samples at Welshs Bight could be collected, due to the lack of good exposure. These altered samples contain sulphides (pyrite, chalcopyrite), sericite, low-Fe, high-Mg chlorite, and quartz but, in contrast to gold-rich samples at previous showings, no carbonate. Sulphide-rich samples at Rogues Harbour contain considerably lower amounts of gold (only up to 535 ppb).

##### Rogues Harbour

Sample	FeO <sub>t</sub>	SiO <sub>2</sub>	CaO	MgO	Na <sub>2</sub> O	K <sub>2</sub> O	Ba	Sr
139	+354	-	-68	+303	-	+42	+2.5	-.8
145	+98	-	-68	+102	-22	+4	-	-.9
215	+244	-	-68	+108	-23	-	-	-1
144	-	-	-42	+56	-20	-	-	-.9

**Table 4-5:** Chemical changes of Rogues Harbour altered samples

See Table 4-4 and Appendix B.7 for explanation.

Considerable amounts of both FeO<sub>t</sub> and MgO have been added to the rocks (Tables 4-3 and 4-5). This is not surprising, given the quantity of iron sulphide and Mg-rich chlorite in the samples. K<sub>2</sub>O is accommodated in sericite, which has replaced feldspar, resulting in losses in CaO, Na<sub>2</sub>O, and Sr.

#### 4.7. Rare Earth Elements

Studies of rare earth elements (REE) behavior in hydrothermal systems are restricted by the lack of data on the partitioning of REE between hydrothermal solutions and rock phases (Cullers and Graf, 1984). Wall rocks can mask REE patterns of initial solutions and can also provide REE to the fluid during alteration. REE data to date on hydrothermal deposits (New Brunswick massive sulphides, Graf, 1977; Dome Mine, Abitibi region, Kerrich and Fryer, 1979) show a wide variation depending upon the mineral analysed, geological setting of the deposit and positioning of the sample within the paragenetic sequence (Cullers and Graf, 1984). REE patterns of hydrothermally altered rocks depend mainly on the gangue mineralogy of the samples analysed, as most sulphide and oxide minerals do not host the REE elements.

Several authors have shown that the LREE are mobile during low temperature alteration, metamorphism and spilitization of oceanic crust (Frey *et al.*, 1974; Hellman and Henderson, 1977; Ludden and Thompson, 1978). Eu anomalies in altered rocks likely are due to the fractionation of REE during fluid/rock interaction or by the preferential alteration of feldspar (Graf, 1977). The latter would result in a negative Eu anomaly for the rock REE pattern.

Several sulphide and altered host rock samples of the Nippers Harbour showings were analysed for REE using the ICP-MS at Memorial University. The results are presented in Appendix D.

Plots of REE abundances were made for each of the lithological units at the

Hill showing. There is not much variation between each of the REE patterns, as shown in Fig. 4-18. Unit 1 quartz-chlorite-sulphide rocks are more depleted in LREE than other units; this may be attributable to the higher degree of alteration in these rocks. The negative Eu anomaly could be a result of the leaching of feldspar in these rocks.

Unit 2 samples (175, 261) show higher LREE abundances and positive Eu anomalies. This likely is a reflection of very minor amounts of feldspar remaining in these samples. Although these samples are quartz-chlorite-sulphide-bearing, as are unit 1 rocks, their alteration, as shown by the REE patterns, is less intense.

Sample 254 from unit 3 is depleted in MREE relative to other Hill samples. The REE pattern of the unaltered unit 4 sample, 250, has a convex-upwards pattern which is discussed in section 4.2.2.

The Burtons Pond samples (298-altered diabase; 311-quartz-carbonate-sulphide vein) display markedly similar HREE but different LREE concentrations (Fig. 4-19). HREE contents are considerably lower than those of relatively unaltered diabase (Fig. 4-4c). LREE have been depleted in sample 298, which consists of quartz, Fe-rich chlorite, sulphides, and gold, but have been enriched substantially in the quartz-sulphide vein (sample 311). It appears that this could be a localized event: LREEs which were added to the fluid during alteration of an initial lithological equivalent to sample 298 could have been redeposited in gangue minerals of sample 311. It is possible that the alteration of plagioclase was involved to produce sample 298, as a negative Eu anomaly is depicted for this

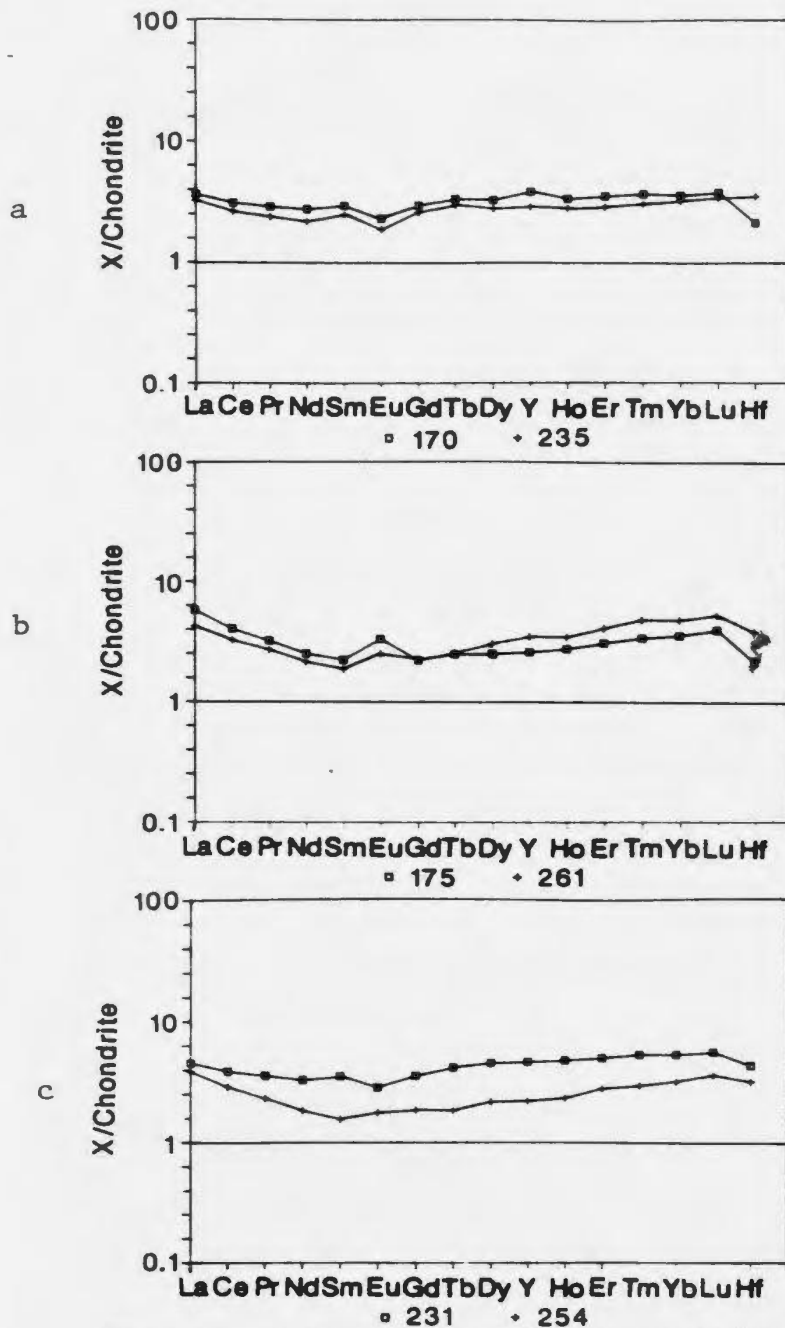


**Figure 4-18:** Rare-earth element diagrams

(a) Unit one altered quartz-chlorite samples, (b) Unit two altered quartz-chlorite samples, (c) Unit three altered quartz-chlorite-albite samples; Hill showing. (Normalized according to Taylor and McLennan (1985)).



sample. Minor albite occurs with quartz in sample 311; this may account for the positive Eu anomaly noted. No minor phases such as apatite, epidote or tourmaline, which are known to concentrate REE, were noted.

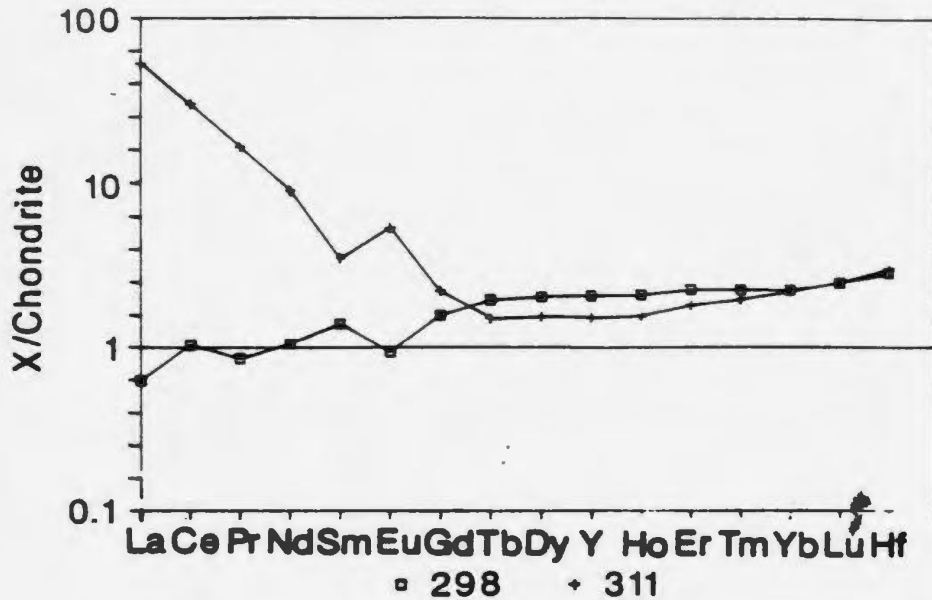


**Figure 4-19:** Rare earth element diagram

Burtens Pond samples. Sample 298 is an altered diabase, and 311 is a quartz-carbonate-sulphide vein (Normalized according to Taylor and McLennan (1985)).

REE patterns for two altered samples, one from Gull Pond (209-altered diabase) and one from Rogues Harbour (139-chlorite schist-altered gabbro), are depicted in Fig. 4-20. The pattern shown by the Gull Pond sample is similar to that shown by the altered diabasites from Unit 3 of the Hill showing, but is slightly more depleted in MREE. The Rogues Harbour chlorite schist, taken from within the main sulphide-quartz zone, shows a similar REE pattern to that of unaltered gabbro (Fig. 4-4b), but is more depleted in LREE and more enriched in MREE. This may be due to the alteration of feldspar and possibly clinopyroxene.

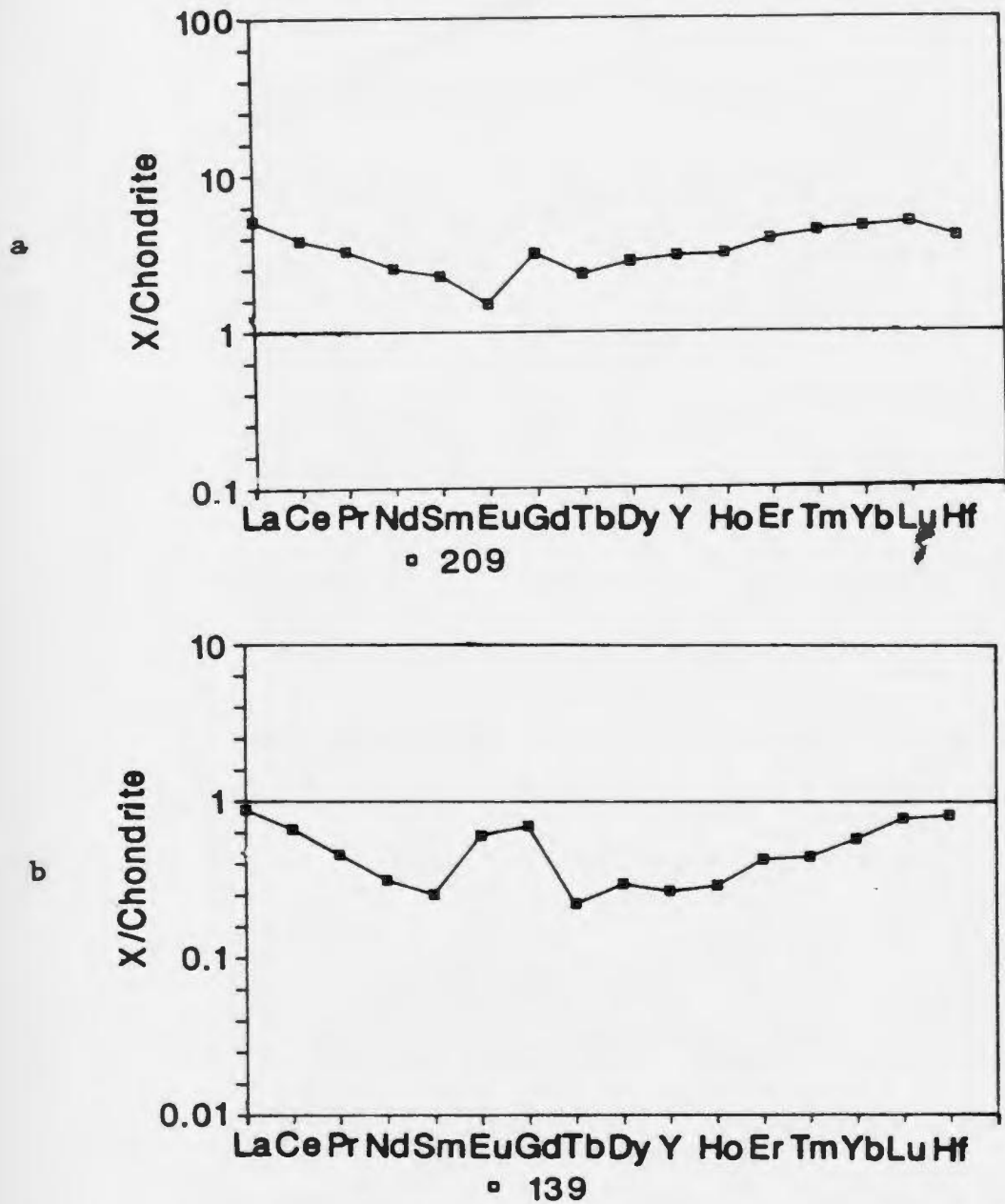


**Figure 4-20:** Rare earth element diagrams

(a) Gull Pond altered diabase sample (209) (b) Rogues Harbour chlorite schist (altered gabbro) sample (139). (Normalized according to Taylor and McLennan (1985)).

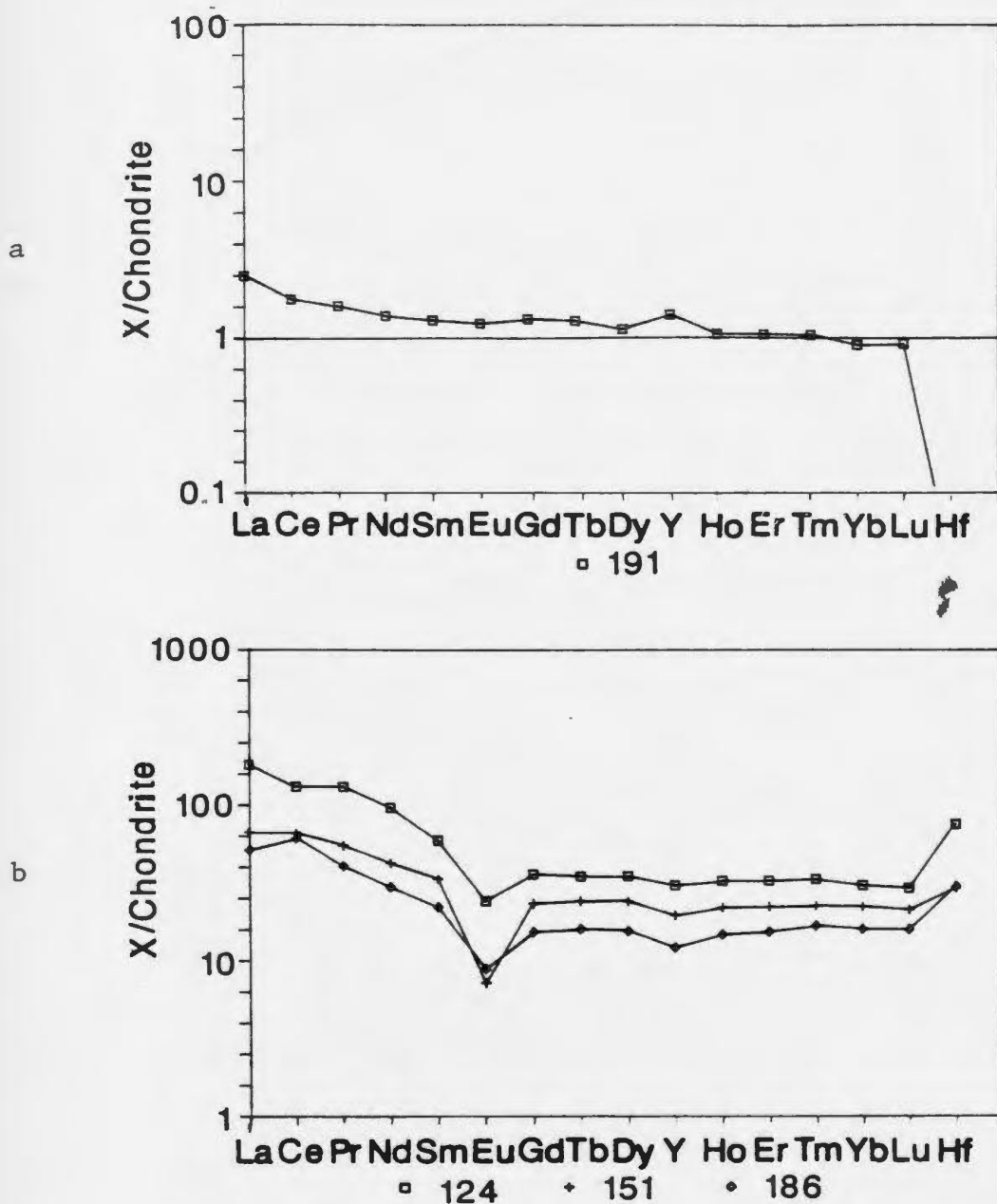


**Figure 4-21:** Rare earth element diagrams

(a) Welshs Bight galena-bearing quartz vein sample (191) (b) Cape St. John rhyolite (124) and QFP (151, 186) samples. (Normalized according to Taylor and McLennan (1985)).

The REE pattern shown by the galena-bearing quartz vein (191) at Welsh Bight is fairly flat (Fig. 4-21a). It does not resemble the patterns shown by the Cape Brule Porphyry (Fig. 4-21b) (samples 151, 186), the Cape St. John rhyolite (sample 124), nor any of the ophiolitic sample patterns (Fig. 4-18, 4-4). The shaft at which sample 191 was found is in close proximity to a fault between QFP and ophiolitic diabase, but the host rock is not readily apparent as only minor sulphidic samples remain around the workings. The gangue minerals in sample 191 (quartz, calcite, minor sericite), which give rise to the REE pattern in Fig. 4-21a, may have been derived from complex reactions between hydrothermal fluid and quartz-feldspar porphyry, producing this REE pattern, or from a completely different and unrelated source.

#### **4.8. Sulphur Isotopes**

##### **4.8.1. Introduction**

Several sulphide-bearing samples were submitted to the Geological Survey of Canada for sulphur isotope analysis. These include 9 Burtons Pond samples, four each from the Hill and Showing No. 2, three from each of the Rogues Harbour and Gull Pond sulphides, and one from Welsh Bight and from a quartz vein near Long Pond. In many cases, more than one type of sulphide mineral (pyrite, pyrrhotite, chalcopyrite, galena) was submitted for analysis.

#### 4.8.2. Background

Sulphur isotope data are used to infer sources and temperatures of sulphur-bearing fluids. Sulphur in hydrothermal fluids probably originates from either an igneous source, as sulphur carried in magmatic fluids or obtained by the leaching of S-bearing minerals in igneous rocks, or a seawater source. Sulphur is fixed as sulphide and/or sulphate minerals depending on the conditions of deposition (Ohmoto and Rye, 1979).

There are, however, inherent problems in the use of sulphur isotopes as source indicators, because ore deposits generally have intricate histories during which the isotopic composition of sulphur may be modified after deposition by thermal metamorphism. The isotopic composition of sulphide minerals depends on both the isotopic composition of all of the sulphur present in the system and on the environmental conditions during deposition. Thus an ore deposit may have a wide range of sulphur isotopic compositions due to different stages of mineralization precipitated under varying conditions. Correct interpretations can be made only when the geology and history of the ore deposit are well understood. Sulphur isotopes can be used to infer sources of sulphur, if the above considerations are noted.

The variation of sulphur isotopic compositions of naturally occurring substances has been summarized by Ohmoto and Rye (1979) (Fig. 4-22). Sulphides in igneous rocks average around 0 per mil  $\delta^{34}\text{S}$ , as do meteorites. Seawater and sedimentary sulphates have large positive values, indicating enrichment in the heavier S isotope,  $^{34}\text{S}$ . The sedimentary sulphides display a wide range of values from -70 per mil to +70 per mil.

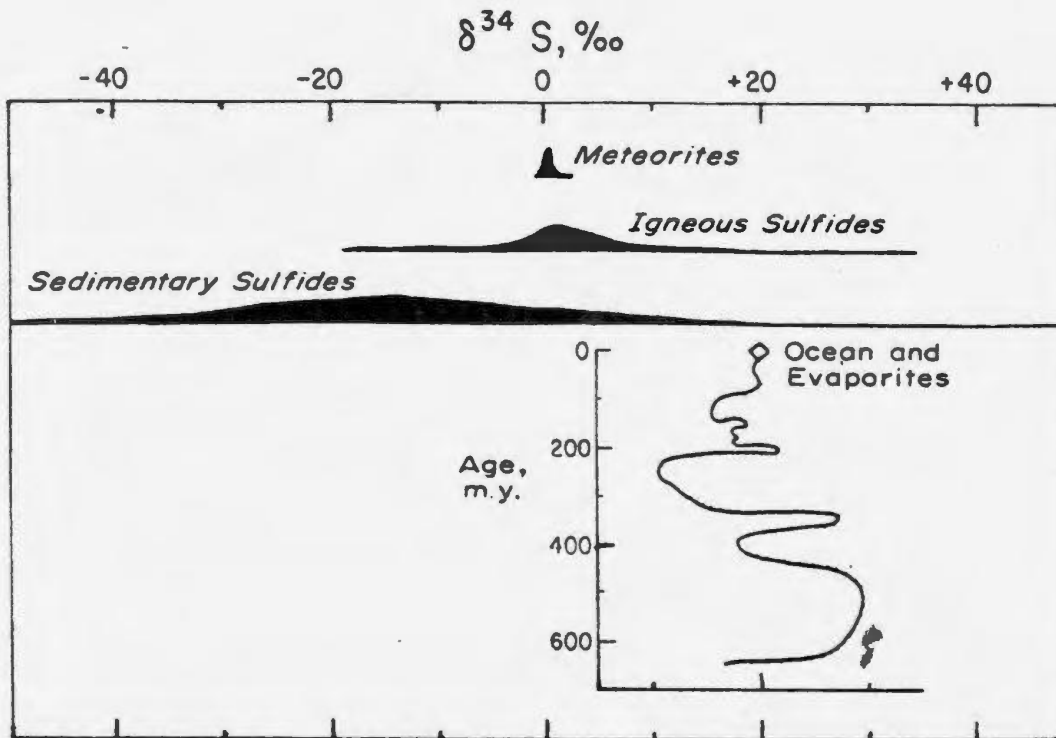


**Figure 4-22:** Sulphur isotopic variation in nature

From Ohmoto and Rye (1979).

Sulphur isotopic data from porphyry copper and stratiform massive sulphide deposits has been summarized by Ohmoto and Rye (1979).  $\delta^{34}\text{S}$  values of sulphides of porphyry coppers fall between -3 and +1 per mil. Temperatures inferred from sulphide-sulphate isotopic temperatures and other geochemically-estimated temperatures lie between 450 and 650°C. This information implies that the S-isotopic sulphide values may be attributed to the addition of sedimentary sulphur to the fluid (Ohmoto and Rye, 1979).

The  $\delta^{34}\text{S}$  values of sulphides in volcanogenic massive sulphide deposits are generally positive and range from -10 up to +20 per mil, with the majority of

values falling between +2 and +8 per mil. Various authors (Sangster, 1968; Peter *et al.*, 1987) have suggested that these sulphides were formed by mixture of magmatic sulphide (near 0 per mil) and  $H_2S$  or  $HS^-$  with positive isotopic values from hydrothermally or bacterially reduced seawater, or sedimentary sulphate. Ohmoto and Rye (1974) and Ripley and Ohmoto (1977) explained this data by means of a model whereby reduction of seawater sulphate occurred by reactions with  $Fe^{2+}$  in basaltic rocks.

Archaean lode gold deposits in Canada and Zimbabwe contain iron sulphides with  $\delta^{34}S$  values ranging from -0.7 to +7 per mil (Crocket and Lavigne, 1984; Wanless *et al.*, 1960; Lambert *et al.*, 1984; Wood *et al.*, 1986; Pattison *et al.*, 1986). Although the isotopic values are not unique to a single source or type, the narrow range close to zero suggests that the sulphur of the fluids was in a reduced form (Roberts, 1987).

#### 4.8.3. Nippers Harbour Results

The Nippers Harbour isotopic results, completed by the OCCGS/GSC Stable Isotope Facility at the University of Ottawa, are compiled in Appendix D and portrayed in the histograms in Figure 4-23. Also tabulated in Appendix D are several unpublished analyses for sulphides at Betts Cove.

The Nippers Harbour samples exhibit a range of  $\delta^{34}S$  values of -0.4 to 8.9 per mil. The relatively good consistency of pyrrhotite-chalcopyrite results suggests, in the most general sense, that these minerals were formed in isotopic equilibrium at each of the showings (Fig. 4-23b).

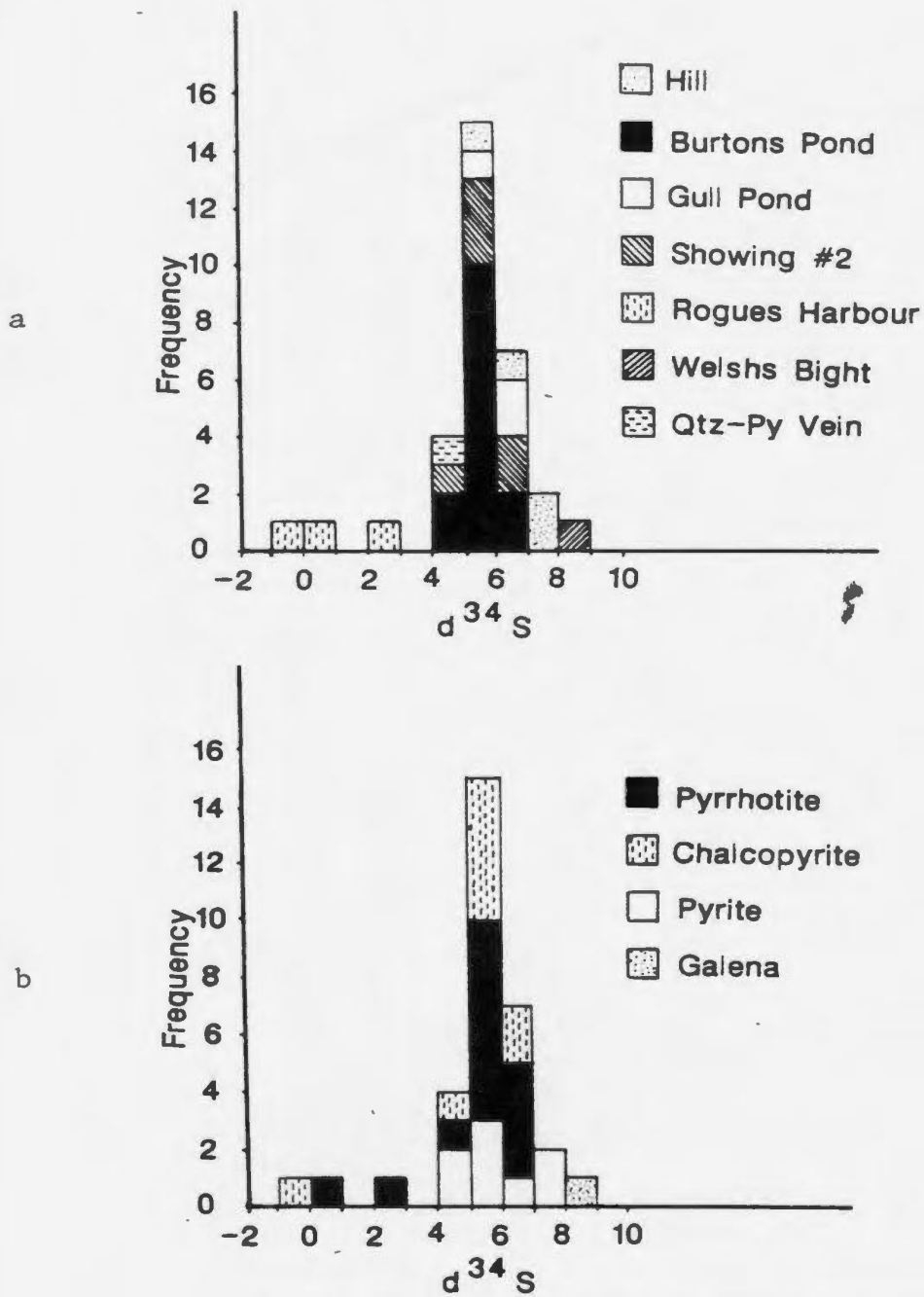


**Figure 4-23:** Sulphur isotope histograms, Nippers Harbour showings

(a) Isotopes displayed according to showing

(b) Isotopes displayed according to mineralogy.



The Rogues Harbour analyses are the most distinct, as they cluster about 0 per mil. This suggests contribution of sulphur from an igneous source, providing no fractionation has taken place since deposition. That source is probably the Cape Brule Porphyry or the mafic ophiolitic rocks, or a combination of both.

The Betts Cove sulphide deposit has been interpreted to be a volcanogenic massive sulphide lens deposited on the seafloor by hydrothermal fluids which have passed through basaltic rock (Upadhyay and Strong, 1973; Saunders, 1985). Its isotopic values are consistent with this interpretation, in that they fall within the published range of values of other massive sulphide deposits. The values are slightly heavier than values for recent Guymas Basin sulphides (-3 to +4.5 per mil) (Peter *et al.*, 1987).

Mineralization at the Hill showing has, based on geological field relations, been suggested to result from deposition under sub-seafloor conditions. The isotopic values (mean 6.8, range 5.9 to 7.4 per mil) are closest to the Betts Cove values but are slightly isotopically lighter, indicating that the sulphur may have been in a more reduced form.

The Burtons Pond, Showing No. 2 and Gull Pond sulphides have similar isotopic compositions, indicating that they may have been deposited under similar conditions. Isotopic values from sulphide pairs of the first two showings were used to calculate temperatures of sulphide formation. Isotopic equilibration between solids, and solids and liquids causes small differences in  $\delta^{34}\text{S}$  values of precipitating sulphide minerals (Sakai, 1957; Thode, 1970). These differences may

reflect the temperature of equilibration (Tatsumi, 1965). Several assumptions must first be made: (1) Both phases formed in equilibrium; (2) No further isotopic exchange occurred after the precipitation of the minerals; and (3) Only pure mineral separates were submitted for analysis (Ohmoto and Rye, 1979).

Experimental study of sulphur isotope fractionation by Sakai (1957), Thode (1970) and Kajiwara and Krouse (1971) confirms the fact that  $\delta^{34}\text{S}$  values of mineral pairs are linearly related to equilibrium temperatures in the form  $10^6/T^2$ . The equation

$$D = A * 10^6 / T^2,$$

(where D is the difference between  $\delta^{34}\text{S}$  values of two coexisting minerals, A is a constant and T is the absolute temperature), expresses this relationship. Table 4-6 lists experimentally calculated constants (A's) for mineral pairs used in this study.

The three temperatures ( $114^\circ \pm 23^\circ$ :Po-Cp pair,  $114^\circ \pm 23^\circ$ :Po-Cp pair,  $209^\circ \text{C} \pm 73^\circ$ :Po-Py pair) obtained for Showing No. 2 are geologically reasonable (within the error limits stated), and suggest that the quartz and sulphides may have been deposited from the same, low temperature fluid.

The results for the Burtons Pond, Showing No. 2 and Betts Cove thermometers are summarized in Table 4-7. Those Burtons Pond and Betts Cove values which are within the acceptable temperature range ( $250 - 600^\circ\text{C}$ ), are comparable and high ( $339$  to  $593^\circ\text{C}$ ). Fluids currently emanating on the seafloor

Mineral Pair	A	Temperature Range (°C)
Pyrrhotite-Chalcopyrite	0.15	250-600
Pyrrhotite-Pyrite	0.30	250-600
Pyrite-Chalcopyrite	0.45	250-600

**Table 4-6:** Sulphur Isotope Thermometers  
After Kajiwara and Krouse, 1971

are of the order of 350°C (Edmond *et al.*, 1979a,b; Von Damm *et al.*, 1983; Bowers *et al.*, 1987). Of the 12 temperature measurements quoted, however, 7 lie outside the range of the experimental temperature range shown in Figure 4-24. Some of the very high temperatures probably reflect disequilibrium, which is discussed in more detail below.

The plot of  $\delta^{34}\text{S}$  mineral vs temperature, shown in Fig. 4-24, indicates again that some disequilibrium must have occurred. Although there is an apparent trend toward isotopically heavier sulphur with decreasing temperature, sample BP-058 indicates a reversal of this trend. This may reflect this isotopic

Showing/ Mineral Sample	T(°C)	Error(°C)	Pair
<b>Burtons Pond</b>			
22001	593	+/-530	Po-Cp
22004	952	+/-267	Po-Cp
22008	434	+/-286	Po-Cp
22058	339	+/-170	Po-Cp
<b>Showing No.2</b>			
296	114	+/-23	Po-Cp
11002	114	+/-23	Po-Cp
11003	209	+/-73	Po-Py
<b>Betts Cove</b>			
A09	1848	+/-1800	Py-Cp
A05	434	+/-95	Py-Cp
A06	315	+/-47	Py-Cp
F444	952	+/-476	Py-Cp
F450	676	+/-270	Py-Cp

**Table 4-7:** Nippers Harbour geological temperatures calculated from sulphur isotope pairs

disequilibrium between the sulphides, which seems likely, given the fact that pyrrhotite in many Burtons Pond samples is weathering to pyrite. The temperatures obtained for the Burtons Pond samples, therefore, are suspect and should not be used. It probably is safe to assume, however, that during precipitation, the activity of sulphur decreased as the sulphides were early forming phases.

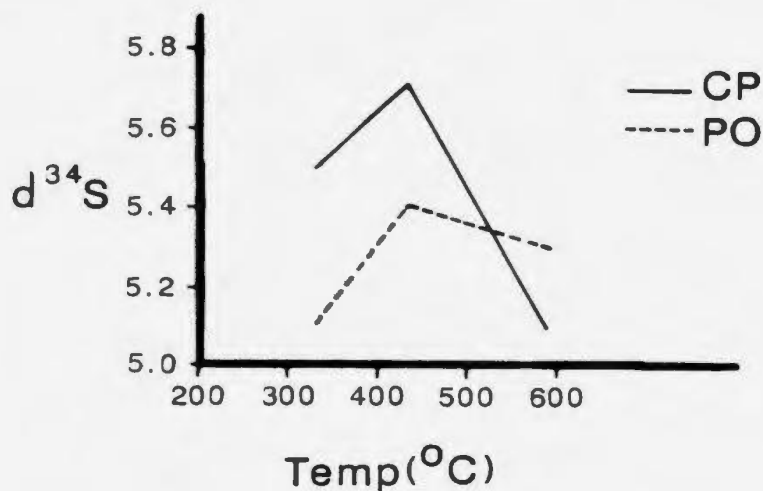


**Figure 4-24:** Temperature vs  $\delta^{34}\text{S}$ ,  
Burtons Pond samples

Galena from Welshs Bight yields the highest  $\delta^{34}\text{S}$  value of 8.9 per mil, which is distinct from all of the other Nippers Harbour values (range -0.1 to 7.4). In any set of co-existing sulphides, galena normally is the heaviest isotopically (Faure, 1977), so the Welshs Bight galena may not necessarily have a genesis different from the other base metal sulphides.

#### 4.9. Lead Isotope, Welshs Bight Showing

Galena from sample 191 was submitted to R.I. Thorpe at the Geological Survey of Canada for isotopic analysis. The results, completed by Geospec Consultants Ltd., Edmonton, under contract to the Geological Survey of Canada, are listed in Table 4-8 and shown in Figure 4-25. Figure 4-25 also shows samples from other Newfoundland showings, taken from Swinden and Thorpe (1984).

Sample	$^{206}\text{Pb}/^{204}\text{Pb}$	$^{207}\text{Pb}/^{204}\text{Pb}$	$^{208}\text{Pb}/^{204}\text{Pb}$
191	17.659	15.464	37.562

**Table 4-8:** Lead isotope results, Welshs Bight

Isotopic Pb data can be used to derive 'model ages' for the samples they represent. These ages indicate the time at which the lead was segregated from its source and subsequently deposited in the crust in a lead-bearing mineral (galena, pyrite) (Faure, 1977). The derivation of a model age is based on the Holmes (1946)-Houtermans (1946) model, which bases the Pb isotopic composition of a sample of lead on a single-stage history, whereby uranium and thorium in the source region decay to radiogenic lead. When the resulting lead (primeval plus radiogenic) is separated from its parents and deposited in a lead mineral, that mineral's isotopic composition is assumed not to change, because it contains no uranium or thorium (Faure, 1977).

R.I. Thorpe calculated model ages for the Nippers Harbour sample relative to other Newfoundland samples, using a Stacey and Kramers (1975) standard lead growth curve to derive a model age. The model has  $T_0 = 3700$ ,  $a_0 = 11.152$ ,  $b_0 = 12.998$ ,  $c_0 = 31.230$  and a  $\mu$  value of 0.74 for their best-fit evolution curve to the 15 leads used. The value for the Welshs Bight lead is 456.8 Ma.

Paleozoic model ages should be interpreted with caution. Although a single-



**Figure 4-25:**  $^{206}\text{Pb}/^{204}\text{Pb}$  vs  $^{207}\text{Pb}/^{204}\text{Pb}$  diagram for Welsh Bight and other Newfoundland samples

stage growth model is adequate to explain Archean lead evolution, considerable source mixing occurs in the Paleozoic (R.I. Thorpe, pers comm., 1987). Swinden and Thorpe (1984) have pointed this out in the case of the New Brunswick Bathurst deposits, which lie along a shallow secondary isochron or mixing line. The error limits associated with model ages are large, thus, it is useful to compare a number of model ages to draw correlations and similarities between geographically and geologically similar leads.

Swinden and Thorpe (1984) pointed out that the metal and lead-isotopic compositions of volcanogenic sulphide deposits in the Newfoundland Central mobile belt are consistent with control by their source region lithologies, which generally are mafic volcanic and intrusive ophiolitic rocks and island-arc mafic volcanic and sedimentary rocks. The Welsh Bight showing also is underlain by ophiolitic rocks. The model age obtained (456.8 Ma) and error limits are within range of ages obtained for the ophiolite (483.4 +/- 3.1/-1.8 Ma; Dunning, 1984) and of the overlying Snooks Arm Group (470 to 485 Ma, Snelgrove, 1931). The lead-isotope analysis, however, is considerably less radiogenic than the Notre Dame Bay values, implying that the two areas have considerably different lead source regions. The Betts Cove analysis is more radiogenic than the Nippers Harbour value, suggesting that its lead source may be ophiolitic.

The Welsh Bight analysis and model age are similar to results for leads from occurrences in the Catchers Pond Group from the Notre Dame Bay area. Lithologically, this Group is distinct from other Notre Dame Bay island-arc sequences, in that it contains approximately 50 percent felsic material (Dean,



1978). Its lead isotope compositions plot in a much less radiogenic position than the main group of Notre Dame Bay values, leading Swinden and Thorpe (1984) to suggest that the source region for the Catchers Pond Group ores was highly depleted in radiogenic lead relative to the underlying regions to the Central Newfoundland island arc.

The age of 475 +/- 10 Ma, obtained by Mattinson (1975) for the Cape Brule Porphyry, has been interpreted as the original age of the pluton. The closeness of this to the calculated Welshs Bight model age (456.80 Ma) and the geological proximity of the showing to the porphyry (on a fault between diabase and QFP) suggests a genetic link between the two. Similarly, at Brents Cove, pyrite occurs in Cape St. John Group metafelsites which are in close proximity to a small pluton of Cape Brule Porphyry (DeGrace *et al.*, 1976). Lead isotope compositions and model ages are similar to those at Welshs Bight (Fig. 4-25).

Lead-isotope values obtained for leads from vein sulphides often are suspect. For example, two analyses of galena from the Silverdale deposit (unpublished data from H.S. Swinden) are distinctly different (Table 4-9). Lead in small vein systems may be derived locally and thus depends on the immediate lithologies rather than a larger-scale feature, such as the ocean crust or a felsic magma with an evolving lead cycle (H.S. Swinden, *pers comm.*, 1988). The plot of  $^{208}/^{204}\text{Pb}$  vs  $^{206}/^{204}\text{Pb}$  shown in Fig. 4-26 substantiates the argument that the Welshs Bight lead may be derived locally, as the value does not plot close to the lead growth curve after Zartman and Doe (1981). If the lead was related to the regional lead-isotope signatures, the value would have plotted closer to the growth curves.

Clearly, further Welshs Bight lead-isotope analyses are needed to solve this problem.

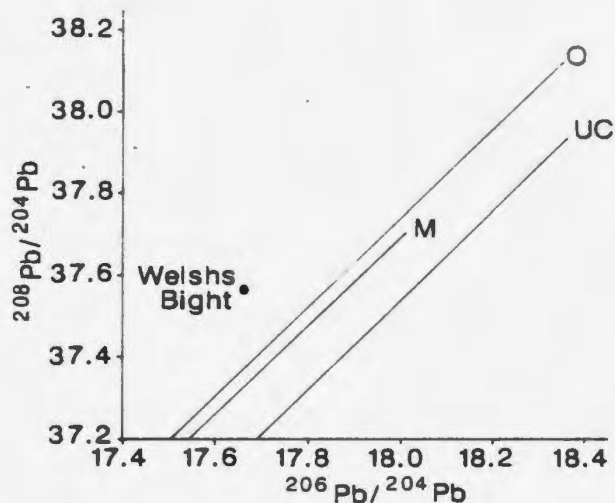


**Figure 4-26:**  $^{206}\text{Pb}/^{204}\text{Pb}$  vs  $^{208}\text{Pb}/^{204}\text{Pb}$  for Welshs Bight sample

Lead growth curves are from Zartman and Doe (1981): O-Orogene, M-Mantle, UC-Upper Crust.

Sample	$^{206}\text{Pb}/^{204}\text{Pb}$	$^{207}\text{Pb}/^{204}\text{Pb}$	$^{208}\text{Pb}/^{204}\text{Pb}$
TQ72-72	17.848	15.500	37.654
TQ83-2	17.853	15.505	37.670

**Table 4-9:** Lead isotope analyses from the Silverdale deposit, Lushs Bight Group

#### 4.9.1. Summary

Unaltered mafic rocks of the Nippers Harbour ophiolite are similar to Betts Cove boninitic-type lavas and dykes in that they have anomalously low  $\text{TiO}_2$  contents, and high  $\text{SiO}_2$ ,  $\text{MgO}$ ,  $\text{Cr}$  and  $\text{Ni}$  relative to other common oceanic basalts. Rocks at Nippers Harbour are slightly more enriched in elements such as  $\text{Y}$ ,  $\text{Zr}$ ,  $\text{Cr}$  and  $\text{Ni}$  than those at Betts Cove, suggesting that the Nippers Harbour ophiolite is derived from a more incompatible element-enriched source than that which generated the Betts Cove Ophiolite.

Units one and two quartz-chlorite-sulphide samples from the Hill showing display enrichments in  $\text{FeO}_t$ ,  $\text{Cu}$  and  $\text{Zn}$ , and depletions in  $\text{Na}_2\text{O}$  and  $\text{CaO}$ . These can be related to the formation of iron-rich chlorite, iron sulphides (pyrite, chalcopyrite), and to the destruction of feldspar by the hydrothermal fluids. Unit three rocks contain the same assemblage as above, as well as minor albite. As a result, their depletions in  $\text{CaO}$  and  $\text{Na}_2\text{O}$  are much less significant.

Alteration at the gold-rich Burtons Pond, Gull Pond and Showing No.2 areas is expressed chemically by the addition of  $\text{FeO}_t$ ,  $\text{S}$ ,  $\text{K}_2\text{O}$ ,  $\text{CO}_2$ ,  $\text{Ba}$ , and some  $\text{MgO}$ , and variable depletions of  $\text{CaO}$ ,  $\text{Sr}$  and  $\text{Na}_2\text{O}$ . These can be accounted for by the formation of iron- and magnesium-rich chlorite, sericite and calcite. Gold enrichment correlates best with enrichments in  $\text{S}$ ,  $\text{FeO}_t$  and  $\text{CO}_2$ . Considerable amounts of  $\text{FeO}_t$  and  $\text{MgO}$ , as well as lesser  $\text{K}_2\text{O}$ , have been added to altered rocks at Rogues Harbour.

LREE have been depleted from most of the altered rocks at each showing.

except for a quartz-sulphide-gold vein at Burtons Pond. This may be attributable to feldspar alteration. MREE have been enriched in the Hill sulphide-chlorite-albite Unit 3 rocks and in an altered gabbro from Rogues Harbour, and depleted in an altered diabase from Gull Pond. The REE pattern shown by the Welshs Bight quartz vein shows enrichment in LREE and depletion in HREE, and its origin is uncertain.

Sulphur isotope values from the Nippers Harbour showings fall within a range of  $-0.5$  to  $+8.9$  per mil and cluster about the value  $+5.5$  per mil. The cluster of Rogues Harbour values about 0 per mil may reflect an igneous source of sulphur, which is likely the mafic ophiolitic rocks or the Cape Brule Porphyry, while temperatures obtained from sulphide pairs from Showing No. 2 are low ( $114^{\circ} \pm 23^{\circ}$  to  $209^{\circ} \pm 73^{\circ}\text{C}$ ). Temperatures calculated from Burtons Pond pairs are suspect due to weathering of pyrrhotite. The Welshs Bight galena may or may not have a different genesis than the other Nippers Harbour sulphides, based on its anomalous but isotopically reasonable value of  $+8.9$  per mil.

The Welshs Bight lead-isotope analysis plots along an isochron with other Newfoundland leads associated with ophiolitic rocks. It plots in a considerably less radiogenic position than the other values, implying that its source may be different or modified from the type of source generating the other leads (the mafic lithologies of the ophiolites themselves). The Welshs Bight analysis is similar to values from showings associated with felsic volcanics (Catcher's Pond) and the felsic Cape Brule Porphyry (Brent's Cove), implying that the lead found in the Welshs Bight galena may be supplied at least in part by the nearby Cape Brule

Porphyry. Furthermore, the model age of the Welshs Bight lead is very close to that of the porphyry. Due to problems with isotopic analyses of vein deposits, additional analyses are needed to support the above arguments.

## Chapter 5

### Fluid Inclusions

#### 5.1. Introduction

Thirty-seven quartz samples were prepared for fluid inclusion studies (see Appendix G). These were collected from most of the showings and from veins in diabase, pyroxenite and quartz-feldspar porphyry (QFP). Of these, only 15 samples had inclusions large enough to be used for microthermometric measurements. Samples K3075, K3275 and K1175 from Burtons Pond, with gold contents of 110, 2200 and unknown ppb, contain quartz occurring with sulphides. Quartz from samples 211, 218, 241 and 243 occurs with the Cu-Fe sulphides at Rogues Harbour, and sample 147 was taken from the large quartz vein which extends across the Rogues Harbour peninsula. Sample number 230 represents a quartz vein from Showing No. 2. Samples 41 and 81 represent quartz veins in diabase which contain traces of epidote and pyrite. Sample 68 is a pure quartz vein in diabase. Sample 180 is found in a shear zone in pyroxenite in Northwest Arm. Samples 94 and 168 were collected from quartz veins found in the QFP unit.

## 5.2. Description of Inclusions

The only inclusions suitable for microthermic studies were those with diameters ranging from 70 to 80  $\mu\text{m}$ , but most were in the range of 5 to 15  $\mu\text{m}$ . The samples contain both primary and secondary inclusions, although in some cases, the distinction between them was not very clear. Primary inclusions are isolated, occur in a random, three-dimensional distribution throughout the crystal, and in some instances, have long axes parallel to a direction of growth (Roedder, 1979). Secondary inclusions are very common, and tend to occur as planar growths outlining fractures (Roedder, 1979), and as trails concentrated along curvilinear cracks. These generally were disregarded, with the exception of some of the Rogues Harbour samples. The sulphides at Rogues Harbour occur as crustiform and vug structures characteristic of open space fillings (see chapter 3), hence the secondary inclusions found along mineralized fractures may relate to the ore fluids that deposited the sulphides.

Two types of fluid inclusions are present in the samples. The first is a simple two-phase, liquid plus vapour inclusion. These are by far the most abundant, and some samples contained inclusions of only this type. These inclusions normally have high liquid to vapour ratios. None of the samples contain simultaneously homogenized inclusions of both liquid and vapour, hence boiling could not be demonstrated. The vapour was probably composed predominantly of  $\text{H}_2\text{O}$  rather than  $\text{CO}_2$ , as the inclusions all homogenized at temperatures above  $31^\circ\text{C}$  (the homogenization temperature for  $\text{CO}_2$ ).

The second type of inclusion contains three or more phases, liquid-vapour






plus one or more solid phases. The solid phases may be either daughter minerals or accidental solids, unrelated to the fluid composition.

Table 5-1 presents a list of the solid phases occurring in the Nippers Harbour samples. The most common solid phase is a high relief, acicular to prismatic crystal which probably is anhydrite (No. 1) (Fig. 5-1a). Another prismatic solid of medium relief, low birefringence and unknown identity (No.2) is also present, and is at times difficult to distinguish from anhydrite. An equant, cubic solid phase, thought to be halite (No.5) (Fig. 5-1a) was also observed. Two solids resembling carbonate (No.3 and No.4) (Fig. 5-1b) were recorded in some samples.

Table 5-2 summarizes the various characteristics of the inclusions in the Nippers Harbour samples.

Within individual samples where solids were present, the inclusions had variable phase ratios, suggesting that the solids in the Nippers Harbour inclusions probably are accidental, or that leakage may have occurred. If a solid is indeed a daughter mineral, one should be able to nucleate it by cooling (for halite) or heating (for carbonates and sulphates). In addition, if a fluid was supersaturated, it should have had time to precipitate a daughter mineral. Holland (1967), however, has pointed out that calcite or sulphates are not always precipitated from solution by simple heating, as a loss of  $\text{CO}_2$  or  $\text{SO}_2$  also is required. This is difficult to accomplish, as fluid inclusions normally are sealed by their host mineral.



No.		Shape	Biref.	Relief	Possible Minerals
1		acicular, prismatic	med, high	high	anhydrite
2		acicular, prismatic	low	med	unknown
3		anhedral	high	high	carbonate
4		cubic	none	high	halite
5		rhombic	high	high	carbonate

**Table 5-1:** Characteristics of fluid inclusion solids

A solid in equilibrium with its host fluid should grow larger or smaller when heated or cooled (Roedder, 1967, 1972) (e.g., carbonates and sulphates should increase in size when heated). No nucleation or change in solid shape was noted in the Nippers Harbour samples, except possibly for halite.

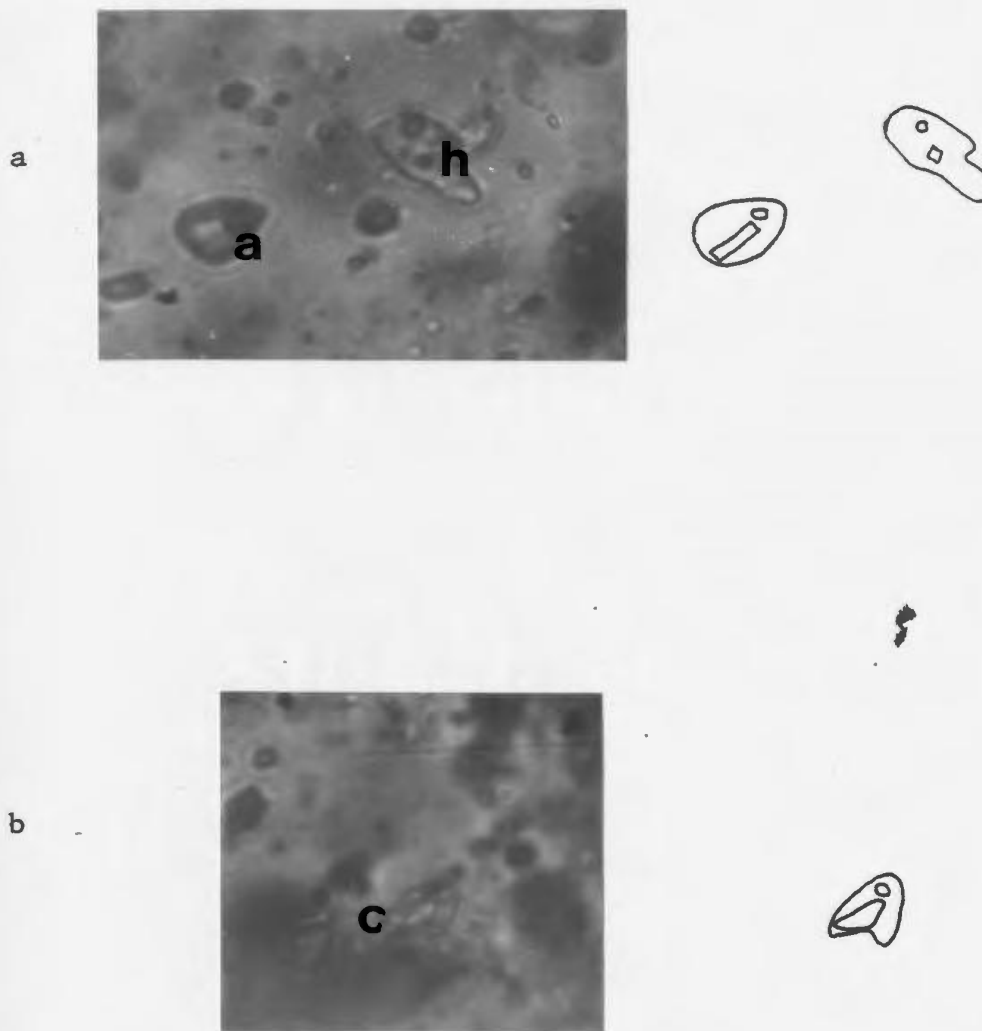


**Figure 5-1:** Photomicrographs of fluid inclusions

(a) Sample 81, PL, Diabase sample, inclusions containing halite

(h) and anhydrite (a) solids. (b) Sample 243, PL, Rogues

Harbour, inclusion containing carbonate (c) solid. Photo

widths a,b 0.13 mm.

SAMPLE	SOLID PHASES	CONTROL/ APPEARANCE OF INCLUSIONS	RELATION TO SULPHIDES	SALINITY (EQUIV. WT% NaCl)	TO	SUBSTITUTED
<u>BURTONS POND</u>						
K1175	2,3,4,5	some primary alignment (pseudo-secondary?)	p-1	3.6 to 11.2	8.4; 196.1 to 247.7	none measured
K3075	2*,5	growth zone	p-1	5.0 to 5.9	196.0 to 266.5	-17.8 to -37.4
K3275	2,3	growth zone	p-1	0 to 3.9	165.3 to 196.8	-12.3 to -20.6
<u>ROQUES HARBOUR</u>						
147*	1,2,4	isolated in polygonal fractures	p-3	11.2 to 20.6	205.8 to 213.7	-33.7 to -70.9
211	1*	isolated in polygonal fractures	s-2	15.6	167.2 to 192.2	-29.4 to -39.0
243	1 or 2*, 4	p-isolated s-aligned along sulphide-filled fractures	p-2 s-1	p-9.2 to 9.7; 15.7 s-15.8 to 20.4	p-173.2 to 219.5 s-156.5 to 171.9	p -28.2 s -23.2 to -43.2
218	-	isolated in polygonal fractures	p-2	2.7 to 11.0	197.6 to 210.0	-17.7 to -21.8
241	1*, 2, 4, 5	s-fracture-related	p-2 s-1	p-3.6 s-17.4 to 17.9	p-223.7 to 258.0 s-176.7 to 220.2	p-12.6 s -18.2 to -32.2

SAMPLE	SOLID PHASES	CONTROL/ APPEARANCE OF INCLUSIONS	RELATION TO SULPHIDES	SALINITY (wt % NaCl)	TH	POTENTIAL
<u>QUARTZ VEIN OF SHOWING NO. 2</u>						
230	2,3,4	growth zone: very dense population of inclusions	p-2	0 to 2.6; 8.4	141.9 to 189.0	none measured
<u>QUARTZ-EPIDOTE-PYRITE VEINS IN DIABASE</u>						
68	-	very dense population of inclusions	p-4	11.5 to 14.6	150.3 to 197.6	-34.8 to -55.1
81	1*		p-4	8.1 to 13.0	165.0 to 214.3	-36.6 to -61.0
41	1*,3		p-4	12.8 to 22.3	121.4 to 166.9	-29.2 to -54.8
<u>QUARTZ VEINS IN GPF</u>						
94	1*	isolated, cut by streams of secondary inclusions	p-4	11.7 to 14.4	98.2 to 171.4	-33.1 to -53.1
168	1*,4	isolated, rare inclusions	p-4	12.2	134.6 to 176.9	-27.0 to -36.5
<u>SHEAR ZONE RELATED QUARTZ VEIN</u>						
180	1*	fills tensional area related to shearing	s-2	10.9 to 14.0	187.1 to 210.9	-22.7 to -30.4

**Table 5-2: Characteristics of Nippers Harbour Fluid Inclusions**

Numbers in solid phases column refer to Table 5-1. Other symbols: p-primary, s-secondary; Relations to sulphides column: 1-high probability, 2-uncertain, 3-low probability, 4-unrelated, data is used for comparison purposes; \*-solid phase is very common.

### 5.3. Freezing Results

Freezing experiments were performed on the Nippers Harbour samples from Burtons Pond, Rogues Harbour, Showing No. 2, diabase, QFP and shear zone related quartz veins. Compositions and salinities were determined from the cooling experiments.

#### 5.3.1. Eutectic Temperature

Melting of a frozen inclusion containing solids and vapour begins at E, a eutectic temperature, which is characteristic for different natural chloride solutions, as summarized in Figure 5-2 and Appendix G. If a solution is more complex, containing salts such as KCl, MgCl<sub>2</sub> or CaCl<sub>2</sub>, which all serve to depress the eutectic, it may be difficult to observe the initial melt fraction (Crawford, 1981). As well, very small volumes of melt are generated at the eutectic, and in small inclusions or inclusions of low salinity, this makes the eutectic temperature determination extremely difficult.

Eutectic temperatures were recorded for 68 inclusions and are presented in Figure 5-2. The Burtons Pond samples contain NaCl, KCl and some MgCl<sub>2</sub>, and are the least complex. Of the initial melting temperatures recorded, all were above the eutectic for CaCl<sub>2</sub>, -49.8°C. Spooner and Bray (1977) documented a similar phenomenon for inclusions in samples from stockwork zones of deposits in Troodos, Cyprus. They recorded spontaneous freezing temperatures of -30°C, which implies that CaCl<sub>2</sub> was not present in the fluids. However, one Burtons Pond measurement was below the eutectic for MgCl<sub>2</sub>, implying that CaCl<sub>2</sub> may have been present, but the eutectic was not recorded.

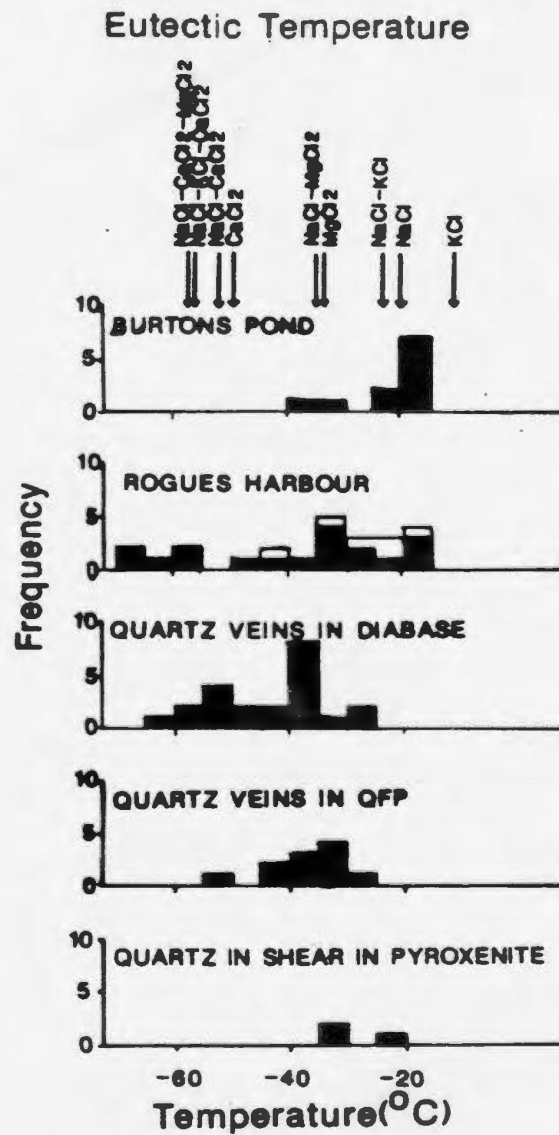


**Figure 5-2:** Nippers Harbour eutectic temperatures

Shaded bars-primary inclusions; open bars-secondary inclusions.

Eutectic temperatures for various salts are taken from Crawford (1981) and Luzhnaya and Vereshtchina (1946).

Secondary inclusions (believed to be related to mineralization) in the Rogues Harbour samples also contain no  $\text{CaCl}_2$ , as the lowest eutectic recorded was  $-43.2^\circ\text{C}$ .

Primary inclusions in the Rogues Harbour samples and in quartz-epidote-pyrite veins in diabase exhibit a wide range of eutectic temperature. They contain  $\text{CaCl}_2$  and  $\text{NaCl}$ , and possibly  $\text{KCl}$  and  $\text{MgCl}_2$ , although this cannot be proven without the aid of other techniques. Fluids in QFP and shear zone inclusions are less complex, as only one inclusion had an initial melting temperature below the eutectic of  $\text{CaCl}_2$ .

### 5.3.2. Salinity

Final melting temperatures were recorded for 58 solid-free inclusions. These temperatures can be used to infer salinity, providing it is known which solid, ice or hydrohalite ( $\text{NaCl}\cdot 2\text{H}_2\text{O}$ ), is the one which melts. Below the eutectic temperature, ice, hydrohalite and vapour can coexist (Fig. 5-3). Both solid phases have similar final melting temperatures (ice,  $0^\circ\text{C}$ ; hydrohalite,  $0.1^\circ\text{C}$ ), but correspond to distinctly different salinities. Furthermore, hydrohalite has a much higher birefringence and relief than ice. Ice also has a tendency to recrystallize into a number of grains upon heating (Roedder, 1972; Crawford, 1981). The solid phase in the Nippers Harbour samples is ice.

The salinities of the Nippers Harbour samples are illustrated in Figure 5-4. The Burtons Pond and Showing No. 2-related samples have low salinities, with ranges of 0 to 11.2 eq. wt. %  $\text{NaCl}$  (mean 4.55 wt. %  $\text{NaCl}$ ) and 0 to 8.6 eq. wt. %

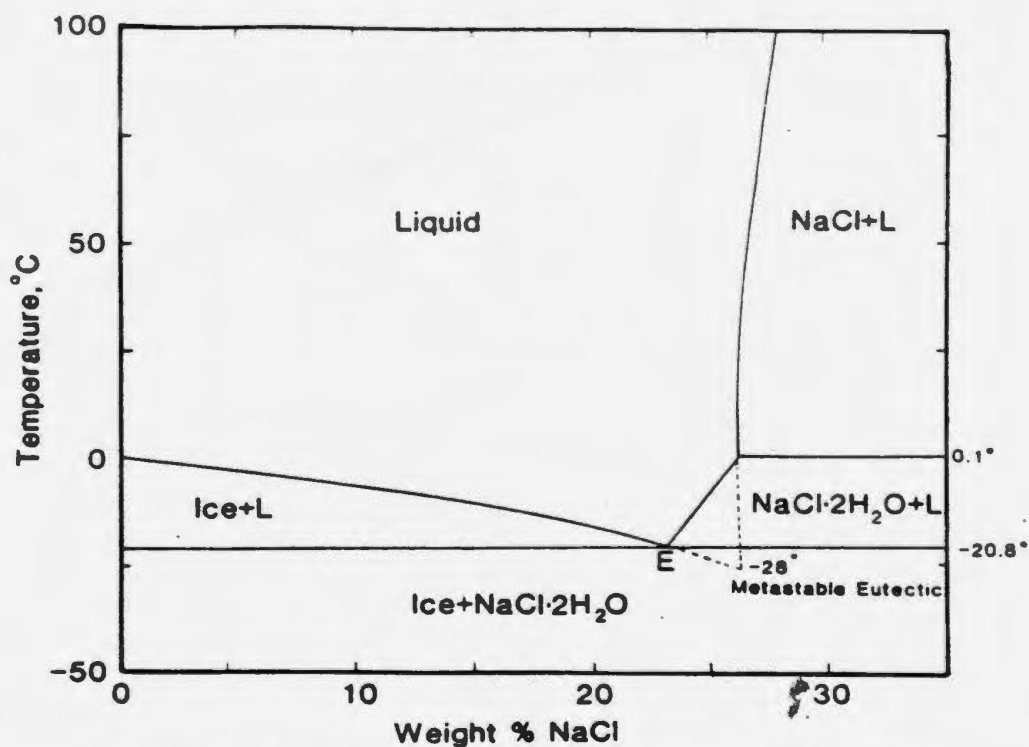


**Figure 5-3:** NaCl-H<sub>2</sub>O system, temperature-composition diagram at 1 atm

All phases coexist with vapour. After Crawford (1981), data from Potter et al., (1978) and Linke (1965).

NaCl (mean 2.42 wt.% NaCl). Rogues Harbour primary and secondary, diabase, QFP and shear zone inclusions all have distinctly higher salinities, with ranges of 2.7 to 20.6 eq. wt% NaCl (mean 12.3 eq. wt% NaCl), 17.4 to 20.4 eq. wt% NaCl (mean 18.7 wt% NaCl), 8.1 to 22.3 eq. wt% NaCl (mean 13.0 eq. wt% NaCl), 9.6 to 14.4 eq. wt% NaCl (mean 12.4 eq. wt% NaCl), and 10.9 to 14.0 eq. wt% NaCl (mean 12.4 eq. wt% NaCl).



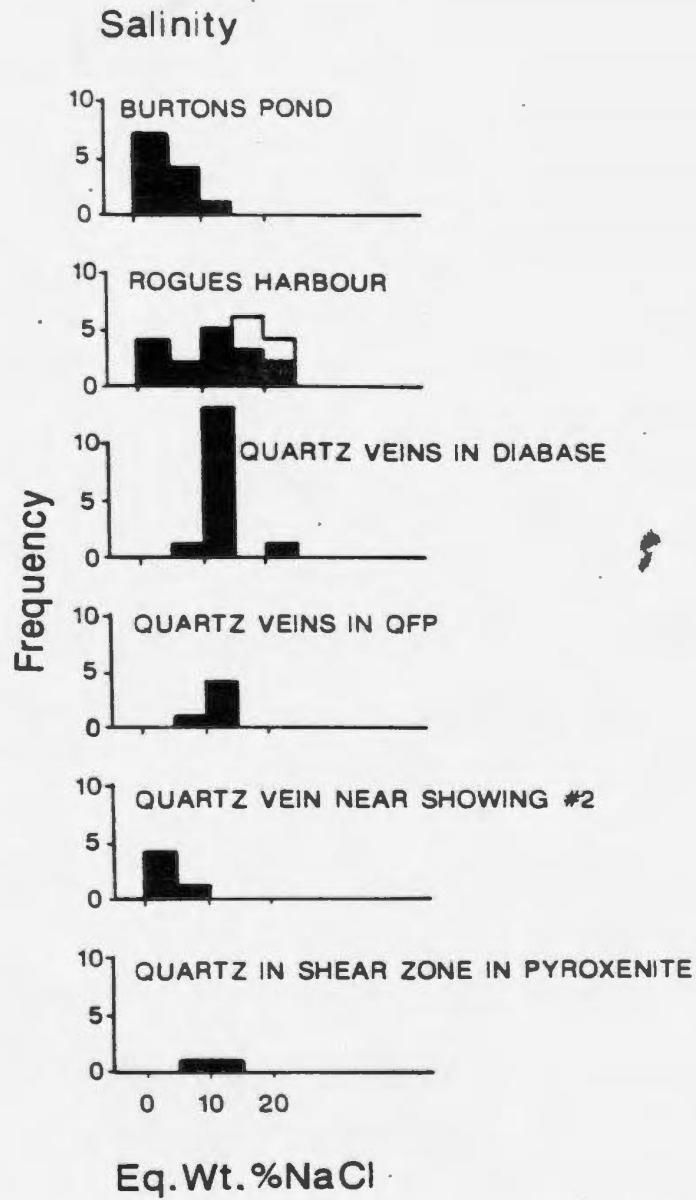


**Figure 5-4:** Nippers Harbour fluid inclusion salinities

Shading of bars as in Fig. 5-2.

## 5.4. Heating Results

### 5.4.1. Homogenization Temperature

Homogenization temperatures were recorded for 85 inclusions, and are summarized in Figure 5-5. Most of the samples homogenized at between 120° and 200°C, with means as follows: Burtons Pond, 193.5°C; Rogues Harbour primary, 198.6°C, secondary, 174.7°C; Showing No. 2, 169.5°C; diabase 169.8°C; QFP, 152.5°C; shear zone, 199.6°C.

Because the precise compositions and densities of the Nippers Harbour inclusions are not known, trapping temperature and pressure cannot be correctly determined from homogenization temperatures using isochores (see Roedder and Bodnar, 1980; Crawford, 1981). Pressure corrections could be estimated if the depths of the deposition were known, and applying these to the diagrams of Potter (1977).

If the Burtons Pond and Showing No. 2 sulphides were generated below the seafloor, then depths corresponding to modern day seafloor hydrothermal deposits might be applied. Rona (1984) has tabulated water depths for 63 such deposits, stating that they are located beneath about 1600 to 5800 m of water. Since the Burtons Pond and Showing No. 2 showings are located in diabase units, an extra depth of 1 to 4 km should be added to the above estimates. The quartz-epidote-pyrite veins in diabase would also correspond to this depth. Pressure corrections of +43°C and +63°C for water depths of 5000 and 7500 m, for a 5% NaCl solution at a homogenization temperature of 170°C, would apply to these

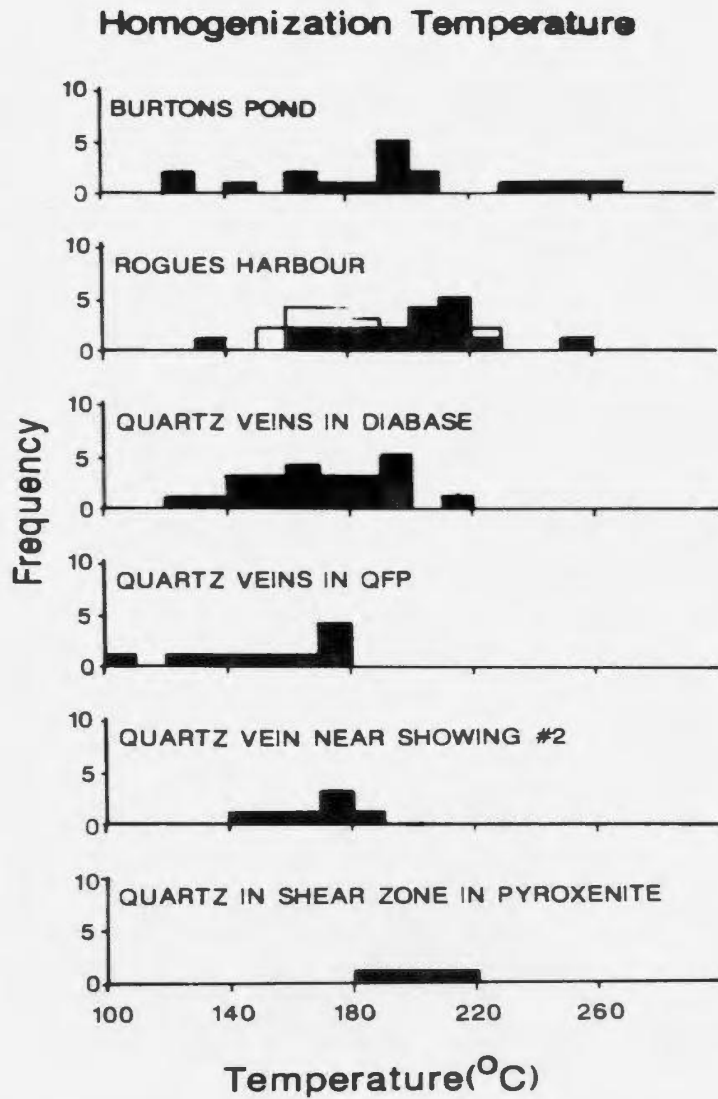


**Figure 5-5:** Nippers Harbour fluid inclusion homogenization temperatures

Shading of bars as in Fig. 5-2.

showings. However, if they were generated during or after obduction, pressure corrections  $< +30^{\circ}\text{C}$  would apply (see diagrams of Potter, 1977).

If the Rogues Harbour sulphides are related to seafloor processes, then depths similar to the above should be used for pressure corrections. However, if the sulphides are instead related to the QFP or other post-obduction processes, then the depth of deposition may be anywhere. Similarly, the inclusions in the QFP and possibly the shear zone may correspond to such a range of depth.

### 5.5. Discussion

Spooner (1981) has summarized the fluid inclusion characteristics of several hydrothermal deposits, which, with the Nippers Harbour inclusions, are reported in Table 5-3.

The Burtons Pond samples most closely resemble those from volcanogenic massive sulphides, implying that the fluids which generated the Burtons Pond ores also may be modified seawater. Burtons Pond salinities are higher than those of the Cyprus samples, and it is possible that these higher salinities result from boiling (which would also greatly influence sulphide deposition). However, no evidence for boiling was noted in the Burtons Pond nor any other Nippers Harbour samples. No vapour-rich inclusions were noted, and the vapour-liquid ratio was fairly constant.

Jehl (1975) recorded salinities and homogenization temperatures for 25 specimens from the Mid-Atlantic Ridge, adjacent zones and transverse fractures. Salinities were of the order of 2 to 16 eq. wt% NaCl, and homogenization

	SALINITY (Wt% NaCl)	HOMOGENIZATION TEMPERATURE ( C)	FLUID	MINERALIZATION TEXTURES
VOLCANO- GENIC MASSIVE SULPHIDES	3.0%	260 to 330	Seawater	Massive sulphide lens or stockwork
EPITHERMAL Au-Ag-Cu- Pb-Zn VEINS OR REPLACEMENT DEPOSITS	0.5 to 12 %	200 to 330	Mainly meteoric	Simple fracture or complex vein systems Crustiform, comb and vug structures
DEPOSITS ASSOCIATED WITH IGNEOUS INTRUSIONS (NO BOILING)	5.0 to 10.0 %	200 to 400	Magmatic+ Meteoric	Massive and disseminated
ARCHEAN LODE GOLD DEPOSITS	2.0 to 4.0%	200 to 490	Magmatic, Meteoric or Seawater; CO <sub>2</sub> -rich	Massive ore and vein systems
BURTONS POND	4.55 %	193.5		Stockwork
ROGUES HARBOUR	18.74 %	174.7		Vug structure in quartz vein
SHOWING NO.2	2.42 %	169.5		Vug and fragmental
DIABASE	13.0 %	169.8		
QFP	12.4 %	152.5		

**Table 5-3:** Fluid Inclusion and Other Characteristics of Selected Hydrothermal Deposits, and of Nippers Harbour Inclusions

Salinities and homogenization temperatures of the Nippers Harbour inclusions are quoted as statistical means. Data from the former is taken from Spooner (1981) and Rona (1984).

temperatures in the range of 124° to 335°C. He concluded that a hydrothermal fluid, operating under low pressure and a high geothermal gradient, was responsible. This fluid originated from seawater which penetrated down to depths of 4 to 5 km in the crust.

The pressure-corrected homogenization temperatures are substantially lower than modern hydrothermal fluids ejecting from seafloor vents (350°C), or from fluid inclusions from ophiolitic stockworks (260° to 330°C) (Spooner, 1980, 1981).

A temperature decline during mineralization is common in hydrothermal ore deposition (Spooner, 1981; Edmond, 1984). This presumably reflects the decay of the heat or fluid source. It is possible that the Burtons Pond samples recorded such a situation.

It is also possible that the temperatures reflect the true hydrothermal fluid temperatures at the time of trapping. The Burtons Pond mineralization may have been generated by modified seawater (as shown by the fluid composition and salinities). It has been suggested that the Burtons Pond mineralization may have formed during or after obduction of the ophiolite, upon reactivation of the Stocking Harbour Fault. If this is true, then the seawater fluids which generated the mineralization may have been released along faults or obduction-related thrust planes during this event.

Saunders (1985) reported that the fluid inclusions measured from Betts Cove may be unrelated to mineralization. Whereas those samples were open space fills

and related to faults that post-date the orebody, the Burtons Pond quartz samples are intergrown intimately with sulphides and are more likely related to the mineralizing event. The Betts Cove inclusions are very similar to those at Burtons Pond, suggesting that the fluids also may have been trapped seawater, released upon later faulting.

The Showing No. 2 quartz vein exhibits salinities in the range of volcanogenic massive sulphide and seawater salinities (mean 2.42 eq. wt% NaCl). Although the homogenization temperature mean is very low (169.5°C), it could represent a waning hydrothermal system (as at Burtons Pond). The sulphides here also could be generated by those mechanisms operating at Burtons Pond.

Primary and secondary inclusions from Rogues Harbour samples display markedly high salinities. The fluid inclusion measurements most closely resemble measurements from epithermal type veins, which may or may not be related to the margins of intrusive stocks (Table 5-4) (Nash, 1973). Similarly, the Rogues Harbour showing may be related to the QFP, as sulphide textures in the Rogues Harbour samples mimic the crustiform and vug structures of epithermal veins. The Rogues Harbour homogenization temperatures are slightly lower than those of vein deposits; this again may be attributable to a decaying heat source.

Measurements from inclusions in QFP, diabase and the shear zone are all similar. The QFP fluids probably are late- or post-magmatic, as the homogenization temperatures are not as high as granitic magmatic temperatures, which are in the order of 450°C and higher (Weisbrod, 1981). Salinities of fluids

in the diabase are much higher than seawater salinities, hence the inclusions measured may have been related to late meteoric and not seawater processes. Boiling probably is necessary to produce such high salinities.

Comparison of fluid inclusion temperatures and those calculated from sulphur isotope pairs (see Section 4.8.3) reveals minor differences. The only possibly reliable sulphur isotope temperatures were those calculated from sulphide pairs from Showing No. 2, which gave temperatures of  $114^{\circ}\pm 23^{\circ}$  and  $209^{\circ}\pm 73^{\circ}\text{C}$ . Fluid inclusion homogenization temperatures from a Showing No. 2-related quartz vein have a mean of  $169.5^{\circ}\text{C}$ . These temperatures all are low ( $<250^{\circ}\text{C}$ ) and comparable. Any differences may reflect a lack of equilibrium between the quartz (which contained the fluid inclusions) and the sulphides (which yielded the sulphur isotope measurements). The fluid inclusions and sulphur isotopes also could have measured different thermal events, in that the sulphides generally precipitated before the vein-sealing quartz.

### 5.6. Summary

Fluid inclusions from Burtons Pond, Showing No. 2, Rogues Harbour, QFP, diabase and shear zone quartz veins yield information about fluid compositions, salinities and homogenization temperatures. The inclusions are a simple liquid-vapour type, several of which contain a variety of solid phases (anhydrite, carbonate, halite, unknown).

Fluids which generated the Burtons Pond and Showing No. 2 mineralization are believed to be modified seawater, based on their compositions (containing



possibly KCl, NaCl, NaCl-MgCl<sub>2</sub>, NaCl-MgCl<sub>2</sub>) and salinities (2.42 to 4.55 eq. wt. % NaCl (means)). The homogenization temperatures (193.5° and 169.5°C means) are lower than temperatures recorded from modern hydrothermal vents (~350°C), suggesting that the Nippers Harbour fluids were generated in a different setting. If these showings formed during or after obduction, the fluids may have been trapped, lower-temperature modified seawater, released during this event or related faulting (e.g. Stocking Harbour Fault).

Inclusions from Rogues Harbour yield eutectic temperatures related to more complex salt compounds (CaCl<sub>2</sub>, NaCl-CaCl<sub>2</sub>, NaCl-KCl-CaCl<sub>2</sub>, NaCl-CaCl<sub>2</sub>-MgCl<sub>2</sub>). Secondary inclusions, believed to be related to mineralization, have high salinities (mean 18.7 eq. wt. % NaCl). These may have been generated by boiling; a phenomenon which also would have caused sulphide precipitation.

## Chapter 6

# Characteristics of Ore-Bearing Hydrothermal Fluids and Genetic Models

### 6.1. Hill Showing

#### 6.1.1. Introduction

The study of ocean-floor, ophiolitic massive sulphide deposits has been carried out for the last three decades. An entire generation of scientists have been involved in this research (Hegleson, 1964, 1969; Bostrom and Peterson, 1966; Degens and Ross (1969), Bender *et al.*, 1971; Corliss 1971; Sillitoe, 1972; Spooner and Fyfe, 1973; Upadhyay and Strong (1973); Strong (1984); Lambert and Sato, 1974; Andrews and Fyfe, 1976; Spooner, 1977; Large, 1977; Finlow-Bates and Large, 1978; Plimer and Finlow-Bates, 1978; Solomon and Walshe, 1979; Henley and Thornley, 1979; Spooner, 1980; Parmentier and Spooner, 1978; Rona, 1978, 1980, 1987; Rona and Lowell, 1980, Rona *et al.*, 1983; Mottl, 1983; Lydon, 1984; Campbell *et al.*, 1984; Strong and Saunders, 1988). Currently, much attention is being focussed on active hydrothermal vents on the seafloor and associated tectonics.

Massive sulphides are considered to be a result of the mixing of hot, seawater-derived hydrothermal solutions and cold seawater at the seafloor

interface. Cold seawater is drawn down into the crust through faults and fractures, is circulated convectively through the rock column, becomes heated and leaches metals from the mafic oceanic rocks. The hot fluids then carry the metals to the surface, where they precipitate metalliferous deposits.

The hydrothermal fluids feeding the deposits have been shown to be contemporaneous seawater through the use of Sr-isotopes (Chapman and Spooner, 1977), hydrogen and oxygen isotopes (Heaton and Sheppard, 1977) and fluid inclusions (Spooners and Bray, 1977; Spooner, 1980) based on stockwork samples from ophiolitic deposits. Heaton and Sheppard (1977) further suggested that some of their data indicated that some of the alteration may not have been caused by modified seawater, but by a meteoric or magmatic component.

#### **6.1.2. Application to the Hill Showing**

Altered rocks of the Hill showing bear strong similarities to those of massive sulphide stockwork zones, but with two important differences. The first is that stockwork zones generally are located beneath the ore lens and form the footwall assemblage. There is no obvious stratified massive sulphide in the Hill area. Unit one breccia ore consists of sulphide-impregnated mafic fragments cemented by quartz-pyrite-chalcopyrite. It is impossible to discern the quantity of sulphide originally present as much of it has been removed by previous excavation.

Secondly, massive sulphide stockwork zones often, but not exclusively, form in pillow basalts at or beneath the seafloor. Host lithologies of the Hill showing are diabases, not pillow lavas. This has, however, been documented elsewhere in

the Betts Cove Ophiolite for massive sulphides at Betts Cove and Tilt Cove (Upadhyay and Strong, 1973; Strong and Saunders, 1988).

Stockwork-mineralized alteration pipes have been documented to extend down into the sheeted dyke complex (Constantinou, 1980; Richards *et al.*, in press). Recently, Richardson *et al.* (1987) documented epidosite zones which they believed to be the root zones of ore-forming fluids at Troodos, Cyprus. These zones occur in the lower part of the sheeted dyke complex and are characterized by epidote-quartz rock (epidosite) which replaces the dykes as sheets and pipes up to 1 km wide. Chemically, the epidosites are depleted in Cu and Zn relative to background diabases. Richardson *et al.* (1987) showed that the quantity of metal removed is sufficient to form massive sulphides and furthermore, that several large Cypriot deposits lie along strike of the epidosites.

Striped zones of epidote- and chlorite-rich rock were mapped stratigraphically below the showing. It is possible that, should epidosites indeed represent the sources of the ore-bearing fluids, the sulphide deposits at the Hill showing may have resulted from precipitation of such fluids.

Upadhyay and Strong (1973) suggested that sulphide precipitation occurs at the pillow-basalt/diabase interface which represents a permeability-temperature boundary, and that precipitation is a result of the mixing of ascending metal-enriched fluids with descending cold seawater. Gillis (1987) further proposed that the ascending solutions are driven by the intrusion of late-stage, shallow-level dykes or other such magmatic event. There is evidence at the Hill showing of intrusion of late diabase dykes into previously hydrothermally altered material.

Shear zones provide permeable conduits for fluids moving through the crust, thus it is probably safe to assume that rocks situated closest to these zones will be the most altered. This is reflected in the unit one and two chlorite-quartz-sulphide rocks which may reflect w/r ratios greater than 50 (Fig. 4-13) (Mottl, 1983). It is possible that unit three chlorite-quartz-albite xenoliths, scattered around the major shear zones, may have formed a cohesive unit before the intrusion of unit four diabases. Hydrothermal activity probably ceased before this later event, as the unit four rocks are represented only by a spilitic (greenschist) assemblage.

Figure 6-1 presents a schematic sequence of events that may have occurred to form the Hill ores and alteration assemblages. Stage I depicts the initial formation of diabase and pillow basalt units. Mixing of hot hydrothermal fluids and cold seawater occurs at this boundary during stage II, precipitating sulphides and forming the alteration assemblages depicted in stage III. Intrusion of fresh diabase dykes in stage IV causes previously altered material to form xenoliths about the two main shear zones.

## **6.2. Gold-Rich Showings - Burtons Pond, Gull Pond, Showing**

### **No. 2**

It has been shown petrographically that hydrothermal mineralization at the gold-rich showings at Nippers Harbour involves the deposition of pyrrhotite (Burtons Pond, Gull Pond) or pyrite (Showing No. 2) and chalcopyrite, with minor sphalerite, in fractures in chlorite-quartz+/-albite (Burtons Pond) or chlorite-sericite-quartz (all three showings) altered rocks. This was followed by

## GEOLOGICAL HISTORY OF THE HILL SHOWING

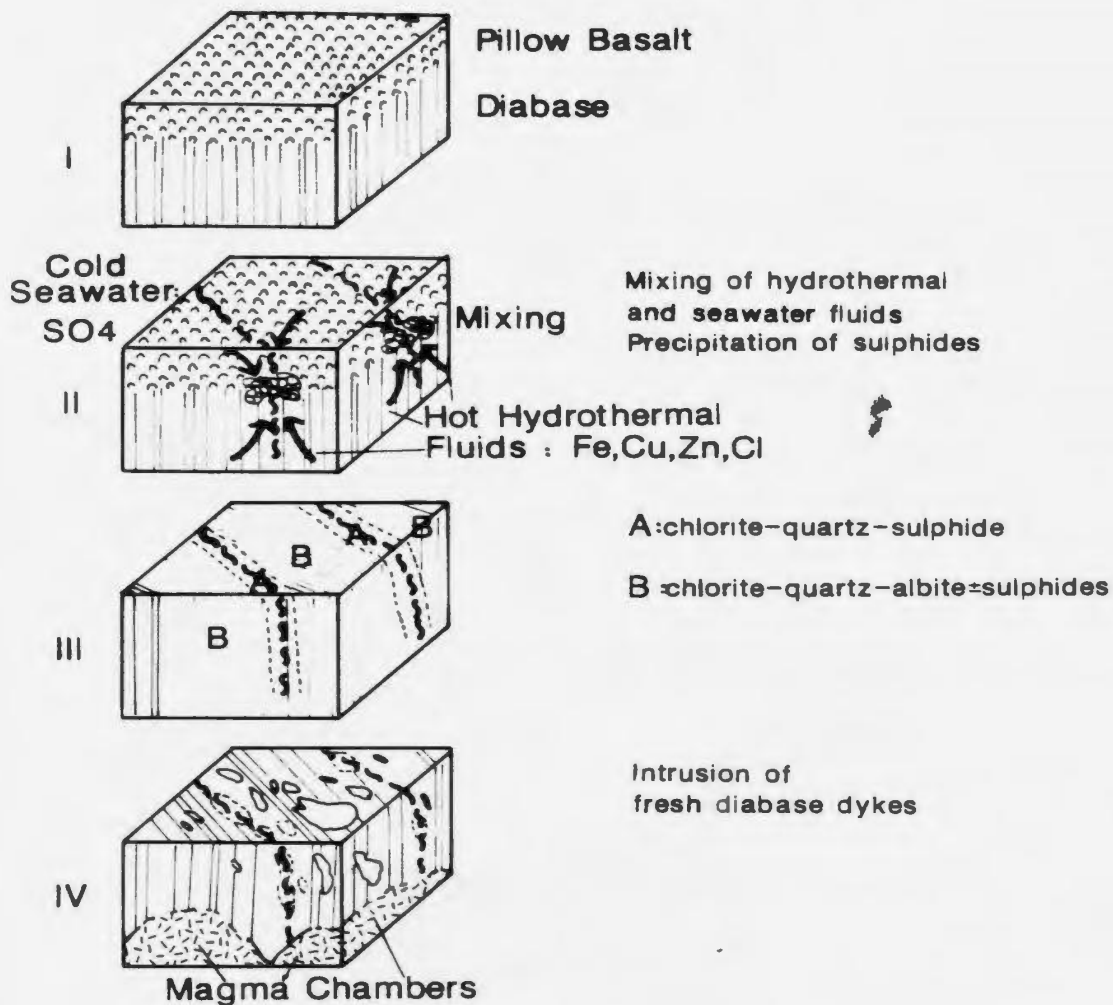


**Figure 6-1:** Schematic model for mineralization at the Hill showing

See text for explanation.

the precipitation of arsenic minerals, calcite and quartz. Gold may have been deposited during this later stage. Fluid inclusion compositions and salinities suggest that modified seawater may have generated the gold-rich ores. This information is used below to discuss the mode of transport and deposition of gold at these showings.

### 6.2.1. Source of Gold

Both Tilling *et al.* (1973) and Romberger (1986a) have presented data which suggests that there is no one particular rock type which is enriched in gold and therefore may serve as a preferred source. Romberger (1986b) postulated that the favourability of a rock as a gold source may depend on how the gold occurs, the chemistry of the rock itself, and the chemistry of the mobilizing solutions.

Despite these facts, there is a clear proximal association between gold deposits and serpentinized ultramafic rocks in both Archaean greenstone belts (Pyke, 1976) and in many Newfoundland occurrences (Tuach, 1987; Tuach *et al.*, 1988). LeBlanc (1986) has suggested that gold is leached from ultramafic rocks during serpeninization by As-CO<sub>2</sub>-rich solutions.

Background gold contents of mafic rocks (samples 32, 62, 69, 72, 84, 105; average 4.8 ppb Au) of Nippers Harbour samples are slightly higher than, but comparable with those of serpentinite (sample 158, 2.5 ppb) or quartz-feldspar porphyry (sample 186, 1.3 ppb). This suggests that that any of these may have been the major source of gold.

### 6.2.2. Modes of Gold Transport

Previous studies on gold transport in hydrothermal solutions have contrasted the solubility of gold-chloride species in acid oxidizing solutions with various gold-sulphide species. Recently, Grigoryeva and Sukneva (1981) have suggested the existence of thio-arsenide complexes, based on relatively high gold solubilities in sulphide solutions containing arsenic, and on the ubiquitous association of arsenic in gold deposits of many different origins (Romberger, 1986b).

Henley (1973) determined the solubility of gold in chloride solutions at temperatures between 300°C and 500°C. He found that gold is transported most commonly as  $\text{AuCl}_2$  at these temperatures, but at lower temperatures, it occurred as  $\text{AuCl}_2^-$  in oxidized chloride solutions. Seward (1973, 1984) measured gold solubility as a function of temperature, pH and sulphide concentration. He demonstrated that gold thio-complexes ( $\text{Au}(\text{HS})_2^-$  and  $\text{Au}_2\text{S}(\text{HS})_2^{2-}$ ) are stable to at least 300°C, and in this temperature range (ie, <300°C), predominate over gold chloride complexes. The latter may be more dominant at higher temperatures (300°C to 500°C), but no data exist for gold thio-complex solubilities at these temperatures.

The solubilities and relative stabilities of gold chloride and thio-complexes are compared in Fig. 6-2. The diagram is calculated at 250°C (a maximum temperature for Nippers Harbour fluids based on fluid inclusion and sulphur isotope thermometers), and assumes a solution containing 3.5 wt.% NaCl and 0.01 M (320 ppm) total sulphur. It uses thermodynamic data of Wagman *et al.* (1969)



and stability constants of Seward (1973). The solubilities shown for gold thio-complexes are several orders of magnitude larger than those of gold chloride complexes. The gold thio-complex solubilities decrease very rapidly with both decreasing and increasing pH, while gold chloride solubilities decrease with decreasing oxygen activity and with increases in pH.

Fig. 6-3 illustrates the effects of stability fields of various iron-sulphide and -oxide phases on the solubility fields of the gold complexes outlined in Fig. 6-2. Fig. 6-3 shows that for the mineral assemblages in the Nippers Harbour showings (pyrrhotite, pyrite, gold, arsenopyrite), gold probably is carried as a thio-complex. Systems dominated by oxidized minerals such as hematite and magnetite probably had gold carried as a chloride complex. Fluid inclusions from Burtons Pond and Showing No. 2, however, feature moderate salinities and eutectics corresponding to common salts (NaCl, KCl, MgCl<sub>2</sub>, CaCl<sub>2</sub>), as well as sulphate (anhydrite) solid inclusions. This suggests that some of the Nippers Harbour gold may have been carried as a chloride complex.

Copper, lead and zinc may be transported in hydrothermal solutions as chloride or bisulphide (thio-) complexes. Chloride complexes of these metals are much more soluble than bisulphide complexes in saline, weakly acid ore-forming fluids with total sulphur  $< 10^{-2}$  M. It has been shown by Anderson (1975) that a solution should carry at least  $10^{-5}$  M of reduced sulphur to produce sulphide ores. Available data for base metal thio-complexes indicate that they are important below 250°C within neutral to alkaline solutions with total sulphur  $> 0.01$  M (Roberts, 1987).

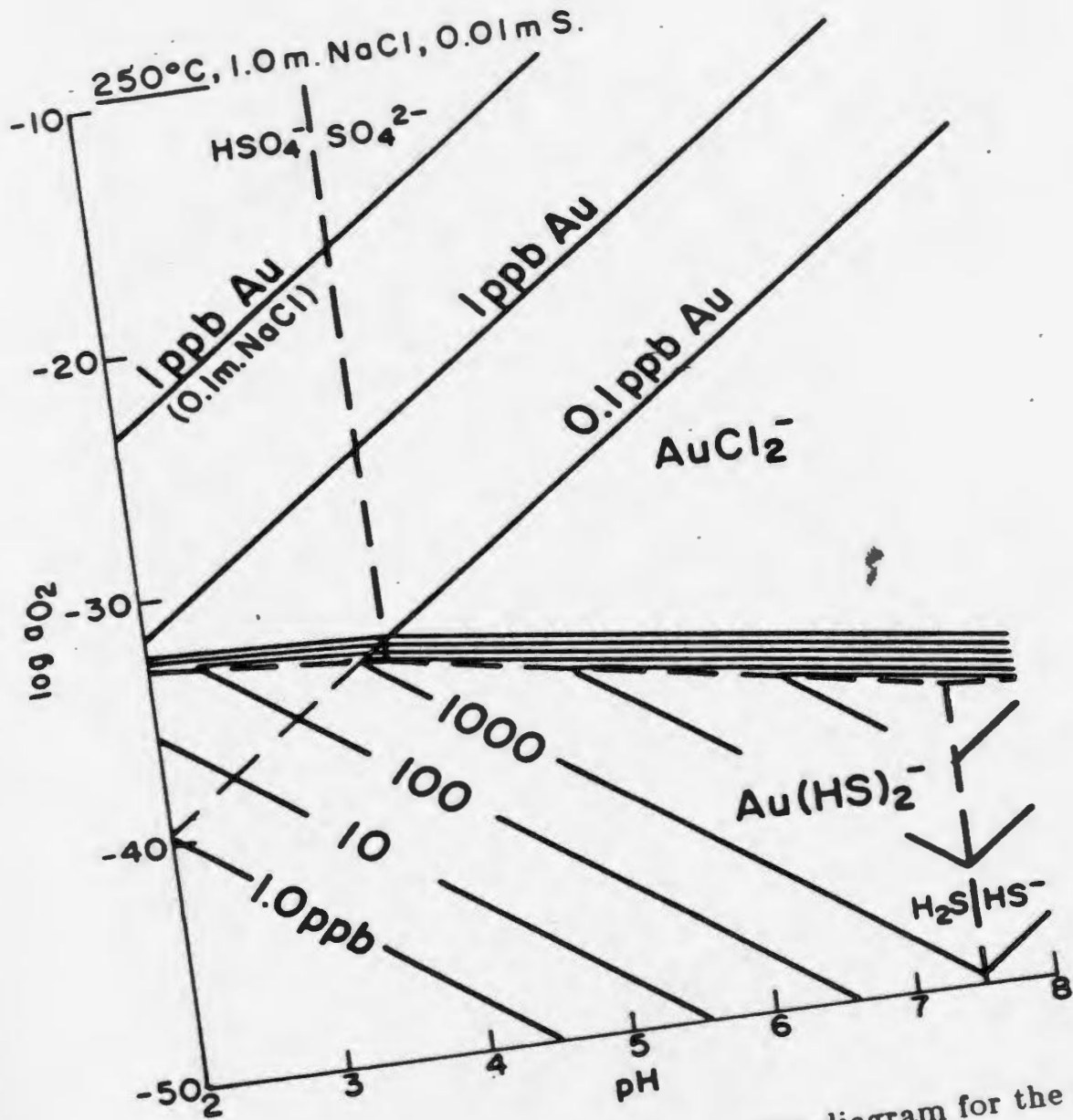


**Figure 6-2:** Calculated oxygen activity diagram for the system Au-NaCl-S-H<sub>2</sub>O at 250°C

From Romberger (1986b). Shows the relative solubilities of gold chloride and thio-complexes; assuming 1 M NaCl and 0.01 M S in aqueous solution.

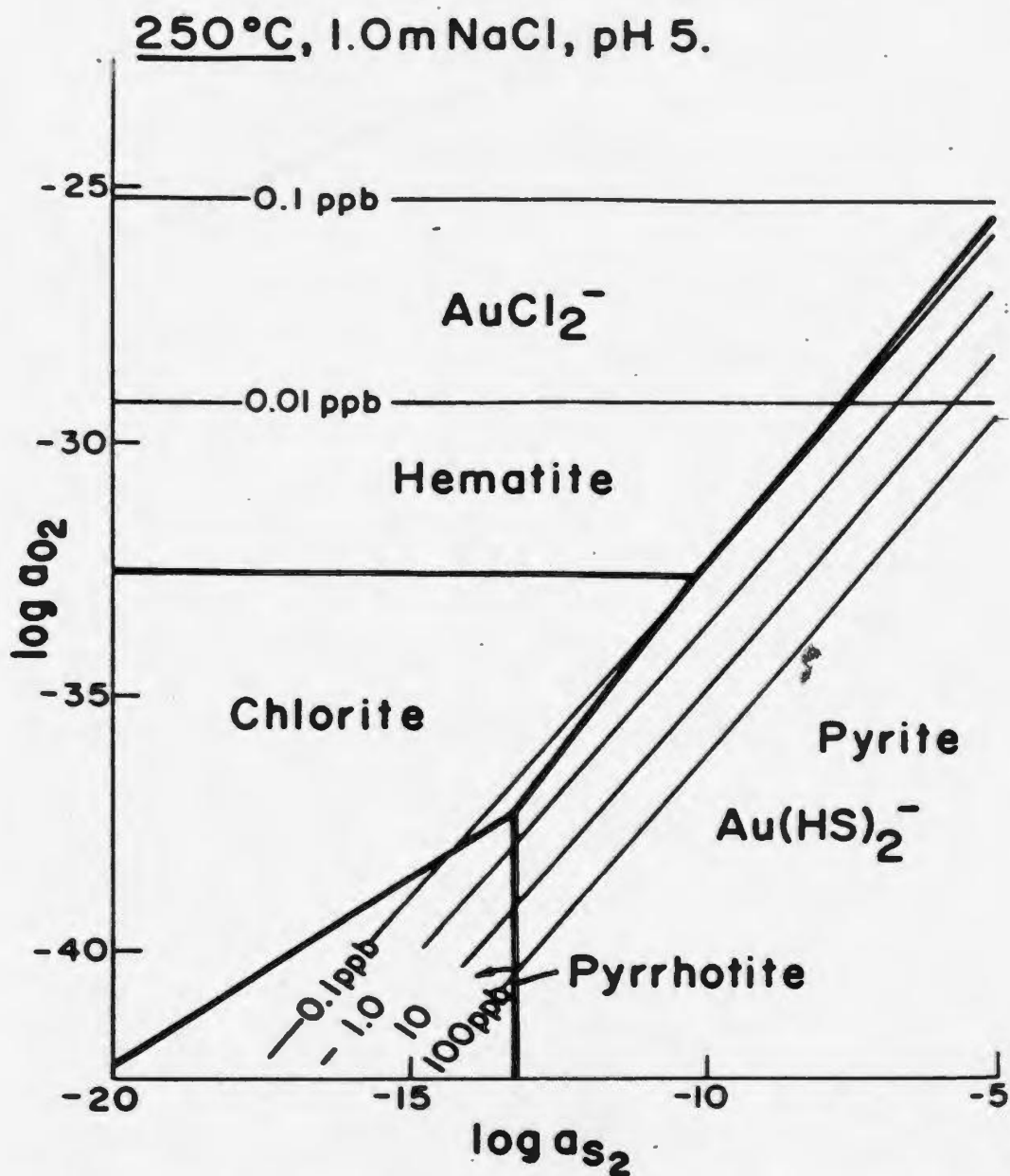


**Figure 6-3:** Calculated oxygen activity-sulphur activity diagram for the system Au-NaCl-S-H<sub>2</sub>O at 250°C and pH 5

From Romberger (1986b). Shows the relative stability of various iron minerals (heavy solid lines) and gold solubility relationships (light solid lines); 1 M NaCl in aqueous solutions.

Deposition of gold from thio-complexes may result from a decrease in temperature at constant pH, oxidation of the complex, or reduction in sulphur activity caused by sulphide precipitation (Seward, 1984; Romberger, 1986b). Any of these may apply to the gold-bearing fluids at Nippers Harbour, especially given the presence of anhydrite in the late quartz-hosted fluid inclusions (oxidation). Fig. 6-3, however, shows that the solubility curves for  $\text{Au}(\text{HS})_2^-$  are subparallel to the phase boundary for chlorite and pyrite. This suggests that gold would not be deposited in systems buffered by this assemblage if reduction in sulphur activity or oxidation are the only deposition mechanisms (Romberger, 1986b). Chlorite and pyrite occur together at Showing No. 2 and more rarely at Gull Pond. Clearly, an alternate mechanism of gold precipitation may have to be found for these areas. As pyrrhotite is the major iron sulphide at Burtons Pond, this problem is less important there.

Fig. 6-4 shows the stability fields for arsenopyrite superimposed on the phase relationships shown in Fig. 6-3. The phase relationships shown in Fig. 6-4 provide a solution to the problem outlined above. They suggest that the mineralizing solutions were dominated by reduced sulphur species and that gold was most likely transported as  $\text{Au}(\text{HS})_2^-$ . In this case, activities of sulphur and oxygen would be  $a_{\text{S}_2} < 10^{-13.5}$ ,  $a_{\text{O}_2} < 10^{-42}$ ; and  $a_{\text{S}_2} < 10^{-9.5}$ ,  $a_{\text{O}_2} < 10^{-42}$ , for Burtons Pond and Gull Pond, and Showing No. 2, respectively.

It is also possible, given the occurrence of arsenic minerals at the Nippers Harbour gold-bearing showings, that gold could have been transported as one of the thio-arsenide complexes of Grigoryeva and Sukneva (1981). Assuming a stoichiometry of  $\text{AuAsS}_2^0$ , the equation:

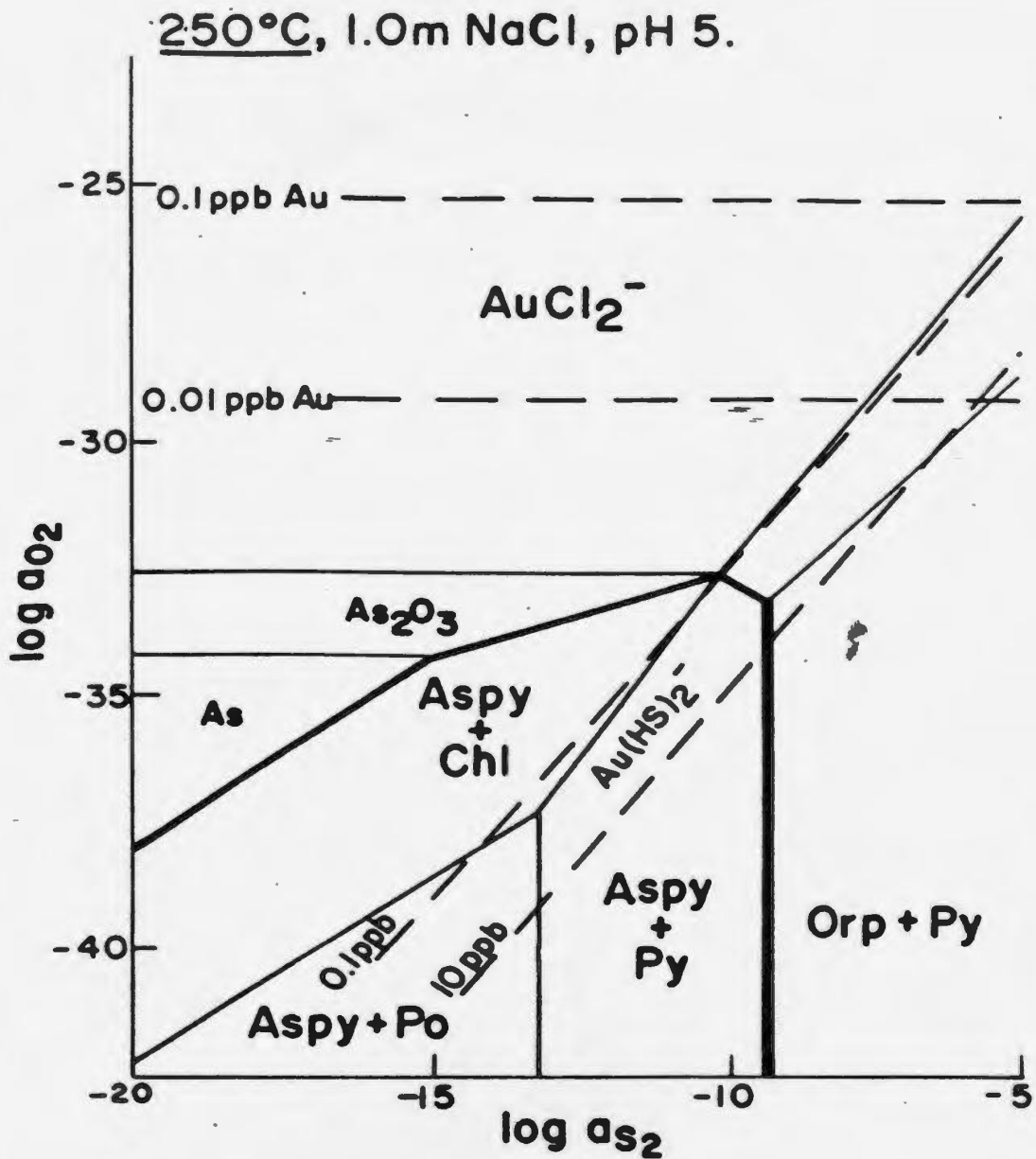


**Figure 6-4:** Calculated oxygen-activity-sulphur activity diagram for the system Au-Fe-As-NaCl-S-H<sub>2</sub>O at 250°C and pH 5

From Romberger (1986b). Shows the stability field of arsenopyrite (heavy solid lines) superimposed on the solution-mineral equilibria of Fig. 6-3.

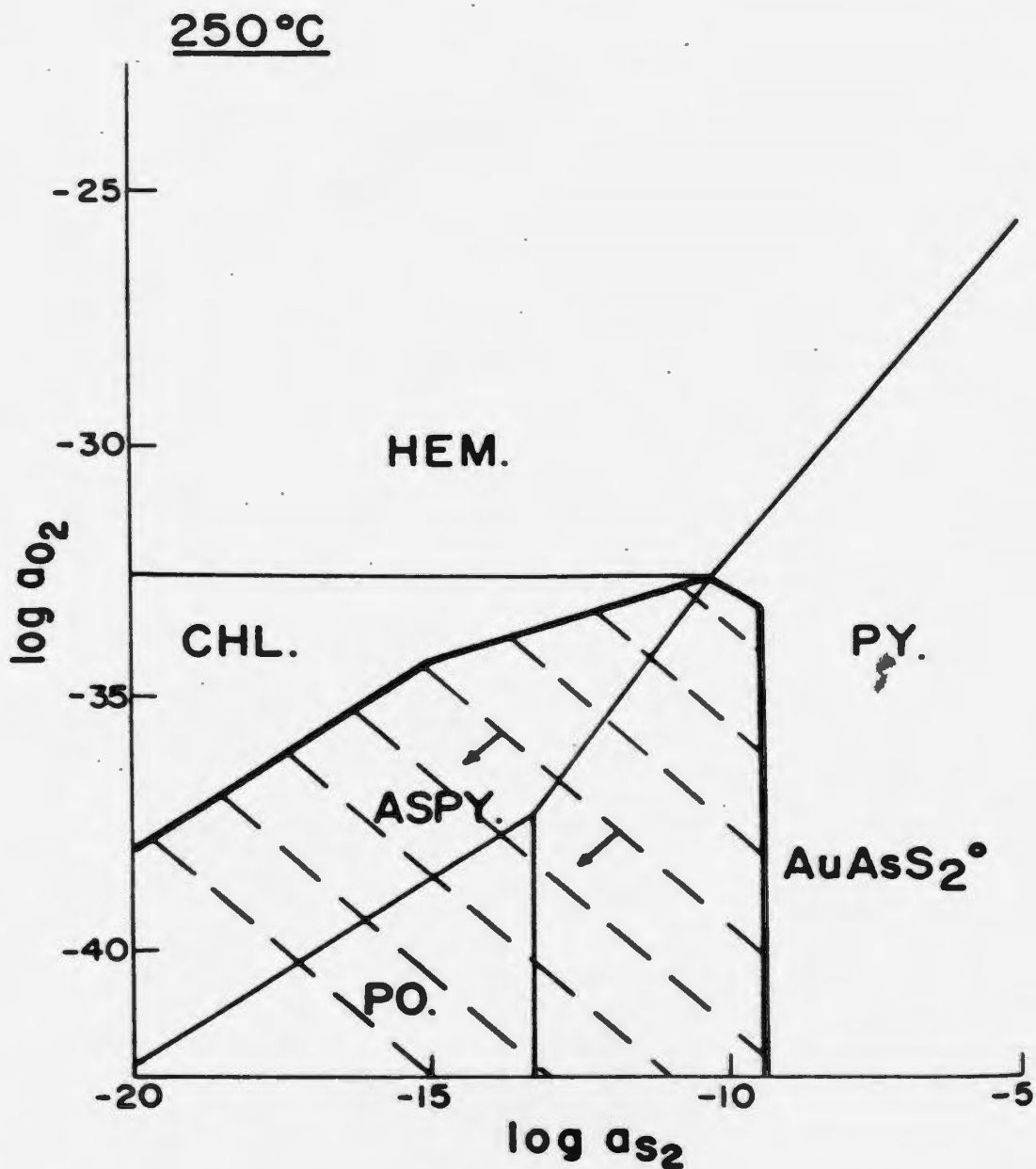
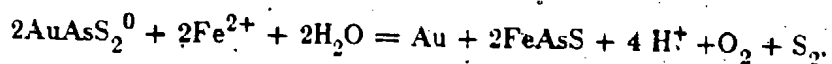


**Figure 8-5:** Calculated oxygen activity-sulphur activity diagram for the system  $Au-Fe-As-NaCl-S-H_2^0$  at 250°C and pH 5

From Romberger (1986b). Shows the solubility of gold as a thio-arsenide complex (dashed lines) superimposed on the stability fields of arsenopyrite (heavy lines). Arrows indicate the direction of decreasing solubility.



would result in the co-precipitation of gold and arsenopyrite as observed at Gull Pond (Fig. 3-17) and Showing No. 2. Arsenopyrite and gold may have also formed at similar times at Burtons Pond (see Fig. 3-14 and Section 3.3.2.2). This equation was used by Romberger (1986b) to calculate gold thio-arsenide solubility contours, as shown in Fig. 6-5. Clearly a decrease in sulphur activity or reduction would cause gold precipitation. Estimates of sulphur and oxygen activities for Nippers Harbour gold-bearing solutions would be similar to those discussed above for thio-sulphide complexes.

### 6.2.3. Genetic Models

The timing of the Burtons Pond and other gold-rich showings is a problem. They could have formed prior to obduction of the ophiolite, as sub-seafloor deposits; during obduction, forming along faults related to thrusting; or after obduction. The Burtons Pond showing occurs on a splay of the Stocking Harbour fault. As discussed earlier, this fault may have been a seafloor feature which was reactivated after ophiolite obduction. The close spatial association of a phase of the Cape Brule porphyry (which is younger than the ophiolite) along the coast (Fig 2-10) confirms this observation. Mineralization may have formed along the Stocking Harbour Fault coevally with the intrusion of the porphyry, and after obduction.

Nickel-arsenide mineralization near the West Zone at Tilt Cove occurs near the contact of the pillow lava and a subsurface fault sliver of talc-carbonate rock

which may be related to the Stocking Harbour Fault. It also is found in calcite veins within the quartz-feldspar porphyry near the West Zone (Papezik, 1964), implying that it formed after solidification of that phase of the porphyry. Should all the nickel-arsenide (and gold) mineralization in the Betts Cove Complex be related, this fact suggests that the Nippers Harbour gold showings may be syn- or post-obduction rather than sub-seafloor-related features.

The listwaenite model for gold mineralization, as presented in Fig. 1-4 (Buisson and LeBlanc, 1986), shows that gold mineralization forms in carbonatized ultramafic rocks. Low temperature (150 to 300°C) NaCl brines, derived both from mantle material and from interaction with seawater, are focussed along major thrusts related to the late stages of ophiolite emplacement. Gold is associated with sulphide or cobalt arsenide mineralization, or with late quartz veins containing pyrite or arsenopyrite.

The Nippers Harbour gold bearing fluids have been shown to have very low CO<sub>2</sub> contents (see Section 4.5.1). Fluids which generated Archaean (Colvine *et al.*, 1984) and Mother Lode (California) (Bohlke and Kistler, 1986) gold deposits, however, are dominated by CO<sub>2</sub> and H<sub>2</sub>O, as shown by fluid inclusions with high CO<sub>2</sub> contents. Colvine *et al.* (1984) inferred that these high densities are a function of fluid entrapment at considerable depths, 5 km or greater. Gold therefore may have been transported as a CO<sub>2</sub> complex, although no research has been done to date on the existence of such complexes. The lack of CO<sub>2</sub>-bearing inclusions in the Nippers Harbour gold-bearing samples implies that the mineralization may have formed at levels more shallow than 5 km.



The fluids which generated gold-rich mineralization in the Mother Lode area, California (Bohlke and Kistler, 1986; Weir and Kerrick, 1987) have some similar features to those of Nippers Harbour. The Mother Lode fluids have the following characteristics:  $T = 250^{\circ}$  to  $325^{\circ}\text{C}$ ,  $X\text{CO}_2 = 0.1$ ,  $\text{pH} = 5.5$  to  $6.0$ ,  $\text{H}_2\text{S} =$  dominant sulphur species,  $a\text{O}_2 = 10^{-32}$  to  $10^{-35}$  (Weir and Kerrick, 1987), which, apart from  $X\text{CO}_2$ , are relatively similar to the Nippers Harbour fluids. Bohlke and Kistler (1986) showed that the fluids were isotopically heavy and  $\text{CO}_2$ -bearing, and did not resemble seawater, magmatic, or meteoric waters. They were probably metamorphic waters, generated from deep sources and set in motion by deep magmatic activity related to east-dipping subduction along the western margin of North America (Bohlke and Kistler, 1986; Weir and Kerrick, 1987). The Nippers Harbour fluids, however, have characteristics (salinities, eutectics) suggesting that they are modified seawater.

The model envisaged for the formation of the Burtons Pond ores is portrayed in Fig. 6-6. Seawater-derived fluids flowed along shallow thrust planes underlying mafic and serpentized ultramafic rocks, leaching metals from both of these units, probably during or after ophiolite emplacement. Gold, as discussed earlier, most likely was carried as a thio-complex, but also may have been partially transported as a thio-arsenide or chloride complex. Fluids were low temperature ( $<250^{\circ}\text{C}$ ), moderate pH ( $\sim 5$ ), and had low oxygen and sulphur activities. Precipitation of sulphides and formation of chloritic and sericitic alteration assemblages occurred when the fluids encountered fault splays. Heat,  $\text{K}_2\text{O}$  and Ba may have been supplied by the coevally forming Cape Brule Porphyry.

Although the Gull Pond and Showing No. 2 showings are not found directly on the Stocking Harbour fault; they are spatially close to the porphyry and are found in fault zones which parallel the major faults. The model depicted in Fig. 6-6 also may apply to the formation of this mineralization.

### **6.3. Rogues Harbour, Welshs Bight**

Both the Rogues Harbour and Welshs Bight showings occur directly on the Stocking Harbour fault, near the Cape Brule quartz-feldspar porphyry. The Welshs Bight lead has been suggested to originate from the porphyry (see Section 4.9). The calcite and arsenopyrite found in the vein sample suggest that sulphide deposition may be related to the same process which generated the gold-rich showings, although no significant gold was documented there.

Sulphur isotopes clustering about 0 per mil at Rogues Harbour suggest an igneous source for the sulphur. Sulphides related to seafloor deposition generally are heavier (2 to 8 per mil), implying that the Cape Brule Porphyry was instead the source of sulphur there. Cu, Fe and Zn may have been derived from the underlying gabbros and deposited with sulphur in fractures in the quartz vein on the Stocking Harbour Fault. Fluid inclusion salinities of secondary inclusions believed to be related to mineralization are very high (15.6 to 20.4 eq. wt. % NaCl), suggesting that boiling (phase separation) occurred. Boiling is also a very efficient mechanism of precipitating sulphides. Several of the altered samples are enriched in  $K_2O$ , which also may have been contributed by the porphyry.

In conclusion, fluids derived from the porphyry, which was intruded along

## GOLD MINERALIZATION MODEL BURTONS POND

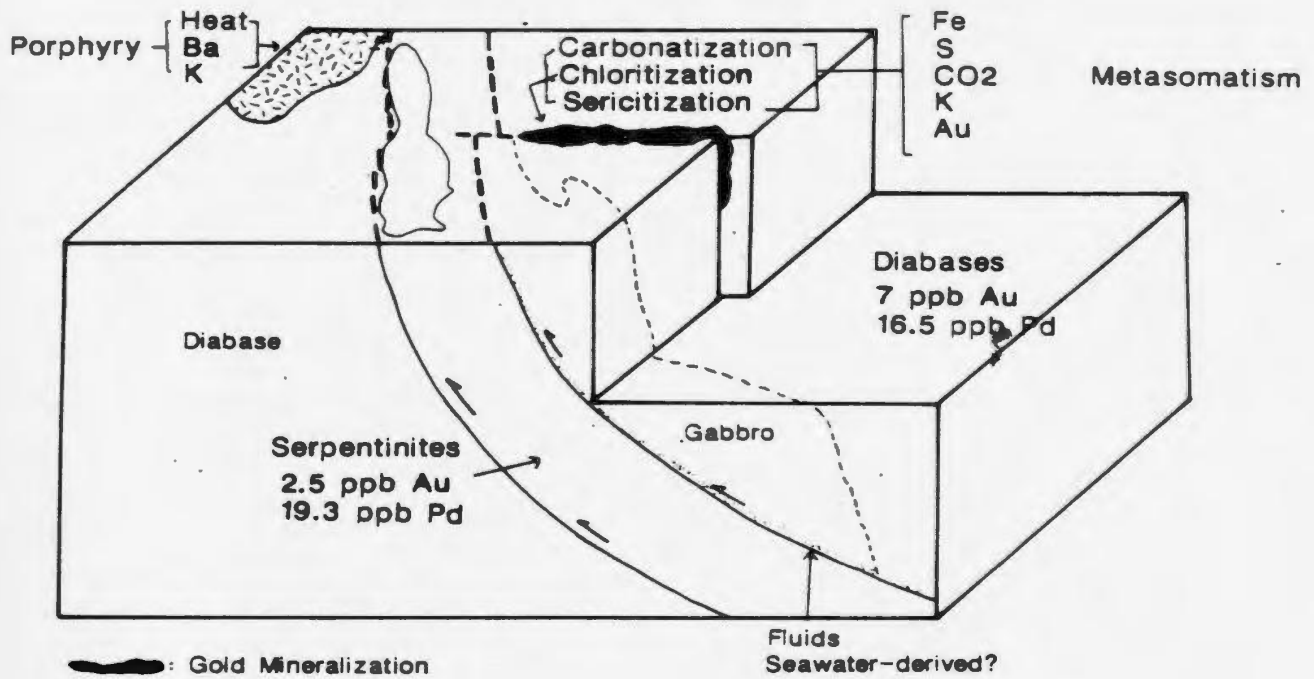


**Figure 6-6:** Model for gold mineralization at Burtons Pond

See text for discussion.

the Stocking Harbour Fault at Rogues Harbour, leached metals and precipitated them in fractures in an earlier quartz vein there, possibly in response to boiling.

## Chapter 7

### Summary and Recommendations

#### 7.1. Summary

The Ordovician Nippers Harbour Ophiolite is considered to be a southward extension of the neighbouring Betts Cove Ophiolite. The Nippers Harbour Ophiolite is overlain unconformably by the Silurian Cape St. John Group, a sequence of subaerial conglomerates, sandstones, basic pyroclastics and subaerial to rhyolitic welded tuffs, and also is intruded by the Silurian Cape Brule Porphyry, a medium to coarse grained, homogeneous quartz-feldspar pluton.

Ultramafic, gabbro and sheeted dyke units of the Nippers Harbour Ophiolite are represented in the map area. Ultramafic rocks are mainly serpentinized dunites with veins of pyroxenite, while gabbros generally are medium-grained to pegmatitic, and are unlayered. Dykes normally are sheeted, displaying narrow chilled and sometimes brecciated margins. Contacts between these ophiolitic units are both gradational and faulted.

The Cape Brule quartz-feldspar porphyry dominates the map area. It contains quartz and feldspar phenocrysts in a fine-grained, quartz-plagioclase-dominant matrix. A distinct phase whose matrix is dominated by orthoclase crops

out along the Stocking Harbour Fault along the coast. Scattered outcrops of Cape St. John Group conglomerate, basaltic dyke, rhyolite and intrusive breccia occur throughout the area.

The map area is dominated structurally by shear zones and faults, especially the Stocking Harbour Fault. Most of the mineralization occurs along, and may be controlled by this fault. The major faults in the area may be early pre-obduction features which have been reactivated upon intrusion of the Cape Brule Porphyry.

Unaltered mafic rocks of the Nippers Harbour Ophiolite are similar to Betts Cove boninitic-like lavas in that they have anomalously low  $\text{TiO}_2$  contents, and high  $\text{SiO}_2$ ,  $\text{MgO}$ ,  $\text{Cr}$  and  $\text{Ni}$  relative to other common basalts. Mafic intrusive rocks at Nippers Harbour are slightly more enriched in elements such as  $\text{Y}$ ,  $\text{Zr}$ ,  $\text{Cr}$  and  $\text{Ni}$  than those at Betts Cove, suggesting that the Nippers Harbour Ophiolite is derived from a more incompatible element-enriched source than that which generated the Betts Cove Ophiolite.

Six major mineralized showings were examined in detail for this study. They all are found in fault zones in altered diabase or gabbro. Sulphide mineralogy is fairly simple, consisting of pyrrhotite or pyrite, chalcopyrite, with lesser and varying sphalerite, arsenopyrite, and electrum ( $\text{Au-Ag}$ ). The latter two minerals appear to have formed later than other sulphides. Galena is found only at the Welshs Bight showing.

The Hill showing is believed to be a sub-seafloor, pre-obduction feature.

Mineralization there consists of pyrite and chalcopyrite in shear zones in quartz-chlorite rocks (units one and two), as well as minor pyrite in quartz-chlorite-albite rocks (unit three). These hydrothermally altered rocks have been intruded by fresh diabase dykes (unit four). Units one and two samples display enrichments in  $\text{FeO}_4$ , Cu and Zn, and depletions in  $\text{Na}_2\text{O}$  and CaO, and can be related to the formation of iron-rich chlorite, iron sulphides (pyrite and chalcopyrite), and to the destruction of feldspar by the hydrothermal fluids. Unit three rocks show less significant depletions in CaO and  $\text{Na}_2\text{O}$ . Mineralization probably occurred by the mixing of hot hydrothermal fluids and cold seawater at the pillow basalt-diabase interface, precipitating sulphides and forming the alteration assemblages described above. Intrusion of fresh diabase dykes (unit four) caused previously altered material to form xenoliths about earlier-formed shear zones.

The Burtons Pond, Gull Pond and Showing No. 2 areas are characterized by high base metal (Cu, Zn) and gold contents. Host rocks are altered to assemblages of chlorite-sericite-quartz (at all three showings), and chlorite-quartz+/-albite and calcite-sericite (Burtons Pond only). Gold is found on the edges of chalcopyrite and pyrrhotite grains, in quartz-calcite gangue and in arsenopyrite, all of which are found in veins cutting altered host rocks. Alteration at these showings is expressed chemically by the addition of  $\text{FeO}_4$ , S,  $\text{K}_2\text{O}$ ,  $\text{CO}_2$ , Ba, and some MgO, and variable depletions of REE, CaO, Sr, and  $\text{Na}_2\text{O}$ , which can be accounted for by the formation of iron- and magnesium-rich chlorite, sericite and calcite. Gold enrichment correlates best with enrichments in S,  $\text{FeO}_4$  and  $\text{CO}_2$ . Temperatures calculated from sulphide pairs using sulphur isotope

values from Showing No. 2 are low ( $114^{\circ} \pm 23^{\circ}$  to  $209^{\circ} \pm 73^{\circ}\text{C}$ ), and generally are in agreement with temperatures from fluid inclusion measurements from Burtons Pond and Showing No. 2, suggesting a possible upper temperature limit of  $250^{\circ}\text{C}$ . Salinities and eutectic temperatures of the gold-bearing fluids are similar to seawater.

Relatively high background gold values suggest that the ophiolitic diabases and gabbros, or serpentinized ultramafic or quartz-feldspar porphyry rocks may have been the source of gold for these showings. Gold was transported probably as a thio-complex, but moderate salinities, anhydrite in fluid inclusion and the ubiquitous presence of arsenic minerals suggest that gold also may have been carried as a chloride or thio-arsenide complex. The fluids had the following characteristics:  $T \leq 250^{\circ}\text{C}$ , pH 5.5, total reduced sulphur  $< 10^{-3}$  M,  $a_{\text{O}_2} < 10^{-4.2}$  M and  $a_{\text{S}_2} < 10^{-13.5}$  M. Mineralization is believed to have formed by the movement of seawater-derived fluids along shallow thrusts, depositing sulphides and gold in splays. Intrusion of the Cape Brule Porphyry may have been coeval with, and possibly the cause of this mineralization.

Other sulphide showings include the Rogues Harbour Cu-bearing and the Welshs Bight Pb-Zn-bearing quartz veins. Sulphur isotopes clustering about 0 per mil at Rogues Harbour suggest an igneous source for sulphur, possibly the Cape Brule Porphyry. Several of the samples are enriched in  $\text{K}_2\text{O}$ , which also may have been contributed by the porphyry. Fluid inclusions from mineralization-related samples have very high salinities, suggesting that the sulphides may have been deposited through boiling.



Lead from the Welshs Bight showing has been suggested to originate from the porphyry. Calcite and arsenopyrite found in the vein suggest that the mineralization may be related to the same process which generated the gold-rich mineralization, although no anomalous gold was documented there.

## 7.2. Recommendations for Future Work

The following list is a compilation of ideas for future work which could be carried out on the mineralized showings in the Nippers Harbour Ophiolite:

- (1) More sample collecting, particularly of Welshs Bight sulphide and host rock samples, and of new drill core which is being provided through further exploration of the Nippers Harbour area.
- (2) Further examination of gold grain associations to provide more evidence for its paragenesis.
- (3) Stable isotope data, possibly on quartz-chlorite pairs from the various showings, to give some idea of fluid temperatures and source(s).
- (4) More Pb isotope data, especially at Welshs Bight and perhaps on pyrite or other sulphide minerals from other showings to further delineate the Pb source(s).

## References

- Abbey, S. 1980. Studies in "Standard Samples" for use in the general analysis of silicate rocks and minerals. Part 6. 1979 Edition of "usable" values. Geological Survey of Canada, Paper 80-14.
- Advocate Mines Limited. 1967. Diamond drilling data, Nippers Harbour. Unpublished report, Newfoundland Department of Mines and Energy, Mineral Development Division, Open File Report 2E/13 (187)
- Anderson, G. M. 1975. Precipitation of Mississippi Valley-type ores. *Economic Geology*, 70, p. 937-942
- Andrews, A. J. and Fyfe, W. S. 1978. Metamorphism and massive sulphide generation in oceanic crust. *Geoscience Canada*, 3, p. 84-94
- Arndt, N. T. and Nesbitt, R. W. 1982. Geochemistry of Munro Township basalts. in: *Komatiites*, eds. N. T. Arndt and E. G. Nisbet, George Allen and Unwin, London, England, p. 309-329
- Bachinski, D. J. 1977. Alteration associated with metamorphosed ophiolitic cupriferous iron sulfide deposits: Whalesback Mine, Notre Dame Bay, Newfoundland. *Mineralium Deposita*, 12, p. 48-63
- Bain, G. W. 1933. Wall rock mineralization along Ontario gold deposits. *Economic Geology*, 28, p. 705-745
- Baird, D. M. 1947. The geology of the Burlington Peninsula, Newfoundland. Ph. D. thesis, McGill University, Montreal
- Baird, D. M. 1948. Copper mineralization in the Betts Cove-Stocking Harbour district, Notre Dame Bay, Newfoundland. *Canadian Mining and Metallurgical Bulletin*, April, p. 211-213
- 1951. The geology of the Burlington Peninsula, Newfoundland. Geological Survey Canada, paper 51-21, 70 p.
- Barton, P. B. Jr. and Skinner, B. J. 1979. Sulfide mineral stabilities. in: *Geochemistry of Hydrothermal Ore Deposits* (2nd ed.), ed. H. L. Barnes. Wiley Interscience, New York, N. Y., p. 278-403
- Bell, K. and Blenkinsop, J. 1978. Reset Rb/Sr whole-rock systems and chemical control. *Nature*, 273, p. 532-534

- Bender, M., Broecker, W., Gornitz, V., Middel, V., Kay, R. and Sun, S. 1971. Geochemistry of three cores from the East Pacific Rise. *Earth Planetary Science Letters*, 12, p. 425-433
- Bohlke, J. K. and Kistler, R. W. 1986. Rb-Sr, K-Ar, and stable isotope evidence for the ages and sources of fluid components of gold-bearing quartz veins in the Northern Sierra Nevada Foothills metamorphic belt, California. *Economic Geology*, 81, p. 266-322
- Bonnatti, E. 1975. Metallogenesis at oceanic spreading centers. *Annual Review Earth Planetary Science Letters*, 3, p. 401-431
- Bostrom, K. and Peterson, M. N. A. 1968. Precipitates from hydrothermal exhalations on the East Pacific Rise. *Economic Geology*, 61, p. 1258-1265
- Bowers, T. S., Campbell, A. C. and Edmond, J. M. 1987. Solution chemistry at ridge crest hot springs. in: *Recent Hydrothermal Mineralization at Seafloor Spreading Centres: Tectonic, Petrologic and Geochemical Constraints. Program and Abstracts*, Feb. 5-6, 1987, McGill University, Montreal, Quebec.
- Boyle, R. W. 1979. The geochemistry of gold and its deposits. *Geological Survey Canada Bulletin*, 280, 584p.
- Buisson, G. and LeBlanc, M. 1985. Gold in carbonatized ultramafic rocks from ophiolite complexes. *Economic Geology*, 80, p. 2028-2029
- 1986. Gold-bearing listwaenite (carbonatized ultramafic rocks) in ophiolite complexes. in: *Metallogeny of Basic and Ultrabasic Rocks*, eds. J. M. Gallagher, R. A. Iscear, C. R. Neary and H. M. Prichard, London Institute Mining and Metallurgy, p. 121-132
- Cameron, W. E. and Nisbet, E. G. 1982. Phanerozoic analogues of komatiitic basalts. in: *Komatiites*, eds. Arndt, N. T. and Nisbet, E. G., George Allen and Unwin, London, p. 29-50
- Cameron, W. E., Nisbet, E. G. and Dietrich, V. J. 1979. Boninites, komatiites and ophiolitic basalts. *Nature*, 280, p. 550-553
- Cameron, W. E., Nisbet, E. G. and Dietrich, V. G. 1980. Petrographic dissimilarities between ophiolitic and ocean-floor basalts. in: *Ophiolite*, ed. A. Panayiotou, *Proceedings International Ophiolite Symposium*, Nicosia, Cyprus, April 1979, Geological Survey Cyprus, p. 182-192

- Campbell, I. H., McCougall, T. J. and Turner, J. S. 1984. A note on fluid dynamic processes which can influence the deposition of massive sulfides. *Economic Geology*, 79, p. 1905-1913
- Cann, J. R. 1970. Rb, Sr, Y, Zr and Nb in some ocean floor basaltic rocks. *Earth Planetary Science Letters*, 10, p. 7-11
- Carmichael, D. M. 1984. Mineral equilibria in metabasites and metagreywackes in the transition from greenschist to amphibolite facies. *Geological Society America, Abstracts with Programs*, 16, p. 464
- Chapman, H. J. and Spooner, E. T. C. 1977.  $^{87}\text{Sr}$  enrichment of ophiolitic sulphide deposits in Cyprus confirms ore formation by circulating seawater. *Earth Planetary Science Letters*, 35, p. 71-78
- Church, W. R. and Riccio, L. M. 1977. Fractionation trends in the Bay of Islands ophiolite, Newfoundland: polycyclic cumulate sequences in ophiolites and their classification. *Canadian Journal Earth Sciences*, 14, p. 1156-1165
- Clark, M. E., Archibald, N. J. and Hodgson, C. J. 1986. The structural and metamorphic setting of the Victory gold mine, Kambalda, Western Australia. in: *Proceedings of Gold '86, an International Symposium on the Geology of Gold*, ed. A. J. Macdonald, Toronto, 1986, p. 243-254
- Coish, R. A. 1977a. Ocean floor metamorphism in the Betts Cove Ophiolite, Newfoundland. *Contributions Mineralogy Petrology*, 60, p. 255-270
- 1977b. Petrology of the mafic units of west Newfoundland ophiolites. Ph. D. thesis, University of Western Ontario, London, Ontario, 227 p.
- Coish, R. A. and Church, W. R. 1978. The Betts Cove ophiolite, Newfoundland: some unusual chemical characteristics. [abstract] *EOS, Transactions American Geophysical Union*, 59, p. 408
- 1979. Igneous geochemistry of mafic rocks in the Betts Cove Ophiolite, Newfoundland. *Contributions Mineralogy Petrology*, 70, p. 29-39
- Coish, R. A., Hickey, R. and Frey, F. A. 1982. Rare earth element geochemistry of the Betts Cove ophiolite, Newfoundland: complexities in ophiolite formation. *Geochimica Cosmochimica Acta*, 46, p. 2117-2134
- Colvine, A. C., Andrews, A. J., Cherry, M. E., Durocher, M. E., Fyon, A. J.,

- Lavigne, M. J. Jr., Macdonald, A. J., Marmont, S., Poulsen, K. H., Springer, J. S. and Troop, D. G. 1984. An integrated model for the origin of Archean lode gold deposits. Ontario Geological Survey Open File Report 5524, 98 p., 7 tables, 53 figs. and 2 appendices
- Constantinou, G. 1980. Metallogenesis associated with Troodos ophiolite. in: Ophiolites, ed. A. Panayiotou, Proceedings International Ophiolite Symposium, Nicosia, Cyprus, April 1979. Geological Survey Cyprus, p. 663-674
- Corliss, J. B. 1971. The origin of metal-bearing submarine hydrothermal solutions. *Journal Geophysical Research*, 76, p. 8123-8138.
- Coyle, M. and Strong, D. F. 1987. Geology of the Springdale Group: a newly recognized Silurian epicontinental-type caldera in Newfoundland. *Canadian Journal Earth Sciences*, 24, p. 1135-1148
- Crawford, M. L. 1981. Phase equilibria in aqueous fluid inclusions. in: *Fluid Inclusions: Applications to Petrology*, eds. L. S. Hollister and M. L. Crawford, Mineralogical Association Canada Short Course Handbook, 6, p. 75-100
- Crocket, J. H. and Lavigne, M. J. 1984. Sulphur sources in the Dickenson gold mine as suggested by sulphur isotopes. in: *Gold '82*, ed. R. P. Foster, Zimbabwe Geological Society, Special Publication No. 1, p. 417-434
- Cullers, R. L. and Graf, J. L. 1984. Rare earth elements in igneous rocks of the continental crust: Intermediate and silicic rocks - Ore petrogenesis. in: *Rare Earth Element Geochemistry*, ed. P. Henderson, Elsevier, Amsterdam, p. 275-316
- Dean, P. L. 1978. The volcanic stratigraphy and metallogeny of Notre Dame Bay, Newfoundland. *Memorial University Newfoundland Geology Report* 7, 204 p.
- Deer, W. A., Howie, R. A. and Zussman, J. 1966. *An Introduction to the Rock Forming Minerals*. Longman Group Ltd, Harlow, England, 528 p.
- Degens, E. T. and Ross, D. A. 1969. (eds.) *Hot Brines and Recent Heavy Metal Deposits in the Red Sea*. Springer, New York, N. Y., 600 p.
- DeGrace, J. R., Kean, B. F., Hsu, E. and Green, T. 1976. Geology of the Nippers Harbour map area (2E/13), Newfoundland. Newfoundland Department Mines and Energy, Mineral Development Division, Report 76-3, 73 p.

- Donoghue, H. G., Adams, W. S. and Harper, C. E. 1959 Tilt Cove copper operation of the Maritimes Mining Corporation Limited, Canadian Institute Mining Metallurgy, Journal, 62, p. 54-73
- Douglas, G. V., Williams, D., Rove, O. N. and others 1940. Copper deposits of Newfoundland. Geological Survey of Newfoundland Bulletin 20, 176 p.
- Dunning, G. R. 1984. The geology, geochemistry, geochronology and regional setting of the Annieopsquotch Complex and related rocks of southwest Newfoundland. Ph. D. thesis, Memorial University of Newfoundland, St. John's, Newfoundland, 402 p.
- Edmond, J. M. 1984. Hydrothermal ore generation within sediment starved and sediment covered ridge areas. Geological Association Canada, Newfoundland Branch, Spring Meeting
- Edmond, J. M., Measures, C., McDuff, R. E., Chan, L. H., Collier, R., Grant, B., Gordon, L. I. and Corliss, J. B. 1979a. Ridge crest hydrothermal activity and the balance of the ocean: the Galapagos data. Earth Planetary Science Letters, 46, p. 1-18
- Edmond, J. M., Measures, C., Mangum, B., Grant, B., Sclater, F. R., Collier, R., Hudson, A., Gordon, L. I. and Corliss, J. B. 1979b. On the formation of metal-rich deposits at ridge crests. Earth Planetary Science Letters, 46, p. 19-30
- Epstein, R. S. 1983. The eastern margin of the Burlington Granodiorite, Newfoundland. M. Sc. thesis, University of Western Ontario, 188 p.
- Faure, G. 1977. Principles of Isotope Geology. John Wiley and Sons, New York, 464 p.
- Finlow-Bates, T. and Large, D. E. 1978. Water depth as major control on the formation of submarine exhalative ore deposits. Geologisches Jahrbuch, D30, p. 27-39
- Flanagan, F. J. 1973. 1972 values for internal geochemical reference standards. Geochimica Cosmochimica Acta, 37, p. 1189-1200
- Frey, F. A., Gryan, W. B. and Thompson, G. 1974. Atlantic Ocean floor: Geochemistry of basalts from Legs 2 and 3 of the DSDP. Journal Geophysical Research, 79, p. 5507-5527
- Froese, E. 1969. Metamorphic rocks from the Coronation mine and surrounding area. Geological Survey Canada, Paper 68-5, p. 55-77

- Fryer, B. J. and Hutchinson, R. W. 1976. Generation of metal deposits on the seafloor. *Canadian Journal Earth Sciences*, 13, p. 126-135
- Fyfe, W. S. and Kerrich, R. 1984. Gold: Natural concentration processes. in: *Gold '82*, ed. A. A. Balkema, Rotterdam, The Netherlands, p. 99-127
- Gale, G. H. 1969. The primary dispersion of Cu, Zn, Ni, Co, Mn, and Na adjacent to sulfide deposits, Springdale Peninsula, Newfoundland. M. Sc. thesis, Memorial University of Newfoundland, St. John's, Newfoundland, 143 p.
- Gillis, K. 1987. Alteration of the upper oceanic crust: Comparison of DSDP Hole 504B and the Troodos Ophiolite. in: *Recent Hydrothermal Mineralization at Seafloor Spreading Centres: Tectonic, Petrologic and Geochemical Constraints, Program and Abstracts, February 5-6, 1987*, McGill University, Montreal, Quebec.
- Graf, J. L. Jr. 1977. Rare earth elements as hydrothermal tracers during the formation of massive sulfide deposits in volcanic rocks. *Economic Geology*, 72, p. 527-548
- Grant, J. A. 1988. The isocdn diagram—a simple solution to Gresens' equation for metasomatic alteration. *Economic Geology*, 81, p. 1976-1982
- Gresens, R. L. 1967. Composition-volume relationships of metasomatism. *Chemical Geology*, 2, p. 47-65
- Grigoryeva, T. A. and Sukneva, L. S. 1981. Effects of sulphur and of antimony and arsenic sulphides on the solubility of gold. *Geochemistry International*, p. 152-158
- Hannington, M. D., Peter, J. M. and Scott, S. D. 1986. Gold in sea-floor polymetallic sulfide deposits. *Economic Geology*, 81, p. 1867-1883
- Hanson, G. N. 1980. Rare earth elements in petrogenetic studies of igneous systems. *Annual Review Earth Planetary Science*, 8, p. 371-406
- Hawkins, J. W., 1980. Petrology of back-arc basins and island arcs: Their possible role in the origin of ophiolites. in: *Ophiolites*, ed. A. Panayiotou, Proceedings, International Ophiolite Symposium, Cyprus, 1979. Geological Survey Department, Cyprus, p. 244-254
- Heaton, T. H. E. and Sheppard, S. M. F. 1977. Hydrogen and oxygen isotope evidence for sea-water hydrothermal alteration and ore deposition, Troodos

complex, Cyprus. in: Volcanic Processes in Ore Genesis, Geological Society London, Special Publication 7, p. 42-57

Hegleson, H. C. 1964. Complexing and Hydrothermal Ore Deposition. Pergamon Press, New York, N. Y., 128 p.

----- 1969. Thermodynamics of hydrothermal systems at elevated temperatures and pressures. *American Journal Science*, 267, p. 724-804

Hellman, P. L. and Henderson, P. 1977. Are rare earth elements mobile during spilitization? *Nature*, 267, p. 38-40

Henley, R. W. 1973. Solubility of gold in hydrothermal chloride solutions. *Chemical Geology*, 11, p. 73-87

Henley, R. W. and Thornley, P. 1979. Some geothermal aspects of polymetallic massive sulfide formation. *Economic Geology*, 74, p. 1600-1612

Hibbard, J. 1982. Significance of the Baie Verte Flexure, Newfoundland. *Geological Society America Bulletin*, 93, p. 790-797

----- 1983. Geology of the Baie Verte Peninsula, Newfoundland. Newfoundland Department Mines and Energy, Mineral Development Division, Memoir 2, 279 p.

Hickey, R. L. and Frey, F. A. 1982. Geochemical characteristics of boninite series volcanics: implications for their source. *Geochimica Cosmochimica Acta*, 46, p. 2099-2115

Higgins, N. C. 1979. Theory, methods and application of fluid inclusion research. Geological Association Canada, Newfoundland Section, Short Course Notes, St. John's, Newfoundland, November 17, 1979, 74 p.

Holland, H. D. 1967. Gangue minerals in hydrothermal deposits. in: *Geochemistry of Hydrothermal Ore Deposits* (1st ed.), ed. H. L. Barnes. Holt, Rhinehart and Winston, p. 382-436

Holmes, A. 1946. An estimate of the age of the earth. *Nature*, 157, p. 680-684

Houtermans, F. G. 1946. Die Isotopenhaufigkeiten im natürlichen Blei und das Alter des Urans. *Naturwissenschaften*, 33, p. 185-186, 219

Humphris, S. E. and Thompson, G. 1978. Hydrothermal alteration of oceanic basalts by seawater. *Geochimica Cosmochimica Acta*, 42, p. 107-125



- Hurley, T. D. 1982. Metallogeny of a volcanogenic gold deposit, Cape St. John Group, Tilt Cove, Newfoundland. B. Sc. thesis, McMaster University, Hamilton, Ontario, 63 p.
- Hurley, T. D. and Crocket, J. H. 1985. A gold-sphalerite association in a volcanogenic base-metal-sulfide deposit near Tilt Cove, Newfoundland. *Canadian Mineralogist*, 23, p. 423-430
- Hutchison, R. W. and Searle, D. L. 1971. Stratabound pyrite deposits in Cyprus and relations to other sulphide ores. in: IAGOD volume, ed. Y. Takeuchi. Society Mining Geologists Japan, Special Issue 3, p. 198-205
- James, R. S., Grieve, R. A. F. and Pauk, L. 1978. The petrology of cordierite-anthophyllite gneisses and associated mafic and pelitic gneisses at Manitouwadge, Ontario. *American Journal Science*, 278, p. 41-63
- Jehl, V. 1975. The metamorphism of the oceanic rocks of the North Atlantic and fluids associated with it. Ph. D. Thesis, University Nancy, 242 p. (in French)
- Jonasson, I. R. and Franklin, J. M. 1987. Nature of alteration zone beneath Galapagos Ridge sulfide mounds. in: *Recent Hydrothermal Mineralization at Seafloor Spreading Centres: Tectonic, Petrologic and Geochemical Constraints, Program and Abstracts, February 5-6, 1987*, McGill University, Montreal, Quebec.
- Kajiwara, Y. and Krouse, H. R. 1971. Sulfur isotope partitioning in metallic sulfide systems. *Canadian Journal Earth Sciences*, 8, 1397-1408.
- Kerrick, R. 1979. Lode gold deposits in greenstone belts, chemical and hydrodynamic constraints. in: *Gold: Exploration and outlook*, eds. T. Anderson, P. Chamois and D. Desnoyers, Adams Club Annual Special Symposium, 8th, February 1979, McGill University, Montreal Proceedings, p. 13-34
- 1983. Geochemistry of gold deposits in the Abitibi greenstone belt. CIM Special Paper 27, 75 p.
- Kerrick, R. and Fryer, B. J. 1979. Archean precious metal hydrothermal systems, Dome Mine, Abitibi Greenstone Belt, II. REE and oxygen isotope relations. *Canadian Journal Earth Sciences*, 16, p. 440-458
- 1981. The separation of rare elements from abundant base metals in Archean lode gold deposits: Implications of low water/rock source regions. *Economic Geology*, 76, p. 160-166

- Kerrick and Fyfe, 1981. The gold-carbonate association: source of  $\text{CO}_2$  and  $\text{CO}$  fixation reactions in Archean lode deposits. *Chemical Geology*, 33, p. 265-294
- Kerrick, R. and Hodder, R. W. 1982. Archean lode gold and base metal deposits: Chemical evidence for metal separation into independent hydrothermal systems. *CIM Special Volume 24*, p. 144-160
- Knuckey, M. J., Comba, C. D. A. and Riverin, G. 1982. Structure, metal zoning and alteration at the Millenbach deposit, Noranda, Quebec. in: *Precambrian Sulphide Deposits*, eds. R. W. Hutchinson, C. D. Spence and J. M. Franklin, Geological Association Canada, Special Paper 25, p. 255-295
- Knuckey, M. J., and Watkins, J. J., 1982. The geology of the Corbet massive sulphide deposit, Noranda district, Quebec, Canada. in: *Precambrian Sulphide Deposits*, eds. R. W. Hutchinson, C. D. Spence - and J. M. Franklin, Geological Association Canada, Special Paper 25, p. 297-317
- Lambert, I. B. and Sato, T. 1974. The Kuroko and associated ore deposits of Japan: A review of their features and metallogenesis. *Economic Geology*, 69, p. 1215-1236
- Lambert, I. B., Phillips, G. N. and Groves, D. L. 1984. Sulphur isotope compositions and genesis of Archaean gold mineralization, Australia and Zimbabwe. in: *Gold '82*, ed. R. P. Foster, Zimbabwe Geological Society, Special Publication No. 1, p. 389-416
- Large, R. 1977. Massive sulfides in volcanic terranes. *Economic Geology*, 72, p. 549-572
- LeBlanc, M. 1986. Co-Ni arsenide deposits, with accessory gold, in ultramafic rocks from Morocco. *Canadian Journal Earth Sciences*, 23, p. 1592-1602
- Linke, W. F. 1965. Solubilities of inorganic and metal-organic compounds. (4th ed.), 2, American Chemical Society, 1914 p.
- Luzhnaya, N. P. and Vereshtchetina, I. P. 1946. Sodium, calcium, magnesium chlorides in aqueous solutions at  $-57^\circ$  to  $+25^\circ\text{C}$  (polythermic solubility). *Zhurnl. Prikl. Khimii*, 19, p. 723-733
- Ludden, J. N. and Thompson, G. 1978. The behaviour of the rare earth elements during submarine weathering of tholeiitic basalt. *Nature*, 274, p. 147-149

- Lydon, J. W. 1984. Ore deposit models - 8 Volcanogenic massive sulphate deposits part I: A descriptive model. *Geoscience Canada*, 11, p. 195-202
- Lydon, J. W. and Galley, A. 1986. Chemical and mineralogical zonation of the Mathiati alteration pipe, Cyprus, and its genetic significance. in: *Metallogeny of Basic and Ultrabasic Rocks*, The Institute of Mining and Metallurgy, London., p. 49-68
- Martin, W. 1983. Once Upon a Mine: Story of Pre-Confederation Mines on the Island of Newfoundland. *Canadian Institute Mining and Metallurgy*, Special Volume 26, 98 p.
- Mattinson, J. M. 1975. Early Paleozoic ophiolite complexes of Newfoundland: Isotopic ages of zircons. *Geology*, 3, p. 181-183
- Miyashiro, A. 1973. The Troodos ophiolite complex was probably formed in an island arc. *Earth Planetary Science Letters*, 19, p. 218-224
- Mottl, M. J. 1983. Metabasalts, axial hot springs, and the structure of hydrothermal systems at mid-ocean ridges. *Geological Society America Bulletin*, 94, p. 161-180
- Mottl, M. J. and Holland, H. D. 1978. Chemical exchange during hydrothermal alteration of basalt by seawater - I. Experimental results for major and minor components of seawater. *Geochimica Cosmochimica Acta*, 42, p. 1103-1115
- Mottl, M. J., Holland, H. D. and Corr, R. F. 1979. Chemical exchange during hydrothermal alteration of basalt by seawater - II. Experimental results for Fe, Mn and sulfur species. *Geochimica Cosmochimica Acta*, 43, p. 869-884
- Nash, J. T. 1973. Geochemical studies in the Park City district, Utah: I. ore fluids in the Mayflower mine. *Economic Geology*, 68, p. 34-51
- Neale, E. R. W. 1957. Ambiguous intrusive relationship of the Betts Cove-Tilt Cove serpentinite belt, Newfoundland. *Geological Association Canada, Proc.*, 9, p. 95-107
- Neale, E. R. W., Kean, B. F. and Upadhyay, H. D. 1975. Post-ophiolite unconformity, Tilt Cove-Betts Cove area, Newfoundland. *Canadian Journal Earth Sciences*, 12, p. 880-886
- Ohmoto, H. and Rye, R. D. 1974. Hydrogen and oxygen isotopic compositions of

fluid inclusions in the Kuroko deposits, Japan. *Economic Geology*, 69, p. 947-953.

----- 1979. Isotopes of sulfur and carbon. in: *Geochemistry of Hydrothermal Ore Deposits* (2nd ed.), ed. H. L. Barnes, Wiley-Interscience, New York, N. Y., p. 509-567

Panayiotou, A. 1980. Cu-Ni-Co-Fe sulphide mineralization, Limassol Forest, Cyprus. *Proceedings of the International Ophiolite Symposium, Nicosia, Cyprus*, p. 102-116

----- 1986. Sulphide and arsenide mineralization associated with the basic and ultrabasic plutonic rocks of the Troodos Ophiolite, Cyprus. in: *Metallogeny of Basic and Ultrabasic Rocks*, Athens, p. 417-447

Papezik, V. S. 1964. Nickel minerals at Tilt Cove, Notre Dame Bay, Newfoundland. *Geological Association Canada, Proc.*, 15, part 2, p. 27-32

Papezik, V. S. and Fleming, J. M. 1967. Basic volcanic rocks of the Whalesback area, Newfoundland. *Geological Association Canada Special Paper* 4, p. 181-192

Parmentier, E. M. and Spooner, E. T. C. 1978. A theoretical study of hydrothermal convection and the origin of the ophiolite sulphide deposits of Cyprus. *Earth Planetary Science Letters*, 40, p. 33-44

Pattison, E. F., Auerbrei, J. A., Hannila, J. J. and Church, J. F. 1986. Gold mineralization in the Casa-Beradi area, Quebec, Canada. in: *Proceedings of Gold '86, an International Symposium on the Geology of Gold*, ed. A. J. Macdonald, Toronto, 1986, p. 170-183

Pearce, J. A. 1975. Basalt geochemistry used to investigate past tectonic environments on Cyprus. *Tectonophysics*, 25, p. 41-67

----- 1980. Geochemical evidence for the genesis and eruptive setting of lavas from Tethyan ophiolites. in: *Ophiolites*, ed. A. Panayiotou. *Proceedings International Ophiolite Symposium, Nicosia, Cyprus, April, 1979*, Geological Survey Cyprus, p. 261-272

Pearce, J. A. and Cann, J. R. 1973. Tectonic setting of basic volcanic rocks determined using trace element analyses. *Earth Planetary Science Letters*, 19, p. 290-300

- Peter, J. M., McConachy, T. F. and Scott, S. D. A geological and geochemical comparison of hydrothermal vent deposits in the Southern Trough of the Guymas Basin, Gulf of California and 11°N, East Pacific Rise. in: Recent Hydrothermal Mineralization at Seafloor Spreading Centres: Tectonic, Petrologic and Geochemical Constraints, Program and Abstracts, February 5-6, 1987. McGill University, Montreal, Quebec.
- Plimer, I. R. and Finlow-Bates, T. 1978. Relationship between primary Fe-sulfide species, sulfur source, depth of formation and age of submarine exhalative sulfide deposits. *Mineralium Deposita* (Berlin), 13, p. 399-410
- Potter, R. W. II. 1977. Pressure corrections for fluid-inclusion homogenization temperatures based on the volumetric properties of the system NaCl-H<sub>2</sub>O. *Journal Research-United States Geological Survey*, 5, p. 603-607
- Potter, R. W. II., Clyne, M. A. and Brown, D. L. 1978. Freezing point depression of aqueous chloride solutions. *Economic Geology* 73, p. 284-285
- Pringle, J. 1978. Rb-Sr ages of silicic igneous rocks and deformation, Burlington Peninsula, Newfoundland. *Canadian Journal Earth Sciences*, 15, p. 293-300
- Pye, E. G. 1960. Geology of the Manitouwadge area. Ontario Department of Mines, 66, part 8, 1957, 114 p.
- Pyke, D. R. 1976. On the relationship of gold mineralization and ultramafic volcanic rocks in the Timmins Area, northeastern Ontario. *Canadian Institute Mining Metallurgy Bulletin*, 69, p. 79-87
- Riccio, L. M. 1972. The Betts Cove Ophiolite, Newfoundland. M. Sc. thesis, University of Western Ontario, London, Ontario, 91 p.
- 1975. Report of mineral exploration on the Burlington Peninsula for 1975. Unpublished report, Philips Management Inc., Newfoundland Department Mines and Energy, Mineral Development Division, Open File Nfld (929)
- Richards, H. G., Cann, J. R. and Jensenius, J. J., in press. Mineralogical and metasomatic zonation of the alteration pipes of Cyprus sulfide deposits. (submitted to *Economic Geology*)
- Richardson, C. J., Cann, J. R., Richards, H. G., and Cowan, J. G. 1987. Metal-depleted root zones of the Troodos ore-forming hydrothermal systems, Cyprus. *Earth Planetary Science Letters*, 84, p. 243-253

- Ripley, E. M. and Ohmoto, H. 1977. Mineralogic, sulfur isotope and fluid inclusion studies of the stratabound copper deposits at the Raul Mine, Peru. *Economic Geology*, 72, p. 1017-1041
- Riverin, G. and Hodgson, C. J. 1980. Wall-rock alteration at the Millenbach Cu-Zn mine, Noranda, Quebec. *Economic Geology*, 75, p. 424-444
- Roberts, R. G. 1987. Ore deposits models #11. Archaean lode gold deposits. *Geoscience Canada*, 14, p. 37-52
- Roedder, E. 1967. Fluid inclusions as samples of ore fluids. in: *Geochemistry of Hydrothermal Ore Deposits* (1st ed.), ed. H. L. Barnes, Holt, Rhinehart and Winston, p. 515-574
- 1972. *Composition of Fluids Inclusions. Data of Geochemistry* (6th Ed.), Chapter JJ, United States Geological Survey Professional Paper 410 JJ, 164p.
- 1979. Fluid inclusions as samples of ore fluids. in: *Geochemistry of Hydrothermal Ore Deposits* (2nd ed.), ed. H. L. Barnes. Holt, Rhinehart and Winston, p. 684-737
- Roedder, E. and Bodnar, R. J. 1980. Geologic pressure determinations from fluid inclusion studies. *Annual Review Earth Planetary Science*, 8, p. 263-301
- Romberger, S. B. 1986a. *Geochemistry of Gold*. U. S. Geological Survey Professional Paper (in press)
- 1986b. The solution chemistry of gold as applied to the origin of hydrothermal deposits. in: L. A. Clark, (ed.), *Gold in the Western Shield*, CIM Special Volume 38, p. 168-186
- Rona, P. A. 1978. Criteria for recognition of seafloor hydrothermal mineral deposits. *Economic Geology*, 73, p. 135-160
- 1980. TAG Hydrothermal Field: Mid-Atlantic Ridge crest at latitude 26°N. *Journal Geological Society London*, 137, p. 385-402
- 1984. Hydrothermal mineralization at seafloor spreading centers. *Earth Science Reviews*, 20, p. 1-104
- 1987. Ocean ridge crest processes. *Reviews of Geophysics*, 25, p. 1089-1114

- Rona, P. A. and Lowell, R. P. 1980. (eds.) Seafloor Spreading Centers Hydrothermal Systems. Benchmark Papers in Geology, 56. Dowden, Hutchinson and Ross, Stroudsburg, Pennsylvania, 424 p.
- Rona, P. A., Bostrom, K., Laubier, L., Smith, K. L. Jr. 1983. (eds.) Hydrothermal Processes at Seafloor Spreading Centers. NATO Conference Series, Series IV: Marine Sciences 12, New York, Plenum Press, 796 p.
- Sakai, H. 1957/ Fractionation of sulfur isotopes in nature. *Geochimica Cosmochimica Acta*, 12, p. 150-169
- Sangster, D. F. 1968. Relative sulfur isotope abundance of ancient seas and stratabound sulphide deposits. *Proceedings Geological Association Canada*, 19, p. 79-86
- Saunders, C. M. 1985. Controls of Mineralization in the Betts Cove Ophiolite. M. Sc. thesis, Memorial University of Newfoundland, St. John's, Newfoundland, 200 p.
- Schroeter, T. G. 1971. Geology of the Nippers Harbour area, Newfoundland. M. Sc. thesis, University of Western Ontario, London, Ontario, 88 p.
- Scott, S. D. 1987. Seafloor sulphides: Lessons of relevance to ancient massive sulphide deposits. in: *Recent Hydrothermal Mineralization at Seafloor Spreading Centres: Tectonic, Petrologic and Geochemical Constraints*. Program and Abstracts, February 5-6, 1987, Montreal, Quebec.
- Seward, T. M. 1973. Thio complexes of gold in hydrothermal ore solutions. *Geochimica Cosmochimica Acta*, 37, p. 379-399
- 1984. The transport and deposition of gold in hydrothermal systems. in: *Gold '86*, ed. R. P. Foster, Geological Survey Zimbabwe Special Publication 1, p. 165-182.
- Seyfried, W. E. and Bischoff, J. L. 1981. Experimental seawater-basalt interaction at 300°C, 500 bars, chemical exchange, secondary mineral formation and implications for the transport of heavy metals. *Geochimica Cosmochimica Acta*, 45, p. 135-147
- Seyfried, W. E. and Mottl, M. J. 1982. Hydrothermal alteration of basalt by seawater under seawater-dominated conditions. *Geochimica Cosmochimica Acta*, 46, p. 985-1002
- Sillitoe, R. H. 1972. Formation of certain massive sulphide deposits at sites of

sea-floor spreading. Institute Mining Metallurgy Transactions, 81, Section B, p. 141-148

Smewing, J. D. 1975. Metamorphism of the Troodos massif, Cyprus. Ph. D. thesis, Open University, Milton Keynes, U. K.

Smirnov, V. I. 1977. Ore deposits of the USSR. Volume III. Pitman Books Ltd., London.

Snelgrove, A. K. 1929. Geological report on Betts Cove Copper Mine. Unpublished report, Norseman Corporation Limited, Newfoundland Department Mines and Energy, Mineral Development Division Open File 2E/13(23)

----- 1931. Geology and ore deposits of Betts Cove-Tilt Cove area, Notre Dame Bay, Newfoundland. Ph. D. thesis, Princeton University, New Jersey. (published in Canadian Mining Metallurgical Bulletin, 24, 43 p.)

Solomon, M. and Walshe, J. L. 1979. The formation of massive sulphide deposits on the sea floor. Economic Geology, 74, p. 797-813

Spooner, E. T. C. 1977. Hydrodynamic model for the origin of the ophiolite cupriferous pyrite ore deposits of Cyprus. in: Volcanic Processes in Ore Genesis, Geological Society London, Special Publication 7, p. 58-71

----- 1980. Cu-pyrite mineralization and seawater convection in oceanic crust - the ophiolitic ore deposits of Cyprus. in: The Continental Crust and its Mineral Deposits, ed. D. W. Strangway, Geological Association Canada Special Paper 20, p. 685-704

----- 1981. Fluid inclusion studies in hydrothermal ore deposits. in: Fluid Inclusions: Applications to Petrology, eds. L. S. Hollister and M. L. Crawford, Mineralogical Association Canada Short Course Handbook, 8, p. 209-240

Spooner, E. T. C. and Bray, C. J. 1977. Hydrothermal fluids of seawater salinity in ophiolitic sulphide deposits in Cyprus. Nature, 266, p. 808-812

Spooner, E. T. C. and Fyfe, W. S. 1973. Sub-sea metamorphism, heat, and mass transfer. Contributions Mineralogy Petrology, 42, p. 287-304

Spooner, E. T. C., Chapman, H. J. and Smewing, J. D. 1977. Strontium isotopic contamination and oxidation during ocean floor hydrothermal



metamorphism of the ophiolitic rocks of the Troodos massif, Cyprus. *Geochimica Cosmochimica Acta*, 41, p. 873-890

- Squires, G. C. 1981. The distribution and genesis of the Tilt Cove sulphide deposits. B. Sc. thesis, Memorial University of Newfoundland, St. John's, Newfoundland, 115 p.
- Stacey, J. S. and Kramers, J. D. 1975. Approximation of terrestrial lead isotope evolution by a two-stage model. *Earth Planetary Science Letters*, 26, p. 207-222
- Strong, D. F. 1980. Geology of the Long Pond-Tilt Cove-Beaver Cove Pond area, western Notre Dame Bay, Newfoundland. Unpublished report, Newmont Mining Canada Ltd., Newfoundland Department Mines and Energy, Mineral Development Division, Confidential File 2E/13(408), 75 p.
- 1984. Geological relationship of alteration and mineralization at Tilt Cove, Newfoundland. in: *Mineral Deposits of Newfoundland- A 1984 Perspective*, ed. H. S. Swinden, Newfoundland Department Mines and Energy, Mineral Development Division, Report 84-3, p. 81-90
- Strong, D. F. and Saunders, C. M., 1988. Ophiolitic sulfide mineralization at Tilt Cove, Newfoundland: Controls by upper mantle and crustal processes. *Economic Geology*, 83, p. 239-255
- Sun, S. S. and Nesbitt, R. W. 1978. Geochemical regularities and significance of ophiolitic basalts. *Geology*, 6, p. 689-693
- Swinden, H. S. and Thorpe, R. I. 1984. Variations in style of volcanism and massive sulfide deposition in Early to Middle Ordovician island-arc sequences of the Newfoundland central mobile belt. *Economic Geology*, 79, p. 1596-1619
- Tatsumi, T. 1965. Sulfur isotope fractionation between coexisting sulfide minerals from some Japanese ore deposits. *Economic Geology*, 60, p. 1645-1659
- Taylor, S. R. and McLennan, S. M. 1985. (eds.) *The Continental Crust: its Composition and Evolution*. Blackwell Scientific Publications, p. 257, 298
- Thode, H. G. 1970. Sulfur isotope geochemistry and fractionation between coexisting minerals. *Mineralogical Society America Special Paper*, 3, p. 133-144

- Thorpe, R. I., Guha, J., Franklin, J. M. and Loveridge, W. D. 1984. Use of the Superior Province lead isotope framework in interpreting mineralization stages in the Chibougamau District. in: Chibougamou- Stratigraphy and Mineralization, eds. J. Guha and E. H. Chown, Canadian Institute Mining and Metallurgy, Special Volume 34, p. 496-516
- Tilling, R. I., Gottfreid, D. and Rowe, J. J. 1973. Gold abundance in igneous rocks and its bearing on gold mineralization. *Economic Geology*, 68, p. 168-186
- Tuach, J. 1987. Granite-related mineralization in Newfoundland, and compilation of gold data in Newfoundland. Newfoundland Department Mines and Energy, Mineral Development Division, Report of Activities for 1987, p. 7-9
- Tuach, J., Dean, P. L., Swinden, H. S., O'Driscoll, C. F., Kean, B. F. and Evans, D. T. W. 1988. Gold mineralization in Newfoundland: A 1988 review. in: Current Research (1988), Newfoundland Department Mines, Mineral Development Division, Report 88-1.
- Upadhyay, H. D. 1973. The Betts Cove Ophiolite and related rocks of the Snooks Arm Group, Newfoundland. Ph. D. thesis, Memorial University of Newfoundland, St. John's, Newfoundland, 224 p.
- 1974. Geology and mineral potential of Betts Cove-Tilt Cove area, Newfoundland. Unpublished Consolidated Morrison Exploration Ltd. report, Newfoundland Department Mines and Energy, Mineral Development Division, Open File 2E/12(329)
- 1978. Phanerozoic peridotitic and pyroxenitic komatiites from Newfoundland. *Science*, 202, p. 1192-1195
- 1982. Ordovician komatiites and associated boninite-type magnesian lavas from Betts Cove, Newfoundland. in: Komatiites, eds. N. T. Arndt and E. G. Nisbet, George Allen and Unwin, Boston, p. 187-198
- Upadhyay, H. D. and Neale, E. R. W. 1979. The Betts Cove - Tilt Cove ophiolite and associated rocks, Newfoundland. *Geological Society America Abstract with Program*, 8, p. 290
- Upadhyay, H. D. and Strong, D. F. 1973. Geological setting of the Betts Cove copper deposits, Newfoundland: an example of ophiolite sulphide mineralization. *Economic Geology*, 68, p. 161-167

- Upadhyay, H. D., Dewey, J. F. and Neale, E. R. W. 1971. The Betts Cove ophiolite complex, Newfoundland: Appalachian oceanic crust and mantle. *Proceedings Geological Association Canada*, 24, No. 1, July 1971
- Varga, R. J. and Moores, E. M. 1985. Spreading structure of the Troodos ophiolite, Cyprus. *Geology*, 13, p. 846-850
- Von Damm, K. L., Grant, B. and Edmond, J. M. 1983. Preliminary report on the chemistry of hydrothermal solutions at 21 North, East Pacific Rise. in: *Hydrothermal Processes at Seafloor Spreading Centers*, eds. P. A. Rona, K. Bostrom, L. Laubier and K. L. Smith. NATO Conference Series IV, Marine Sciences, Plenum Press, New York, p. 360-390
- Wagman, D. D., Evans, W. H., Parker, V. B., Halow, I., Bailey, S. M. and Schumm, R. H. 1969. Selected values of chemical thermodynamic properties. *Natural Bureau Standard Technical Note 270-4*, p. 39-42
- Walford, D. C. and Franklin, J. M. 1982. The Anderson Lake mine, Snow Lake, Manitoba. in: *Precambrian Sulphide Deposits*, eds. R. W. Hutchinson, C. D. Spence, and J. M. Franklin, *Geological Association Canada, Special Paper 25*, p. 481-523
- Wanless, R. K., Boyle, R. W. and Lowdon, J. A. 1960. Sulphur isotope investigations of the gold-quartz deposits of the Yellowknife District. *Economic Geology*, 55, p. 1591-1621
- Weir, R. H. Jr. and Kerrick, D. M. 1987. Mineralogic, fluid inclusion, and stable isotope studies of several gold mines in the Mother Lode, Tuolumne and Mariposa Counties, California. *Economic Geology*, 82, p. 328-344
- Weisbrod, A. 1981. Fluid inclusions in shallow intrusives. in: *Fluid Inclusions: Applications to Petrology*, eds. L. S. Hollister and M. L. Crawford, *Mineralogical Association Canada Short Course Handbook*, 6, p. 209-240
- Whitehead, R. E. S., Davies, J. F. and Cameron, R. A. 1980. Carbonate and alkalic alteration patterns in the Timmins gold mining area. *Ontario Geological Survey Miscellaneous Paper*, 93, p. 244-258
- Whitmore, D. R. E. 1969. Geology of the Coronation copper deposit. *Geological Survey Canada, Paper 68-5*, p.37-54
- Williams, H. 1976. Tectonic stratigraphic subdivision of the Appalachian orogen. *Geological Society America Abstracts with Program*, 8, p.1279-1295

1978 Tectonic lithofacies map of the Appalachian orogen.  
Memorial University Newfoundland, Map 1.

Winchester, J. A. and Floyd, P. A. 1976. Geochemical magma type discrimination: application to altered and metamorphosed basic igneous rocks. *Earth Planetary Science Letters*, 28, p. 459-469

Wood, P. C., Burrows, D. R., Thomas, A. V. and Spooner, E. T. C. 1986. The Hollinger-McIntyre Au-quartz vein system, Timmins, Ontario, Canada: Geological characteristics, fluid properties and light stable isotopes. in: *Proceedings of Gold '86, an International Symposium on the Geology of Gold*, ed. A. J. Macdonald, Toronto, 1986, p. 56-80

Zartman, R. E. and Doe, B. R. 1981. Plumbotectonics - the model. *Tectonophysics*, 75, p. 135-162

## Appendix A

### Mineralogy of Samples

Symbols used: fel: felspar; q: quartz; ak: actinolite; ch: chlorite; ep: epidote; ca: calcite; cr: chromite; ti: sphene; py: pyrite; cp: chalcopyrite; pn: pyroxene; sup: serpentine; sc: sericite; po: pyrrhotite; sp: sphalerite; asp: arsenopyrite; Au: electrum; gn: galena; or: orthoclase; o: others; jas: jasper; brav: bravoite; Ni: nickel-telluride; db: diabase; op: opaques; rk: rock fragments; P-pervasive alteration; S-semi-pervasive alteration; U-essentially unaltered.

## HILL

	fel	q	ak	ch	ep	ca	cr	ti	py	cp
Unit One										
159		X	X	X			X		X	X
170		X		X	X	X		X	X	X
199		X		X	X				X	X
235		X		X	X				X	X
Unit Two										
175		X		X	X				X	
195		X		X	X				X	X
260		X		X	X			X	X	X
261		X		X	X				X	X
Unit Three										
174	X	X		X	X				X	X
231	X	X		X	X					
232	X	X	X	X	X				X	
253		X	X	X	X				X	
258	X	X		X	X				X	
Unit Four										
250	X	X	X		X				X	
251	X		X	X	X	X		X		
252	X	X	X	X						
254	X	X	X	X						
256	X	X	X					X		

## BURTONS POND

	pn	fel	q	ak	ch	ep	ca	sup	sc	ti	cr	po	cp	sp	asp	py	Au
8		X		X		X											
10	X	X						X									
13								X									
16		X		X		X											
20	X	X		X													
298P		X	X	X	X					X	X	X	X	X	X	X	X
301U		X	X	X	X												
302P		X	X	X	X			X				X					
304U		X	X	X	X												
307S		X		X		X	X					X	X			X	
309S		X	X	X	X	X	X					X	X				
311P		X	X		X	X		X				X	X	X	X		X
K875U		X			X						X	X					
K9250		X		X													
K1125S		X		X	X		X	X				X					
K1375			X	X								X	X				X
K1275P			X		X	X						X					
K1698P				X	X		X	X				X	X				
K2675U		X		X							X	X					
K2825S		X	X	X	X												
K3075P		X	X		X		X			X			X				
K3275S		X	X	X	X	X	X					X	X				
K3500U		X		X			X										
K3728P			X	X	X	X	X			X		X	X				
K4293U		X		X		X	X	X				X	X				
KA3175P			X	X	X	X						X	X	X			X
KA3350P		X	X		X		X				X	X	X		X		X
KA4301U		X	X	X	X		X										
22001P		X	X	X		X	X					X	X				
22004P			X	X	X		X				X	X	X	X	X		X
22011P			X	X	X		X					X	X	X	X		
22016U		X		X		X				X		X	X	X	X		

## CULL POND

	fel	q	ak	ch	ep	ca	sc	po	cp	asp	py	Au-Ag
Host Rocks												
206		X	X	X	X		X	X				
207		X	X	X			X					
262		X			X				X	X	X	X
264	X	X	X				X					
269	X	X					X					

## Massive Sulphide Samples

53	X				X	X		X	X	X		X
190	X				X	X		X		X		
204	X			X		X	X	X	X			
205	X							X	X	X		X
208	X					X	X	X	X			
265				X	X	X	X	X	X	X	X	
266	X		X		X	X	X	X	X	X	X	

## SHOWING #2

	fel	q	ak	ch	ep	ca	sc	po	cp	asp	py	o
Host Rocks												
290	X	X	X			X	X		X		X	
11009	X	X	X	X	X							

## Sulphide-rich Samples

32	X					X	X	X	X		X	
229	X		X	X		X	X	X	X		X	
277	X					X					X	jas
292	X			X		X	X	X	X	X	X	Au-Ag
296	X				X				X		X	
11002	X			X		X			X		X	
11003	X			X		X			X		X	



## ROGUES HARBOUR

	fel	q	ak	ch	sc	cr	py	cp	sp	asp	po	o
--	-----	---	----	----	----	----	----	----	----	-----	----	---

## Host Rocks

134	X	X	X	X			X					
139		X		X		X	X	X				
144	X		X	X			X					
145	X	X		X			X					
215		X		X	X		X	X				

## Sulphide-rich Samples

131		X		X			X	X				
133		X					X	X			X	
140		X		X			X	X			X	
211		X					X	X				
216		X					X	X				
217		X		X			X	X	X	X		brav
221		X					X	X			X	
244				X			X	X				Ni-Te
245		X						X			X	

## WELSHS BIGHT

	q	ca	gn	sp	cp	asp	po
40	X		X				
191	X	X	X	X	X	X	X

## REGIONAL QUARTZ VEINS

	q	py	cp
41	X	X	
44	X		X
83	X	X	X
109	X	X	

## DIABASE/GABBRO

	pn	fel	q	ak	ch	ep	ca	sc	ti	py	sup
49		X	X	X	X					X	
59		X	X	X	X						
62	X	X	X	X	X						
65		X	X	X	X		X				
84	X		X	X		X	X				
105	X	X			X		X				
121	X	X	X	X	X					X	
122		X		X		X	X				

## PYROXENITES/DUNITE

155	X	X	X								
179	X	X	X	X							
148											X
156											X

## CAPE ST. JOHN GROUP

36	X	X		X	X	X	X	X	X		
97	X	X		X	X					X	
123	X	X	X		X						
178	X	X			X					X	
267		X	X	X	X	X					
157	X	X									

## QUARTZ-FELDSPAR PORPHYRY

	Phenocrysts						Groundmass			
	q	fel	or	db	op	rk	q	fel	or	ch
37	X	X	X	X	X		X	X		
151	X	X	X		X		X	X	X	
165	X	X	X	X			X		X	
185	X	X	X				X	X		
186	X	X	X	X			X	X	X	
227	X	X			X	X	X	X		X
KN14780	X	X	X				X	X		X
KN17062	X	X	X	X			X	X		

## Appendix B

### Analytical Methods

#### B.1. Major Elements

##### B.1.1. Memorial Samples

Sixty-three samples were analysed for major elements by atomic absorption. 0.1000 g of 100 mesh rock powder from each sample was weighed into a flask. 5 mL of concentrated HF+50 mL saturated Boric Acid solution was added to each flask to dissolve the sample. This mixture was diluted by adding 145 mL of distilled water. Analysis of MgO and CaO requires further dilution with lanthanum oxide solution and distilled water. The samples were compared to standards containing known amounts of the major oxides. Initial readings for % absorption were obtained for the standards, then for the sample and for the standards just lower and just higher than the samples. The following formula was then applied to the readings to calculate the amount of a particular oxide:

$$\% \text{oxide} = \% \text{LS} + (\% \text{A sample} - \% \text{A LS}) / (\% \text{A HS} - \% \text{A LS}) * (\% \text{HS} - \% \text{LS}) * 2$$

(A = Absorption; LS = low standard; HS = high standard)

Loss on ignition (LOI) was determined by weighing a known amount of rock powder in a crucible before and after ignition at 1000°C.

Precision estimates were unavailable.

### **B.1.2. GSC Samples**

Fifty-nine rock powders were submitted by the Geological Survey of Canada to the X-Ray Assay laboratories Ltd, Don Mills Ontario for major element analysis. The samples were analysed by X-ray Fluorescence Spectrometry.

1.3 g of sample was roasted at 950°C for 1 hour, fused with 5 g of lithium tetraborate and the melt cast into a 40 mm button. This button was then analysed using a Philips PW1600 simultaneous xray fluorescence spectrometer. Each major element has a particular fixed channel through which it was analysed by making counts over 60 seconds. The accumulated counts for each element were compared to standards which were used to calibrate the machine (Abbey, 1980).

Loss on ignition was calculated by weighing the original 1.3 g sample after the roasting at 950°C. Totals of all elements were determined and any samples with sums less than 98% or greater than 101% were repeated.

Instrumental precision is better than 0.5%. Errors of 1 to 2% are associated with elements with low counts.

## B.2. Trace Elements

### B.2.1. Memorial Samples

X-ray fluorescence was used at Memorial to analyse trace elements. Pellets were made by thoroughly combining 10 +/- g of rock powder with 1.4 to 1.5 g of binder (Bakelite brand phenyl resin) using a mechanical shaker. The mixtures were pressed into pellets and baked for approximately 20 minutes at 200°C.

The elements Pb, U, Th, Rb, Sr, Y, Zr, Nb, Ga, Zn, Cu, Ni, La, Ti, V and Cr were analysed using a standard 16 element package designated TRACEF. Analyses of Ba, Sc, Ca and repeats were carried out using a separate program known as TRACEA. Standards W-1, DTS-1 and BCR-1 were analysed with the Nippers Harbour samples to give estimates of precision and accuracy (Table B-1).

### B.2.2. GSC Samples

A variety of methods were utilized by the X-ray assay labs (under contract by the GSC) to analyse trace elements. Cd, Ca, Co, Cu, Fe, Pb, Mg, Mn, Ni, Ag and Zn were analysed by Direct-Current Plasma Emission Spectrometry. 0.25g of sample was mixed with 2 mL of nitric acid for one half hour in a water bath, then 1 mL of hydrochloric acid was added. This mixture was allowed to digest for a further 2 hours, and was shaken regularly.

The elements Na, Cr, K and Ti underwent a slightly different process: 0.25 g of sample was mixed with 2 mL of nitric acid and 10 mL of hydrofluoric acid and heated to dryness. 1 mL of 1:1 sulphuric acid and 5 mL of hydrofluoric acid were added after cooling and the sample was again heated to dryness. After a

## TRACE ELEMENTS

	W-1 (n=8)	S.D.	PUB	DTS-1 (n=2)	S.D.	PUB
Pb	0	4	8	2	1.4	14.2
U	8	4.2	0.58	7	4.2	0
Th	2	6.4	2.42	4	0	0.01
Rb	20	5.6	21	0	2	0.053
Sr	190	7	190	0	1	0.35
Y	22	5.4	25	0	1	0.05
Zr	96	9.2	105	4	1	3
Nb	9	3.0	9.5	0	1	<3
Ga	17	5.0	16	0	1	0.2
Zn	99	5.3	86	34	0	45
Cu	117	15.8	110	0	0	7
Ni	74	5.9	76	2292	15.6	2269
La	9	17.7	9.8	0	0	0.04
Ti	1.05	0.03	-	.03	0	.07
V	261	9.0	240	13	2.2	10.3
Cr	127	22.0	120	4056	7.8	4000

	BCR-1 (n=10)	S.D.	PUB
Ba	752	51.4	675
Sc	34	3.5	33

**Table B-1:** Precision and accuracy estimate for  
MUN trace element analyses

'n' refers to number of times the standard was analysed; S.D. is the standard deviation; Pub refers to the published value for the analysis from Flanagan (1973).

second cooling, 2 mL of hydrochloric acid was added and the sample was again heated to dissolve any residue. The total pre-analysis procedure took approximately four hours.

Each set of samples were brought up to volume with lithium buffer. The samples were then run on the simultaneous direct current plasma emission spectrometer, along with standards and previously analysed samples.

As, Ba, Nb, Rb, Sr, S, Y and Zr were analysed by x-ray fluorescence. 5 g of sample was used to make a 40 mm pellet, which was loaded into a Philips PW1400 wavelength dispersive x-ray spectrometer for analysis. Various standards were used, depending on the element being analysed.

Se was analysed by acid extraction. Here, a 0.25 g sample was mixed with 15 mL of a 2:2:1 mixture of HF, HNO<sub>3</sub> and NClO<sub>4</sub> until vapours were produced. Distilled water was added many times, heated to vapour each time then the final time, taken to volume. Se was extracted with 0.1% solution of 2,3-diaminonaphthaline (DAN) and MIBK, from an aliquot of digestate, keeping tight control over sulfosalicylic acid, EDTA and pH. The MIBK fraction extracted was analysed using an atomic absorption spectrometer, and the Se content determined by comparison of the curve obtained with standard curves of Se standards.

CO<sub>2</sub>% was determined using coulometry. 0.02 g to 0.10 g of sample were combined with 2N HClO<sub>4</sub> to release CO<sub>2</sub>. The CO<sub>2</sub> was passed through the coulometer cell, which was filled with an aqueous solution of monoethanolamine

coulometer cell, which was filled with an aqueous solution of monoethanolamine and a colourmetric indicator. The gas quantitatively absorbed formed a strong titratable acid with the monoethanolamine, and caused the indicator colour to fade. To maintain equilibrium, the coulometer electrically generated a base to restore the original colour.  $\text{CO}_2$  was calculated as the total amount of current required for the complete titration. Detection limits were 0.01%.

$\text{H}_2\text{O}^+$  (crystallized or combined water) was measured as follows. 1.0 g of sample was dried for 3 hours at  $110^\circ\text{C}$  to remove any moisture. The dried sample was combined with PbO and heated in a pyrex test tube during which time any water vapour was condensed on a piece of preweighed paper in the upper part of the test tube. This test tube section was then cooled using ice in a polyethylene jacket and weighed. The  $\text{H}_2\text{O}^+$  present in the sample was equivalent to the weight gained on the paper.

### **B.3. Precious Metals**

#### **B.3.1. Memorial Samples**

40 samples were analysed for precious metals (Au, Ru, Rh, Pd, Os, Ir and Pt) by ICP at Memorial University. The pre-analysis procedure was as follows: 15.0 g of sample, 9.6 g of Ni, 6.0 g of S, 18.0 g of sodium carbonate, 36.0 g of borax and 6.0 g of silica (10 g for ultramafics) were weighed into a clay crucible and mixed thoroughly. Amounts of Ni and/or S were reduced for samples with high concentrations of these elements, as determined by a previous method. Samples containing high amounts of Cu had to be run a second time due to



hours and allowed to cool. A NiS button was recovered after breaking the crucible. It was weighed, crushed to small chips and transferred to a 1000 mL pyrex beaker. The weight of NiS transferred was then determined to check for loss on crushing.

After adding 500 mL of concentrated HCl to the beaker, it was covered with a watchglass, placed on a hotplate for at least 3 hours. This allowed the NiS to dissolve, in most cases resulting in a black, precious-metal bearing residue.

After cessation of NiS dissolution, the mixture was cooled, then 7 mL of Te solution was added. The solution was brought slowly to the boiling point over 30 minutes, then 12 mL of  $\text{SnCl}_2$  solution was added, forming a black Te precipitate. The mixture was boiled vigorously for half an hour to coagulate the precipitate.

The mixture was again allowed to cool until warm, then filtered with 0.45  $\mu$  pore size cellulose nitrate membrane filter paper. The paper was transferred to a refluxing test tube. Five mL of concentrated  $\text{HNO}_3$  was added, a condenser attached, and the tube heated at  $100^\circ\text{C}$  until the filter paper dissolved. Five mL of concentrated HCl was added through the top of the column and refluxed for 20 minutes to completely dissolve the precipitate.

The tube was allowed to cool for 10 minutes. The reflux condenser was washed down with distilled water, then transferred to a 125 mL polypropylene bottle and made up to 100 mL with distilled water. 3 g of Cd/Tl spike was added and the mixture was well shaken.

Precious metals were analysed on a SCIEX ELAN inductively coupled plasma/mass spectrometer (ICP/MS). Precision estimates based on the standards SU-1A and SARM-7 are listed in Table B-2, along with detection limits for each element for each run carried out.

### PRECIOUS METALS

#### Detection Limits

	Ru	Rh	Pd	Re	Os	Ir	Pt	Au
Run 1	.033	.012	.271	.03	.788	.138	.052	2.893
Run 2	12.819	.035	.102	9.324	1.551	.07	.233	15.354
Run 3	.199	.039	.248	-	-	-	-	-

	SU-1A	S.D.	PUB	SARM-7	S.D.	PUB
Ru	35.8	.28	-	275.87	3.45	430
Rh	51.0	.28	0.08	204.86	13.07	240
Pd	303.55	1.48	0.37	1398.3	79.29	1530
Re	7.85	0.92	-	-	-	-
Os	9.7	0.56	-	-	-	-
Ir	20.65	0.49	-	-	-	-
Pt	361.05	9.26	410	-	-	-
Au	127.15	9.26	150	-	-	-

(All values (except S.D.) in ppb.)

**Table B-2:** Detection limits, precision and accuracy estimates for MUN precious metal analyses

Detection limits are all given in ppb. S.D. refers

to standard deviation; MUN refers to the published MUN

value for the standard sample.

### B.3.2. GSC Samples

Fifty-nine samples were submitted by the GSC to the XRAL labs for precious metal analysis. The elements Au, Pt and Pd were analysed by neutron activation. Sensivities were 1-2 ppb for a 20 gram sample. These analyses were carried up to about 10,000 ppb.

20 g of sample were weighed on a top loader electronic balance to within +/- 0.1 grams. This was added to a 20 g assay crucible which contained 85-90 g of flux. A fixed amount of reducing agent was also added, as well as five mg of silver for samples to be analysed for gold.

After mixing, the sample-flux combination was fused at an average temperature of 980° Celcius for about 45 minutes. The melts were poured, and after cooling, 24-35 g lead buttons were recovered, deslagged, and put into preheated cupels in a cupellation furnace. The buttons were then cupellated at about 900° Celcius for 30 minutes. The silver bead was recovered and analysed by neutron activation. The metal (Au, Pt, Pd) content was measured by gamma spectrometry and an irradiation was carried out.

### B.4. Rare Earth Elements and Traces - MUN

Rare earth elements and selected trace elements were analysed by ICP at Memorial University. Approximately 0.1 g of sample were weighed into a 100 mL teflon beaker. 10 to 15 mL of HF and 10 to 15 mL of concentrated HNO<sub>3</sub> were added to the beaker and evaporated to near dryness. 10 mL of 8N HNO<sub>3</sub> were then added and again evaporated to near dryness. If there was any residue, equal

volumes of 8N HNO<sub>3</sub> and 6N HCl were added and evaporated. A further evaporation with 8N HNO<sub>3</sub> was then carried out. The samples were then taken into solution by adding about 10 mL of 0.2N HNO<sub>3</sub> and heating for a few minutes if necessary. The samples were then taken to a final volume of 90 mL in 0.2N HNO<sub>3</sub>. If the sample did not contain silicate minerals, an initial dissolution with 6N HCl and 8N HNO<sub>3</sub> was used instead of the HF/HNO<sub>3</sub> dissolution.

Two tubes were used in the final analysis. Tube No.1 contained 9 g of sample solution and 1 g of 0.2N HNO<sub>3</sub>. Tube No.2 contained 9 g of sample solution and 1 g of a mixed spike solution.

Precision and accuracy estimates for the two runs based on the standard SY-2 are listed in Table B-3.

### **B.5. Sulphur Isotopes**

32 samples were submitted to the OCCGS/GSC Stable Isotope Laboratory at the University of Ottawa for sulphur isotope analysis. Sulphide samples were separated by magnetic and hand picking methods, then crushed, sieved (usually from -115 to +230 mesh) and superpanned. Sulphide fractions were further separated utilizing an Isodynamic Frantz magnetic separator model L-1 (115 Volts, 2.2 Amps).

Sulphur was extracted as SO<sub>2</sub> by oxidation with Cu<sub>2</sub>O at 1000°C and analyzed on a VG-Isogas Micromass 602E spectrometer. Before and after each run of about 12 samples, two internal standards with δ<sup>34</sup>S values of 1.13 and 30.5 per mil were tested.

REES			
	SY-2 (n=2)	S.D.	Std. Value
La	61.822	2.57	67.6
Ce	142.32	5.87	152
Pr	18.158	0.65	19.0
Nd	68.390	0.56	72.0
Sm	14.559	0.34	15.2
Eu	2.378	0.14	2.35
Gd	14.594	0.50	14.9
Tb	2.814	0.06	2.84
Dy	18.854	0.11	19.8
Ho	4.341	0.11	4.42
Er	13.978	0.23	14.7
Tm	2.261	0.06	2.35
Yb	16.599	0.13	17.2
Lu	2.766	0.03	2.81
Hf	8.198	0.34	8.8
Y	96.056	0.46	116

**Table B-3:** Precision and accuracy estimates for  
MUN REE analyses

S.D. refers to standard deviation. Pub refers to the published MUN values for standard sample SY-2.

### B.6. Lead Isotopes

Lead isotope results for the galena sample submitted to R.I. Thorpe were completed by Geospec Consultants Ltd, Edmonton. Sample preparation involved dissolving a small galena fragment in 10 mL of high purity 2N HCl and evaporating the solution slowly until  $PbCl_2$  crystallized. These crystals were washed in 4N HCl, dried and dissolved in water. A 1 to 2  $\mu$  aliquot was next loaded on a rhenium filament in a silica-gel phosphoric acid mixture (Thorpe *et al.*, 1984). Isotopic analyses were completed on a micromass MM-30 mass spectrometer.

The 2 $\sigma$  error limits for the ratios  $^{206}\text{Pb}/^{204}\text{Pb}$ ,  $^{207}\text{Pb}/^{204}\text{Pb}$  and  $^{208}\text{Pb}/^{204}\text{Pb}$  are 0.042, 0.052 and 0.058%, respectively, for analyses by Geospec Consultants Ltd over the 1983 to 1987 period (R.I. Thorpe, pers comm. 1987). These limits are based on duplicate measurements made over this time interval, and also on results for specimens that can reasonably be considered isotopically identical, although not strictly duplicate.

### B.7. Sample Calculation - Mass Balancing

Mass balance calculations were carried out for all samples according to the method outlined in Lydon and Galley (1986). The procedure is as follows:

#### B.7.1. Part A - Determination of Ratio of Oxide to Immobile Element,

Zr

e.g. molar  $\text{FeO}_t$  // molar  $\text{FeO}_t$  + molar (Zr \* 1000)

This works out as:

$$\frac{\text{FeO}_t(\text{wt } \%) / \text{Atomic wt. FeO}_t}{\text{FeO}_t(\text{wt } \%) / \text{Atomic wt. FeO}_t + ((\text{Zr}(\text{ppm}) * 1000) / 91.22)} = x \text{ (mol/kg)}$$

After ratios have been worked out for each sample, a range of ratios for unaltered samples was determined for each oxide (called A to B)

**B.7.2. Part B - Determination of Gain/Loss of Component , as g/kg of original rock**

Assuming initial Zr contents of 15 ppm Zr for Burtons Pond samples and 21 ppm Zr for all other samples, proceed as follows:

e.g.  $\text{FeO}_t$  ratios for Burtons Pond samples,

Unaltered  $\text{FeO}_t$  range is .38 (+0) (A) to .21 (-0) (B).

Use sample K2825, a gold-rich sample, with a  $\text{FeO}_t/\text{FeO}_i + (\text{Zr} \cdot 1000)$  ratio of 0.45.

For an upper limit on unaltered ratio, molar  $\text{FeO}_t/\text{molar FeO}_i + (\text{Zr}_{\text{init}} \cdot 1000/91.22) = 0.38 \text{ mol}/100 \text{ g}$ . We assume  $\text{Zr}_{\text{init}} = 15 \text{ ppm}$ . Therefore,

molar  $\text{FeO}_t/\text{molar FeO}_i + (15 \cdot 1000/91.22) = 0.38 \text{ mol}/100 \text{ g}$ . Therefore,  $\text{FeO}_t = 0.09225 \text{ mol}/100\text{g}$ .

For sample K2825, molar  $\text{FeO}_t/\text{molar FeO}_i + 0.164 = 0.45 \text{ mol}/100 \text{ g}$ . Therefore,  $\text{FeO}_t = 0.13418 \text{ mol}/100\text{g}$ .

The difference between K2825 and the upper unaltered range is:

$$0.13418 - 0.09225 \text{ mol}/100 \text{ g} = \sim 70 \text{ g}/\text{kg original rock}.$$

If a sample had been depleted in  $\text{FeO}_t$ , then the lower limit for the unaltered sample range of that oxide would have been used in this calculation.

**B.7.3. Atomic Weight used in Calculations**

Compound	Atomic Wt.	Compound	Atomic Wt.
FeO <sub>t</sub>	159.6	SiO <sub>2</sub>	60.086
CaO	56.08	MgO	40.312
Na <sub>2</sub> O	62.0	K <sub>2</sub> O	94.204
Ba	137.40	Sr	87.62
S	32.064	Zr	91.22

**B.7.4. Graphs Used to Estimate Metasomatic Enrichments and Depletions**



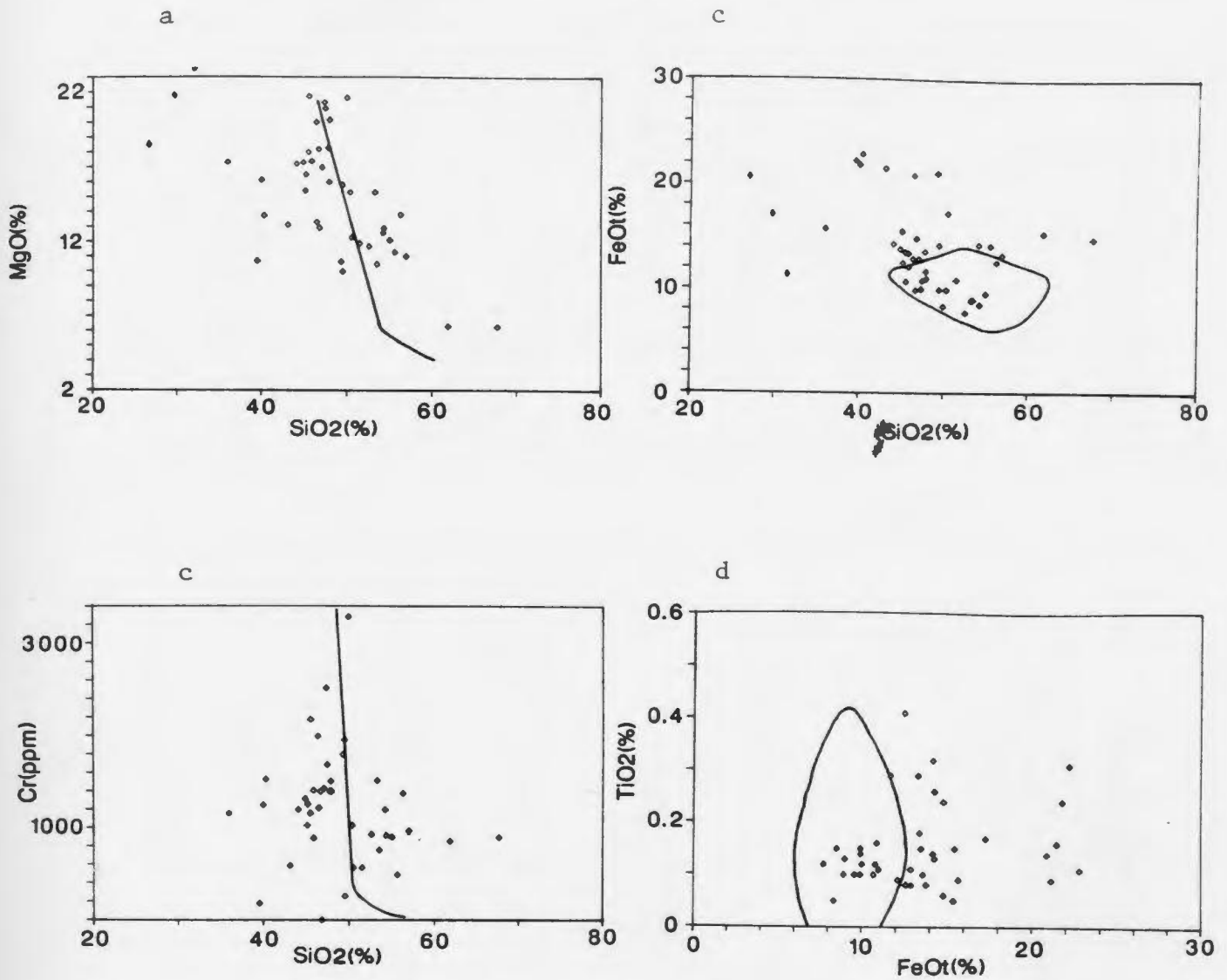


**Figure B-1:** Variation diagrams

(a) SiO<sub>2</sub> vs MgO (b) SiO<sub>2</sub> vs Cr (c) SiO<sub>2</sub> vs FeO<sub>t</sub> (d) FeO<sub>2</sub> vs TiO<sub>2</sub>, Burton's

Pond. Lines in a,b represent trends for unaltered samples shown in Fig. 4-8a,b.

Envelopes in c,d represent fields for unaltered samples shown in Fig. 4-9a,b.

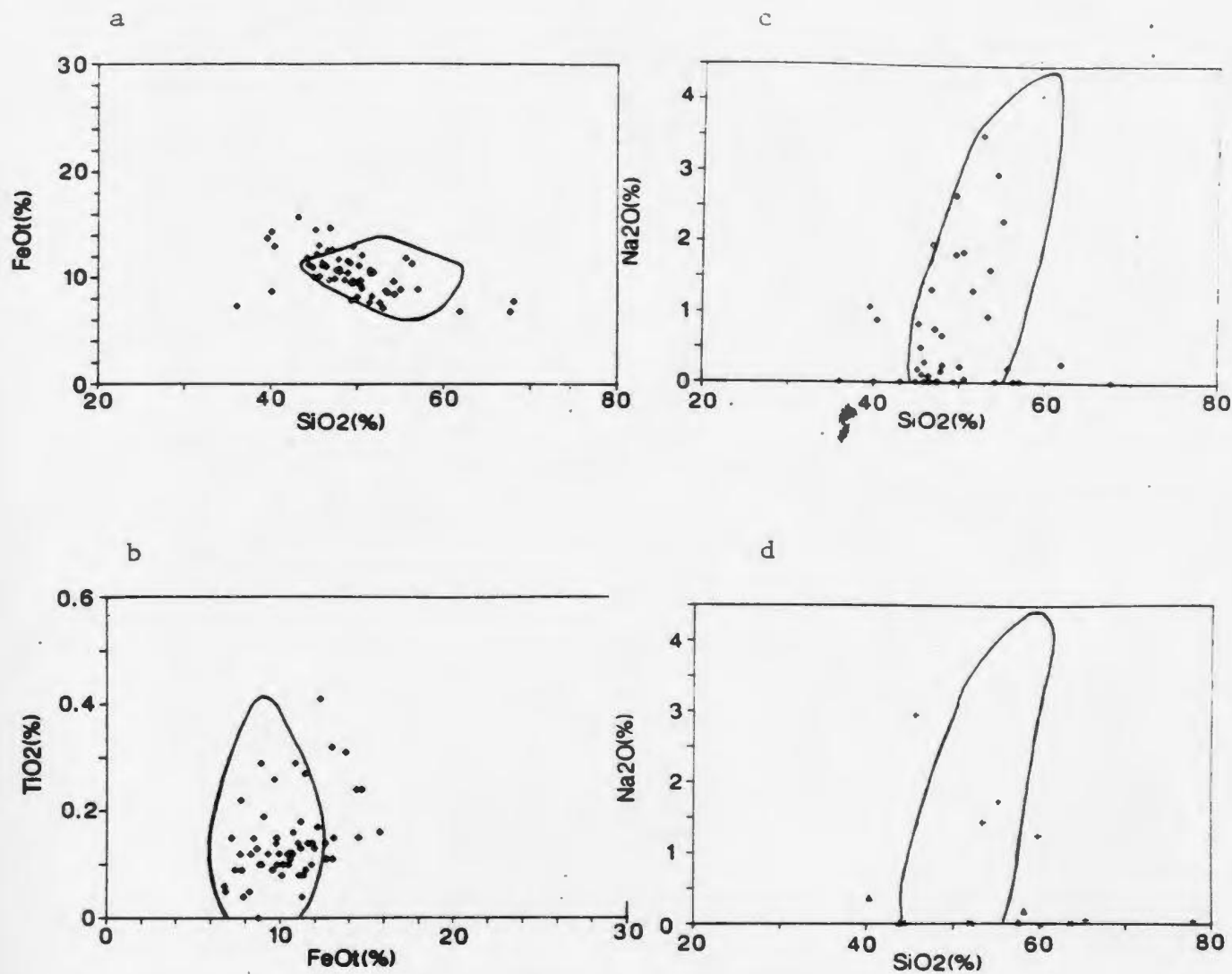


**Figure B-2: Variation diagrams**

(a) SiO<sub>2</sub> vs FeO<sub>t</sub> (non-sulphide) (b) FeO<sub>t</sub>(non-sulphide) vs TiO<sub>2</sub>, Burtons Pond  
 (c),(d) SiO<sub>2</sub> vs Na<sub>2</sub>O (c)-Burtons Pond, (d)-Other Showings. Symbols for (d):  
 (+)-Gull Pond; (Δ)-Rogues Harbour; (χ)-Showing No. 2. Envelopes represent fields  
 for unaltered samples from Fig. 4-9a,b (for a,b) and Fig. 4-10a (for c,d).

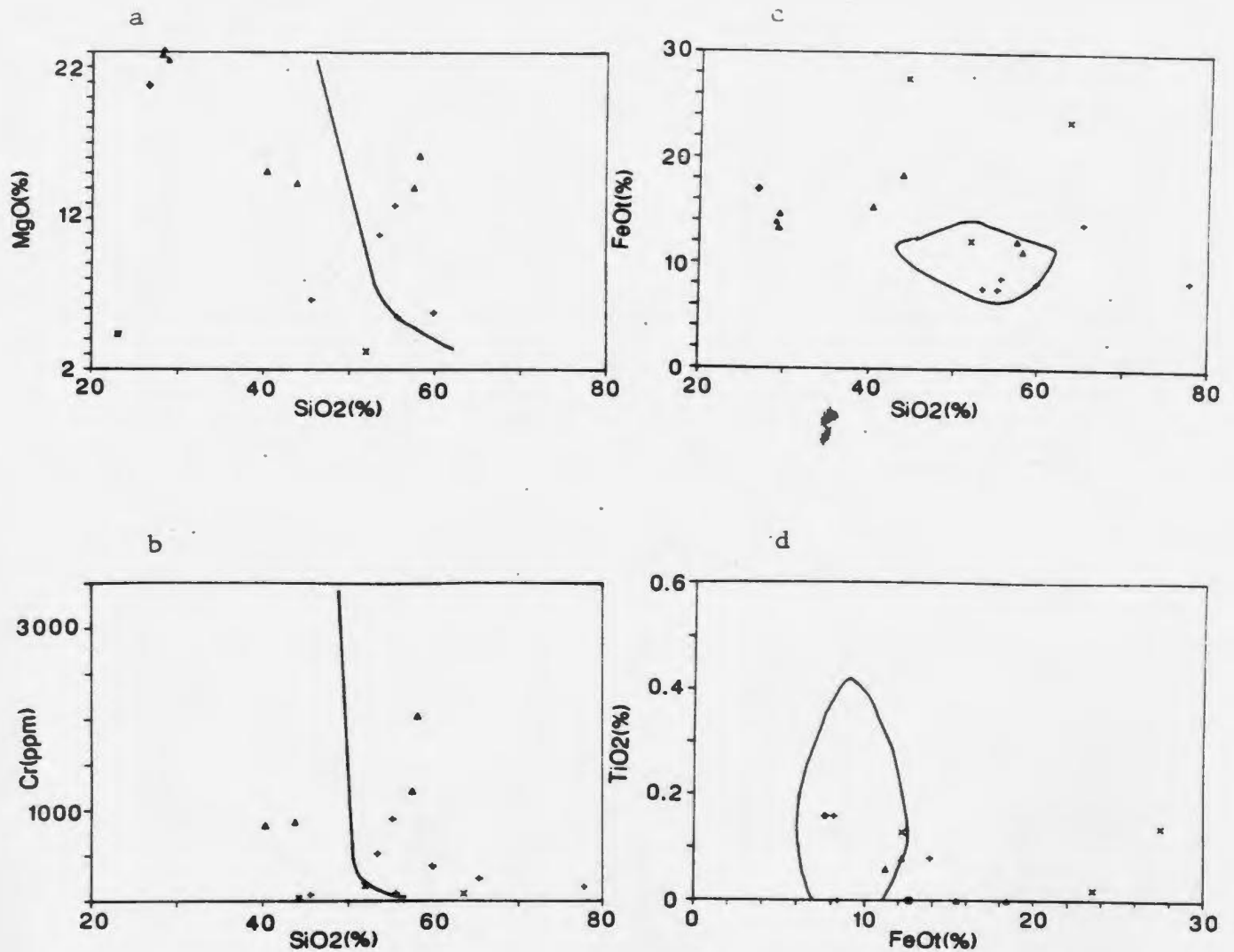


**Figure B-3:** Variation diagrams

(a) SiO<sub>2</sub> vs MgO (b) SiO<sub>2</sub> vs Cr (c) SiO<sub>2</sub> vs FeO<sub>t</sub> (d) FeO<sub>t</sub> vs TiO<sub>2</sub> for Gull Pond, Rogues Harbour, Showing No. 2. Symbols as in Fig. B-2 (d). Lines in a,b represent trends for unaltered samples shown in Fig. 4-8a,b. Envelopes in c,d represents fields for unaltered samples shown in Fig. 4-9a,b.

**Appendix C**  
**Major and Trace Element Analyses**

	Sample Number				
	159	170	199	235	175
SiO2	60.0	50.0	60.8	51.3	52.9
TiO2	0.28	0.24	0.20	0.28	0.12
Al2O3	8.10	7.45	7.73	10.7	12.0
Fe2O3	19.63	27.12	15.99	20.91	17.52
MnO	0.08	0.09	0.11	0.07	0.17
MgO	6.36	4.30	4.73	4.45	10.64
CaO	0.78	0.78	2.40	1.60	1.32
Na2O	0.01	0.01	0.05	1.59	0.03
K2O	0.10	0.03	0.03	0.11	0.01
P2O5	0.05	0.02	0.02	0.03	0.04
LOI	4.10	8.56	4.79	8.36	5.85
TOTAL	99.49	98.60	96.25	99.40	100.60
Pb	0	0	0	0	0
U	8	10	8	8	20
Th	3	0	2	9	2
Rb	0	0	0	0	0
Sr	0	0	154	58	44
Y	6	6	3	13	6
Zr	20	22	20	28	19
Nb	4	4	4	3	3
Ga	3	2	0	12	10
Zn	98	43	290	34	217
Cu	5849	2468	20460	463	479
Ni	34	25	41	3	62
La	0	0	0	0	0
Ti	1900	2600	2500	5500	2400
V	242	221	183	331	365
Cr	354	308	236	47	464
Ba	-	0	4	7	0
Sc	-	34	19	-	44

	Sample Number				
	195	260	261	174	231
SiO2	43.9	48.4	59.3	53.8	47.3
TiO2	0.40	0.56	0.20	0.20	0.36
Al2O3	10.2	10.7	12.4	13.2	14.0
Fe2O3	27.62	23.48	14.88	17.24	18.77
MnO	0.08	0.08	0.15	0.17	0.16
MgO	4.02	2.41	5.05	10.64	9.33
CaO	1.46	1.98	1.36	1.32	3.02
Na2O	1.46	2.12	1.57	0.03	0.14
K2O	0.08	0.25	0.11	0.01	0.02
P2O5	0.02	0.01	0.07	0.04	0.04
LOI	10.67	8.84	3.64	5.85	5.37
TOTAL	99.54	98.83	98.73	98.44	98.51
Pb	14	0	0	0	0
U	11	20	12	2	4
Th	0	1	2	0	0
Rb	0	8	2	3	3
Sr	45	85	55	42	53
Y	13	15	9	12	14
Zr	34	45	28	26	30
Nb	4	4	2	1	5
Ga	8	5	12	11	12
Zn	42	57	54	78	55
Cu	748	4164	2546	2478	63
Ni	0	0	0	0	0
La	0	0	0	0	0
Ti	6500	7500	3300	3300	4600
V	300	309	460	544	378
Cr	5	0	0	0	247
Ba	3	43	16	25	0
Sc	35	35	47	59	46

	Sample Number				
	232	248	253	258	250
SiO2	57.5	50.8	52.4	57.7	52.3
TiO2	0.08	0.00	0.08	0.44	0.60
Al2O3	12.7	13.8	11.2	11.6	13.0
Fe2O3	16.99	12.55	16.85	18.32	13.66
MnO	0.13	0.17	0.21	0.19	0.14
MgO	4.75	10.04	9.95	7.42	6.18
CaO	2.90	5.88	2.60	8.22	5.66
Na2O	0.84	3.14	0.38	3.18	2.28
K2O	0.06	0.10	0.02	0.23	0.04
P2O5	0.02	0.02	0.03	0.02	0.05
LOI	3.64	3.01	4.80	2.08	5.58
TOTAL	99.61	99.51	98.52	100.73	99.49
Pb	0	0	0	0	0
U	0	6	1	0	9
Th	0	0	0	0	0
Rb	0	3	0	0	0
Sr	59	69	22	8	102
Y	9	5	6	13	16
Zr	30	21	22	33	45
Nb	3	4	1	1	3
Ga	10	6	8	7	10
Zn	60	63	97	62	127
Cu	241	91	150	113	248
Ni	4	125	76	9	17
La	0	0	0	0	0
Ti	2400	1800	2400	7400	9100
V	401	321	320	434	338
Cr	0	609	671	0	22
Ba	18	31	1	0	9
Sc	50	58	53	44	46

	Sample Number				
	251	252	254	256	1
SiO2	53.2	52.7	52.8	53.5	45.9
TiO2	0.20	0.04	0.04	0.16	0.14
Al2O3	14.5	10.5	12.4	14.9	8.54
Fe2O3	10.18	9.33	10.18	8.75	20.6
MnO	0.22	0.26	0.23	0.19	0.14
MgO	8.50	13.60	10.64	7.42	13.1
CaO	6.98	7.36	6.00	8.22	2.80
Na2O	3.04	1.65	3.04	3.18	2.80
K2O	0.08	0.06	0.16	0.23	0.03
P2O5	0.04	0.03	0.02	0.02	0.03
LOI	2.69	3.36	3.01	2.08	7.23
TOTAL	99.63	98.89	98.52	98.65	98.7
Pb	3	0	8	0	4
U	2	12	2	9	-
Th	4	1	0	0	-
Rb	0	0	1	5	6
Sr	91	37	73	116	6
Y	9	6	9	7	<2
Zr	26	18	24	22	15
Nb	3	4	2	1	30
Ca	11	7	8	11	-
Zn	327	436	145	148	350
Cu	156	48	54	106	12000
Ni	86	234	118	42	340
La	0	0	0	0	-
Ti	2500	1200	2000	1900	750
V	332	269	270	278	180
Cr	321	1158	732	60	1300
Ba	13	8	-	52	240
Sc	53	-	-	49	-
As	-	-	-	-	51
Se	-	-	-	-	17.0
H2O	-	-	-	-	4.9
CO2	-	-	-	-	0.03
S	-	-	-	-	4.94



	Sample Number				
	2	6	8	10	13
SiO2	47.7	46.2	51.1	49.1	39.6
TiO2	0.12	0.24	0.12	0.04	0.00
Al2O3	7.47	15.2	16.6	4.71	0.82
Fe2O3	10.9	14.65	8.19	7.89	8.71
MnO	0.21	0.11	0.11	0.06	0.13
MgO	21.0	12.75	7.78	17.00	37.20
CaO	8.44	0.96	8.08	4.80	0.96
Na2O	<0.01	1.94	3.24	0.20	0.01
K2O	0.05	0.04	1.42	0.02	0.01
P2O5	0.02	0.04	0.05	0.00	0.00
LOI	4.31	6.61	2.22	5.72	11.48
TOTAL	100.5	98.74	98.91	99.54	98.92
Pb	4	1	0	4	0
U	-	5	6	12	0
Th	-	11	9	2	0
Rb	6	0	22	0	1
Sr	6	43	169	0	5
Y	<2	7	4	0	0
Zr	15	25	14	8	5
Nb	20	1	3	0	0
Ga	-	9	11	2	0
Zn	83	69	13	26	41
Cu	18	4606	5	177	2
Ni	730	104	73	1424	1639
La	-	0	0	0	0
Ti	750	3800	900	300	200
V	190	443	280	89	60
Cr	1500	2	41	2979	2558
Ba	60	9	143	0	11
Sc	-	66	53	19	16
As	36	-	-	-	-
Se	<0.1	-	-	-	-
H2O	3.8	-	-	-	-
CO2	0.09	-	-	-	-
S	Nil	-	-	-	-

	Sample Number				
	16	20	298	299	300
SiO2	47.8	44.3	53.3	44.9	40.6
TiO2	0.12	0.04	0.27	0.41	0.15
Al2O3	16.7	8.91	8.77	12.6	10.2
Fe2O3	10.64	11.34	12.4	12.4	20.2
MnO	0.16	0.16	0.11	0.19	0.12
MgO	9.76	22.40	10.3	16.4	12.3
CaO	8.00	7.30	1.91	5.56	1.07
Na2O	3.05	0.39	<0.01	0.84	<0.01
K2O	0.46	0.05	0.02	0.22	0.02
P2O5	0.05	0.03	0.03	0.04	0.02
LOI	2.97	5.06	6.16	5.62	9.23
TOTAL	99.71	99.98	93.5	99.4	94.1
Pb	0	0	8	2	10
U	6	12	-	-	-
Th	0	2	-	-	-
Rb	7	0	6	10	6
Sr	155	0	6	30	2
Y	5	5	6	6	<2
Zr	18	20	12	21	18
Nb	3	3	10	10	40
Ga	11	7	-	-	-
Zn	46	37	260	160	400
Cu	8	0	26000	1700	28000
Ni	116	681	300	430	130
La	6	0	-	-	-
Ti	140	900	170	250	750
V	310	184	140	160	210
Cr	222	2004	940	1400	500
Ba	53	0	440	90	440
Sc	70	32	-	-	-
As	-	-	12	24	490
Se	-	-	38.0	0.8	31.0
H2O	-	-	4.2	5.0	6.9
CO2	-	-	0.87	0.40	<0.01
S	-	-	2.61	0.06	3.39

	Sample Number				
	301	302	303	304	305
SiO2	47.5	56.2	90.5	54.1	45.2
TiO2	0.12	0.08	0.05	0.15	0.15
Al2O3	7.46	5.76	1.66	10.4	8.88
Fe2O3	10.0	12.6	3.20	8.51	15.5
MnO	0.18	0.22	0.02	0.16	0.18
MgO	21.4	13.8	1.54	12.9	15.5
CaO	8.14	6.78	0.13	7.41	8.72
Na2O	<0.01	<0.01	<0.01	2.95	0.19
K2O	0.04	0.03	0.03	0.18	0.04
P2O5	0.02	0.02	0.01	0.02	0.02
LOI	5.00	3.93	2.31	2.62	5.62
TOTAL	100.2	99.6	99.5	99.6	100.2
Pb	2	6	4	4	2
Rb	6	6	6	10	6
Sr	6	6	<2	80	8
Y	<2	<2	2	4	<2
Zr	9	9	6	15	9
Nb	10	30	10	10	30
Zn	82	270	250	55	1900
Cu	30	120	11000	19	1900
Ni	650	360	71	220	200
Ti	700	440	150	900	920
V	190	120	30	210	220
Cr	2500	1200	250	910	980
Ba	40	40	170	70	70
As	66	24	33	12	15
Se	<0.1	1.5	8.0	0.4	2.5
H2O	4.0	3.2	0.9	1.8	4.3
CO2	<0.01	0.08	0.01	0.20	<0.01
S	Nil	0.71	1.31	Nil	0.52

	Sample Number				
	306	307	309	310	311
SiO2	45.7	44.9	44.8	67.3	38.4
TiO2	0.09	0.08	0.15	0.06	0.30
Al2O3	8.64	7.61	9.87	3.88	14.7
Fe2O3	12.1	13.8	13.3	14.7	21.6
MnO	0.18	0.19	0.21	0.09	0.14
MgO	17.3	17.3	17.7	6.23	10.4
CaO	10.7	10.3	6.32	2.35	2.05
Na2O	<0.01	<0.01	0.49	<0.01	1.05
K2O	0.03	0.03	0.03	0.04	0.02
P2O5	0.02	0.02	0.02	0.02	0.02
LOI	4.62	5.54	5.31	4.54	8.47
TOTAL	99.6	100.0	98.4	99.4	97.2
Pb	<2	2	6	6	46
Rb	6	6	6	6	6
Sr	4	4	12	4	22
Y	<2	<2	4	<2	<2
Zr	9	9	12	6	18
Nb	10	20	<10	10	30
Zn	220	110	140	49	380
Cu	1800	1000	2100	980	13000
Ni	640	390	290	420	220
Ti	500	450	900	300	1900
V	140	170	220	82	530
Cr	1400	1200	1100	880	170
Ba	50	60	80	70	250
As	230	51	42	57	390
Se	0.2	3.3	1.2	14.0	21.0
H2O	4.0	3.8	4.9	2.3	4.2
CO2	<0.01	<0.01	0.03	<0.01	0.04
S	0.34	2.20	0.19	4.80	5.00

	Sample Number				
	K677	K875	K925	K1025	K1125
SiO2	50.1	45.7	50.1	48.4	50.1
TiO2	0.12	0.10	0.05	0.14	0.13
Al2O3	9.49	7.95	4.86	14.1	11.0
Fe2O3	9.43	10.7	8.34	12.4	12.2
MnO	0.17	0.17	0.15	0.16	0.18
MgO	16.3	21.7	21.6	10.6	13.3
CaO	7.92	8.46	10.8	5.90	6.24
Na2O	1.99	0.11	0.23	2.39	2.18
K2O	0.09	0.06	0.06	0.34	0.32
P2O5	0.02	0.02	0.02	0.02	0.02
LOI	3.54	4.77	3.39	4.39	4.08
TOTAL	99.4	100.1	100.1	98.9	99.9
Pb	2	2	2	2	4
Rb	6	6	6	20	20
Sr	28	6	6	86	48
Y	2	<2	<2	<2	2
Zr	9	<3	6	12	12
Nb	10	10	20	30	10
Zn	52	50	37	61	55
Cu	56	98	110	220	190
Ni	540	960	1300	150	280
Ti	740	710	320	1000	820
V	20	170	120	320	230
Cr	1400	1900	3500	550	1200
Ba	40	40	40	80	80
As	30	120	120	27	<3
Se	1.1	1.2	0.6	1.6	3.1
H2O	3.1	4.6	1.4	4.0	3.7
CO2	0.09	0.03	0.07	0.36	0.31
S	0.08	0.27	0.04	0.49	0.57

	Sample Number				
	K1275	K1325	K1425	K1698	K2152
SiO2	55.1	48.0	67.0	50.6	47.4
TiO2	0.14	0.16	0.09	0.19	0.29
Al2O3	10.7	10.6	5.82	15.9	9.08
Fe2O3	14.1	16.4	9.54	9.10	11.6
MnO	0.14	0.13	0.12	0.15	0.16
MgO	11.2	11.7	8.33	9.10	15.8
CaO	1.35	0.81	3.59	7.44	9.51
Na2O	0.20	0.05	<0.01	2.45	0.66
K2O	0.09	0.03	0.02	1.01	0.28
P2O5	0.02	0.03	0.02	0.03	0.03
LOI	5.93	6.93	3.77	4.00	3.93
TOTAL	99.1	95.0	98.4	100.1	99.0
Pb	2	<2	<2	4	4
Rb	6	6	6	24	10
Sr	10	6	6	150	30
Y	2	<2	<2	4	4
Zr	15	18	9	15	15
Nb	10	20	<10	10	<10
Zn	140	660	68	64	100
Cu	2000	16000	1100	110	1800
Ni	150	160	130	92	340
Tl	770	940	480	1200	1900
V	260	250	130	310	230
Cr	500	650	570	290	1600
Ba	140	320	110	140	90
As	81	21	12	<3	3
Se	4.8	8.1	3.5	<0.1	1.1
H2O	5.7	5.8	3.4	2.9	3.6
CO2	0.25	0.07	1.26	1.07	0.88
S	1.36	3.05	1.13	Nil	0.45

	Sample Number				
	K2425	K2525	K2675	K2825	K2975
SiO2	51.7	49.7	49.0	38.8	49.3
TiO2	0.12	0.09	0.10	0.23	0.27
Al2O3	12.0	7.87	7.55	9.10	11.5
Fe2O3	10.5	9.67	10.8	21.1	11.5
MnO	0.16	0.17	0.18	0.15	0.19
MgO	14.5	19.5	19.1	15.6	15.7
CaO	5.45	8.37	8.54	4.54	5.87
Na2O	1.35	0.36	0.28	<0.01	1.13
K2O	0.39	0.14	0.10	0.05	0.29
P2O5	0.02	0.02	0.02	0.03	0.03
LOI	4.08	4.16	4.23	7.08	4.31
TOTAL	100.4	100.3	100.2	96.9	100.3
Pb	2	2	<2	<2	2
Rb	12	28	6	6	12
Sr	48	16	12	6	38
Y	2	<2	<2	<2	4
Zr	12	9	21	12	15
Nb	20	30	<10	<10	20
Zn	64	49	65	380	61
Cu	190	1.5	1200	13000	33
Ni	270	580	650	440	380
Ti	810	630	600	1300	1400
V	240	200	170	200	240
Cr	820	1800	1700	1200	1200
Ba	120	50	60	230	130
As	3	6	30	78	9
Se	<0.1	<0.1	1.2	29.0	<0.1
H2O	4.4	3.8	3.8	5.2	4.3
CO2	0.05	0.03	0.15	0.07	0.05
S	Nil	Nil	0.15	4.38	Nil

	Sample Number				
	K3075	K3175	K3275	K3500	K3728
SiO2	49.0	44.3	53.6	48.7	51.0
TiO2	0.32	0.17	0.10	0.15	0.16
Al2O3	15.0	9.87	9.09	11.5	12.1
Fe2O3	14.1	12.9	8.96	9.91	10.8
MnO	0.16	0.17	0.14	0.18	0.23
MgO	9.94	16.8	15.4	16.0	11.8
CaO	2.58	5.69	6.95	6.62	4.95
Na2O	2.62	0.29	0.95	1.54	1.30
K2O	0.11	0.03	0.06	0.08	0.04
P2O5	0.03	0.03	0.02	0.02	0.02
LOI	5.00	6.08	5.00	5.47	6.62
TOTAL	98.9	96.5	100.5	100.4	99.1
Pb	<2	4	4	4	4
Rb	8	6	6	6	6
Sr	38	12	38	30	26
Y	6	3	<2	20	2
Zr	18	12	9	12	12
Nb	10	20	10	20	10
Zn	110	180	84	110	160
Cu	2800	13000	640	27	350
Ni	110	340	830	950	190
Tl	2200	1000	580	900	900
V	330	230	200	240	260
Cr	280	990	1500	1600	590
Ba	120	240	70	50	60
As	3	9	15	33	6
Se	3.1	15.0	<0.1	<0.1	<0.1
H2O	5.0	5.2	4.1	4.6	5.2
CO2	0.53	0.82	1.18	1.38	2.54
S	0.68	1.29	0.04	Nil	0.04



	Sample Number				
	K4086	K4293	K4605	K4905	K41586
SiO2	45.0	52.9	46.6	50.3	53.4
TiO2	0.14	0.13	0.10	0.15	0.13
Al2O3	11.2	13.2	10.9	11.2	11.4
Fe2O3	11.1	7.22	9.90	9.92	8.99
MnO	0.19	0.13	0.16	0.14	0.17
MgO	19.6	11.2	18.1	15.2	10.5
CaO	6.60	7.48	7.34	5.92	10.1
Na2O	0.92	3.64	1.32	1.85	1.60
K2O	0.08	0.51	0.14	0.10	0.47
P2O5	0.02	0.02	0.02	0.02	0.02
LOI	5.31	3.39	5.00	4.85	2.93
TOTAL	100.3	99.9	99.8	99.8	99.9
Pb	4	4	4	6	6
Rb	6	16	6	6	12
Sr	26	120	40	34	100
Y	2	2	2	6	<2
Zr	12	33	9	12	12
Nb	10	<10	10	<10	20
Zn	48	39	51	57	110
Cu	1.5	13	11	58	1500
Ni	180	160	670	400	180
Ti	810	840	510	940	1200
V	240	210	200	250	190
Cr	820	490	1500	1000	720
Ba	80	100	70	80	150
As	<3	<3	6	6	3
Se	<0.1	<0.1	<0.1	<0.1	1.3
H2O	4.8	2.3	4.5	4.2	2.5
CO2	0.08	0.72	0.72	0.59	0.94
S	Nil	Nil	Nil	0.04	0.17

	Sample Number				
	KA2196	KA2923	KA3125	KA3175	KA3225
SiO2	52.0	47.3	49.4	37.6	54.1
TiO2	0.12	0.11	0.14	0.11	0.10
Al2O3	13.1	9.09	10.5	8.68	9.56
Fe2O3	10.6	13.0	9.91	21.2	9.42
MnO	0.16	0.20	0.18	0.16	0.16
MgO	9.37	17.1	15.8	12.8	11.9
CaO	8.94	8.50	7.75	5.64	7.75
Na2O	3.18	0.76	1.82	0.83	2.25
K2O	0.22	0.09	0.27	0.06	0.19
P2O5	0.02	0.02	0.02	0.02	0.02
LOI	2.39	4.16	3.62	6.08	2.77
TOTAL	100.2	100.5	99.7	93.4	98.4
Pb	6	<2	<2	<2	2
Rb	6	6	10	6	6
Sr	96	18	64	14	72
Y	2	<2	2	<2	<2
Zr	12	6	12	9	9
Nb	10	20	10	10	20
Zn	56	82	72	840	90
Cu	42	450	1300	26000	3100
Ni	94	350	400	820	240
Ti	840	610	830	550	540
V	450	290	220	160	220
Cr	380	1300	1900	1500	940
Ba	80	60	100	390	120
As	<3	24	36	24	6
Se	<0.1	<0.1	0.2	8.0	0.8
H2O	2.5	4.0	3.4	3.9	2.6
CO2	<0.01	0.02	0.02	0.01	0.38
S	Nil	0.09	0.07	5.83	0.36

	Sample Number				
	KA3350	KA3750	KA4301	22001	22004
SiO2	29.3	52.2	50.7	55.9	70.9
TiO2	0.07	0.12	0.22	0.05	0.06
Al2O3	6.32	11.0	13.6	4.94	3.48
Fe2O3	12.8	7.67	7.68	13.9	7.85
MnO	0.12	0.14	0.13	0.12	0.09
MgO	14.1	11.6	9.93	5.67	4.12
CaO	13.3	9.26	7.60	4.85	0.65
Na2O	<0.01	3.47	4.14	0.27	<0.01
K2O	0.05	0.12	0.12	0.05	0.05
P2O5	0.02	0.02	0.04	0.02	0.02
LOI	5.23	3.47	4.08	4.54	3.23
TOTAL	81.5	99.2	98.7	90.5	90.6
Pb	<2	4	6	<2	68
Rb	6	6	6	<10	<10
Sr	26	60	84	10	<10
Y	<2	2	6	<10	<10
Zr	6	12	21	<10	<10
Nb	<10	20	20	10	20
Zn	310	39	57	390	220
Cu	46000	31	17	>4000	>4000
Ni	450	260	260	370	340
Ti	440	600	1400	200	260
V	140	250	350	110	72
Cr	1300	910	850	860	460
Ba	560	30	80	270	430
As	30	3	6	34	790
Se	9.6	<0.1	<0.1	11	21
H2O	4.0	2.2	2.7	2.8	1.9
CO2	6.79	1.72	2.53	1.90	0.25
S	4.99	Nil	Nil	5.12	3.79



	Sample Number				
	22006	22008	22009	22011	22013
SiO2	44.7	45.3	47.0	49.7	45.5
TiO2	0.08	0.09	0.11	0.26	0.10
Al2O3	6.46	8.22	6.95	8.40	7.55
Fe2O3	12.4	19.4	10.8	13.0	12.5
MnO	0.15	0.12	0.17	0.14	0.17
MgO	19.4	9.76	19.7	11.6	17.1
CaO	9.23	0.46	9.12	3.08	7.80
Na2O	0.09	<0.01	0.25	<0.01	0.16
K2O	0.06	0.05	0.07	0.05	0.07
P2O5	0.02	0.02	0.02	0.03	0.02
LOI	3.85	8.39	3.77	5.16	4.31
TOTAL	96.8	92.1	98.2	91.7	95.5
Pb	<2	<2	<2	<2	<2
Rb	20	<10	<10	<10	<10
Sr	<10	<10	<10	<10	<10
Y	<10	<10	<10	<10	<10
Zr	<10	<10	<10	<10	<10
Nb	10	10	10	30	20
Zn	48	600	38	240	54
Cu	82	>4000	52	>4000	930
Ni	730	380	450	330	390
Ti	240	330	420	1900	450
V	160	190	160	160	170
Cr	2510	1780	1420	1240	1350
Ba	70	430	60	420	90
As	170	150	35	19	75
Se	2.3	19	0.8	48	1.1
H2O	3.9	5.0	3.3	4.4	3.9
CO2	0.92	0.45	0.63	0.78	1.26
S	1.04	6.97	0.21	2.76	1.04

	Sample Number				
	22016	54	206	207	209
SiO2	42.3	54.8	75.9	52.4	55.3
TiO2	0.13	0.28	0.00	0.16	0.16
Al2O3	8.73	15.3	6.91	12.5	11.1
Fe2O3	13.7	10.22	8.23	7.56	7.66
MnO	0.18	0.13	0.01	0.14	0.15
MgO	16.50	7.24	0.66	10.75	12.95
CaO	8.94	4.58	0.16	5.82	6.34
Na2O	0.04	3.09	0.04	1.40	1.73
K2O	0.05	0.22	2.22	1.87	2.02
P2O5	0.03	0.10	0.03	0.04	0.05
LOI	5.16	3.30	3.40	5.49	2.74
TOTAL	96.0	99.26	97.56	98.13	100.20
Pb	<2	0	234	4	0
U	-	9	9	6	14
Th	-	1	62	13	9
Rb	<10	3	60	65	64
Sr	<10	86	0	22	24
Y	<10	10	0	9	12
Zr	<10	22	12	22	34
Nb	<30	2	0	2	1
Ga	<20	9	6	10	6
Zn	220	20	2	17	18
Cu	>4000	0	3398	78	15
Ni	330	39	16	0	0
La	-	1	0	0	0
Ti	720	2500	1000	1400	1600
V	200	321	177	274	253
Cr	1320	62	164	524	904
Ba	100	20	148	252	260
Sc	-	52	28	56	55
As	120	-	-	-	-
Se	1.5	-	-	-	-
H2O	0.00	-	-	-	-
CO2	1.6	-	-	-	-
S	1.36	-	-	-	-

	Sample Number				
	262	264	269	290	11009
S102	63.6	51.0	58.2	56.5	51.1
TiO2	0.08	0.20	0.16	0.16	0.13
Al2O3	6.54	11.0	11.4	12.4	15.9
Fe2O3	13.47	10.53	7.97	6.43	12.0
MnO	0.04	0.18	0.12	0.18	0.20
MgO	1.93	15.40	5.65	4.05	3.15
CaO	0.82	4.12	5.56	9.17	13.4
Na2O	0.05	1.71	1.22	0.30	<0.01
K2O	1.77	0.21	2.76	2.59	0.06
P2O5	0.03	0.004	0.00	0.01	0.03
LOI	9.03	4.72	4.35	9.14	2.47
TOTAL	97.36	99.07	97.36	100.0	98.5
Pb	41	1	3	0	<2
U	1	12	9	-	-
Th	16	9	4	-	-
Rb	53	7	105	16	<10
Sr	17	19	34	16	310
Y	2	6	10	9	<10
Zr	10	25	15	20	<10
Nb	3	4	3	2	10
Ga	3	10	9	9	<20
Zn	39	52	14	16	39
Cu	5456	0	796	52	3300
Ni	39	238	60	23	110
La	0	0	0	-	-
Ti	800	1400	1400	1300	580
V	175	273	235	266	330
Cr	248	1555	390	18	170
Ba	-	30	314	84	60
As	-	-	-	-	8
Se	-	-	-	-	-
H2O	-	-	-	-	1.7
CO2	-	-	-	-	0.67
S	-	-	-	-	0.36

	Sample Number				
	134	139	144	145	215
SiO2	49.0	40.0	57.9	57.2	43.4
TiO2	0.32	0.00	0.06	0.08	0.00
Al2O3	8.92	19.0	5.05	9.75	13.5
Fe2O3	9.01	15.32	11.19	12.10	18.28
MnO	0.13	0.04	0.08	0.02	0.05
MgO	18.90	15.05	16.15	14.00	14.25
CaO	5.94	0.04	1.56	0.08	0.04
Na2O	0.07	0.37	0.18	0.02	0.01
K2O	0.36	1.32	0.01	0.03	0.00
P2O5	0.02	0.02	0.06	0.06	0.00
LOI	6.87	8.10	7.37	6.09	9.59
TOTAL	99.54	99.26	99.55	99.43	99.54
Pb	0	0	0	0	3
U	6	10	11	6	8
Th	6	4	5	0	2
Rb	10	43	0	0	0
Sr	16	6	2	2	0
Y	5	6	5	4	0
Zr	12	11	7	20	15
Nb	2	2	2	3	2
Ga	5	10	6	7	10
Zn	33	48	50	2	45
Cu	53	242	1521	204	1357
Ni	386	105	123	33	44
La	0	0	0	0	0
Ti	700	600	1300	1400	1000
V	201	186	310	382	246
Cr	1635	833	2043	1214	873
Ba	21	98	0	0	0
Sc	48	52	99	-	59

	Sample Number				
	39	49	59	62	65
SiO2	55.2	57.2	58.0	65.2	57.3
TiO2	0.20	0.24	0.28	0.40	0.16
Al2O3	14.3	14.2	14.2	11.1	14.2
Fe2O3	7.63	11.72	10.30	9.13	9.16
MnO	0.11	0.08	0.17	0.12	0.12
MgO	5.31	4.32	4.81	3.29	5.16
CaO	14.10	0.18	4.56	3.20	7.44
Na2O	0.07	1.19	3.87	3.46	2.53
K2O	0.01	3.02	0.21	0.04	0.09
P2O5	0.00	0.02	0.22	0.13	0.01
LOI	1.88	6.26	2.48	2.41	2.37
TOTAL	98.81	98.43	99.10	98.48	98.54
Pb	0	4	0	0	0
U	12	11	6	14	9
Th	0	0	0	2	0
Rb	1	53	0	0	1
Sr	88	13	73	74	109
Y	6	7	8	13	7
Zr	19	34	28	42	22
Nb	1	1	2	3	4
Ga	12	13	13	12	10
Zn	11	5	101	51	21
Cu	11	74	37	88	5
Ni	32	5	4	0	16
La	0	0	0	0	0
Ti	1600	3000	3100	3900	1900
V	278	503	405	222	346
Cr	61	3	0	0	71
Ba	0	257	6	8	10
Sc	42	62	54	39	53



	Sample Number				
	84	105	121	122	155
SiO2	54.0	62.4	51.5	59.9	52.1
TiO2	0.04	0.24	0.00	0.08	0.00
Al2O3	14.6	12.7	8.98	13.3	4.20
Fe2O3	8.79	11.24	9.05	7.77	7.76
MnO	0.11	0.09	0.11	0.12	0.14
MgO	5.62	3.02	17.65	5.29	24.65
CaO	10.98	7.74	8.56	8.26	6.34
Na2O	0.19	1.19	0.57	4.32	0.21
K2O	0.01	0.02	0.05	0.04	0.03
P2O5	0.02	0.02	0.00	0.12	0.00
LOI	4.87	2.22	3.18	1.42	3.82
TOTAL	99.23	100.88	99.65	100.62	99.25
Pb	0	0	0	0	0
U	1	3	6	0	4
Th	0	4	0	0	5
Rb	0	0	1	0	1
Sr	156	75	25	84	2
Y	9	13	5	8	2
Zr	22	29	12	21	11
Nb	3	3	2	3	3
Ga	10	10	5	10	6
Zn	15	7	13	3	23
Cu	0	0	0	0	17
Ni	40	0	401	37	405
La	0	0	0	0	0
Ti	1900	3700	800	1700	400
V	280	478	217	276	150
Cr	56	0	1538	60	2102
Ba	0	0	4	0	0
Sc	36	51	48	43	47

	Sample Number				
	179	148	156	36	97
S102	50.9	39.1	42.3	44.2	44.8
T102	0.00	0.04	0.00	2.20	2.32
Al2O3	7.60	0.83	6.00	15.1	13.7
Fe2O3	8.43	10.09	5.54	11.72	12.31
MnO	0.14	0.08	0.13	0.23	0.17
MgO	20.25	38.85	14.65	8.08	6.54
CaO	7.56	0.18	10.14	7.58	7.68
Na2O	0.13	0.01	0.01	2.97	2.90
K2O	0.02	0.00	0.00	0.48	0.07
P2O5	0.03	0.00	0.02	0.49	0.28
LOI	5.24	11.32	18.13	4.43	7.57
<b>TOTAL</b>	<b>100.30</b>	<b>100.50</b>	<b>98.38</b>	<b>97.48</b>	<b>98.34</b>
Pb	0	0	6	5	0
U	6	0	4	16	5
Th	0	0	4	5	0
Rb	0	0	1	16	0
Sr	0	2	36	340	131
Y	3	2	3	27	28
Zr	21	4	16	163	164
Nb	2	2	3	9	9
Ga	7	0	7	15	19
Zn	33	23	32	68	63
Cu	15	0	27	39	45
Ni	298	1816	405	64	49
La	0	5	0	0	5
Ti	500	100	400	22400	17700
V	154	47	211	283	330
Cr	2389	3773	1822	177	69
Ba	0	0	0	119	9
Sc	40	15	41	33	38

	Sample Number				
	123	178	267	124	157
SiO2	66.8	50.8	54.8	76.9	58.1
TiO2	1.04	1.88	1.64	0.20	0.68
Al2O3	14.2	15.0	14.5	10.9	13.6
Fe2O3	5.23	10.47	8.54	2.90	5.54
MnO	0.11	0.15	0.12	0.02	0.09
MgO	1.12	6.87	5.40	0.14	7.20
CaO	2.78	6.82	5.04	0.18	4.52
Na2O	3.15	3.15	5.72	3.99	4.66
K2O	4.10	0.11	0.05	3.51	0.10
P2O5	0.24	0.36	0.37	0.00	0.37
LOI	1.12	3.55	2.39	0.21	4.66
TOTAL	99.89	99.16	98.57	98.95	99.47
Pb	18	0	0	-	15
U	17	0	6	1	17
Th	15	4	7	16	17
Rb	124	1	0	68	0
Sr	313	219	135	36	569
Y	52	27	29	77	19
Zr	380	163	204	601	185
Nb	13	9	12	20	7
Ga	21	19	15	19	17
Zn	79	58	28	13	51
Cu	6	39	54	0	40
Ni	0	167	33	0	135
La	30	9	18	78	42
Ti	7500	19500	18200	2100	7800
V	66	270	221	1	160
Cr	0	126	84	0	296
Ba	1081	87	18	813	851
Sc	11	36	-	0	20

	Sample Number				
	37	151	165	185	186
SiO <sub>2</sub>	77.5	75.8	76.8	73.7	76.4
TiO <sub>2</sub>	0.04	0.08	0.12	0.08	0.08
Al <sub>2</sub> O <sub>3</sub>	10.8	11.5	11.5	10.9	11.5
Fe <sub>2</sub> O <sub>3</sub>	0.21	1.23	1.65	3.85	1.43
MnO	0.01	0.03	0.02	0.02	0.01
MgO	0.09	0.50	0.48	0.49	0.05
CaO	0.94	0.48	0.22	6.40	0.18
Na <sub>2</sub> O	3.35	3.52	2.49	2.10	3.42
K <sub>2</sub> O	4.23	4.60	5.06	0.01	4.80
P <sub>2</sub> O <sub>5</sub>	0.04	0.02	0.01	0.04	0.00
LOI	1.08	0.62	1.02	0.97	0.73
TOTAL	98.29	98.38	98.35	98.76	98.60
Pb	26	12	17	0	10
U	9	11	13	2	2
Th	14	17	26	0	12
Rb	84	146	145	0	132
Sr	45	16	39	111	24
Y	51	55	46	7	42
Zr	119	138	196	64	152
Nb	19	22	16	4	17
Ga	15	19	20	13	14
Zn	0	34	27	0	18
Cu	0	0	6	7	5
Ni	0	10	2	0	0
La	18	34	33	0	12
Ti	800	1000	1500	2000	1400
V	3	1	2	44	2
Cr	0	21	0	0	0
Ba	369	201	622	0	353
Sc	7	4	7	22	7

	Sample Number		
	227	KN14780	KN17062
SiO2	76.1	76.1	73.0
TiO2	0.08	0.09	0.12
Al2O3	11.2	12.0	12.2
Fe2O3	1.20	1.43	1.87
MnO	0.03	0.04	0.06
MgO	0.45	0.40	0.63
CaO	0.78	1.66	1.96
Na2O	3.49	3.96	2.89
K2O	4.24	2.57	4.72
P2O5	0.00	0.02	0.02
LOI	0.75	1.70	1.54
TOTAL	98.32	100.0	99.1
Pb	28	26	26
U	10	-	-
Th	26	-	-
Rb	178	140	150
Sr	25	20	50
Y	86	160	100
Zr	45	54	67
Nb	29	30	30
Ga	19	-	-
Zn	45	54	67
Cu	4	15	12
Ni	12	6	21
La	5	-	-
Ti	600	500	1000
V	5	4	4
Cr	17	8	44
Ba	48	160	330
Sc	9	-	-
As	-	9	3
Se	-	<0.1	<0.1
H2O	-	0.6	0.7
CO2	-	1.15	1.15
S	-	Nil	Nil

## Appendix D

# REE Analyses, Chondrite Normalizing Values, and Sulphur Isotopes

### D.1. REE analyses

## Sample Number

8            8\*            10            13            16

## Rare Earth Elements, Y and Hf

La	0.730	0.801	0.197	0.087	0.903
Ce	1.463	1.554	0.265	0.140	1.795
Pr	0.161	0.208	0.038	0.018	0.215
Nd	0.682	0.761	0.138	0.063	0.856
Sm	0.162	0.281	0.050	0.029	0.233
Eu	0.184	0.103	0.020	0.006	0.118
Gd	0.400	0.475	0.053	0.038	0.405
Tb	0.051	0.052	0.012	0.007	0.077
Dy	0.441	0.433	0.100	0.053	0.595
Y	3.077	3.357	0.667	0.348	4.068
Ho	0.121	0.123	0.027	0.012	0.179
Er	0.462	0.499	0.103	0.053	0.627
Tm	0.078	0.091	0.018	0.010	0.106
Yb	0.642	0.664	0.138	0.078	0.827
Lu	0.111	0.115	0.022	0.012	0.144
Hf	0.199	0.240	0.069	0.146	0.367

## Sample Number

156            170            170\*            235            175

## Rare Earth Elements, Y and Hf

La	0.638	1.185	1.333	1.193	2.134
Ce	1.490	2.529	2.947	2.514	3.883
Pr	0.168	0.349	0.393	0.325	0.440
Nd	0.706	1.645	1.952	1.547	1.791
Sm	0.192	0.583	0.677	0.574	0.514
Eu	0.033	0.157	0.200	0.162	0.290
Gd	0.227	0.814	0.901	0.798	0.676
Tb	0.041	0.168	0.193	0.173	0.144
Dy	0.294	1.140	1.241	1.062	0.963
Y	1.887	7.466	8.621	6.503	5.851
Ho	0.076	0.257	0.285	0.239	0.236
Er	0.258	0.820	0.871	0.714	0.771
Tm	0.045	0.121	0.130	0.109	0.122
Yb	0.341	0.806	0.886	0.803	0.894
Lu	0.058	0.121	0.144	0.131	0.153
Hf	0.380	0.362	0.382	0.634	0.397



## Sample Number

261            231            254            250            298

## Rare Earth Elements, Y and Hf

La	1.569	1.669	1.420	1.649	0.231
Ce	3.127	3.712	2.771	4.457	0.987
Pr	0.372	0.490	0.318	0.697	0.117
Nd	1.528	2.338	1.301	3.803	0.747
Sm	0.433	0.815	0.359	1.390	0.323
Eu	0.219	0.248	0.154	0.695	0.081
Gd	0.690	1.088	0.567	1.882	0.481
Tb	0.148	0.241	0.106	0.395	0.113
Dy	1.170	1.721	0.828	2.656	0.776
Y	7.892	10.425	4.956	15.142	4.660
Ho	0.297	0.407	0.199	0.613	0.179
Er	1.030	1.246	0.609	1.796	0.563
Tm	0.174	0.190	0.106	0.271	0.080
Yb	1.205	1.326	0.799	1.839	0.557
Lu	0.205	0.213	0.138	0.282	0.095
Hf	0.692	0.778	0.572	1.285	0.513

## Sample Number

311            209            208            208\*            204

## Rare Earth Elements, Y and Hf

La	19.638	1.900	0.462	0.411	0.445
Ce	28.801	3.694	0.895	0.787	1.121
Pr	2.278	0.451	0.100	0.087	0.128
Nd	6.410	1.805	0.420	0.341	0.503
Sm	0.815	0.525	0.111	0.093	0.141
Eu	0.466	0.131	0.055	0.043	0.032
Gd	0.676	0.965	0.155	0.118	0.131
Tb	0.087	0.135	0.029	0.024	0.027
Dy	0.590	1.064	0.219	0.215	0.187
Y	3.429	6.819	1.544	1.315	1.117
Ho	0.134	0.267	0.057	0.048	0.049
Er	0.454	0.965	0.198	0.178	0.156
Tm	0.070	0.156	0.036	0.031	0.028
Yb	0.547	1.152	0.228	0.226	0.184
Lu	0.096	0.188	0.041	0.037	0.029
Hf	0.540	0.716	0.131	0.067	0.045

## Sample Number

139            245            245\*            202            292\*

## Rare Earth Elements, Y and Hf

La	0.324	0.173	0.236	0.408	0.355
Ce	0.637	0.289	0.383	0.789	0.686
Pr	0.063	0.026	0.032	0.088	0.083
Nd	0.224	0.086	0.098	0.308	0.274
Sm	0.059	0.010	0.002	0.097	0.072
Eu	0.053	0.000	-----	0.021	0.022
Gd	0.214	0.014	0.004	0.089	0.085
Tb	0.013	0.002	0.000	0.018	0.015
Dy	0.114	0.015	0.006	0.161	0.104
Y	0.608	0.063	0.085	0.999	0.799
Ho	0.025	0.004	0.002	0.034	0.031
Er	0.108	0.012	0.008	0.136	0.109
Tm	0.016	0.002	0.001	0.024	0.024
Yb	0.145	0.014	0.014	0.201	0.177
Lu	0.030	0.003	0.003	0.037	0.030
Hf	0.147	0.043	0.012	0.068	0.082

## Sample Number

296                      191                      124                      124\*                      151

## Rare Earth Elements, Y and Hf

La	0.329	0.923	61.480	66.982	24.525
Ce	0.390	1.699	115.356	126.180	63.433
Pr	0.040	0.220	16.449	17.971	7.511
Nd	0.173	0.984	63.773	68.558	29.955
Sm	0.034	0.298	12.754	13.574	7.714
Eu	0.017	0.107	2.270	2.085	0.625
Gd	0.037	0.403	10.667	10.899	7.109
Tb	0.009	0.074	1.875	2.004	1.399
Dy	0.059	0.429	11.929	13.166	9.088
Y	0.428	3.146	57.220	67.921	43.600
Ho	0.015	0.089	2.471	2.744	1.858
Er	0.046	0.260	7.282	8.061	5.495
Tm	0.008	0.037	1.061	1.180	0.799
Yb	0.071	0.223	6.657	7.478	5.479
Lu	0.010	0.035	1.007	1.106	0.804
Hf	0.030	0.006	11.642	13.489	5.239

## Sample Number

186

---

Rare Earth Elements, Y and Hf

---

La	19.092
Ce	58.823
Pr	5.556
Nd	21.035
Sm	5.074
Eu	0.768
Gd	4.673
Tb	0.922
Dy	5.885
Y	27.216
Ho	1.240
Er	3.799
Tm	0.594
Yb	3.945
Lu	0.602
Hf	5.316

Note - Samples 204, 208 and 245 are massive sulphides and were not used in the discussions.

**D.2. Chondrite Values**

Chondrite Values  
(After Taylor and McLennan, 1985)

---

La	0.367	Dy	0.381
Ce	0.957	Y	2.25
Pr	0.137	Ho	0.0851
Nd	0.711	Er	0.249
Sm	0.231	Tm	0.0356
Eu	0.087	Yb	0.248
Gd	0.306	Lu	0.0381
Tb	0.058	Hf	0.179

---

## D.3. Sulphur Isotopes

SULPHUR ISOTOPES

<u>Sample</u>	<u>Mineral</u>	<u>Value</u>	<u>Sample</u>	<u>Mineral</u>	<u>Value</u>
<u>NIPPERS HARBOUR</u>					
Hill					
159	Py	7.4	292	Py	4.5
235	Py	6.6	296	Po	5.5
250	Py	7.4	296	Cp	6.5
260	Py	5.9	11002	Po	6.0
Burtons Pond					
310	Po	5.4	11002	Cp	5.0
22001	Po	5.3	11003	Po	6.0
22001	Cp	5.1	11003	Py	5.3
22003	Po	4.9	11004	Py	5.0
22004	Po	5.0	Rogues Harbour		
22004	Cp	5.7	133	Cp	-0.4
22007	Cp	5.0	244	Po	2.9
22008	Po	5.4	245	Po	0.1
22008	Cp	5.7	Welshs Bight		
22011	Cp	6.6	191	Gn	8.9
22058	Po	5.1	Regional Quartz Vein		
22058	Cp	5.5	109	Py	4.3
Gull Pond					
204	Po	5.4			
205	Po	6.3			
206	Po	6.7			

<u>Sample</u>	<u>Mineral</u>	<u>Value</u>	<u>Sample</u>	<u>Mineral</u>	<u>Value</u>
<u>BETTS COVE</u>					
F275	Py	7.7	09	Py	6.1
F375	Py	8.9	010	Py	7.4
F450	Py	8.6	011	Py	9.5
F450	Cp	8.1	012	Py	7.4
01	Py	9.7	C200	Py	7.6
02	Py	6.9	A09	Py	6.7
05	Py	6.7	A09	Cp	6.6
05	Cp	7.6	026	Cp	7.4
06	Py	8.6	036	Cp	8.8
06	Cp	7.3	F444	Py	8.2
07	Py	7.8	F444	Cp	7.9

Estimates of precision and accuracy for sulphur isotope measurements were unavailable. Errors for each analysis were assumed to be 0.1 per mil.



## Appendix E

### Precious and Base Metal Analyses

#### E.1. Precious and Base Metal Analyses

Sample	Cu ppm	Zn ppm	Pb ppm	Co ppm	Ag ppm	Au ppb
<b>Hill</b>						
159	5849	98	0	-	-	-
170	2468	43	0	-	-	45.5
199	20460	290	0	-	-	92.2
235	463	34	0	-	-	-
260	4164	57	0	-	-	191.2
175	479	217	0	-	-	-
195	748	42	14	-	-	-
261	2548	54	0	-	-	21.8
174	2478	78	0	-	-	51.2
231	63	55	0	-	-	3.7
258	113	62	0	-	-	14.0
250	248	127	0	-	-	37.2
254	54	145	8	-	-	10.5
256	108	148	0	-	-	4.9
<b>Burtons Pond</b>						
1s	12000	350	4	110	15.0	5200
2	18.0	83.0	4	57	<0.5	4
6s	4808	89	1	-	-	5727.5*
298s	26000	280	8	71	23.0	3200
299	1700	160	2	61	1.5	140
300s	28000	400	10	410	47.0	19970*
301	30.0	82.0	2	58	<0.5	5
302	120	270	6	59	<0.5	41

Sample	Cu ppm	Zn ppm	Pb ppm	Co ppm	Ag ppm	Au ppb
303s	11000	250	4	62	12.0	550
304	19.0	55.0	4	44	<0.5	30
305s	1900	100	2	38	2.0	1100
306s	1800	220	<2	48	1.5	1300
307s	1000	110	2	78	1.0	1300
309	2100	140	6	45	1.0	190
310s	980	49.0	6	120	2.0	2600
311s	13000	380	46	210	14.0	16155*
K677	56.0	52.0	2	47	<0.5	50
K875	98.0	50.0	2	66	<0.5	310
K925	110	37.0	2	56	<0.5	18
K1025	220	61.0	2	57	<0.5	120
K1125	190	55.0	4	62	<0.5	3100
K1275s	2000	140	2	110	2.5	700
K1325s	16000	660	<2	64	19.0	240
K1425s	1100	68.0	<2	33	2.5	88
K1698	110	64.0	4	33	1.5	6
K2152	1800	100	4	56	0.5	370
K2425	190	64.0	2	40	0.5	51
K2525	1.5	49.0	2	47	<0.5	34
K2675	1200	65.0	<2	62	2.0	140
K2825s	13000	380	<2	220	15.0	>10000
K2975	33.0	61.0	2	49	0.5	110
K3075s	2800	110	<2	44	1.5	520
K3175s	13000	180	4	58	8.5	2200
K3275	640	84.0	4	46	1.5	290
K3500	27.0	110	4	49	0.5	42
K3728	350	160	4	35	1.5	950
K4086	1.5	48.0	4	44	<0.5	11
K4293	13.0	39.0	4	30	<0.5	29
K4605	11.0	51.0	4	47	<0.5	79
K4905	58.0	57.0	6	43	<0.5	320
KA1586s	2500	110	6	38	2.5	790
KA2196	42.0	56.0	6	37	0.5	10
KA2923	450	82.0	<2	44	1.0	310
KA3125	1300	72.0	<2	46	0.5	130
KA3175s	26000	840	<2	160	19.0	>10000
KA3225s	3100	90.0	2	40	1.0	420
KA3350s	46000	310	<2	85	14.0	>10000
KA3750	31.0	39.0	4	36	<0.5	140

Sample	Cu ppm	Zn ppm	Pb ppm	Co ppm	Ag ppm	Au ppb
KA4301	17.0	57.0	6	37	<0.5	16
22001s	>4000	390	<2	63	16.0	1800
22004s	>4000	220	68	550	16.0	2500
22006	82.0	48.0	<2	110	0.5	50
22008s	>4000	600	<2	120	26.0	1600
22009	52.0	38.0	<2	54	<0.5	55
22011s	>4000	240	<2	63	18.0	3300
22013s	930	54.0	<2	64	<0.5	250
22016s	>4000	220	<2	73	3.5	8700

## Gull Pond

53	30482	253	93	-	-	13443.7
204	17006	51	206	-	-	19151.4
205	15970	116	275	-	-	10048.6
208	23131	296	410	-	-	24713.0
206	3398	2	234	-	-	9831.7
266	2785	25	117	-	-	-
207	78	17	4	-	-	48.4
209	15	18	0	-	-	74.2

## Showing No.2

32	1174	17	6	-	-	329.8
292	330	15	1	-	-	2520.8
296	12604	107	97	-	-	14033.2
11002	1500	19.0	34	290	1.5	>10000
11003	220	10.0	<2	150	<0.5	890
11004	1900	50.0	<2	240	1.5	1900
277	0.0	0.0	0.0	-	-	4.2

## Rogues Harbour

131	18602	269	0	-	-	204.2
133	16524	16	0	-	-	135.1
140	22574	70	9	-	-	402.8
211	15342	106	13	-	-	374.3
217	11323	90	0	-	-	177.3
221	14050	126	0	-	-	80.2
244	6534	0	0	-	-	97.9

Sample	Cu ppm	Zn ppm	Pb ppm	Co ppm	Ag ppm	Au ppb
245	52627	179	8	-	-	535.4
134	242	33	0	-	-	8.5
215	1357	45	3	-	-	36.4
Welshs Bight						
191	473	16118	4930	-	-	41.2
40	0	0	12353	-	-	-
Quartz-Sulphide Veins						
83	202	0	0	-	-	2.4
44	247	0	0	-	-	2.1
109	392	269	2	-	-	271.6
41	25	0	0	-	-	3.4
Diabase/Ultramafic						
39	11	11	0	-	-	7.2
62	88	51	0	-	-	3.2
69	-	-	-	-	-	1.9
72	23	14	6	-	-	10.7
74	1110	77	0	-	-	19.4
84	0	15	0	-	-	4.0
105	0	7	-	-	-	2.0
156	27	32	6	-	-	2.5
QFP						
186	5	18	10	-	-	1.3

Sample	Ru ppb	Rh ppb	Pd ppb	Re ppb	Os ppb	Ir ppb	Pt ppb	PGEt ppb
Hill								
170*	-	-	-	0.2	-	0.0	2.0	-
199*	0.07	0.11	5.63	1.1	0.5	0.0	0.8	8.21
260*	0.08	0.07	3.52	2.9	0.0	0.0	1.7	8.27
261*	0.19	0.08	0.55	0.1	2.8	0.1	1.2	5.02
174*	0.1	0.08	1.31	0.0	0.1	0.0	1.6	3.17
231	1.8	0.2	6.7	-	0.4	0.0	2.5	11.6
258	2.1	0.0	1.5	0.6	0.5	0.0	0.9	5.6
250	0.2	0.1	22.7	0.7	-	-	2.1	25.8
254	0.5	0.6	32.3	0.1	0.3	0.1	10.2	44
256	4.0	0.2	25.7	0.2	1.7*	0.1	6.6	38.5
Burtons Pond								
1s	-	-	23	-	-	-	10	-
2	-	-	16	-	-	-	10	-
6s*	-	-	-	-	0.5	0.1	1.7*	-
298s	-	-	13	-	-	-	<10	-
299	-	-	16	-	-	-	10	-
300s*	0.46	0.3	14.65	0.1	1.9	0.0	5.3	22.71
301	-	-	13	-	-	-	<10	-
302	-	-	13	-	-	-	<10	-
303s	-	-	4	-	-	-	<10	-
304	-	-	19	-	-	-	<10	-
305s	-	-	21	-	-	-	10	-
306s	-	-	16	-	-	-	<10	-
307s	-	-	28	-	-	-	<10	-
309	-	-	19	-	-	-	10	-
310s	-	-	15	-	-	-	10	-
311s*	0.19	0.10	6.62	-	0.9	0.0	1.8*	9.61
K677	-	-	17	-	-	-	10	-
K875	-	-	19	-	-	-	<10	-
K925	-	-	17	-	-	-	<10	-
K1025	-	-	13	-	-	-	<10	-
K1125	-	-	25	-	-	-	<10	-
K1275s	-	-	15	-	-	-	<10	-
K1325s	-	-	19	-	-	-	<10	-
K1425s	-	-	10	-	-	-	<10	-
K1698	-	-	31	-	-	-	10	-
K2152	-	-	23	-	-	-	<10	-

Sample	Ru ppb	Rh ppb	Pd ppb	Re ppb	Os ppb	Ir ppb	Pt ppb	PGEt ppb
K2425	-	-	35	-	-	-	<10	-
K2525	-	-	30	-	-	-	<10	-
K2675	-	-	21	-	-	-	<10	-
K2825s	-	-	16	-	-	-	<10	-
K2975	-	-	13	-	-	-	<10	-
K3075s	-	-	20	-	-	-	10	-
K3175s	-	-	26	-	-	-	10	-
K3275	-	-	23	-	-	-	10	-
K3500	-	-	29	-	-	-	<10	-
K3728	-	-	26	-	-	-	<10	-
K4086	-	-	64	-	-	-	10	-
K4293	-	-	13	-	-	-	<10	-
K4605	-	-	24	-	-	-	10	-
K4905	-	-	26	-	-	-	10	-
KA1586s	-	-	37	-	-	-	10	-
KA2196	-	-	29	-	-	-	<10	-
KA2923	-	-	27	-	-	-	10	-
KA3125	-	-	21	-	-	-	10	-
KA3175s	-	-	20	-	-	-	20	-
KA3225	-	-	28	-	-	-	<10	-
KA3350s	-	-	21	-	-	-	10	-
KA3750	-	-	23	-	-	-	<10	-
KA4301	-	-	16	-	-	-	10	-
22001	-	-	29	-	-	-	<10	-
22004	-	-	15	-	-	-	<10	-
22006	-	-	16	-	-	-	<10	-
22008	-	-	24	-	-	-	10	-
22009	-	-	8	-	-	-	<10	-
22011	-	-	18	-	-	-	10	-
22013	-	-	12	-	-	-	10	-
22016	-	-	19	-	-	-	10	-

## Gull Pond

53*	-	-	-	0.7	1.5	0.1	4.0	-
204*	-	1.57	6.44	0.8	0.7	0.1	1.6	11.21
205*	-	-	-	1.1	3.6	0.0	3.4	-
208*	0.49	0.21	14.28	2.1	1.6	0.1	5.0	23.78
206*	-	0.99	14.65	-	2.4	0.0	3.9	21.94
207*	-	-	-	0.0	-	0.0	5.5	-
209*	-	-	-	0.0	0.0	0.0	4.4	-

Sample	Ru ppb	Rh ppb	Pd ppb	Re ppb	Os ppb	Ir ppb	Pt ppb	PGEt ppb
Showing No.2								
32	1.2	0.2	6.5	-	0.9	0.0	1.1	9.9
292*	-	0.0	34.82	0.1	0.0	-	2.9	37.82
296*	0.32	0.0	5.13	0.1	-	-	0.7	6.25
11002	-	-	34	-	-	-	<20	-
11003	-	-	8	-	-	-	<10	-
11004	-	-	5	-	-	-	<10	-
277	0.2	0.1	7.4	0.1	-	0.0	0.8	12.8
Rogues Harbour								
131*	0.29	0.18	6.20	0.1	0.2	0.0	3.5	10.47
133*	0.82	0.69	4.07	0.1	0.2	0.1	4.9	10.88
140*	0.19	0.04	5.02	-	9.5	0.1	0.8	15.65
211*	0.11	0.07	2.21	-	1.1	0.1	0.9	4.49
216*	0.11	0.04	13.87	0.1	-	0.0	1.0	15.12
221*	0.28	0.38	4.35	0.1	0.5	-	5.1	10.71
244*	0.42	0.47	12.68	-	3.0	0.1	5.5	22.17
245*	0.52	0.0	11.75	0.2	2.2	0.1	2.3	17.07
134	-	-	-	0.0	-	0.0	8.8	-
215	-	-	-	-	8.4	0.1	3.1	-
Welshs Bight								
191	0.1	0.9	3.3	0.6	-	0.0	0.2	5.1
Quartz-Sulphide Veins								
83	4.3	0.1	2.7	0.2	2.3	0.0	1.0	10.6
44	5.9	0.3	4.5	-	1.1	0.0	1.6	13.4
109	0.2	0.1	4.7	0.3	3.1	0.0	1.1	9.5
41	0.3	0.1	8.1	0.1	0.3	-	0.9	9.8
Diabase/Ultramafic								
39	0.3	0.2	27.6	0.0	-	0.0	3.7	31.8
62	3.1	0.1	2.3	-	0.8	0.0	0.7	7.0
69	3.0	0.1	15.5	0.5	0.7	0.0	2.1	21.9
72	2.8	0.1	15.2	0.0	0.4	0.0	1.7	20.2

Sample	Ru ppb	Rh ppb	Pd ppb	Re ppb	Os ppb	Ir ppb	Pt ppb	PGEt ppb
74	0.3	0.2	23.6	0.2	-	-	1.5	25.8
84	4.0	0.1	24.4	-	0.5	0.0	4.1	33.1
105	2.3	0.1	6.8	-	0.8	0.0	1.5	11.5
156	0.7	0.7	19.3	0.1	0.0	0.0	10.9	31.7
QFP								
186	5.0	0.0	1.0	0.1	0.6	0.0	0.7	7.4

NOTE: A '\*' after a sample number indicates that that sample had to be re-run for Ru, Rh and Pd due to its high Cu content. The values presented for these elements are those from the second run.



## E.2. Sample Descriptions and Locations

### E.2.1. Sample Descriptions

---

#### HILL

159, 170, 199, 235: 'Unit One' Hill rocks comprising diabase breccias cemented by quartz-pyrite-chalcopyrite. Sulphide contents reach up to 40 percent in hand sample, with pyrite contents > chalcopyrite.

260, 175, 195, 261: 'Unit Two' Hill rocks comprising sheared chloritic/pyritic rock with lesser chalcopyrite.

174, 231, 258: 'Unit Three' Hill rocks comprising chloritized diabase containing the mineral assemblage chlorite-quartz-albite+/-pyrite/chalcopyrite.

250, 254, 256: 'Unit Four' Hill rocks comprising splitized (greenschist) diabases, non-hydrothermally altered.

---

#### BURTONS POND Sulphide-bearing Samples:

6, 298, 300, 305, 306, 307, 309, 310, K1325, K1425, K2825, K3075, K3175, KA1586, KA2923, KA3175, KA3225, 22001, 22008, 22011, 22013, 22016: Chloritized, silicified, carbonatized diabase with stringers of pyrrhotite-chalcopyrite+/-arsenopyrite+/-sphalerite+/-pyrite-calcite-quartz +/-albite

1, 303, 311, K1275, KA3350, 22004: Mainly sulphide (as above), quartz and calcite (in veins).

## Host and Other Rocks:

2, 299, 302, 309, K677, K875, K1025, K, K1698, K2152, KK3275, K3728,  
K4086, K4293, K4605, K4905, KA 2196, KA3125, KA3750, 22006, 22009 :

Hydrothermally altered diabases and gabbros

301, 304, K925, K1425, K2425, K2525, K2675, K2975, K3500, K4301 :

Relatively unaltered diabases and gabbros

---

## GULL POND

53, 204, 205, 208: Massive sulphide: Pyrrhotite/chalcopyrite<sup>a</sup> with minor  
arsenopyrite, < 10 percent gangue minerals.

206, 266: Mainly massive sulphide- pyrrhotite/ chalcopyrite/ arsenopyrite  
with up to 50 percent gangue- chlorite/quartz/sericite.

207, 209: Intensely sheared, chlorite-sericite-quartz rock adjacent to sulphide  
band.

---

## SHOWING NO.2

32, 292, 296, 11002, 11003, 11004: Samples from quartz-sulphide vein  
containing varying amounts of crudely banded and brecciated chalcopyrite,  
pyrite, arsenopyrite, quartz, calcite, and chlorite-quartz-sericite fragments.

277. Carbonate-jasper vein sample near main quartz-sulphide vein.

---

#### WELSHS BIGHT

191: Sphalerite-galena-chalcopyrite-pyrite-calcite-bearing quartz vein.

040: Quartz vein with fracture-filling galena.

---

#### REGIONAL QUARTZ-SULPHIDE VEINS

83, 44: Quartz vein with < 5 percent chalcopyrite, pyrite.

109: Quartz vein with ~ 25 percent pyrite, minor chalcopyrite.

41: Quartz vein with minor pyrite.

---

#### DIABASE/ULTRAMAFIC SAMPLES

39, 62, 69, 72: Unaltered diabase.

74: Diabase in a chloritic shear zone.

84, 105: Tectonized, quartz-calcite veined diabase.

156: Serpentinized ultramafic xenolith in gabbro.

---

#### QUARTZ-FELDSPAR PORPHYRY

186: Quartz, plagioclase, K-feldspar phenocrysts in a K-feldspar-quartz matrix.

### E.2.2. Sample Locations

Locations for most of the Nippers Harbour samples are depicted in Figs. E-1 to E-6. Those not included are:

1,2,6,2201,2208,22011,22013,22016 - samples from Burtons Pond dump.

Samples preceded by 'K' - samples from drill hole 4, Burtons Pond; sample number refers to depth (in cm) down hole.

Samples preceded by 'KA' - samples from drill hole 2, Burtons Pond; sample number refers to depth (in cm) down hole.

Samples preceded by 'KN' - samples from drill hole 2E/13-DDH 7, drilled by Advocate Mines Ltd in 1967; near Gull Pond.

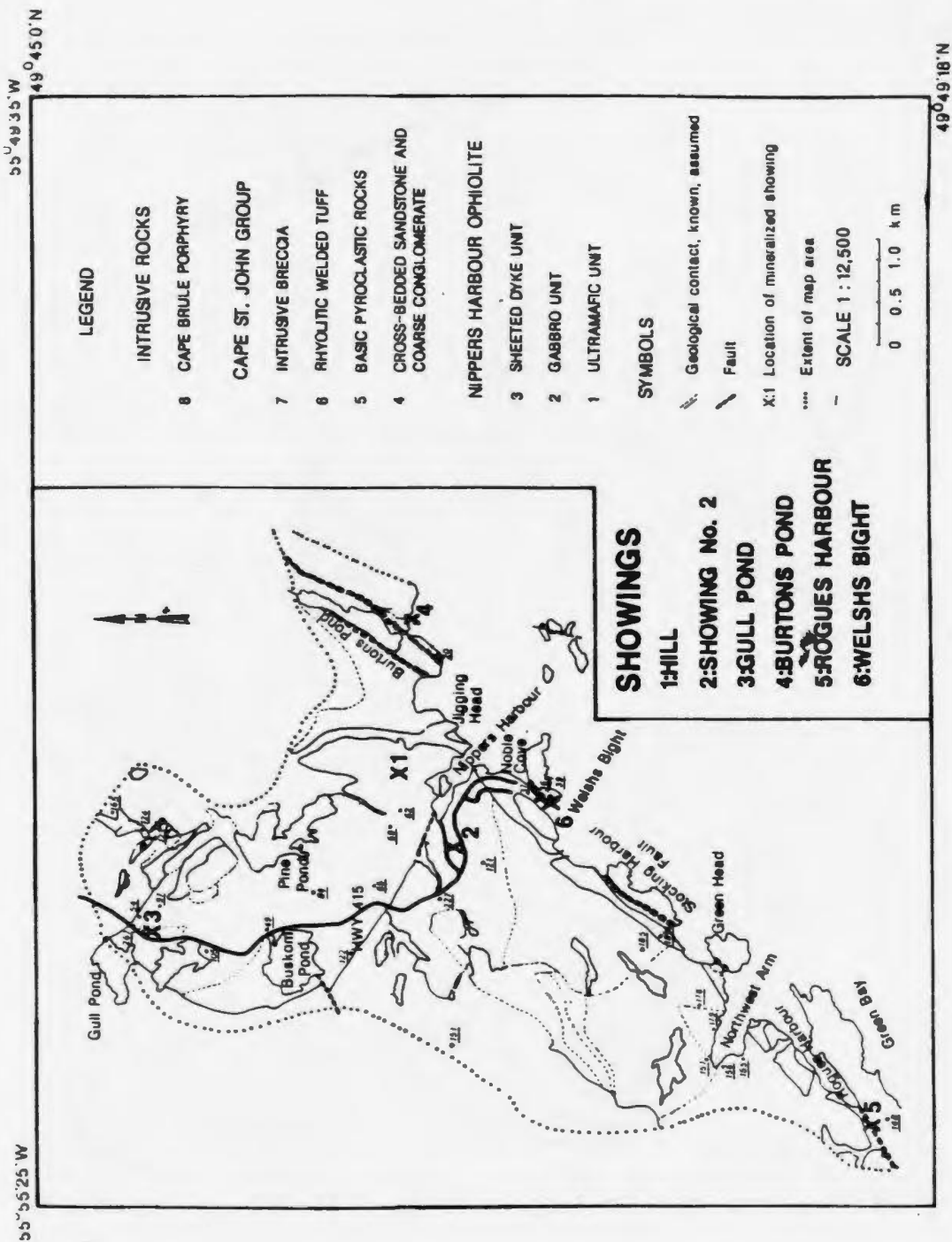


**Figure E-1:** Locations for regional diabase/gabbro, pyroxenite/dunite, Cape St. John Group and QFP samples

Adapted from Fig. 2-1. Samples plotted are: Diabase/gabbro-(20,39,49,54,59, 62,65,84,105,121,122); Pyroxenite/dunite-(155,179,148,156); Cape St. John Group-(36,97,123,124,178,267,157); QFP-(37,151,165,185,186,227)

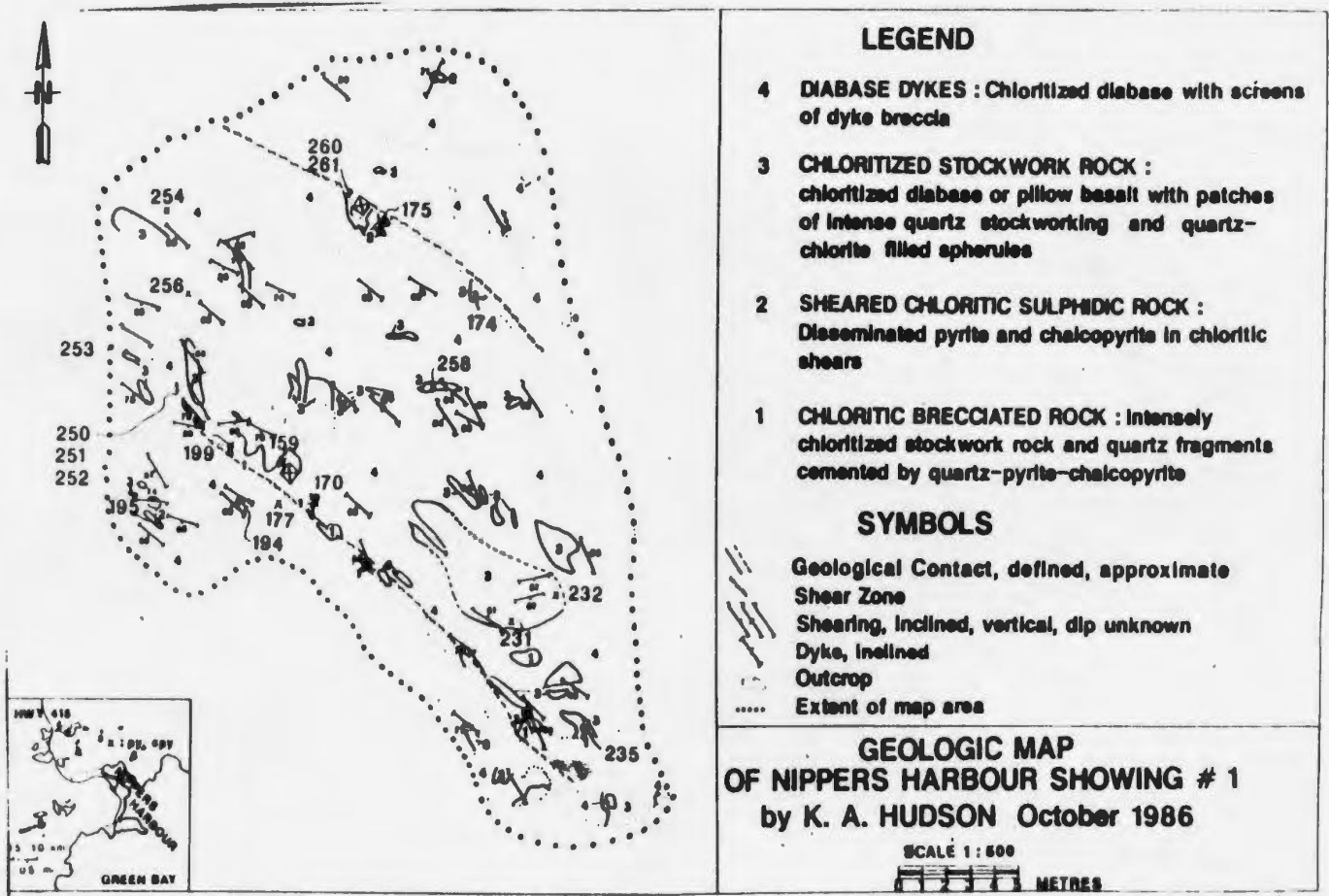


**Figure E-2:** Locations for Hill Showing samples

Adapted from Fig. 3-1. Samples plotted are-

(159, 170, 199, 235, 175, 195, 260, 261, 174, 231, 232, 253,  
 258, 177, 194, 250, 251, 252, 254, 256)

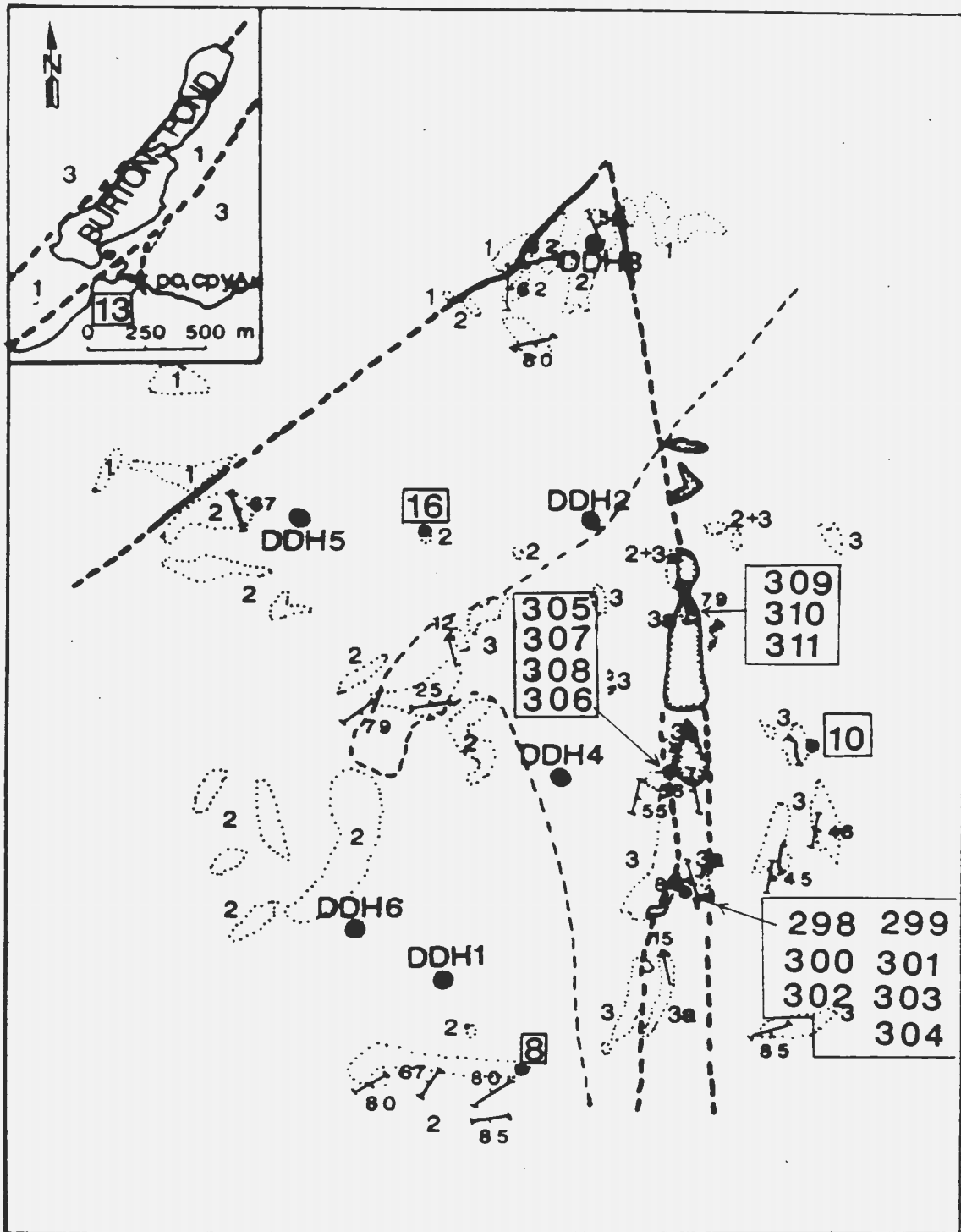


**Figure E-3:** Locations for Burton's Pond samples

Adapted from Fig. 3-5. Samples plotted are: (8,10,13,16,298 to 311)

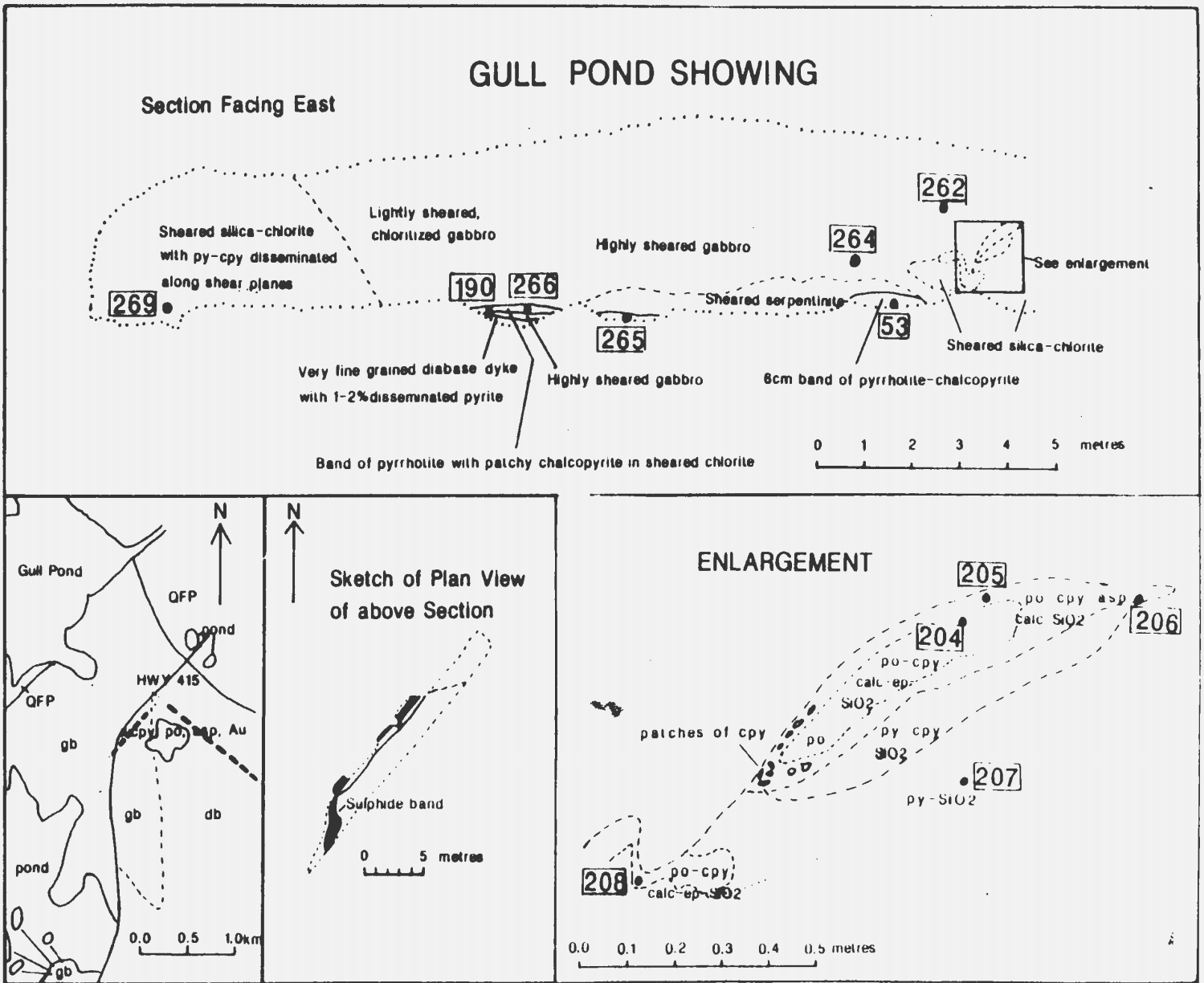


**Figure E-4:** Locations for Gull Pond samples

Adapted from Fig. 3-15. Samples plotted are—(206, 207, 262,

264, 269, 53, 190, 204, 205, 208, 265, 266)



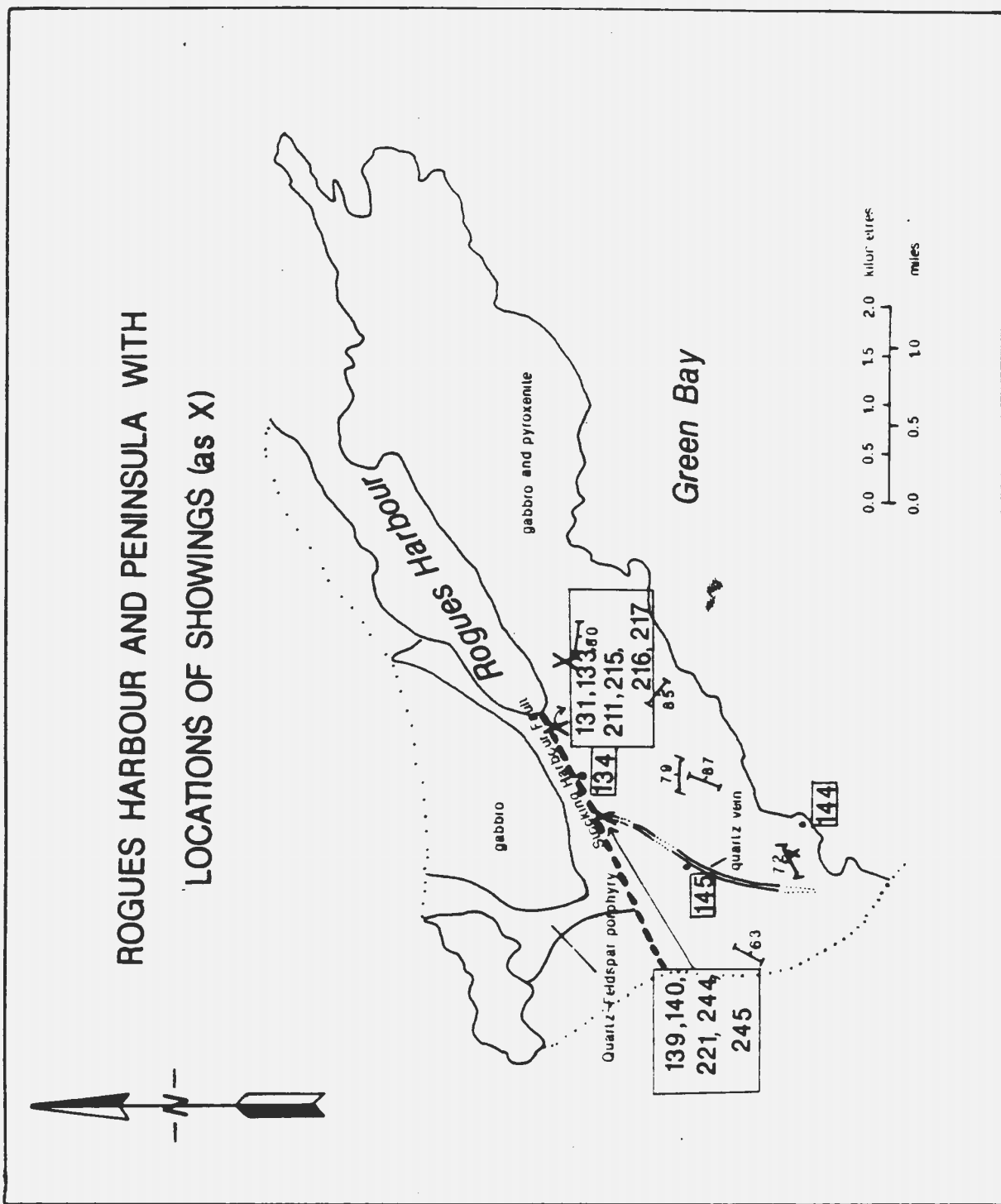


**Figure E-5:** Locations for Rogues Harbour samples

Samples plotted are: (134,139,144,145,215,131,133,140,211,216,217,221,244,245)

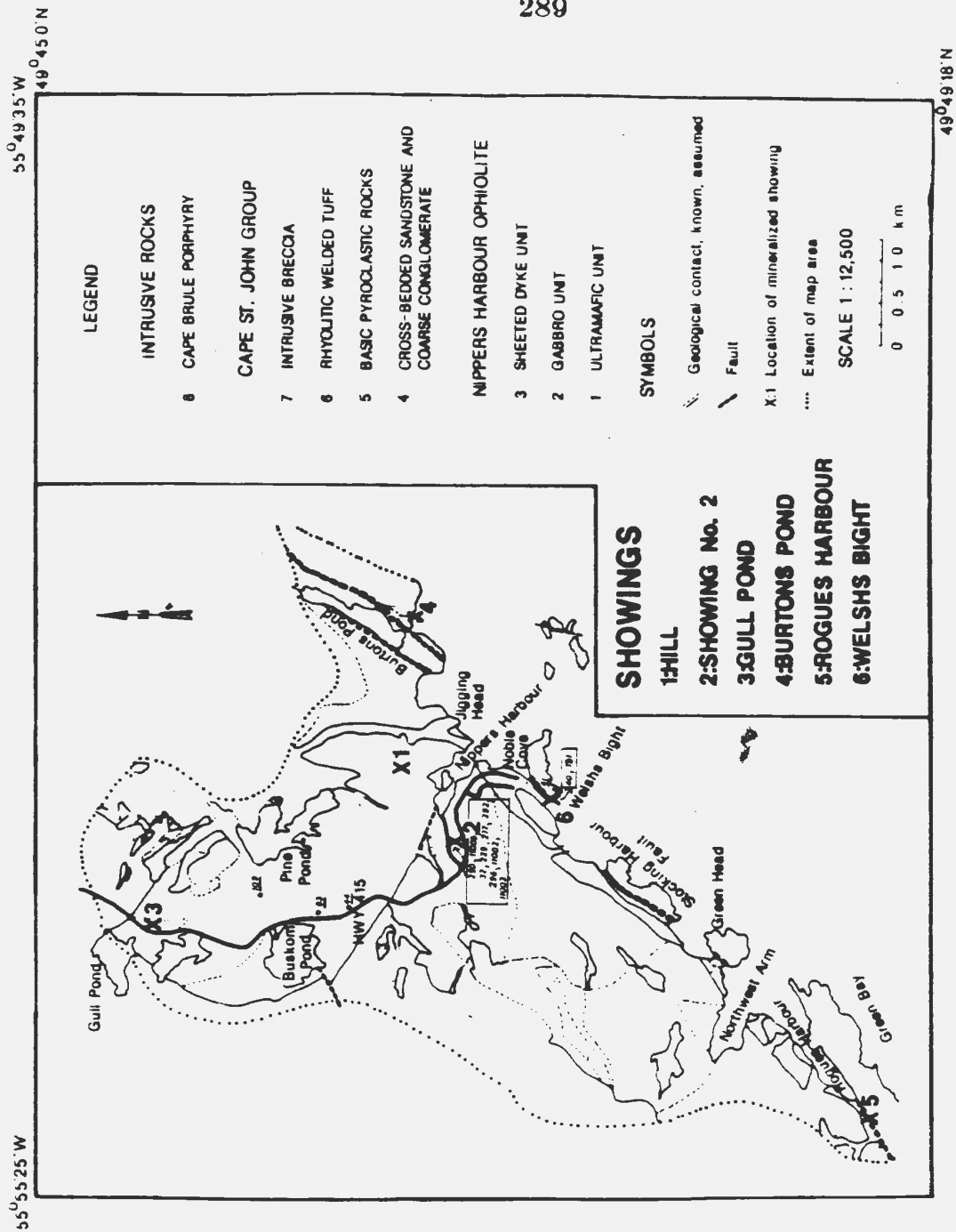


**Figure E-6:** Locations for Showing No.2, Welshs Bight, and Regional Quartz Vein samples

Adapted from Fig. 2-1. Samples plotted are: Showing No.2-(290,11009,32,229, 277,292,296,11002,11003); Welshs Bight-(40,191); Quartz Veins-(41,44,83,109)

## Appendix F

### Electron Microprobe Data

(Sample numbers are followed by the number of analyses carried out for a particular sample.)

## AMPHIBOLES

Sample	8 (3)		74 (2)		159 (1)	
Si	51.37	7.916	56.11	8.050	54.88	8.365
Al	2.82	0.511	15.80	2.699	0.26	0.044
Mg	14.77	3.392	3.01	0.644	13.49	3.064
Fe	14.97	1.927	9.05	1.086	16.62	2.166
Mn	0.25	0.031	0.14	0.017	0.17	0.018
Ca	11.40	1.188	13.47	2.067	12.15	1.981
Na	0.75	0.221	0.37	0.101	0.05	0.013
K	0.08	0.013	0.03	0.004	0.01	0.000
Ti	0.12	0.013	0.05	0.004	0.00	0.000
Cr	0.02	0.000	0.02	0.000	0.04	0.000
Ni	0.02	0.000	0.00	0.000	0.04	0.000
t	96.69	15.905	98.06	14.642	97.70	15.602

Sample	177 (3)		194 (4)		209 (3)	
Si	55.46	8.425	54.90	7.994	53.33	7.944
Al	0.32	0.058	3.55	0.606	2.73	0.477
Mg	10.95	2.478	18.54	4.025	17.71	3.931
Fe	20.18	2.563	10.07	1.222	10.63	1.325
Mn	0.16	0.018	0.22	0.025	0.18	0.021
Ca	12.14	1.975	10.64	1.658	11.74	1.871
Na	0.11	0.026	0.49	0.137	0.53	0.148
K	0.01	0.000	0.03	0.004	0.04	0.017
Ti	0.00	0.000	0.11	0.008	0.02	0.043
Cr	0.02	0.004	0.36	0.038	0.02	0.026
Ni	0.01	0.000	0.05	0.004	0.02	0.004
t	99.37	15.546	98.96	15.721	97.65	15.808

## AMPHIBOLES

Sample	250 (4)		266 (3)		298 (3)	
Si	59.72	8.145	53.09	7.669	51.18	8.267
Al	16.90	2.713	15.24	2.594	4.04	0.759
Mg	6.12	1.241	5.69	1.225	16.15	3.880
Fe	5.34	0.608	11.44	1.382	13.35	1.800
Mn	0.15	0.016	0.12	0.013	0.29	0.038
Ca	6.84	0.997	13.66	2.111	10.60	1.835
Na	5.62	1.485	0.03	0.004	0.14	0.060
K	0.04	0.004	0.01	0.000	0.02	0.003
Ti	0.06	0.004	0.05	0.004	0.18	0.019
Cr	0.01	0.000	0.02	0.000	0.08	0.008
Ni	0.01	0.000	0.03	0.000	0.05	0.003
c	100.80	15.212	99.38	15.001	96.08	16.672

Sample	307 (3)		311 (2)		313 (4)	
Si	55.88	8.152	50.07	8.301	55.85	8.248
Al	2.47	0.424	20.02	3.912	0.95	0.160
Mg	17.29	3.759	13.27	3.280	17.55	3.862
Fe	11.39	1.387	11.79	1.635	10.70	1.317
Mn	0.08	0.038	0.10	0.009	0.30	0.035
Ca	11.68	1.824	0.11	0.014	12.76	2.015
Na	0.13	0.034	3.57	1.143	0.02	0.004
K	0.10	0.017	0.02	0.000	0.04	0.004
Ti	0.02	0.000	0.02	0.000	0.01	0.000
Cr	0.08	0.008	0.01	0.000	0.00	0.000
Ni	0.01	0.000	0.04	0.004	0.04	0.000
c	99.37	15.644	99.02	18.299	98.20	15.799

## AMPHIBOLES

Sample	K437 (3)		K875 (3)		K1275 (2)	
Si	52.12	7.867	53.53	7.712	56.55	8.358
Al	3.58	0.634	5.64	0.956	1.02	0.173
Mg	17.18	3.866	19.58	4.203	15.00	3.305
Fe	11.22	1.413	7.13	0.858	13.93	1.722
Mn	0.15	0.017	0.08	0.008	0.02	0.026
Ca	11.65	1.882	11.31	1.746	12.27	1.943
Na	0.26	0.074	1.66	0.460	0.06	0.013
K	0.06	0.010	0.14	0.021	0.02	0.004
Ti	0.26	0.026	0.11	0.008	0.00	0.000
Cr	0.09	0.007	0.24	0.025	0.02	0.004
Ni	0.05	0.003	0.13	0.012	0.00	0.000
t	96.62	15.799	99.55	16.010	99.13	15.548

Sample	K1698 (5)		K2625 (6)		K2825 (2)	
Si	57.70	8.949	54.03	8.164	56.34	8.074
Al	0.46	0.084	3.23	0.577	2.64	0.444
Mg	16.18	3.742	19.82	4.468	18.95	4.045
Fe	13.13	1.699	6.73	0.846	9.03	1.081
Mn	0.34	0.042	0.16	0.018	0.16	0.012
Ca	12.37	2.053	11.99	1.942	12.21	1.872
Na	0.11	0.031	0.44	0.126	0.28	0.075
K	0.01	0.000	0.09	0.014	0.04	0.006
Ti	0.01	0.000	0.06	0.004	0.10	0.010
Cr	0.02	0.000	0.41	0.048	0.13	0.056
Ni	0.03	0.001	0.10	0.010	0.07	0.006
t	100.36	16.601	97.06	16.217	99.92	15.681

## AMPHIBOLES

Sample	KA3175 (2)		KA3350 (4)	
Si	54.88	8.233	54.90	8.064
Al	2.36	0.414	2.78	0.478
Mg	12.25	2.738	17.84	3.905
Fe	17.98	2.254	9.63	1.181
Mn	0.38	0.044	0.18	0.021
Ca	11.21	1.800	12.08	1.900
Na	0.49	0.141	0.47	0.129
K	0.01	0.000	0.03	0.044
Ti	0.00	0.000	0.07	0.004
Cr	0.02	0.013	0.16	0.017
Ni	0.01	0.000	0.05	0.004
t	99.61	15.637	98.19	15.708

## CHLORITES

Sample	139 (3)		170 (8)		174 (3)	
Si	28.69	5.692	24.34	5.332	26.02	5.480
Al	20.57	4.812	20.52	5.297	21.05	5.220
Mg	22.92	6.781	10.04	3.276	13.43	4.213
Fe	13.38	2.219	32.94	6.033	27.89	4.905
Mn	0.06	0.005	0.19	0.030	0.24	0.037
Ca	0.05	0.005	0.03	0.004	0.02	0.000
Na	0.01	0.000	0.02	0.007	0.04	0.012
K	0.01	0.000	0.01	0.000	0.00	0.000
Ti	0.05	0.005	0.04	0.002	0.05	0.006
Cr	1.43	0.221	0.02	0.001	0.03	0.000
Ni	0.03	0.000	0.03	0.001	0.03	0.000
t	87.20	19.742	88.18	19.983	88.80	19.874

## CHLORITES

Sample	195 (3)		199 (2)		206 (2)	
Si	27.22	5.889	29.58	6.126	26.77	4.687
Al	20.76	5.090	17.56	4.282	21.60	4.456
Mg	11.10	3.527	15.50	4.782	20.88	5.447
Fe	27.71	4.932	25.71	4.448	16.43	2.405
Mn	0.21	0.030	0.22	0.036	0.30	0.041
Ca	0.08	0.009	0.07	0.012	0.01	0.000
Na	0.62	0.024	0.00	0.000	0.01	0.000
K	0.01	0.003	0.02	0.003	0.02	0.005
Ti	0.04	0.006	0.01	0.000	0.06	0.005
Cr	0.04	0.003	0.07	0.009	0.05	0.005
Ni	0.02	0.000	0.04	0.003	0.01	0.000
t	87.81	19.513	88.78	19.701	86.13	17.050

Sample	213 (2)		215 (2)		229 (3)	
Si	28.20	5.589	28.74	5.575	23.34	5.278
Al	22.32	5.211	22.44	5.130	21.45	5.717
Mg	22.52	6.654	23.17	6.702	4.36	1.467
Fe	13.47	2.228	14.75	2.392	38.45	7.277
Mn	0.05	0.005	0.05	0.005	0.51	0.093
Ca	0.02	0.000	0.04	0.005	0.01	0.000
Na	0.03	0.011	0.05	0.017	0.01	0.000
K	0.02	0.000	0.01	0.000	0.01	0.000
Ti	0.07	0.005	0.01	0.000	0.03	0.000
Cr	0.21	0.029	0.22	0.131	0.02	0.000
Ni	0.05	0.005	0.02	0.000	0.02	0.000
t	86.96	19.738	89.50	19.957	88.20	19.832



## CHLORITES

Sample	235 (3)		260 (3)		K875 (3)	
Si	27.58	5.870	26.91	5.840	31.82	5.277
Al	19.63	4.920	19.50	4.993	17.00	3.378
Mg	13.10	4.152	9.47	3.068	26.52	6.663
Fe	26.02	4.627	30.84	5.605	10.87	1.528
Mn	0.22	0.037	0.30	0.053	0.14	0.015
Ca	0.08	0.012	0.06	0.010	0.21	0.034
Na	0.03	0.006	0.03	0.010	0.01	0.000
K	0.04	0.006	0.07	0.015	0.00	0.000
Ti	0.09	0.012	0.09	0.010	0.00	0.000
Cr	0.02	0.000	0.04	0.004	0.45	0.059
Ni	0.03	0.000	0.02	0.000	0.06	0.005
t	86.32	19.643	87.33	19.608	86.58	16.959

Sample	K1275 (3)		K3728 (2)	
Si	29.91	5.821	26.79	5.539
Al	20.79	4.770	20.93	5.096
Mg	21.99	6.381	18.34	5.648
Fe	16.74	2.725	20.59	3.549
Mn	0.32	0.051	0.30	0.048
Ca	0.02	0.000	0.01	0.000
Na	0.02	0.005	0.04	0.012
K	0.01	0.000	0.01	0.000
Ti	0.00	0.000	0.00	0.000
Cr	0.13	0.074	0.09	0.054
Ni	0.04	0.000	0.00	0.000

## EPIDOTES

Sample	8 (2)		74 (2)		174 (5)	
Si	38.97	3.261	38.42	3.270	39.40	3.307
Al	24.80	2.446	23.01	2.308	23.67	2.341
Mg	0.06	0.007	0.00	0.000	0.01	0.000
Fe	10.02	0.700	11.50	0.818	10.73	0.753
Mn	0.05	0.002	0.12	0.006	0.11	0.007
Ca	23.29	2.087	23.58	2.150	23.33	2.098
Na	0.03	0.002	0.01	0.000	0.01	0.001
K	0.01	0.000	0.01	0.000	0.00	0.000
Ti	0.03	0.000	0.06	0.004	0.07	0.002
Cr	0.04	0.000	0.05	0.002	0.03	0.000
Ni	0.04	0.000	0.03	0.000	0.02	0.000
t	97.34	8.506	96.79	8.558	97.38	8.509

Sample	195 (2)		235 (2)		250 (3)	
Si	38.67	3.245	39.74	3.265	38.95	3.224
Al	25.31	2.502	26.78	2.573	26.41	2.578
Mg	0.00	0.000	0.01	0.000	0.00	0.000
Fe	9.63	0.674	8.08	0.554	8.53	0.590
Mn	0.06	0.002	0.10	0.004	0.04	0.002
Ca	23.02	2.069	23.21	2.042	23.45	2.080
Na	0.00	0.000	0.02	0.002	0.00	0.000
K	0.01	0.000	0.00	0.000	0.00	0.000
Ti	0.03	0.000	0.03	0.000	0.03	0.000
Cr	0.02	0.000	0.02	0.000	0.02	0.000
Ni	0.02	0.000	0.03	0.000	0.02	0.000
t	96.74	8.492	97.81	8.440	97.44	8.473

## EPIDOTES

Sample	260 (3)		265 (3)		266 (3)	
Si	40.11	3.326	37.71	3.258	38.01	3.251
Al	23.54	2.299	22.55	2.294	23.39	2.357
Mg	0.00	0.000	0.00	0.000	0.01	0.000
Fe	11.73	0.813	12.49	0.902	11.88	0.848
Mn	0.09	0.004	0.09	0.005	0.07	0.005
Ca	23.14	2.056	22.77	2.107	22.77	2.086
Na	0.03	0.002	0.01	0.000	0.00	0.000
K	0.01	0.000	0.01	0.000	0.00	0.000
Ti	0.07	0.002	0.11	0.005	0.04	0.002
Cr	0.00	0.000	0.04	0.000	0.02	0.000
Ni	0.01	0.000	0.04	0.002	0.01	0.000
$\Sigma$	98.71	8.502	95.81	8.574	96.19	8.550

Sample	296 (2)		311 (1)	
Si	42.02	3.378	38.81	3.293
Al	25.53	2.417	23.91	2.392
Mg	0.00	0.000	0.00	0.000
Fe	9.02	0.606	11.12	0.787
Mn	0.04	0.002	0.08	0.005
Ca	23.23	2.000	22.21	2.020
Na	0.00	0.000	0.01	0.000
K	0.00	0.000	0.00	0.000
Ti	0.01	0.000	0.08	0.005
Cr	0.00	0.000	0.04	0.000
Ni	0.01	0.000	0.01	0.000
$\Sigma$	99.88	8.403	96.26	8.502

## FELDSPARS

Sample	KA3175 (3)		KA3350 (2)		296 (2)	
	Si	68.89	12.029	70.73	12.072	50.02
Al	19.10	3.929	19.61	3.940	31.61	5.369
Mg	0.05	0.010	0.01	0.000	1.43	0.304
Fe	0.15	0.020	0.18	0.025	2.77	0.330
Mn	0.01	0.000	0.02	0.000	0.00	0.000
Ca	0.25	0.046	0.64	0.115	0.02	0.000
Na	11.53	3.904	10.72	3.545	0.08	0.021
K	0.04	0.005	0.04	0.005	9.20	1.688
Ti	0.00	0.000	0.00	0.000	0.00	0.000
Cr	0.00	0.000	0.01	0.000	0.00	0.000
Ni	0.00	0.000	0.03	0.000	0.01	0.000
t	100.04	19.943	102.00	19.702	95.20	14.930

## SERICITES

## SERICITES

Sample	213 (2)		215 (3)		229 (3)	
	Si	49.94	7.222	52.72	8.838	48.03
Al	31.81	5.422	28.80	5.694	32.71	5.673
Mg	1.52	0.324	2.00	0.495	0.56	0.121
Fe	1.47	0.176	1.46	0.203	2.37	0.289
Mn	0.00	0.000	0.02	0.000	0.00	0.000
Ca	0.02	0.002	0.00	0.000	0.00	0.000
Na	0.12	0.032	0.14	0.041	0.13	0.034
K	9.63	1.776	9.88	2.110	9.54	1.789
Ti	0.01	0.000	0.01	0.000	0.02	0.000
Cr	0.00	0.000	0.11	0.056	0.02	0.000
Ni	0.01	0.000	0.01	0.000	0.00	0.000
t	94.52	14.954	95.15	17.437	93.38	14.979

## PRECISION AND ACCURACY OF ELECTRON MICROPROBE RUNS

	Run 1		Run 2		Run 3		Run 4		Run 5	
	Wt%	SD	Wt%	SD	Wt%	SD	Wt%	SD	Wt%	SD
Na	1.42	.04	1.27	.05	1.37	.03	1.38	.02	1.27	.04
Mg	16.03	.13	15.84	.13	16.32	.03	15.89	.12	16.03	.14
Al	8.34	.21	7.95	.14	8.21	.02	8.11	.08	8.07	.05
Si	50.84	.97	50.55	.09	50.53	.25	51.18	.41	50.08	.23
K	0.00	.0	0.00	.0	0.00	.01	0.00	.02	0.00	.01
Ca	16.06	.01	15.75	.11	15.64	.13	15.44	.35	16.29	.29
Ti	0.86	.04	0.79	.00	0.83	.00	0.84	.00	0.83	.03
Cr	0.14	.02	0.13	.00	0.16	.01	0.14	.00	0.16	.01
Mn	0.10	.02	0.09	.02	0.09	.01	0.13	.00	0.11	.03
Fe	6.14	.07	6.23	.05	6.29	.08	6.03	.11	6.38	.09
Ni	0.05	.00	0.04	.00	0.06	.00	0.06	.00	0.04	.02
total	99.98		98.66		99.50		99.21		99.25	
Spls	260(ep,ch) K2625(ak)		229(ch,sc)		250(ep,ak) 265(ep) 266(ep,ak) 74(ep,ak) 298(ak)		195(ep,ch) 235(ep,ch) 199(ep,ch) 213(ch,sc)		170(ch) 174(ep,ch) 311(ep,ak) 250(ep)	

	Run 6		Run 7		Run 8		Run 9		Published	
	Wt%	SD	Wt%	SD	Wt%	SD	Wt%	SD	Values	
Na	1.38	.04	1.29	.04	1.28	.03	1.37	.04	1.27	
Mg	16.01	.20	16.06	.03	16.39	.03	16.13	.02	16.65	
Al	8.16	.10	7.90	.07	7.73	.08	8.12	.06	7.86	
Si	49.50	.26	50.00	.31	51.69	.39	50.32	.30	50.73	
K	0.01	.00	0.01	.01	0.01	.01	0.01	.01	0.00	
Ca	15.69	.17	16.05	.07	16.23	.06	16.21	.10	15.82	
Ti	0.78	.01	0.81	.01	0.16	.01	0.81	.01	0.74	
Cr	0.13	.01	0.14	.01	0.45	.01	0.15	.01	0.00	
Mn	0.14	.00	0.12	.00	0.14	.00	0.14	.00	0.13	
Fe	6.24	.08	6.26	.02	6.50	.04	6.19	.02	6.77	
Ni	0.06	.02	0.04	.00	0.07	.00	0.05	.00	0.00	
total	98.18		98.67		100.65		99.50		99.97	
Spls	KA3350(fel) 139(ch) 296(ep,sc)		KA3350(ak) K875(ak,ch) K1698(ak) 307(ak) KA3175(fel)		215(ch,sc) KA3175(ak) 177(ak) K2825(ak) K1275(ch,ak) K3728(ch)		206(ch) 8(ak,ep) 209(ak) 313(ak) 194(ak) K437(ak)			

Samples (Spls) analysed for each run are given below the run number. Symbols are as follows: ch:chlorite, ep:epidote, fel:feldspar, ak:actinolite, sc:sericite, SD:standard deviation.

## Appendix G

### Fluid Inclusion Methodology

Higgins (1979) outlines the complete procedure for preparation of fluid inclusion sections and the components necessary for microthermic studies. Sections cut for fluid inclusion study are doubly polished and are ideally between 0.5 and 0.2 mm thick. Samples must be cut and ground carefully to insure that frictional heating does not decrepitate the inclusions.

A U.S.G.S. Heating/Freezing Stage was used for microthermic studies. It consists of (1) a heating/freezing stage attached to a petrographic microscope stage; (2) a temperature monitor/control unit; (3) a pressurized liquid nitrogen container. Higgins (1979) added a rubber tube, attached along-side the sample and the lens, to prevent icing up of the sample and the objective lens.

The stage had been previously calibrated for heating runs by melting a small amount of several standard, powdered chemicals between glass cover slips and comparing the measured melting temperature with the actual melting temperature of each compound. The calibration curve is depicted in Fig. G-1.

Salinities were derived using the NaCl-Freezing point curve depicted in Fig. G-2. A list of salinities obtained from this diagram is presented in Table G-1. Eutectic temperatures are summarized in Table G-2.

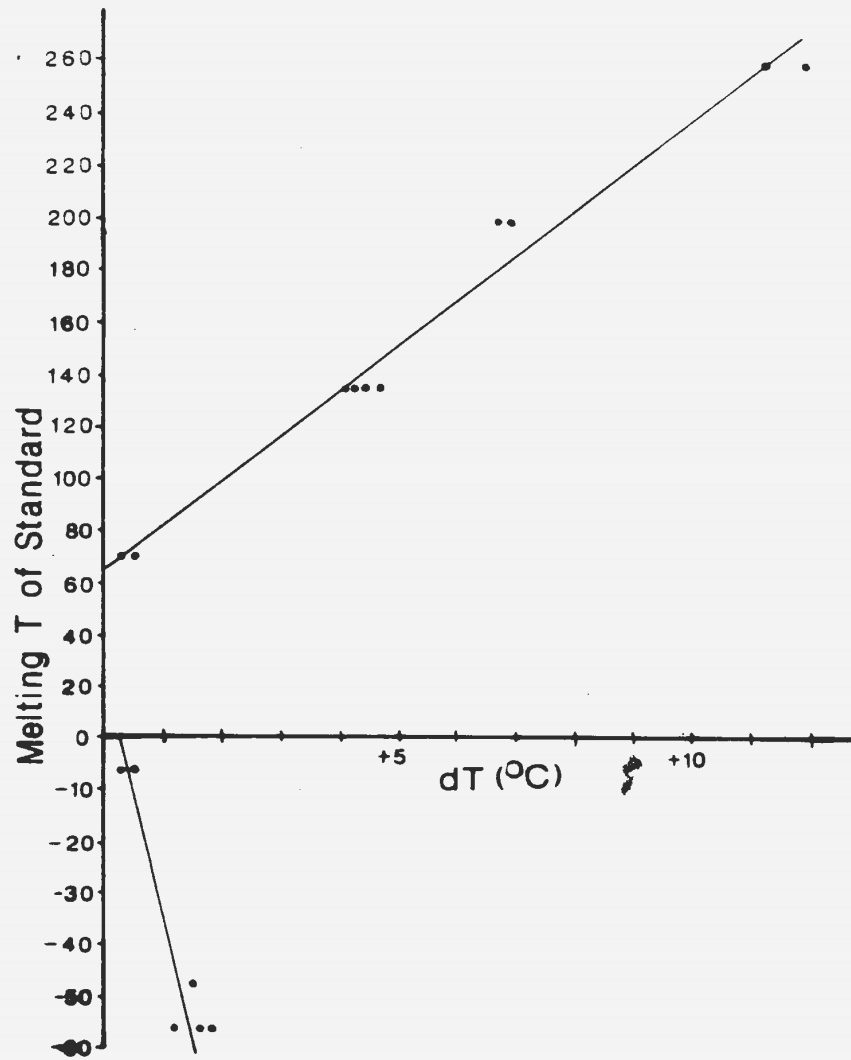


**Figure G-1:** Calibration curve for fluid inclusion runs

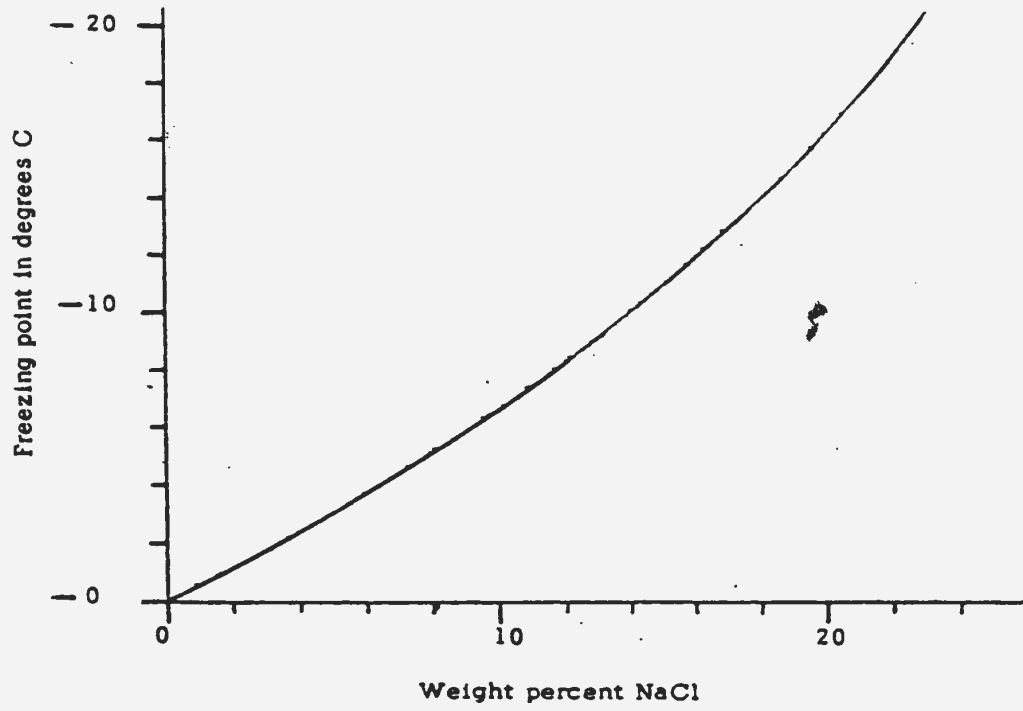


**Figure G-2:** Freezing points of pure NaCl solutions



NaCl ‰	T <sub>m</sub> ice	NaCl ‰	T <sub>m</sub> ice	NaCl ‰	T <sub>m</sub> ice	NaCl ‰	T <sub>m</sub> ice
0.1	-0.1	3.1	-1.9	6.1	-3.8	9.1	-5.9
0.2	-0.1	3.2	-1.9	6.2	-3.8	9.2	-6.0
0.3	-0.2	3.3	-2.0	6.3	-3.9	9.3	-6.1
0.4	-0.2	3.4	-2.0	6.4	-4.0	9.4	-6.1
0.5	-0.3	3.5	-2.1	6.5	-4.0	9.5	-6.2
0.6	-0.4	3.6	-2.2	6.6	-4.1	9.6	-6.3
0.7	-0.4	3.7	-2.2	6.7	-4.2	9.7	-6.4
0.8	-0.5	3.8	-2.3	6.8	-4.3	9.8	-6.4
0.9	-0.5	3.9	-2.3	6.9	-4.3	9.9	-6.5
1.0	-0.6	4.0	-2.4	7.0	-4.4	10.0	-6.6
1.1	-0.6	4.1	-2.5	7.1	-4.5	10.1	-6.7
1.2	-0.7	4.2	-2.5	7.2	-4.5	10.2	-6.8
1.3	-0.8	4.3	-2.6	7.3	-4.6	10.3	-6.8
1.4	-0.8	4.4	-2.7	7.4	-4.7	10.4	-6.9
1.5	-0.9	4.5	-2.7	7.5	-4.7	10.5	-7.0
1.6	-0.9	4.6	-2.8	7.6	-4.8	10.6	-7.1
1.7	-1.0	4.7	-2.9	7.7	-4.9	10.7	-7.2
1.8	-1.1	4.8	-2.9	7.8	-5.0	10.8	-7.2
1.9	-1.1	4.9	-3.0	7.9	-5.0	10.9	-7.3
2.0	-1.2	5.0	-3.1	8.0	-5.1	11.0	-7.4
2.1	-1.2	5.1	-3.1	8.1	-5.2	11.1	-7.5
2.2	-1.3	5.2	-3.2	8.2	-5.2	11.2	-7.6
2.3	-1.4	5.3	-3.2	8.3	-5.3	11.3	-7.6
2.4	-1.4	5.4	-3.3	8.4	-5.4	11.4	-7.7
2.5	-1.5	5.5	-3.4	8.5	-5.5	11.5	-7.8
2.6	-1.5	5.6	-3.4	8.6	-5.5	11.6	-7.9
2.7	-1.6	5.7	-3.5	8.7	-5.6	11.7	-8.0
2.8	-1.7	5.8	-3.6	8.8	-5.7	11.8	-8.1
2.9	-1.7	5.9	-3.6	8.9	-5.8	11.9	-8.1
3.0	-1.8	6.0	-3.7	9.0	-5.8	12.0	-8.2
12.1	-8.3	15.1	-11.1	18.1	-14.2	21.1	-17.9
12.2	-8.4	15.2	-11.2	18.2	-14.3	21.2	-18.0
12.3	-8.5	15.3	-11.3	18.3	-14.5	21.3	-18.1
12.4	-8.6	15.4	-11.4	18.4	-14.6	21.4	-18.3
12.5	-8.7	15.5	-11.5	18.5	-14.7	21.5	-18.4
12.6	-8.7	15.6	-11.6	18.6	-14.8	21.6	-18.5
12.7	-8.8	15.7	-11.7	18.7	-14.9	21.7	-18.7
12.8	-8.9	15.8	-11.8	18.8	-15.0	21.8	-18.8
12.9	-9.0	15.9	-11.9	18.9	-15.2	21.9	-18.9
13.0	-9.1	16.0	-12.0	19.0	-15.3	22.0	-19.1
13.1	-9.2	16.1	-12.1	19.1	-15.4	22.1	-19.2
13.2	-9.3	16.2	-12.2	19.2	-15.5	22.2	-19.4
13.3	-9.4	16.3	-12.3	19.3	-15.6	22.3	-19.5
13.4	-9.5	16.4	-12.4	19.4	-15.8	22.4	-19.6
13.5	-9.6	16.5	-12.5	19.5	-15.9	22.5	-19.8
13.6	-9.6	16.6	-12.6	19.6	-16.0	22.6	-19.9
13.7	-9.7	16.7	-12.7	19.7	-16.1	22.7	-20.1
13.8	-9.8	16.8	-12.8	19.8	-16.2	22.8	-20.2
13.9	-9.9	16.9	-12.9	19.9	-16.4	22.9	-20.3
14.0	-10.0	17.0	-13.0	20.0	-16.5	23.0	-20.5
14.1	-10.1	17.1	-13.1	20.1	-16.6	23.1	-20.6
14.2	-10.2	17.2	-13.2	20.2	-16.7	23.2	-20.8
14.3	-10.3	17.3	-13.3	20.3	-16.9		
14.4	-10.4	17.4	-13.5	20.4	-17.0		
14.5	-10.5	17.5	-13.6	20.5	-17.1		
14.6	-10.6	17.6	-13.7	20.6	-17.2		
14.7	-10.7	17.7	-13.8	20.7	-17.4		
14.8	-10.8	17.8	-13.9	20.8	-17.5		
14.9	-10.9	17.9	-14.0	20.9	-17.6		
15.0	-11.0	18.0	-14.1	21.0	-17.8		

**Table G-1:** Salinities obtained from freezing point measurements

Compound	Eutectic Temp (°C)
KCl	-10.6
NaCl	-20.8
NaCl-KCl	-22.9
MgCl <sub>2</sub>	-33.6
NaCl-MgCl <sub>2</sub>	-35
CaCl <sub>2</sub>	-49.8
NaCl-KCl-CaCl <sub>2</sub>	-56
NaCl-CaCl <sub>2</sub> -MgCl <sub>2</sub>	-57

**Table G-2:** Eutectic temperatures corresponding to common salts

From Crawford (1981) and Luzhnaya and Vereshtchetina (1946).



00045

8

